Electrochemical Society

NOW YOU WILL KNOW THEY ARE FROM GREAT LAKES CARBON

This New Emblem is your assurance of carbon and graphite products—production engineered to the highest standards of quality.

The emblem is being introduced in all of our packaging — in electrode end protectors, nipple cartons, palletized anodes, palletized carbon brick, and drums of carbonaceous materials.

Watch for this emblem — it identifies products made to give you matchless performance.

ELECTRODE GLC DIVISION

GREAT LAKES CARBON CORPORATION

18 EAST 48TH STREET, NEW YORK 17, N.Y. OFFICES IN PRINCIPAL CITIES

GRAPHITE ELECTRODES • ANODES • AND SPECIALTIES

EDITORIAL STAFF

H. H. Uhlig, Chairman, Publication Committee

Cecil V. King, Editor

Norman Hackerman, Technical Editor

Ruth G. Sterns, Managing Editor

U. B. Thomas, News Editor

H. W. Salzberg, Book Review Editor

Natalie Michalski, Assistant Editor

DIVISIONAL EDITORS

W. C. Vosburgh, Battery

Milton Stern, Corrosion, I

R. T. Foley, Corrosion, II

T. D. Callinan, Electric Insulation

Abner Brenner, Electrodeposition

H. C. Froelich, Electronics

D. H. Baird, Electronics—Semiconductors

Sherlock Swann, Jr., Electro-Organic, I

Stanley Wawzonek, Electro-Organic, II

John M. Blocher, Jr., Electrothermics and Metallurgy, I

A. U. Seybolt, Electrothermics and Metallurgy, II

N. J. Johnson, Industrial Electrolytic

C. W. Tobias, Theoretical Electrochemistry, I

A. J. deBethune, Theoretical Electrochemistry, II

REGIONAL EDITORS

Howard T. Francis, Chicago

Joseph Schulein, Pacific Northwest

J. C. Schumacher, Los Angeles

G. W. Heise, Cleveland

G. H. Fetterley, Niagara Falls

Oliver Osborn, Houston

Earl A. Gulbransen, Pittsburgh

A. C. Holm, Canada

J. W. Cuthbertson, Great Britain

T. L. Rama Char, India

ADVERTISING OFFICE

ECS
1860 Broadway, New York 23, N. Y.

ECS OFFICERS

Sherlock Swann, Jr., President
University of Illinois, Urbana, Ill.

W. C. Gardiner, Vice-President
Olin Mathieson Chemical Corp., Niagara Falls, N. Y.

R. A. Schaefer, Vice-President
Cleveland Graphite Bronze Div., Clevite Corp., Cleveland, Ohio

Henry B. Linford, Vice-President and Interim Secretary
Columbia University, New York, N. Y.

Lyle I. Gilbertson, Treasurer
Air Reduction Co., Murray Hill, N. J.

Robert K. Shannon, Executive Secretary
National Headquarters, The ECS, 1860 Broadway, New York 23, N. Y.

Journal of the Electrochemical Society

JANUARY 1959 **VOL. 106 • NO. 1**

CONTENTS

Editorial

"Science, The News, and The Public" 4C

Technical Papers

The Flade Potential of Iron Passivated by Various Inorganic Corrosion Inhibitors. *H. H. Uhlig and P. F. King* 1

Some Observations on the Mechanism of Inhibition. *A. C. Makrides* 7

Oxidation of Titanium, Zirconium, and Hafnium. *G. R. Wallwork and A. E. Jenkins* 10

The Electrical Resistance of Oxide Films on Zirconium in Relation to Corrosion. *R. D. Misch and F. H. Gunzel, Jr.* 15

The Structure of Electro-Deposited Nickel. *B. C. Banerjee and A. Goswami* 20

The System $ZnO \cdot CdO \cdot B_2O_3$, Phase Relationships, and Fluorescence. *D. E. Harrison and F. A. Hummel* 24

Activation of ZnS and (Zn,Cd)S Phosphors by Gold and Other Elements. *S. T. Henderson, P. W. Ranby, and M. B. Halstead* 27

Particle Size Effects and the Distribution of Barriers in Electroluminescent Zinc Sulfide Phosphors. *P. Goldberg* 34

A Method for the Purification of Selenium. *S. Nielsen and R. J. Heritage* 39

Electrodeposition of High-Purity Chromium. *F. E. Block, P. C. Good, and G. Asai* 43

Some Effects of Pressure on Consumable Electrode Arc Melting. *J. W. Suiter* 47

Tungsten Zone Melting by Electron Bombardment. *R. G. Carlson* 49

Vapor Pressure of Niobium. *R. Speiser, P. Blackburn, and H. L. Johnston* 52

The Occurrence of Impurities in Rock Salt, Solar Salt, and Purified Sodium Chloride. *A. Bloomberg and K. Ladenburg* 54

The Oxygen Electrode, I. Isotopic Investigation of Electrode Mechanisms. *M. O. Davies, M. Clark, E. Yeager, and F. Hovorka* 56

Technical Notes

Magnesium-Bismuth Oxide Dry Cells. *C. K. Morehouse and R. Glicksman* 61

Corrosion Product and Inhibitor Films on Aluminum. *H. W. McCune* 63

Additives and Grain Refinement. *D. A. Vermilyea* 66

Measurement of Carbon-Metal Contact Resistances. *H. L. Foltz and M. R. Hertz* 67

Technical Review

Electrodeposition of Powders for Powder Metallurgy. *C. L. Mantell* 70

Brief Communication

On the Hydrogen Evolution Reaction. *R. J. Brodd* 74

Current Affairs 11C-19C

Published monthly by The Electrochemical Society, Inc., from Manchester, N. H., **Executive Offices, Editorial Office** and **Circulation Dept.**, and **Advertising Office** at 1860 Broadway, New York 23, N. Y., combining the JOURNAL and TRANSACTIONS OF THE ELECTROCHEMICAL SOCIETY. Statements and opinions given in articles and papers in the JOURNAL OF THE ELECTROCHEMICAL SOCIETY are those of the contributors, and The Electrochemical Society assumes no responsibility for them. Nondeductible subscription to members $5.00; subscription to nonmembers $18.00. Single copies $1.25 to members, $1.75 to nonmembers.

Copyright 1959 by The Electrochemical Society, Inc.

Entered as second-class matter at the Post Office at Manchester, N. H., under the act of August 24, 1912.

SARGENT-SLOMIN ANALYZERS
are standard equipment in prominent laboratories

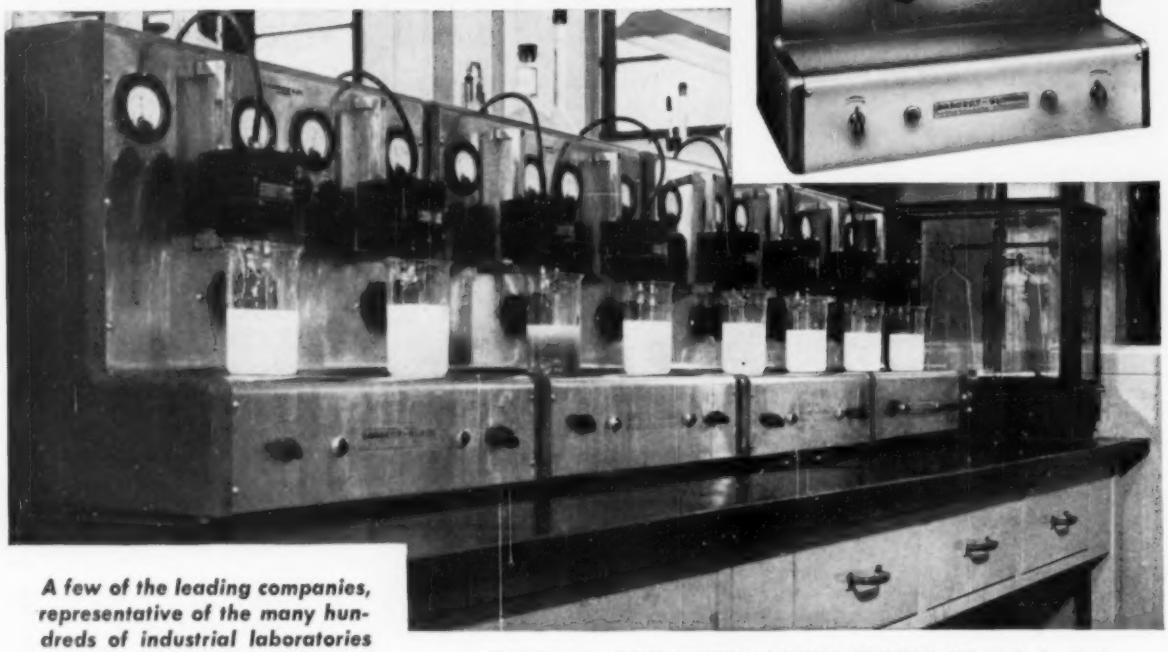

Photo Courtesy INTERNATIONAL HARVESTER COMPANY, Melrose Park, Illinois

A few of the leading companies, representative of the many hundreds of industrial laboratories using the Sargent - Slomin and Heavy Duty Analyzers for control analyses . . .

AMPCO METAL, Inc.
ANDERSON LABORATORIES
CALERA MINING COMPANY
EUREKA WILLIAMS COMPANY
THE FEDERAL METAL CO.
FORD MOTOR COMPANY
THE GLIDDEN COMPANY—Chemical, Metal and Pigment Division
HOT POINT CO.
HOWARD FOUNDRY COMPANY
INTERNATIONAL HARVESTER COMPANY
KENNAMETAL Inc.
McQUAY - NORRIS MANUFACTURING CO.
NATIONAL LEAD COMPANY, Fredericktown, Missouri
PIASECKI HELICOPTER CORPORATION
REVERE COPPER & BRASS INCORPORATED
THE RIVER SMELTING & REFINING COMPANY
SILAS MASON COMPANY
THE STUDEBAKER CORPORATION
THOMPSON PRODUCTS, INC.

Sargent-Slomin Electrolytic Analyzers are recommended for such electro analytical determinations as: Copper in—ores, brass, iron, aluminum and its alloys, magnesium and its alloys, bronze, white metals, silver solders, nickel and zinc die castings. Lead in—brass, aluminum and its alloys, bronze, zinc and zinc die castings. Assay of electrolytical copper, nickel and other metals.

Sargent analyzers are completely line operated, employing self-contained rectifying and filter circuits. Deposition voltage is adjusted by means of autotransformers, with meters indicating volts and amperes and controls on the panel. An easily replaceable fuse guards against circuit overload. Maximum D.C. current capacity 5 to 15 amperes; maximum D.C. voltage available, 10 volts.

Sargent-Slomin Analyzers stir through a rotating chuck operated from a capacitor type induction motor, having a fixed speed of 550 r.p.m. with 60 cycle A.C. current or 460 r.p.m. with 50 cycle A.C. current. Motors are sealed against corrosive fumes and are mounted on cast metal brackets, sliding on ½" square stainless steel rods, permitting vertical adjustment of electrode position over a distance of 4". Pre-lubricated ball-bearings support the rotating shaft. All analyzers accommodate electrodes having shaft diameters no greater than 0.059 inch. Stainless steel spring tension chucks permit quick, easy insertion of electrodes and maintain proper electrical contact. Special Sargent high efficiency electrodes are available for these analyzers. Illustrated above is one model of the five types of Sargent-Slomin and Heavy Duty Analyzers.

S-29465 ELECTROLYTIC ANALYZER—Motor stirred, Two Position, 5 Ampere. With two adjustable heaters, pilot lights and control knobs. For operation from 115 volt, 50 or 60 cycle A.C. circuits.....**$530.00**

SARGENT
SCIENTIFIC LABORATORY INSTRUMENTS • APPARATUS • SUPPLIES • CHEMICALS

E. H. SARGENT & COMPANY, 4647 W. FOSTER, CHICAGO 30, ILLINOIS
DETROIT 4, MICH. • DALLAS 35, TEXAS • BIRMINGHAM 4, ALA. • SPRINGFIELD, N. J.

Sylvania announces a new low cost plan for converting germanium scrap

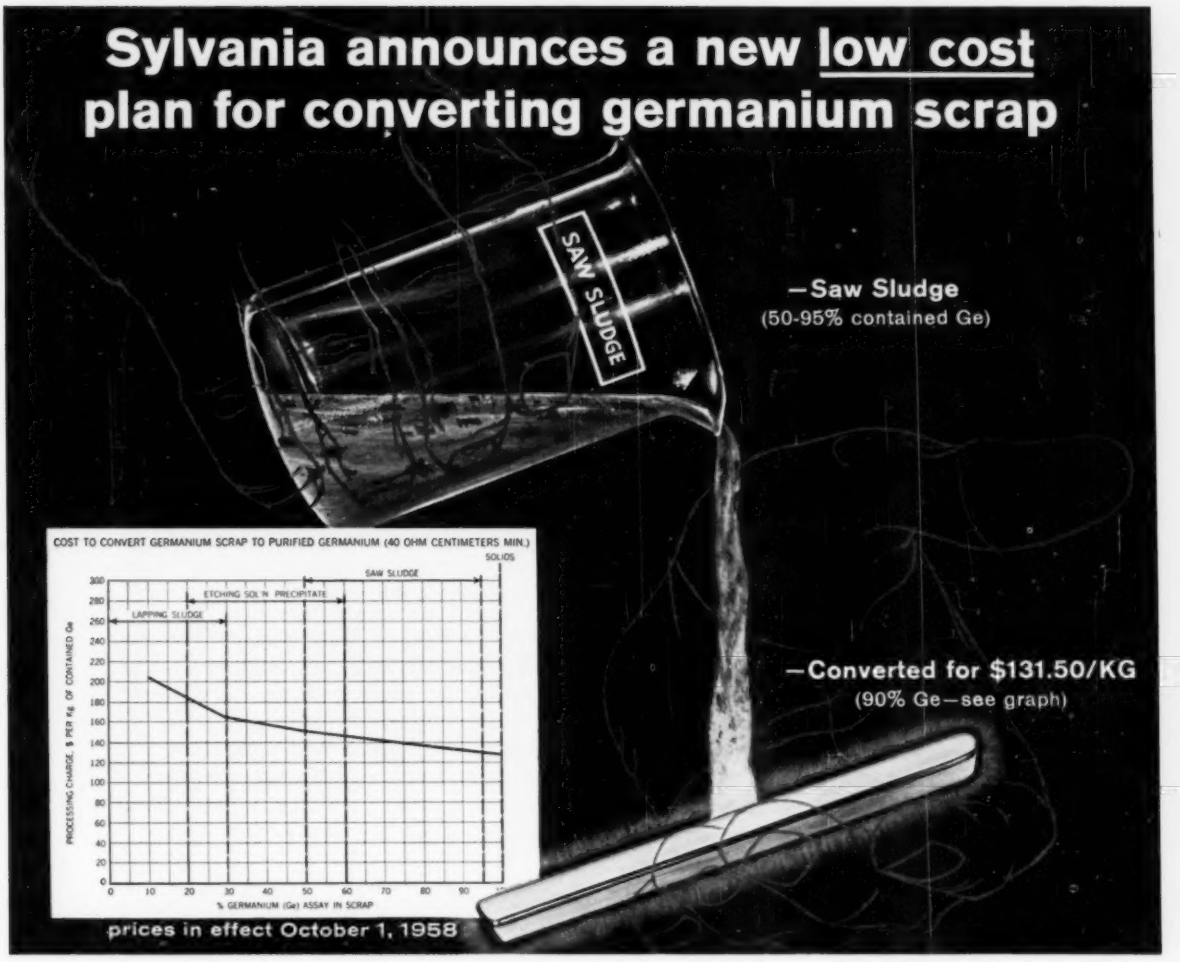
SAW SLUDGE
—Saw Sludge
(50-95% contained Ge)
COST TO CONVERT GERMANIUM SCRAP TO PURIFIED GERMANIUM (40 OHM CENTIMETERS MIN.)
SOLIDS
SAW SLUDGE
ETCHING SOL'N PRECIPITATE
LAPPING SLUDGE
PROCESSING CHARGE, $ PER Kg. OF CONTAINED Ge
% GERMANIUM (Ge) ASSAY IN SCRAP
—Converted for $131.50/KG
(90% Ge—see graph)
prices in effect October 1, 1958

Weigh your in-plant germanium scrap conversion with these important advantages of Sylvania's new plan.

LOWER COST

As a leading supplier of semiconductor materials, Sylvania's volume processing of germanium makes possible new low prices for scrap recovery—makes *all* your scrap more valuable regardless of percentage of contained germanium.

NO HIDDEN WASTE

Do-it-yourself scrap conversion has hidden costs other than labor and overhead. Inaccurate analyses and low percentage yields can waste valuable material. Sylvania provides you an accurate analysis and guarantees 100% return of contained germanium.

UNIFORM QUALITY

For your scrap Sylvania returns high purity germanium ingots or cut pieces produced under the same standards which have made Sylvania a leading supplier to the industry. Minimum resistivity of 40 ohm cm is guaranteed. You'll get maximum yields in growing doped single crystals.

NO TIME DELAY

Upon receipt and analysis of your germanium scrap, Sylvania will replace it with purified material directly from stock, or delivery schedules can be arranged to meet your production planning requirements.

Call in your Sylvania Representative. He'll give you complete details on this important new germanium buying concept. You can discuss all your Semiconductor Materials requirements with him, too.

SYLVANIA

Sylvania Electric Products Inc.
Chemical & Metallurgical Div.
Towanda, Penna.

TUNGSTEN • MOLYBDENUM • CHEMICALS • PHOSPHORS • SEMICONDUCTORS

Editorial

"Science, The News, and The Public"

THE above is the title of a report recently issued by the National Association of Science Writers (available for $1.00, New York University Press, New York 3, N. Y.). For many years NASW has striven to improve the quality of science news reporting for the general public. At first the fight was uphill, but today the importance of scientific technology in everyday life has forced even the most conservative news management to recognize the need for accurate accounts of scientific events and developments. Consequently, all major press associations, most metropolitan newspapers, and the mass circulation magazines have science specialists on their staffs.

While it was quite evident that the popularity of science news was increasing, NASW felt the need of a more definite picture: does such news get through to a wide public, is it understood, appreciated, effective; what do people think of science and scientists, and of the stories they read or hear on radio and television? About two years ago the Association secured funds for a survey, which was conducted by the Survey Research Center of the University of Michigan. A questionnaire was prepared, and personal interviews lasting an hour or more were held with 1,919 adults, selected as a representative cross section of the entire population in that manner known only to public opinion pollsters.

This 43-page report is the result. The findings were not unexpected but, if anything, interest in all kinds of science news items and stories is keener and more widespread than had been anticipated. Three-fourths of those interviewed could recall at least one specific science item; 38% said they read *all* the medical news, 28% all the nonmedical science items, in their newspapers. Women prefer medical, men favor nonmedical, stories. The amount of science news read increases with the education of the reader. Some 28% would like more nonmedical science, 30% would like more comics; 8% confused science and science fiction, even when the latter was so labeled (on television). A very small number would delete science news to make room for other things, while 20% would reduce space given to society, crime, and sports, to permit more science coverage. A common complaint was that science reports do not give enough details.

To quote from the conclusions: "Science stories, even of the less widely read non-medical variety . . . have greater reading in depth than Washington political coverage and foreign events. . . . Reporters and script writers, given more training and more time for assignments, would be able to provide more details, greater background, better interpretation, and, it is hoped, higher accuracy."

What has this to do with our Society? For one thing, we have tried to get local publicity for our National Meetings, with but little success. Surely some of our activities, or the background stories of the research which is sponsored, presented, and published, have interest for a segment of the public. Possibly a committee should be formed to study the situation, decide whether we do have news for the public, and, if so, investigate methods of presenting it.

—CVK

How to save 77 years

The boy Galileo sat in the sanctuary of Pisa's great cathedral, observing the movement of a lamp which had been set swinging by a sudden gusty draft. The chain by which it was suspended from the high ceiling was of such a length that the arcs decreased but slowly. Strange thing, though. No matter how far the pendulum swung, its movement consumed the same time. Galileo made a note of that. The year was 1581.

The old man sat at his writing desk, sixty years and a thousand disputes later, writing down a new theory. The regularity of a swinging pendulum might be combined with a spring mechanism to improve the unreliable clocks of that day. So Galileo scribbled on, and did nothing more about it. A number of years after his death Huygens took the notes and invented the pendulum clock. *Seventy-seven years had elapsed since the boy made the observation upon which it was based!*

The creative thinker today still need not have a specific use in mind when, by equation or formula, he branches off from the accepted to the hitherto unknown. The classic invention of this decade, the transistor, evolved in the Bell Telephone Laboratories as scientists sought a deeper understanding of semiconductors. On the other hand, another great invention, the feedback amplifier, came from the acutely creative mind of one Bell engineer faced with a specific problem.

Current Bell Laboratories activities—in such areas as data transmission, radar and submarine cable development—call for the coordinated efforts of all types of thinkers and all types of approaches. One type complements another.

Today, seventy-seven years would not have elapsed between the swinging lamp and the swinging clock pendulum—certainly not at Bell Labs, where ideas, though not rushed, are carefully advanced toward fruitful application in national defense, industry and communications. An important part of this harvest is the efficiency of America's telephone service, unequalled anywhere else in the world.

BELL TELEPHONE LABORATORIES

WORLD CENTER OF COMMUNICATIONS RESEARCH AND DEVELOPMENT

GRACE SILICON

(ultra-high-purity)

"For want of a nail the battle was lost" becomes painfully true when translated to lack of purity in the semi-conductor material you choose for your transistors, diodes or other silicon devices.

The Pechiney process, used in the manufacture of Grace Silicon, is noted for a product with low boron content as well as overall high purity.

May we suggest that whenever top quality silicon is desired—silicon combining both high purity and uniform quality—you get in touch with GRACE ELECTRONIC CHEMICALS, INC., at PLaza 2-7699, 101 N. Charles Street in Baltimore.

GRACE ELECTRONIC CHEMICALS, INC.

101 N. Charles St., Baltimore, Maryland

Subsidiary of W. R. GRACE & CO.

The Flade Potential of Iron Passivated by Various Inorganic Corrosion Inhibitors

Herbert H. Uhlig and Peter F. King[1]

Department of Metallurgy, Massachusetts Institute of Technology, Cambridge, Massachusetts

ABSTRACT

The characteristic potential obtained just before decay of passivity (Flade potential) was measured for iron passivated by ferrates, nitrites, chromates, molybdates, tungstates, conc. HNO_3, and by anodic polarization in H_2SO_4. The Flade potential is linear with pH, of slope 0.059 up to approximately pH 4.5. Above this value up to pH 11.5, the potentials tend to follow an extension of the data in acids in the case of iron passivated by chromates and nitrites, but reach a constant value for iron passivated anodically or by conc. HNO_3. The standard Flade potential (pH = 0) for various passivators is increasingly noble in the order: nitrite (−0.50 v); chromate, ferrate, molybdate (−0.54 v); tungstate (−0.61 v); and anodic polarization or conc. HNO_3 (−0.64 v). The average of these values is in reasonable accord with previously reported values and only small observed deviations from the average indicate that the structure and composition of the passive film on iron is largely independent of the passivation process.

This is explained by a primary passive film consisting essentially of a monolayer of chemisorbed oxygen atoms through gaps of which a layer of O_2 molecules is chemisorbed. The calculated free energy of formation of such a film (−30,000 cal/mole ads. O), the chemical equivalents of passive film substance (0.01 coulomb/cm^2), and the oxidizing capacity (12×10^{-6} equivalents/cm^2) are all consistent with independent data obtained by others for oxygen adsorption on iron, coulometry, and reaction of the passive film with CrO_3^- to form CrO_4^{--}.

The mechanism of passivity, accordingly, is proposed to consist of: (*a*) adsorption of the passivator on the metal or metal oxide surface; (*b*) depolarization of cathodic areas by the passivator accompanied by anodic passivation of residual small areas of exposed metal; the adsorbed oxygen film is formed at anodes by discharge and combination of OH^- at current densities above approximately 17 amp/cm^2 in accord with data of Franck; and (*c*) very slow formation of iron oxides with continual repair of the adsorbed oxygen film by electrochemical action, as described, at pores in the oxide. Oxide formation is accelerated by elevated temperatures and presence of certain anions, e.g., Cl^-.

It is proposed that the greater stability of the passive film formed by some passivators is accounted for by supplementary adsorption of the passivator on the passive film, accompanied by shift of the Flade potential to a less noble value.

In 1911, Flade (1) showed that if iron is passivated in concentrated HNO_3 or by anodic polarization in dilute H_2SO_4, the decay of passivity with time is represented: first, by a steep fall of potential in the active direction; second, by a less steep change lasting for a fraction of a minute to several minutes; and third, by a steep descent to the active value. The value of potential immediately preceding the steep descent was called by Flade the "umschlagspunkt" and by later workers the Flade potential. This critical potential was shown by Flade to be more noble the higher the concentration of acid in which the decay took place, and also that the value at constant pH became more active by about 50 mv as the temperature was decreased from 15° to 0°C. Franck (2) showed that the Flade potential E_F for iron in acid media accurately followed the relation (A.C.S. Sign Convention):

$$E_F(\text{volt}) = -0.58 + 0.058\,\text{pH}$$

suggesting, therefore, a reversible thermodynamic relationship to pH of the activating acid. Rocha and Lennartz (3) measured the Flade potentials for Fe-Cr alloys and Cr in H_2SO_4, their values for which showed a slope of potential plotted with pH of 0.058 for alloys below about 12% Cr and 2 x 0.058 for alloys of higher Cr content. Earlier, Müller and Cupr (4) provided data for potential behavior of Cr which show on plotting vs. pH a slope of 0.058 characteristic for spontaneous activation of Cr in various acids, and 2 x 0.058 for Cr activated by cathodic polarization. Recently Cartledge and Sympson (5) demonstrated that iron passivated by sodium molybdate, tungstate, and chromate or by potassium pertechnetate also exhibits Flade potentials that are linear with pH, of slope 0.058, the average absolute values for which parallel those by Franck for iron passivated in con-

[1] Present address: Dow Chemical Company, Midland, Michigan.

centrated HNO_3 or anodically in H_2SO_4. The present measurements explore Flade potentials for iron passivated by ferrates and nitrites in addition to chromates, molybdates, tungstates, concentrated HNO_3, and by anodic polarization in H_2SO_4. The experimental procedure differs somewhat from that used by Cartledge and Sympson, and the pH range is increased to include the alkaline region.

Experimental Procedure

Electrodes of about 2 cm^2 area were prepared from mild steel. This composition has an advantage over higher purity iron in that passivity is found to be more stable during transfer from the passivating solution to the activating solution. Carbon steels are more readily passivated by concentrated HNO_3 than is pure iron (6), probably because of cementite present as a second phase in the carbon steels which acts as the noble component of a galvanic couple, hastening anodic passivation of the metallic phase (ferrite). For example, coupling of platinum to iron also hastens passivity. Cementite, accordingly, stabilizes passivity probably by allowing galvanic action to continue during transfer of the specimen. Flade showed earlier (1) that carbon steel or electrolytic iron exhibits essentially the same "umschlagspunkt."

The electrode was assembled with a nickel wire silver soldered to a stem machined on the steel specimen, the wire being enclosed by an 8 mm diameter glass tube. A Teflon gasket maintained a water-tight seal between steel and glass tube at one end, with constant contact being effected by means of a screw, nut, and rubber grommet attached to the wire at the other end. The gasket was machined so as to insure against crevices or leakage which if not avoided made it difficult to obtain optimum passivity.

Passivator solutions were made up from reagent grade salts and distilled water in the following concentrations: (*a*) 0.0025*M* and 0.1*M* $NaNO_2$, (*b*) 0.0025*M* K_2CrO_4, (*c*) 0.0025*M* Na_2WO_4, (*d*) 0.0025*M* Na_2MoO_4. In addition, concentrated CP HNO_3 was used, and 0.1% K_2FeO_4 solution prepared according to the method described by Thompson, Ockerman, and Schreyer (7).

Electrodes were passivated by immersion in one of the above solutions for a period of usually several minutes up to 1 hr, or whatever time was required to achieve a stable noble potential. Electrodes were then washed successively in 3 beakers of distilled water, and finally immersed in water adjusted to a known pH by means of HNO_3, H_2SO_4, or NaOH. It made no apparent difference whether HNO_3 or H_2SO_4 was used for adjustment in the lower pH range. The decay of potential vs. time was measured with reference to Ag-AgCl, 0.1*N* KCl electrode using a Na_2SO_4 salt bridge and employing an electronic galvanometer and portable potentiometer. Corrections were not made for liquid junction potentials. Typical decay curves are shown in Fig. 1. The potential obtained just before the abrupt drop was recorded as the Flade potential. Cartledge and Sympson used instead the average value of the potential at the plateau preceding breakdown, but this procedure differs from that first described by Flade. It seems to us more likely that the potential corresponding to the thinnest passive film, i.e., just before the steep decline, represents the equilibrium state between film and solution, and that it is this potential in which we have most interest. In any case, however, the relatively large experimental error in determining the Flade potential makes the particular procedure in this regard of small consequence. This is evident from the relatively good correspondence of our data with those of Cartledge and Sympson.

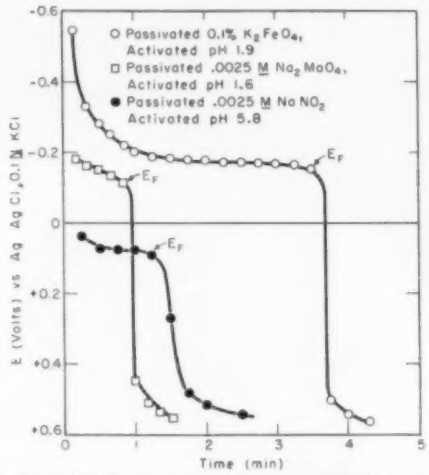

Fig. 1. Potential decay of passive iron and Flade potential E_F

The procedure used by the latter authors for activating their electrodes consisted of adding sodium sulfate to the passivator solution until passivity decayed, without removal of the electrode. Our method was to remove the electrode from the passivator solution, wash it, and then place it in an aqueous solution of known pH. The latter procedure produced a sharper change from the passive to active state, with apparently less experimental scatter.

Results

Flade potentials determined as described above, where each point represents one or more runs, are plotted vs. pH in the acid range up to pH 4.5 in Fig. 2 and 3. Although a single line of slope 0.059 and intercept at −0.57 v for pH = 0 might have been drawn through all the points with maximum deviation of about ±150 mv, the pattern of data favors individual straight lines through points relating to a

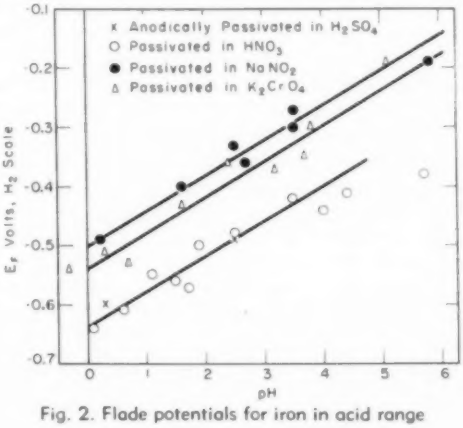

Fig. 2. Flade potentials for iron in acid range

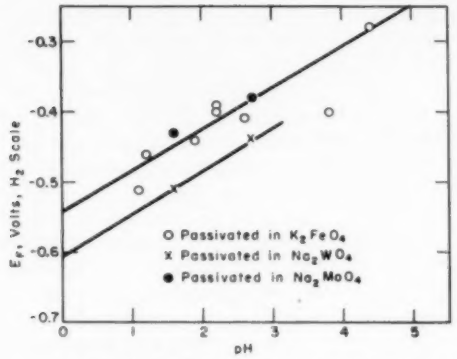

Fig. 3. Flade potentials for iron in acid range

given passivator. All lines so drawn have a slope of approximately 0.059, but the intercepts are increasingly noble in the following order:

Passivator	Approx. intercept, pH = 0 (H_2 scale) v
1. $NaNO_2$	—0.50
2. K_2CrO_4, K_2FeO_4, Na_2MoO_4	—0.54
3. Na_2WO_4	—0.61
4. Anodic polarization in H_2SO_4; conc. HNO_3	—0.64

Measurements in the near-neutral and alkaline range were not as reproducible, and passivator solutions behaved with greater individual differences in comparison to their behavior in acid environments. Data are plotted in Fig. 4.

Potentials of Fig. 2 and 3 agree in slope with those reported by Franck, and by Cartledge and Sympson. The average intercept at pH = 0 of —0.57 v is also close to the average value of their data. However, drawing the best line through individual points for passivation by HNO_3, or anodically in H_2SO_4, produces an intercept of —0.64 v, which is more noble than the average by 0.07 v. This value can be compared with the still more noble standard Flade potential reported by Rocha and Lennartz for iron anodically passivated in H_2SO_4 equal to —0.68 v.

There is a tendency for Flade potentials of iron previously passivated in K_2CrO_4 and then activated in alkaline solutions to follow an extrapolation of data obtained in acid media as indicated by the dotted line of Fig. 4. Two points for $NaNO_2$ fall

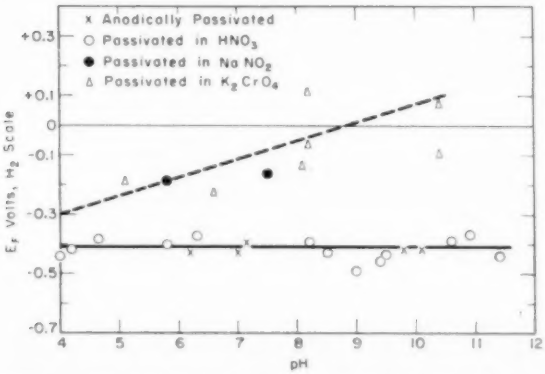

Fig. 4. Flade potentials for iron in near-neutral and alkaline ranges.

within the same region. These data as mentioned earlier are inherently more difficult to reproduce, particularly since breakdown of passivity is sluggish in the alkaline region and sometimes does not occur at all within a reasonable time. More definite conclusions are reached in this region for iron passivated in concentrated HNO_3 or by anodic polarization. Flade potentials lie on a line of zero slope from pH 4 to 11.4, the mean value for which, —0.41 v, is considerably more noble than comparable values for nitrite or chromate.

Discussion

It is significant that all Flade potentials whether in the alkaline or acid region are more noble by several tenths volt than corresponds to potentials for any of the several oxides of iron in equilibrium with metallic iron (8, 9). Hence, the passive film does not appear to be any single known iron oxide. Vetter (9, 10), in order to account for the facts, hypothesized a high potential gradient within a film of Fe_2O_3 overlying a film of Fe_3O_4. Göhr and Lange (11) and Schottky (12) discussed various possible ionic equilibria within the oxide or at the oxide surface.

Göhr and Lange by assuming equilibrium between a layer of γFe_2O_3 overlying a layer of Fe_3O_4, and making certain assumptions regarding the free energy of formation of γFe_2O_3, show that the following reaction may account for the Flade potential:

$$Fe_3O_4 + 1/2\ H_2O \rightarrow 3/2\ \gamma Fe_2O_3 + 2H^+ + 2e$$

Heusler, Weil, and Bonhoeffer (13) concur in a model based on γFe_2O_3 overlying Fe_3O_4. Cartledge (14) suggested an inner oxide, e.g., an abnormal "FeO," in contact with an outer iron oxide in a higher oxidation state to account for the Flade potential.

Some of the assumptions upon which these proposals are made immediately run into difficulty in explaining the Flade potential of Cr (0.2 v) which is also more noble than corresponds to Cr_2O_3 in equilibrium with Cr and for which only one known oxide forms on the metal surface. Furthermore, the total observed thickness of passive film substance, assuming it to be an oxide, is hardly sufficient to accommodate two layers of oxides. For example, the approximate number of chemical equivalents of passive film substance on iron as measured by coulometry (15) or by the oxidizing capacity of the film (16) corresponds to only 0.01 coulomb/cm^2 apparent surface. Assuming that the roughness factor for pickled iron is similar to the measured value of 4 for 18-8 stainless steel pickled in hydrochloric-sulfuric acids (17), the value becomes 0.0025 coulomb/cm^2 absolute surface. This figure becomes larger as iron is polarized to more noble potentials, but becomes smaller as the Flade potential is approached where the passive film reaches minimum thickness consistent with retention of passivity. Hence assuming 0.0025 coulomb/cm^2, the average thickness is 14Å if the passive film is composed of Fe_3O_4, and it can be thinner;[2] if it is γFe_2O_3, the corresponding

[2] Employing for Fe_3O_4 and γFe_2O_3 equivalent weights and densities of 28.9, 26.6, and 5.2, 5.1, respectively. The above thickness of the passive film should not be confused with thicker layers of oxide (25-100Å) residual on iron surfaces after passivity has decayed. This matter is discussed later.

thicknes is 13Å. But the unit cell dimensions of Fe_3O_4 and γFe_2O_3 are 8.3 to 8.4Å (18, 19), the sum of which is 16.7Å. Hence, it does not seem likely that thermodynamic properties of bulk oxides, as employed by Göhr and Lange, for example, can have much significance with respect to properties of the passive film near the Flade potential where the total thickness is less than the sum of the unit cell dimensions. Along the same lines, it is difficult to conceive of a high potential gradient ($>10^6$ v/cm) in a Fe_2O_3 film overlying Fe_3O_4 as hypothesized by Vetter, where the Fe_2O_3 layer has a thickness less than the dimensions of the unit cell. A third difficulty with this duplex oxide film model is that, so far, it has not been able to explain the ability of the passive film to oxidize CrO_2^- to CrO_4^{--} as measured by Uhlig and O'Connor (16).

These difficulties are overcome by the suggestion (20) that the passive film is not an abnormal oxide or double oxide, but is essentially chemisorbed oxygen instead, and that the Flade potential corresponds to the following equilibrium:

$$3H_2O + Fe\ surface \leftrightarrows O \cdot O_2\ (adsorbed\ on\ Fe) + 6H^+ + 6e \qquad [1]$$

The standard potential for this reaction (pH = 0) is −0.58 v according to Franck's data or −0.64 v according to Fig. 2. The structure $O \cdot O_2$ (ads. on Fe) signifies a complete monolayer of chemisorbed oxygen atoms through gaps of which a further layer of O_2 molecules is chemisorbed in accord with the suggested structure of chemisorbed oxygen on tungsten (21). This structure is consistent with the observed approximate 0.01 coulomb/cm² apparent surface of passive film substance. At the Flade potential, as mentioned earlier, the film is somewhat thinner than corresponds to $O \cdot O_2$, and may more nearly correspond to a film of atomic oxygen. For passive potentials more noble than the Flade potential, the film probably contains not only chemisorbed oxygen additional to an atomic monolayer, but also adsorbed OH, the amount depending on the extent to which iron is polarized anodically by the passivation process.

On breakdown of passivity in accord with:

$$O \cdot O_2\ (ads.\ on\ Fe) + 2Fe + 3H_2O \rightarrow Fe(OH)_2$$

a residual film of Fe_2O_3, 60A thick is accounted for, in reasonable agreement with measurements of Schwarz (22) and Gulbransen (23). It is the decomposed passive film which was observed by electron diffraction measurements of Mayne and Pryor (24) which they reported as γFe_2O_3.

A major support for chemisorbed oxygen as the composition of the passive film comes from thermodynamic data. From Tompkin's measurements (25) on the direct chemisorption of gaseous oxygen on iron, $\Delta H^\circ = -75{,}000$ cal/mole O_2. The standard entropy of adsorption ΔS° is approximately equal to −46.2 e.u. (26) with a standard state of half surface coverage. Hence, since ΔH° is not sensitive to the extent of surface coverage (27) we can use the relation ΔG°, the free energy of adsorption, $= \Delta H^\circ - T\Delta S^\circ = -61{,}300$ cal/mole oxygen adsorbed. Accordingly:

$$3/2\ O_2 + Fe\ surface \rightarrow O \cdot O_2\ (ads.\ on\ Fe)$$
$$\Delta G^\circ = -3/2 \times 61{,}300\ cal \qquad [2]$$
$$3H_2O \rightarrow 6H^+ + 3/2\ O_2 + 6e^-$$
$$\Delta G^\circ = 170{,}000\ cal\ (28) \qquad [3]$$

Adding [2] and [3]:

$$3H_2O + Fe\ surface \rightarrow O \cdot O_2\ (ads.\ on\ Fe) + 6H^+ + 6e^-$$
$$\Delta G^\circ = +78{,}000\ cal \qquad [4]$$

The corresponding standard potential E° equal to $-\Delta G^\circ/6F$ is −0.56 v. This value agrees within reasonable limits with the measured values of −0.58, −0.64, and −0.68 v quoted previously.

Bonhoeffer (29) and his co-workers showed that passivation of iron in concentrated HNO_3 proceeds by an electrochemical reaction in which nitrous acid, HNO_2, acts as a strong cathodic depolarizer. The major part of the iron surface serves as cathode resulting in very high current densities reaching approximately 17 amp/cm² (2) at small residual anodic surfaces. These high anodic current densities produce the passive film, which in turn becomes the seat of the continuing cathodic reaction, thereby favoring spread of passivity over all the surface.

The nitrous acid resulting from reduction of HNO_3 plays a very important part as depolarizer, therefore, in passivation by nitric acid. It is proposed herewith that the passivators reported in this paper act also by depolarization to produce the passive state, and that the resulting composition and structure of the passive film are basically the same in all cases. The similarity of Flade potentials makes this conclusion plausible. Chromates, for example, first adsorb on the iron surface, and on iron oxides if present, and as such act as cathodic depolarizers. Since adsorption and depolarization occur over the entire surface, current densities at gaps in the adsorbed film easily reach the order of 17 amp/cm². The ultimate passive film, which is essentially chemisorbed oxygen resulting from discharge and combination of OH^-, is formed by anodic polarizaton. It is formed at a rate measurably slower than for nitric acid presumably because of the slower rate of cathodic reduction of chromates as compared with HNO_2.[2] This slower re-

[2] Uhlig and O'Connor (16) proposed that ferrates or similar higher valence iron compounds form when iron reacts with concentrated HNO_3 and that such compounds adsorbed on iron probably constitute the passive film. They calculated the amount of adsorbed ferrate on the iron surface from the ability of the passive film to oxidize CrO_2^- to CrO_4^{--} in NaOH solution.

It now appears from the foregoing data that it is not necessary to assume formation of ferrates as such as source of the observed oxidizing property of the film. Instead, adsorbed oxygen expressed as $O \cdot O_2$ (ads. on Fe) can also account for the facts. This adsorbed oxygen is related to the ferrate structure in that strongly alkaline media convert the adsorbed film continuously to ferrates in accord with the reaction:

$$O \cdot O_2\ (ads.\ on\ Fe) + Fe + 2NaOH \rightarrow Na_2FeO_4 + H_2O + Fe\ surface$$

as is observed when iron is polarized anodically in concentrated NaOH.

In dilute NaOH, ferrates act as passivators in accord with:

$$2Na_2FeO_4 + 5H_2O + Fe\ surface \rightarrow O \cdot O_2\ (ads.\ on\ Fe) + 2Fe(OH)_2 + 4NaOH$$

Iron immersed in K_2FeO_4, therefore, preforms the passive film and no initial reaction occurs on subsequent immersion of iron into conc. HNO_3, a reaction that is necessary otherwise to form a minimum concentration of HNO_2 to serve as depolarizer (16).

The herein-described mechanism of passivation by chromates (and similar passivators) modifies the earlier proposal by one of us that the primary passive film consists of chromate adsorbed directly on the metal. From present data, formation of such a film more likely is the first stage of passivation. This is followed by formation of the anodically produced oxygen film, which is actually the primary passive film. Iron oxides form more slowly as a third stage process, but they contribute relatively less to corrosion resistance compared to the adsorbed oxygen film which continues at the base of pores in such oxide layers so long as chromates are present in solution. Elevated temperatures and certain anions (e.g., Cl^-) accelerate formation of iron oxide and accompanying reduction of chromate.

duction can account for the fact that it requires only seconds for passivation of iron in conc. HNO_3 but about ½ to 1 hr for the passive film to form completely in chromates as indicated by potential measurements (30), and from experiments on the effect of pre-immersion of iron in chromates on the rate of reaction with concentrated HNO_3 (31).[4]

The above described reaction of iron with dichromate can proceed as follows:

$$Cr_2O_7^{--} + 14H^+ + 6e^- \rightarrow 2Cr^{+++} + 7H_2O \qquad E^\circ = 1.33 \text{ v} \qquad [5]$$

$$3H_2O + \text{Fe surface} \rightarrow 6e^- + 6H^+ + O\cdot O_2 \text{ (ads. on Fe)} \qquad E^\circ = -0.54 \text{ v} \qquad [6]$$

Adding [5] and [6]:

$$Cr_2O_7^{--} + 8H^+ + \text{Fe surface} \rightarrow 2Cr^{+++} + 4H_2O + O\cdot O_2 \text{ (ads. on Fe)} \qquad E^\circ = 0.79 \text{ v} \qquad [7]$$

The positive value of emf for reaction [7] indicates that the reaction can go spontaneously; in other words, dichromate can produce the chemisorbed passive film by anodic polarization in the same way as can conc. HNO_3 or direct anodic polarization in H_2SO_4. It is reasonable that a similar reaction should occur in alkaline media forming perhaps basic chromic chromate (32) as end product, but free energy data for this reaction are not available.

According to reaction [7], each mole $Cr_2O_7^{--}$ which is reduced to form the passive film forms two moles Cr^{+++}. If Cr^{+++} so produced is retained on the metal surface, perhaps as hydrated Cr_2O_3 or adsorbed as the ion, the amount so formed is an indication of the number of equivalents of passive film substance per unit surface. Geary (33) found 3×10^{16} Cr atoms/cm² or 5×10^{-8} g-atom/cm² retained on an iron surface after passivation by dichromate using radioactive Cr as tracer. In this experiment, the iron surface was hydrogen-reduced at 1000°C, then exposed to deaerated 0.0005*M* $Cr_2O_7^{--}$ solution of pH 1.9 for 2 to 17.5 hr avoiding contact with air. The iron surface was washed in distilled water before counting. The same approximate amount of residual Cr was reported by Brasher and Stove (34), by Powers and Hackerman (35), and by Cohen and Beck (36) for air-exposed iron. This quantity of chromium, calculated in accord with conditions of reaction [7], corresponds to 2.5×10^{-8} mole $O\cdot O_2$ (ads. on Fe)/cm²[5] or 15×10^{-8} equivalents of passive film substance per cm². This value is in good agreement with the maximum amount of passive film substance on iron (2×10^{-8} mole $O\cdot O_2$ ads. on Fe/cm² or 12×10^{-8} equivalents of passive film substance/cm²) found by O'Connor (16) from the oxidizing capacity of the passive film.[6] It is also in accord with Weil's value of about 0.01 coulomb/cm² passive film substance as determined by coulometry ($15 \times 10^{-8} \times 96{,}500 = 0.014$ coulomb).

It is probable that most other passivators operate by a mechanism similar to that outlined above for chromates. This mechanism explains why sulfates or perchlorates are not passivators even though they have the XO_4^{n-} structure. Ions of this kind either do not reduce, or do so too slowly to fulfill the requirements of a cathodic depolarizer. On the other hand, oxidizing substances such as chlorides for which the minimum current density for anodic passivation is very high or infinite, also do not meet the requirements of a passivator. Hypochlorous acid and ferric chloride are in this category. Alkaline inhibitors such as Na_3PO_4, Na_2CO_3, and NaOH act as passivators only in the presence of dissolved oxygen (37, 38) and hence the cathodic reduction of these substances is not required for passivation. Instead, most alkaline substances probably displace adsorbed H, the latter tending to form whenever iron is exposed to an aqueous environment, and favor adsorption of OH^- together with oxygen on the metal surface. Hence for these substances an adsorbed oxygen-hydroxyl ion film can form directly without the necessity of anodic polarization. This same situation applies to Cr and the stainless steels which become spontaneously passive on exposure to air.

Dissolved oxygen is also required for passivation of iron by molybdates and tungstates (38). A possible explanation is that oxygen as well as the passivator adsorbs on the metal thereby increasing cathodic and decreasing anodic areas. This extension of cathodic sites and limitation of anodic sites favors attainment of the critical current density necessary for anodic passivation. Oxygen may be necessary, in other words, because molydates and tungstates are not sufficiently good cathodic depolarizers on a clean iron surface, but they become effective if the galvanic current accompanying their cathodic reduction is restricted to smaller anodic areas as when oxygen is present on the surface.

With chromates, dissolved oxygen is not necessary for passivation, but oxygen does increase the rate of passivation (31) in accord with the mechanism just described.

The passive film formed by pertechnetates may also consist essentially of chemisorbed oxygen. From data by Cartledge and Smith (39) for the reaction:

$$TcO_2(c) + 2H_2O \rightarrow TcO_4^-(aq) + 4H^+ + 3e \qquad E^\circ = -0.738 \text{ v} \qquad [8]$$

it is concluded that the following reaction is spontaneous:

$$2TcO_4^- + 2H^+ + \text{Fe surface} \rightarrow O\cdot O_2 \text{ (ads. on Fe)} + H_2O + 2TcO_2 \qquad E^\circ = +0.20 \text{ v} \qquad [9]$$

Radioactive counts by Cartledge (40) on an iron surface passivated by TcO_4^- corresponding to amounts of Tc much less than 4×10^{-8} g-atom/cm² suggests that reduced TcO_4^-, whatever its composition, enters solution rather than precipitating or adsorbing on the metal surface, in contrast to the situation for

[4] When the passive film is previously formed by immersion of iron in O_2-saturated 0.1% $K_2Cr_2O_7$ for more than but not less than ½ hr, no measurable iron reacts on subsequent immersion in concentrated HNO_3, whereas for air-exposed iron, omitting chromate immersion, about 0.04 mg/cm² (16) reacts before the iron-HNO_3 reaction subsides. In deaerated 0.1% $K_2Cr_2O_7$, the time to reach optimum passivity is longer (approx. 2 hr).

[5] This calculated amount should be reduced by the amount of chromate irreversibly adsorbed on the passive film itself. Since a close-packed monolayer of CrO_4^{--} (diam. = 5.4Å) on a surface of roughness factor = 3 amounts to only 0.2×10^{-8} mole/cm², the correction is small.

[6] The reaction studied by O'Connor is assumed (20) to be the following:

$$O\cdot O_2 \text{ (ads. on Fe)} + Fe + OH^- + CrO_2^- + H_2O \rightarrow Fe(OH)_3 + CrO_4^{--}$$

$$\Delta G^\circ = -33{,}000 \text{ cal}$$

He found that a maximum of 2×10^{-8} mole CrO_4^{--} was formed per cm² of passive iron, which was reported as equivalent to 2×10^{-8} mole ferrate/cm² instead of 2×10^{-8} mole $O\cdot O_2$ (ads. on Fe)/cm².

chromates. There is also the possibility that a monolayer or partial monolayer of adsorbed TcO_4^- can in itself satisfy surface affinities, as does CO adsorbed on 18-8 in HCl, without reduction. This seems less likely in view of the fact that Cl^- or SO_4^{--} can and do stimulate reduction of TcO_4^- by metallic iron (41), similar to accelerated reduction of other passivators in presence of these ions.

The slightly more active standard Flade potentials for iron passivated by nitrites and chromates as compared with concentrated HNO_3 or anodic passivation in H_2SO_4 (Fig. 2) is evidence of a slightly greater stability of the passive film formed by the first two substances. This stability is also evident from the usually longer time it requires for passivity to break down using chromates as compared with the less stable passive film formed by HNO_3 or by anodic polarization. The greater stability can be accounted for by adsorption of the passivator substance itself, subsequent to the passivation process, directly on the chemisorbed oxygen film, thereby reducing the over-all free energy of the system. Adsorption of passivator on an underlying oxide layer was proposed by Powers and Hackerman (35, 42) based on contact potential measurements, where, however, an adsorbed oxygen layer would also fit the facts. For example, the following adsorption can occur:

$$O \cdot O_2 \text{ (ads. on Fe)} + H_2CrO_4 \rightarrow$$

$$O \cdot O_2 \cdot H \cdot H \cdot CrO_4 \text{ (ads. on Fe)}$$

the free energy change for which is calculated to be −13,700 cal based on −0.54 v for the standard Flade potential for iron passivated by chromates compared to −0.64 v in concentrated HNO_3. If there is supplementary adsorption of Fe^{+++} or $Fe(NO_3)_3$ on the passive film in HNO_3, as seems likely, the calculated ΔG° is for displacement of such an adsorbate by H_2CrO_4. In other words, the interaction between passivator and passive film on which passivator is adsorbed can account for slight variations in Flade potential and for the observed differences in stability of the passive film. On this basis, nitrites adsorb on the passive film more strongly than do chromates, ferrates, and molybdates (Fig. 2, 3), and the latter in turn more strongly than tungstates.

Reasons for the constant Flade potential in the region of pH 4 to 11.5 when iron is passivated anodically or by HNO_3 probably depend on change in mechanism of passive film breakdown for less acid environments. It is known that corrosion of iron in HNO_3 or H_2SO_4 continues even when it is passive, hence, it is not unlikely that the surface pH rises and that an insoluble basic ferric salt or ferric hydroxide forms as end product of passive decay in solutions of pH as low as 4 to 5.

Since considerable ferric nitrate or ferric sulfate forms at the iron surface just prior to passivity, we can assume with justification that Fe^{+++} or $Fe(NO_3)_3$ adsorbs on the passive film. Accordingly a plausible reaction accounting for breakdown of passivity, which is independent of pH, is the following:

$$2Fe^{+++} \cdot O \cdot O_2 \text{ (ads. on Fe)} + 3H_2O \rightarrow 2Fe(OH)_3 - 6e$$

$$\Delta G^\circ = -75{,}440 \text{ cal}$$

The standard free energy change for this reaction is based on standard free energies of formation of $Fe(OH)_3$(s), Fe^{+++}(aq), $O \cdot O_2$ (ads. on Fe) and H_2O(l), equal to −166,000, −2,530, −81,500,[†] and −56,690 cal per mole, respectively, discounting the small free energy of adsorption of Fe^{+++} on the passive film. The standard potential is accordingly 0.54 v, or −0.54 v for the same reaction written as an oxidation step. This is to be compared with the observed potential of −0.41 v (Fig. 4). The difference of 0.13 v is probably due, other than to experimental error, to free energy of adsorption of Fe^{+++} not included in the calculation, and possibly to reaction products differing in composition from $Fe(OH)_3$. The above reaction does not go when iron is passivated by chromates and similar passivators because soluble ferric salts are not formed in high concentration, and hence are not adsorbed on the passive film. Accordingly, for such passivators breakdown of passivity in alkalies follows a course not much different from that in acids, as is observed.

Acknowledgment

The authors are grateful for support of this research by the Office of Naval Research.

Manuscript received March 7, 1958. This paper was prepared for delivery before the Ottawa Meeting, Sept. 28-Oct. 2, 1958.

Any discussion of this paper will appear in a Discussion Section to be published in the December 1959 JOURNAL.

REFERENCES

1. F. Flade, *Z. physik. Chem.*, **76**, 513 (1911).
2. U. F. Franck, *Z. Naturforsch.*, **4a**, 378 (1949).
3. H. J. Rocha and G. Lennartz, *Arch. Eisenhüttenw.*, **26**, 117 (1955).
4. E. Müller and V. Cupr., *Z. Elektrochem.*, **43**, 42 (1937).
5. G. Cartledge and R. Sympson, *J. Phys. Chem.*, **61**, 973 (1957).
6. "Corrosion Handbook," p. 140, edited by H. H. Uhlig, John Wiley & Sons, Inc., New York (1948).
7. G. Thompson, L. Ockerman, and J. Schreyer, *J. Am. Chem. Soc.*, **73**, 1379 (1951).
8. H. Beinert and K. Bonhoeffer, *Z. Elektrochem.*, **47**, 536 (1941).
9. K. Vetter, "International Symposium on Passivity," Heiligenberg, West Germany, September 1957.
10. K. Vetter, *Z. Elektrochem.*, **58**, 230 (1954).
11. H. Göhr and E. Lange, *Naturwiss.*, **43**, 12 (1956); *Z. Elektrochem.*, **61**, 1291 (1957).
12. W. Schottky, "Halbleiterprobleme," II, p. 233, F. Vieweg u. Sohn., Braunschweig (1955).
13. K. Heusler, K. Weil, and K. Bonhoeffer, *Z. physik. Chem., N. F.*, **15**, 149 (1958).
14. G. Cartledge, *J. Phys. Chem.*, **60**, 1571 (1956).
15. K. Weil, *Z. Elektrochem.*, **59**, 11 (1955).
16. H. Uhlig and T. O'Connor, *This Journal*, **102**, 562 (1955).
17. T. O'Connor and H. Uhlig, *J. Phys. Chem.*, **61**, 402 (1957).
18. L. Welo and O. Baudisch, *Phil. Mag.*, **50**, 399 (1925).
19. A. Claassen, *Proc. Phys. Soc.*, **38**, 482 (1926).
20. H. H. Uhlig, "International Symposium on Passivity," Heiligenberg, West Germany, September 1957.
21. J. Becker, *Ann. N. Y. Acad. Sci.*, **58**, 723 (1954).
22. W. Schwarz, *Z. Elektrochem.*, **59**, 11 (1955).
23. E. Gulbransen, *Trans. Electrochem. Soc.*, **82**, 375 (1942).
24. J. Mayne and M. Pryor, *J. Chem. Soc., (London)*, **1949**, 1831.

[†] Per 3/2 mole O_2.

25. Quoted by B. Trapnell, "Chemisorption," p. 215, Academic Press, New York (1955).
26. Ref. (25), p. 212. Approximated from the value for N_2 chemisorbed on Fe. The value for oxygen has not been reported.
27. Ref. (25), p. 213.
28. "Oxidation Potentials," W. M. Latimer, Prentice-Hall, Inc., New York (1952).
29. K. F. Bonhoeffer, *Z. Metallkunde*, **44**, 77 (1953).
30. R. M. Burns, *J. Appl. Phys.*, **8**, 400 (1937).
31. H. Uhlig and H. Gatos, *This Journal*, **99**, 250 (1952).
32. Ref. (28), p. 249.
33. H. Uhlig and A. Geary, *This Journal*, **101**, 221 (1954).
34. D. Brasher and E. Stove, *Chem. & Ind.*, **1952**, No. 8, 171.
35. R. Powers and N. Hackerman, *This Journal*, **100**, 314 (1953).
36. M. Cohen and A. Beck, "International Symposium on Passivity," Heiligenberg, West Germany, September 1957.
37. H. H. Uhlig, *Metaux & Corrosion*, **23**, 204 (1947).
38. M. Pryor and M. Cohen, *This Journal*, **100**, 203 (1953).
39. G. Cartledge and W. Smith, Jr., *J. Phys. Chem.*, **59**, 1111 (1955).
40. G. Cartledge, *ibid.*, **59**, 979 (1955).
41. G. Cartledge, *Corrosion*, **11**, 355t (1955); *J. Phys. Chem.*, **60**, 28 (1956).
42. N. Hackerman and R. Powers, *J. Phys. Chem.*, **57**, 139 (1953).

Some Observations on the Mechanism of Inhibition

A. C. Makrides

Metals Research Laboratories, Electro Metallurgical Company, Division of Union Carbide Corporation, Niagara Falls, New York

ABSTRACT

Thiocyanic and citric acids are efficient inhibitors of dissolution of iron in dilute HNO_3 solutions. It is concluded that inhibition does not generally involve "poisoning" the combination step in the hydrogen evolution reaction. Some observations on the kinetics of dissolution of iron in dilute HNO_3 solutions are also presented.

There is little doubt that organic compounds which inhibit dissolution of metals in acids adsorb at the metal-solution interface. There are a number of ways in which the resultant adsorbed film could modify the kinetics of the dissolution process. It has been suggested (1) that adsorbed inhibitor on iron deactivates "active centers" at which the reaction

$$H_{ads} + H_{ads} \rightarrow H_2(g) \qquad [1]$$

between adsorbed hydrogen atoms takes place. According to this view, inhibition of iron dissolution is closely associated with occurrence of reaction [1].

Polarization studies with some organic compounds led Elze and Fischer (2) to the conclusion that inhibition of hydrogen discharge governs the process of dissolution in the presence of inhibitors. The particular inhibitors used by these authors had a negligible effect in the presence of an oxidizing agent (Fe^{+++}). From this result, it was maintained that inhibitors function only if reaction [1] above, which according to Elze and Fischer (2) is sensitive to inhibitors, is included in the over-all dissolution process.

It was pointed out (3, 4) that work of King and Hillner (5) indicates that some organic compounds function as inhibitors in strongly oxidizing solutions where reaction [1] is unimportant. However, the relevance of the work of King and Hillner (5) to the elucidation of the mechanism of inhibitor action was questioned on the ground that the observed decrease in dissolution rate may have been due to pH changes of the bulk solution (6).

Makrides and Hackerman (4, 7) found that butyl thiourea inhibits dissolution of iron in $FeCl_3$-HCl solutions. Any bulk effect of butyl thiourea at the concentrations employed was negligible. It was of interest, therefore, to establish whether other compounds function as inhibitors in oxidizing solutions where reaction [1] may be neglected.

Experimental

The rotating cylinder technique was used (8). Armco iron cylinders (99.92-99.96% iron content), 0.94 cm in diameter and about 8 cm long, were rotated at 250 cm/sec linear speed in 400 ml of solution. The cylinders were polished with 2/0 emery paper and were degreased with CCl_4. Only the lateral surface was exposed to solution, the top and bottom parts as well as the edges being covered with paraffin. The exposed area was measured for each cylinder.

Nitric acid solutions of desired concentration were made from stock by dilution. The HNO_3 concentration was determined by titration. Water was doubly distilled, one distillation being from dilute, alkaline $KMnO_4$.

Stock solutions containing HSCN and citric acid were prepared by dissolving a weighed quantity of the corresponding potassium salt in an equivalent quantity of HNO_3 solution. Desired inhibitor concentrations were obtained by diluting stock with HNO_3 solutions of selected concentration. With this procedure, the hydrogen ion concentration in solutions containing inhibitors was at least equal, and generally greater, than in corresponding solutions without inhibitors.

All solutions were thermostated to within $\pm 0.1°C$.

Results and Discussion

Solutions similar to the ones employed by King and Hillner (6) were used originally. First order rate constants were calculated from

$$k = \frac{2.30\,V_s}{At} \log \frac{X_\infty}{X_\infty - X} \qquad [2]$$

Here, V_s is the volume of solution, A the projected surface area, X the weight loss in time t (300 sec), and X_∞ the calculated weight loss for $t \to \infty$. Table I shows that k varied, with no apparent trend, over the concentration range examined. If the (Cl^-) concentration is varied, while that of (H^+) is constant, k at first is independent of C_{Cl^-}, but shows a maximum at larger (Cl^-) concentrations (Table II). Tables I and II indicate that the rate in solutions containing (Cl^-) depends both on total concentration and on the ratio of KNO_3 to HCl concentration.

These results are in general agreement with the work of Abramson and King (9) who have shown that dissolution of iron in KNO_3-HCl solutions is complex. Since there is no apparent reason for using such mixtures, rather than HNO_3 alone, the procedure of King and Hillner (6) was modified to exclude chloride ion.

Dissolution rates in HNO_3 are given Tables III through VI. The results may be summarized as follows: (*a*) approximately two moles of hydrogen ion are consumed per mole of iron dissolved; (*b*) the rate constant decreases regularly with increasing HNO_3 concentration; (*c*) addition of KNO_3 increases the dissolution rate; with $C_{NO_3^-} \sim 2C_{H^+}$, the rate constant increased by about 15% (Table V); (*d*) addition of (H^+) increases the dissolution rate considerably more than addition of (NO_3^-); with $C_{H^+} \sim 2C_{NO_3^-}$, the rate increased by a factor of about 2 (Table VI).

Observations (*a*), (*c*), and (*d*) suggest that in HNO_3 solutions diffusion of (H^+) largely determines the rate at which dissolution takes place. The (H^+) concentration at the interface, therefore, may be considered negligible. The (NO_3^-) concentration at the interface is also less than in the bulk, but the decrease probably does not exceed 20-25%. While it is not possible to state whether (H^+) is consumed by reaction with reduction products of (NO_3^-) or by reaction with (NO_3^-) after discharge, it may be concluded, in view of the excess of (NO_3^-) over (H^+) at the interface,[1] that the concentration of adsorbed atomic hydrogen is negligible. Under these conditions, the contribution of reaction [1] to the overall rate may be neglected.

The decrease of the specific rate constant with increasing HNO_3 concentration is probably caused, at least in part, by changes of the diffusion coefficient. Since the reaction is under diffusion control,

$$k = D/\delta$$

where δ, the equivalent thickness of the boundary layer, may be assumed independent of concentration (10, 11); D, however, is a function of concentration. Any simple correction for this dependence is not possible here, particularly in view of the unknown

[1] Electrical neutrality is, of course, preserved by an equivalent amount of ferrous ion.

Table I

$T = 30° \pm 0.1°C$; $V = 250$ cm/sec

Concentration, M	k, cm/sec*
0.030 KNO_3 + 0.0124 HCl	0.0387
0.060 KNO_3 + 0.0248 HCl	0.0344
0.090 KNO_3 + 0.0372 HCl	0.0321
0.120 KNO_3 + 0.0496 HCl	0.0404

* King and Hillner (5) find $k = 0.0351$ for 0.06 KNO_3 + 0.02 HCl at the same (250 cm/sec) linear speed.

Table II

$T = 30° \pm 0.1°C$; $V = 250$ cm/sec

Concentration, M	k, cm/sec
0.0231 HNO_3	0.0400
0.0231 HNO_3 + 0.000125 KCl	0.0406
0.0231 HNO_3 + 0.00250 KCl	0.0412
0.0231 HNO_3 + 0.00375 KCl	0.0409
0.0231 HNO_3 + 0.00500 KCl	0.0413
0.0231 HNO_3 + 0.0113 KCl	0.0430
0.0231 HNO_3 + 0.0226 KCl	0.0426
0.0231 HNO_3 + 0.0452 KCl	0.0410

Table III

$T = 30° \pm 0.1°C$; $t = 300$ sec

HNO_3 concentration, M	Wt. loss, mg	Wt. loss from (H^+) consumption, mg*
0.0357	122	120
0.0462	171	162
0.0925	288	260

* Calculated from decrease in (H^+), as determined by titration, assuming $2H^+$ are consumed per mole iron dissolved.

Table IV

$T = 30° \pm 0.1°C$; $V = 250$ cm/sec

HNO_3 concentration, M	k, cm/sec
0.0126	0.0422
0.0231	0.0400
0.0357	0.0384
0.0462	0.0356
0.0925	0.0318

Table V

$T = 30° \pm 0.1°C$; $t = 300$ sec

Concentration, M	Wt. loss, mg/10 cm²	k, cm/sec
0.0231 HNO_3	62.0	0.0400
0.0231 HNO_3 + 0.0020 KNO_3	66.0	0.0430
0.0231 HNO_3 + 0.0040 KNO_3	67.0	0.0436
0.0231 HNO_3 + 0.0075 KNO_3	65.5	0.0426
0.0231 HNO_3 + 0.0125 KNO_3	68.5	0.0452
0.0231 HNO_3 + 0.0250 KNO_3	69.5	0.0465

Table VI

$T = 30° \pm 0.1°C$; $t = 300$ sec

Concentration, M	Wt. loss, mg/10 cm²*
0.0231 HNO_3	62.0
0.0231 HNO_3 + 0.0077 $HClO_4$	81.0
0.0231 HNO_3 + 0.0128 $HClO_4$	88.5
0.0231 HNO_3 + 0.0256 $HClO_4$	105.5

* Weight loss in $HClO_4$ solutions only was 3-3.5 mg.

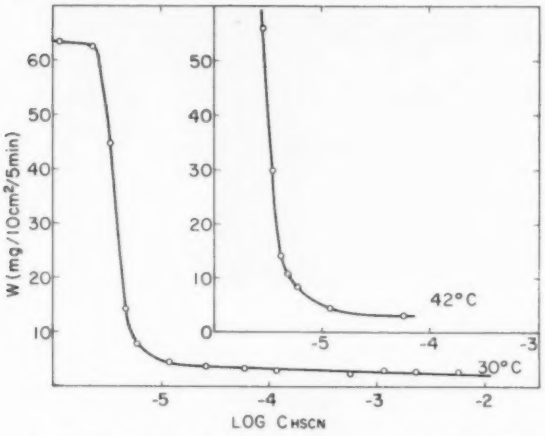

Fig. 1. Rate of dissolution in 0.0231M HNO_3 solutions containing HSCN.

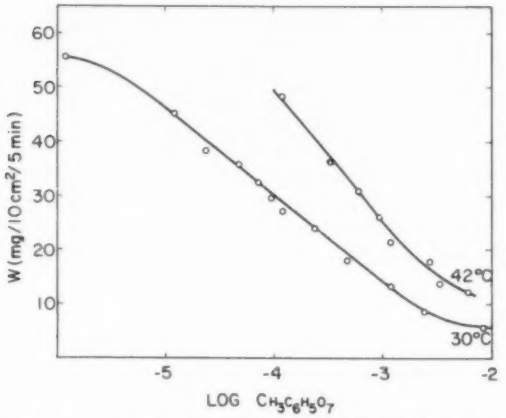

Fig. 2. Rate of dissolution in 0.0231M HNO_3 solutions containing citric acid.

effect of ferrous (or ferric) ions on the activity coefficient of (H^+). There is also the possibility that lack of constancy of k denotes that first order kinetics do not adequately describe the dissolution process in HNO_3 solutions.

Inhibition

Thiocyanic and citric acids were used as inhibitors. HSCN is known to be a good inhibitor in nonoxidizing H_2SO_4 solutions (12), while $H_3C_6H_5O_7$ appeared to be a promising inhibitor according to King and Hillner (6). Runs were made at 30° and 42°C. Results are given in Fig. 1 and 2. In both cases, the solution was 0.0231M HNO_3.

Both compounds proved to be efficient inhibitors. HSCN in particular shows essentially complete inhibition at concentrations above 5×10^{-6} to 1×10^{-5}M. Runs for periods up to 30 min showed that at least half the weight loss observed in this concentration range occurred while the system achieved a steady state. If, as commonly assumed, inhibitors function by adsorption, at small concentrations an appreciable amount of HSCN is removed from solution. At small times, therefore, the solution next to the surface may be depleted and the rate at which adsorption takes place is then limited by the rate of HSCN transport to the interface. From the weight loss-time curve in 5×10^{-6}M HSCN solutions, it was estimated that the time required for adsorption to come to completion was of the order of 1 min.

Of the two compounds used, HSCN is the better inhibitor. It may be inferred that it is adsorbed more firmly. This is borne out by the essentially negligible change in rate observed on raising the temperature to 42°C. The same temperature increase, however, shifts the curve for citric acid toward higher dissolution rates.

It is perhaps worth while to point out again that in neither case can the observed decrease in rate be attributed to a decrease in hydrogen ion concentration of the bulk solution.

Conclusions

Inhibition of iron dissolution under conditions where reaction [1] is negligible by compounds which also inhibit dissolution of iron in nonoxidizing acids suggests that the mechanism of inhibition does not involve, generally, poisoning of the combination reaction between adsorbed hydrogen atoms.

Manuscript received July 17, 1958.

Any discussion of this paper will appear in a Discussion Section to be published in the December 1959 JOURNAL.

REFERENCES

1. J. O'M. Bockris and B. E. Conway, *J. Phys. Coll. Chem.*, **53**, 527 (1949).
2. J. Elze and F. Fischer, *This Journal*, **99**, 259 (1952).
3. A. C. Makrides, *ibid.*, **101**, 635 (1954).
4. A. C. Makrides and N. Hackerman, *J. Phys. Chem.*, **59**, 707 (1955).
5. C. V. King and E. Hillner, *This Journal*, **101**, 79 (1954).
6. C. V. King and E. Hillner, *ibid.*, **101**, 635 (1954).
7. A. C. Makrides and N. Hackerman, *Ind. Eng. Chem.*, **47**, 1773 (1955).
8. A. C. Makrides, N. M. Komodromos, and N. Hackerman, *This Journal*, **102**, 363 (1955); A. C. Makrides and N. Hackerman, *ibid.*, **105**, 156 (1958).
9. M. B. Abramson and C. V. King, *J. Am. Chem. Soc.*, **61**, 2290 (1939).
10. J. N. Agar, *Disc. Faraday Soc.*, **1**, 26 (1947).
11. C. V. King, *J. Am. Chem. Soc.*, **57**, 828 (1935).
12. L. Cavallaro and G. Bolognesi, *Atti Accad. Sci. Ferrara*, **24**, No. 1 (1946-47).

Oxidation of Titanium, Zirconium, and Hafnium

G. R. Wallwork and A. E. Jenkins

School of Metallurgy, New South Wales University of Technology, Sydney, Australia

ABSTRACT

A metallographic study of the high-temperature oxidation of titanium, zirconium, and hafnium has shown that alterations in the rate equations relating to such processes may be associated with the establishment of oxygen diffusion gradients in the surface layers of the metal. It has been shown that these diffusion gradients in the metal extend in depth during an initial period in which the total rate of oxidation is given by the familiar parabolic equation. Subsequent changes in oxidation behavior have been related to observed alterations in the form of these gradients.

The high-temperature oxidation of the metals titanium, zirconium, and hafnium has been investigated on many occasions over the last decade. However, there is still much uncertainty concerning the oxidation characteristics of these metals, and the aim of this investigation has been to extend the available experimental results, most of which have been obtained from gravimetric or volumetric oxidation rate measurements.

Earlier work on the oxidation of Ti and Zr (1-3) has shown that, following an initial period, the parabolic rate equations become linear with further passage of time. Smeltzer and Simnad (4) investigated the oxidation of Hf and reported that logarithmic, parabolic, and linear equations describe the oxidation of this metal over the temperature range 350°-1200°C.

The structure of scales formed on Ti in air has been described by Morton and Baldwin (5) and in air and oxygen by Kinna and Knorr (6), and the scales formed on pure Zr in oxygen in the temperature range 500°-700°C have been described by Belle and Mallett (7).

Previous work by one of the authors (1, 2) has indicated the need for a more detailed metallographic examination of the oxidized specimens, and this has now been carried out subsequent to the development of a suitable metallographic technique.

Experimental Procedure

Metal specimens (1.0 x 0.5 x 0.1 cm) prepared as described by Jenkins (1) were oxidized in pure oxygen produced by the thermal decomposition of potassium permanganate. The system was initially evacuated to 15μ Hg, flushed with oxygen, re-evacuated, and then filled to atmospheric pressure. A furnace operating at the required temperature was drawn over a silica tube which contained a specimen hanging from a Pt wire in the oxygen atmosphere. The iodide-refined Ti metal was supplied by the Phillips Laboratories, Eindhoven, and the analysis was reported by Corbett (8). The Hf-free Zr was obtained from the U.S.A.E.C. and the Hf, containing 3-4% Zr, was supplied by the Westinghouse Electric Corporation. The oxidized specimens were mounted on edge in a cold setting polyester resin and abraded on 120, 320, and 400 mesh SiC papers followed by wax laps made from 400, 600, and 850 mesh SiC. Polishing was carried out by first rubbing lightly on a napless cloth impregnated with 1μ diamond paste and then on selvyt cloth carrying an aqueous paste of MgO. The thickness of scale was measured with a filar eyepiece on cross sections of metallographically polished, oxidized specimens. The presence of oxygen in the Ti lattice could be detected by an increase in hardness of the metal, and measurements were therefore made on specimen cross sections utilizing a Leitz microhardness instrument with a standard 124° diamond indenter.

Results

Titanium

Experiments performed in the range 800°-1000°C for long periods indicated that scaling of Ti was influenced greatly by the extent of an oxygen diffusion gradient in the metal phase of the oxidizing specimen. It was noted that the form of this gradient altered during the oxidation at corners and sides of strip specimens, and that ultimately the gradient beneath the main faces of such specimens was affected by the penetration of oxygen to the center of the strip. Further discussion relating to the form of scaling under such conditions is left to a later stage, and the following comments concern the scaling observed on flat surfaces of thick specimens.

The scales.—Two different types of scale were observed. Below 800°C only thin, gray adherent films were obtained, e.g., 0.2 mm thick after 75 hr at 750°C, which on metallographic examination in polarized light proved to be translucent. The gray appearance of the oxidized specimens is considered to be due to reflections from the metal surface beneath the translucent rutile. Above 800°C the scales were pale yellow, and microscopically they exhibited a characteristic form of lamination or banding. On closer examination these layers appeared to alternate in color from translucent yellow to gray, Fig. 1. Platinum marker experiments using wires wrapped around the original specimens showed that the oxide was formed at the metal/oxide interface, and this conclusion was later verified by the use of

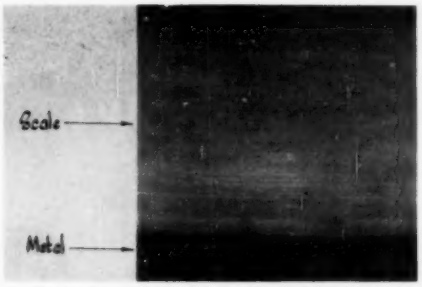

Fig. 1. Scale formed on Ti metal oxidized for 72 hr at 850°C, showing the characteristic form of lamination or banding. (Polarized light, x 250).

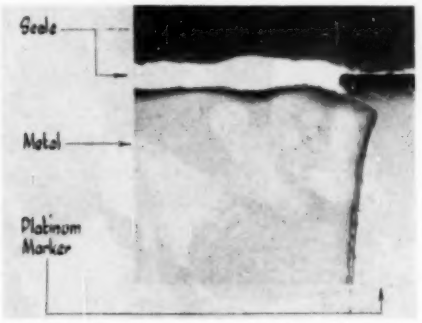

Fig. 2. Scale formed on Ti oxidized for 24 hr at 800°C, showing the inward movement of scale past the Pt marker. (Polarized light, x 125).

Pt plugs inserted through the specimens (Fig. 2). X-ray diffraction studies of the scales and metal cores confirmed that rutile was the only oxide present. The scales, although separated from the metal core on cooling from the oxidation temperature, must have remained in close contact with the oxidizing metal during the tests as they were readily absorbed by the metal when the gaseous supply of oxygen was withdrawn and the tests contained in vacuum for some hours at the same temperature.

The metal core.—Metallographic examination of a cross section of metal cores from oxidized specimens showed that the surface layers contained oxygen in solid solution. In the etched condition these cores taken from specimens oxidized below 800°C showed an oxygen saturated zone outlined by a fine black line just beneath the surface. Above this temperature a much wider band appeared Fig. 3. Previous work (1) had shown that microhardness traverses could be used to follow the form of an oxygen diffusion gradient in Ti. This technique was used to establish the form of the gradients below the saturated surface zone in each section. For each temperature a particular oxygen gradient was established in the core, the extent of penetration being initially time dependent. However, with increasing time the gradient reached a steady state, an example being given in Fig. 4. The time necessary to produce this condition decreased with increasing temperature and coincided with the change from a parabolic to a linear rate equation.

Zirconium and Hafnium

Scales, formed on both metals between 700° and 950°C, were dark gray and adhered to the metal core on cooling. However, the scales were white where they had lifted away from the metal during oxidation. Metallographic examination revealed some cavities penetrating to the metal surface in an otherwise dense, featureless scale structure devoid of layering. Belle and Mallett (7) published a photomicrograph of scale formed on Zr heated in oxygen between 500° and 700°C, and the similarity with the results obtained in the present study indicates that the form of the scale remains unchanged in the range 500°-950°C. Measurements of scale thickness after 24 hr showed a linear increase with respect to both time and temperature. Microhardness traverses revealed that steady oxygen gradients were also established in the cores of these two metals; the periods necessary to accomplish this increased in the order Ti, Zr, and Hf.

"Edge Effect"

Above 800°C, the scales formed on Ti were sufficiently thick to examine in detail, particularly along the edges and corners. At such sites, the yellow translucent scale was invariably thinner than on the main faces and had a crystalline structure distinct from the banded structure obtained elsewhere, Fig. 5. The form of the oxygen gradient in the metal core beneath these edges was traced and its total depth of penetration is shown in Fig. 6 for a specimen oxidized at 850°C for 72 hr.

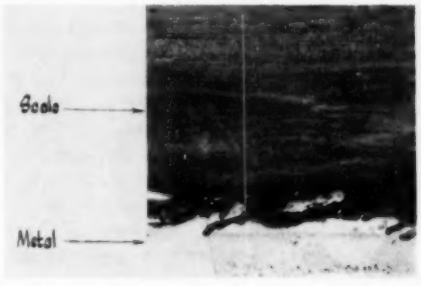

Fig. 3. Same as Fig. 2. The oxygen-saturated zone in the metal core shows as a dark etching band in bright-field illumination. (x 250).

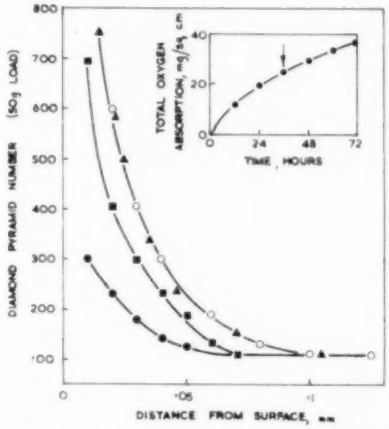

Fig. 4. Penetration hardness curves, showing the development of the gradient and the change from a parabolic to linear rate equation on specimens oxidized at 850°C. ●, 12 hr; ■, 24 hr; ▲, 36 hr; ○, 48 hr.

Fig. 5. Section through the center of a specimen of Ti showing the scale formed on a corner ("edge effect"), oxidized at 850°C, for 72 hr. (Polarized light, x 50).

Quite clearly the extent of oxygen penetration into the metal core at the edges was greater than on the flat faces and this affected the form and thickness of the scale at these sites.

Oxidation of Thin Specimens

In the early stages of the investigation, the importance of maintaining oxygen-free metal at the center of reacting specimens was not fully appreciated. Although specimens 1 cm thick were used in later experiments, oxidation at 1000°C for periods in excess of approximately 5 hr produced scaling changes which were attributed to an interruption in the movement of the diffusing oxygen gradient in the metal. This was apparently caused by oxygen penetrating to the center zone of the specimens because the onset of a change in scaling behavior at these high temperatures was noted to vary with the thickness of the specimen. Results of tests carried out under conditions where the diffusion gradient was affected are given in Fig. 7-9. Figure 7 is a cross section of a thin Ti specimen oxidized at 850°C for 72 hr. Initially a normal layered pale yellow scale of considerable thickness was produced (the layers were not reproduced in Fig. 7 so that other features could be high-lighted). However, due to the thinness of the metal specimen, the diffusion

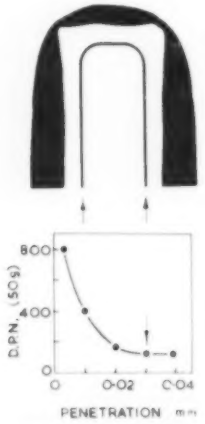

Fig. 6. Shadowgraph of the scale formed on the end of a Ti specimen oxidized for 72 hr at 850°C, showing the position of the extremity of the oxygen gradient and its position in relation to the scale.

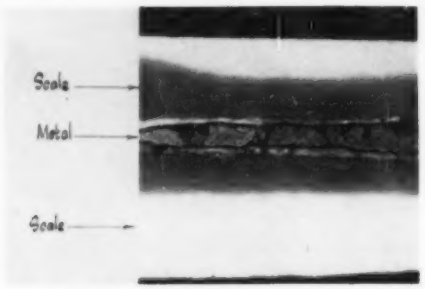

Fig. 7. Scale formed on a thin Ti specimen oxidized for 72 hr at 850°C, showing the effect of through oxidation.

gradients have met in the center, preventing further unhindered progress of the gradients. It is suggested that as a result of a reduced rate of oxygen diffusion into the metal core discoloration of the laminated scale commenced with the onset of cation diffusion outward through the scale toward the gas/scale interface. The metal core eventually received sufficient oxygen to become completely saturated and even produced a film of lower oxide (mainly purple Ti_2O_3) on the large solid particles remaining. As a general rule, the conversion of oxygen-saturated Ti to rutile will by-pass the lower oxides because, as suggested in the following discussion, very thin layers or fragments of oxygen-saturated Ti which have split off from the core are intermittently converted to rutile.

Two additional observations were made on specimens oxidized above 950°C (Fig. 8 and 9). Whenever oxidation conditions permitted the penetration of oxygen to the center zone of each metal specimen, a line of demarcation could be observed in the scale on metallographic examination (Fig. 8). This photomicrograph was prepared from a specimen oxidized at 1000°C for 6 hr, the specimen thickness being such that oxygen penetrated to the center regions. Marker experiments proved that this demarcation line represented the original metal surface. Scale appearing between this line and the metal surface apparently formed during the initial period of oxidation prior to the oxygen penetrating to the center of the metal and possessed the characteristic layered structure (Fig. 1). However, the

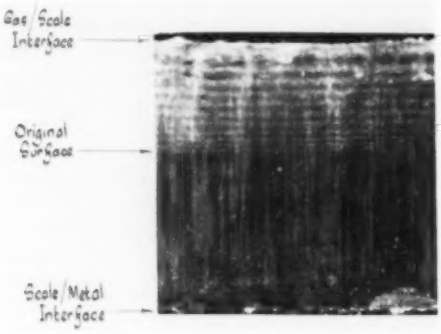

Fig. 8. Scale formed on a Ti specimen oxidized for 6 hr at 1000°C, in which the gradient in the core has been reduced by through oxidation. The columnar structure and the layering in the outer and inner sections of the scale are shown.

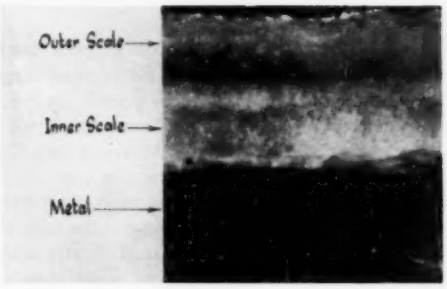

Fig. 9. Scale formed on Ti oxidized for 24 hr at 1000°C, showing the saturated metal core and the two recrystallized layers in the scale.

scale formed between the demarcation line and the gas interface must have been produced as a result of the diffusion of metal cations to the gas interface, and it is evident that the periodicity of the banding has lengthened noticeably toward the end of the oxidation. This portion of the scale forms when the demand for oxygen by the metal phase is reduced for some reason, such as oxygen penetrating to the center of the metal. Microhardness traverses on the remnant metal core beneath the scale shown in Fig. 8 revealed a decrease in oxygen concentration at the surface and a rise at the center, which supports the suggestion concerning reduced oxygen demand by the core. The scale exhibited a gray metallic luster, except at the corners and edges which consisted of large equiaxed crystals. The unusual columnar structure superimposed on the scale structure in Fig. 8 appears to be the result of some cooling phenomenon. The authors believe that a similar observation has been made on rapidly cooled UO_2 crystal aggregates.

Figure 9, taken from a thin specimen oxidized for 24 hr at 1000°C, shows a photomicrograph of the scale produced when the metal core has become completely saturated with oxygen. The two-layer scale is composed of equiaxed translucent yellow crystals of rutile, probably formed at the temperature of test. The core contains a second phase, TiO, which apparently has been rejected during cooling of the saturated solution comprising the core.

Discussion

Earlier work (1, 3) has established that after a brief interval Ti and Zr oxidize according to parabolic rate equations transforming to linear for prolonged periods of time. It is now suggested that the rate equation obeyed by Hf also undergoes a transformation from parabolic to linear upon the establishment of a steady oxygen gradient in the core of the oxidizing specimens. Apart from Loriers' explanation (9) based on a change in scale porosity this transformation has been interpreted in the past as indicating a transition from a diffusion-controlled process (parabolic equation) to a process in which resistance to further diffusion is offered by a barrier of fixed dimensions (linear equation). This barrier was believed to exist in the oxide scale, and the diffusion process was thought to be one in which oxygen penetrated by an anion vacancy mechanism. Metallographic examination has not yet revealed any obvious barrier in any of the scales examined, and density measurements (1) show a 7% porosity at room temperature for rutile scales formed on Ti between 700° and 950°C. However, x-ray diffraction, metallographic, and microhardness techniques have shown that a saturated surface zone together with a steady oxygen gradient is established eventually in the metal core after a period which coincides with the change from parabolic to linear oxidation.

It is now proposed that the scale is not operating as a diffusion barrier in the temperature range considered and that the oxidaiton of Ti, Zr, and Hf is controlled by interstitial diffusion of oxygen in the metal phase. It is considered that the exposure of clean surfaces of these metals to oxygen at high temperatures results first in a rapid gas absorption together with a transient increase in temperature, the gas concentration also rising in the surface layer. Scale formation probably follows the establishment of a saturated surface layer. The conversion of oxygen-saturated metal to rutile is considered to involve an exfoliation of very thin surface layers from the core, conversion to rutile following immediately as the detached metal is exposed to an atmosphere of relatively high oxygen potential. At the high temperature involved, the semiplastic oxide, under stress, would tend to sinter to the previously formed scale, although the junction line may well prove not to be perfect and so lead to the layered scale structure. No layering has been observed in the scales formed on Zr or Hf and this could indicate a difference in the conversion process at the metal/oxide interface.

Scale thickness measurements suggest that the actual scaling rate remains constant during the initial period of parabolic oxidation, whereas the rate of total oxygen absorption decreases with time, the decrease probably reflecting the establishment of the oxygen gradient in the metal core. This would explain the observed parabolic to linear transition in the rate of total oxygen absorption, because a stage must be reached at which the oxygen absorption by the metal core balances the conversion reaction at the metal/oxide interface. Oxygen entering the core then would be used periodically to establish saturated conditions in the core surface and to convert the detached layers to rutile. The following modified parabolic equation should apply during the establishment of the oxygen gradient in the metal,

$$\frac{dn}{dt} = \frac{K_1}{K_2 + n}$$

where n is the number of oxygen molecules absorbed at time t, and K_1 and K_2 are the rate constants for the diffusion and interface reactions. Integrating between the limits (n_0, n), $(0, t)$ we obtain the equation

$$n - n_0 = \Delta n = 2K_1 \left(\frac{t}{\Delta n}\right) - 2(n_0 + K_2)$$

Mathematical substitution in this equation will result in evaluation of the constants K_1 and K_2.

Finally, the influence of the diffusion gradient on the oxidation of Ti is revealed if, for some reason, the gradient of the core is upset. This can occur at corners and edges of specimens where the gradient is extended in depth and also over the main faces of thin specimens in which oxygen has penetrated to the center of the core. When this occurs, the gradient is apparently reduced, the absorption of oxygen by the core is therefore reduced and, if the specimen is scaling in the linear region, the scaling rate must then decrease. The experimental results suggest that the subsequent alteration in scaling behavior then depends on the temperature. Below about 900°C, it appears that a thinner scale remains over such sites, with the possibility of recrystallization at the corners and edges. However, at higher temperatures, it appears that the decrease in the absorption of oxygen at the core surface results in a longer period elapsing between the continuous process of saturation and separation of the core surface layers. Cation diffusion out through the attached scale structure is then observed. Once the usual exfoliation process occurs at the core surface, cation diffusion is halted temporarily until actual contact between scale and core again develops, and this is registered in the widening layered structure (Fig. 8) observed in the outer scale zone of those specimens which have produced a double scale. If this explanation is correct, it would be expected that, as a result of further oxidation of the core and therefore a slower rate of oxygen absorption, an increase in the period elapsing between the detachment of core surface layers would be observed. The result would be that the outermost scale layers formed by cation diffusion, having been the most recent formed, should show the widest banding. It is concluded from the absence of such effects below 850°C (cation diffusion is seen to have commenced in Fig. 4) that the ratio of the diffusivity of Ti cations in rutile to that of interstitial oxygen in the metal may perhaps be increasing with increasing temperature and at a rate such that oxidation at temperatures in the vicinity of 1200°C involves only outward diffusion of the metal cation to the gas-scale interface. Finally, when complete oxygen saturation of the core is approached at high temperatures, it is considered that the scale must eventually recrystallize to form the characteristic pale yellow rutile shown in Fig. 9. Oxygen demand by the core must then be very low, and cation diffusion would operate only as long as contact existed between the scale and the core.

Conclusion

The results of this investigation suggest that the scaling behavior of Ti, Zr, and Hf is controlled by the diffusion of oxygen in the metal phase. The presence of oxygen in the metal core has been used to explain the change in the rate equations during the oxidation of these metals. In the past this has been attributed to a scale barrier of constant thickness, but no such barrier has been detected. However, a diffusion barrier of constant depth is eventually established in the metal core and this is associated with the parabolic to linear transformation. It is considered that the actual isothermal scaling rate for these metals may well prove to be approximately constant, and that the initial parabolic rate of oxygen absorption is associated with the establishment of an oxygen diffusion gradient in the metal core as well as the scaling reaction. Further discussions based on these proposals has produced an explanation for certain effects commonly observed during the high-temperature oxidation of Ti.

Finally, a number of metals other than Ti, Zr, and Hf exhibit a significant oxygen solubility at high temperatures, and therefore their scaling behavior is being examined now along similar lines.

Acknowledgments

The work described in this paper was carried out in the School of Metallurgy at the New South Wales University of Technology, Australia. During the period involved, one of the authors (G.R.W.) held an Australian Atomic Energy Commission Postgraduate Studentship. The authors wish to express their thanks to Professor Rupert Myers for the provision of laboratory facilities and to the Australian Atomic Energy Commission for continued financial support.

Manuscript received March 10, 1958.

Any discussion of this paper will appear in a Discussion Section to be published in the December 1959 JOURNAL.

REFERENCES

1. A. E. Jenkins, *J. Inst. Metals*, **82**, 213 (1953-4).
2. A. E. Jenkins, *ibid.*, **84**, 1 (1955-6).
3. L. F. Kendall, A.E.C. Research & development report H.W. 39190 Sept. (1955).
4. W. W. Smeltzer and M. T. Simnad, *Acta Met.*, **5**, 328 (1957).
5. P. H. Morton and W. M. Baldwin, Jr., *J. Metals*, **4**, 854 (1952).
6. W. Kinna and W. Knorr, *Z. Metallk.*, **47**, 594 (1956).
7. J. Belle and M. W. Mallett, *This Journal*, **101**, 339 (1954).
8. J. A. Corbett, *Analyst*, **76**, 652 (1951).
9. J. Loriers, *Compt. rend.*, **231**, 522 (1950).

The Electrical Resistance of Oxide Films on Zirconium in Relation to Corrosion

R. D. Misch and F. H. Gunzel, Jr.

Argonne National Laboratory, Lemont, Illinois

ABSTRACT

The conductivity of anodic and corrosion films on zirconium was found to increase during heating in vacuum. The conductivity changes at 450°C were studied on anodic films which were 0.6, 0.75, 0.9, and 1.5 μ in thickness. The change in conductivity was attributed to the diffusion of anion vacancies into the oxide with an estimated diffusion coefficient of 4×10^{-12} cm^2 sec^{-1}. Corrosion films produced in water at 350°C appeared to have higher diffusion coefficients. Among the materials zirconium, Zircaloy-1, and Zircaloy-2, specimens of zirconium had the highest corrosion rates and diffusivities (as judged by the conductivity changes). Consequently, an effect of vacuum heating on corrosion was expected and subsequently confirmed. Enhanced oxide growth was observed after corroded specimens were heated at 600°C for 1 min. The increase in weight gain was greater than would be expected from a simple restoration of dissolved oxide.

The corrosion of zirconium in water at high temperature is a sensitive function of metal composition (1). Consideration of this problem has focused attention on changes in the oxide film as a result of additives. An analysis of such effects has been given by Thomas (2). The present study was designed to determine whether the resistance of the oxide plays a role in the corrosion process.

In the case of highly conductive oxides like FeO the effect of small concentrations of impurities is negligible. Zirconium oxide, however, is an insulator at room temperature, and impurities might be expected to decrease its electrical resistivity. Consequently, the resistivity of the corrosion film should reflect the presence of various impurities. The incorporation of such impurities in the oxide has been observed in a 2.5% Sn-Zr alloy where the Sn was found in solid solution in the ZrO_2 layer (3).

Other elements such as Ti, U, Fe, Cr, and Ni have ionic sizes favorable for substitutional replacement of Zr^{4+} in the oxide lattice. Titanium and uranium increase the corrosion rate of Zr in water, while the other elements in small amounts cause a decrease. One may conclude that crystallographic changes are not of primary importance so that emphasis can be directed to changes in the oxide defect structure as determining corrosion behavior. Resistance measurements should be of value in resolving this problem.

A study of the resistance of corrosion films at room temperature was made by Akimov and Clark (4). The film was touched with a mercury droplet. The present technique is similar to that of Savage (5) who examined the resistance of electrical contacts. Contact with the oxide was made with a wire probe, and the underlying Zr formed the other contact.

The oxide on a metal is not a homogeneous, isotropic solid, and the role of inclusions and defects cannot be overlooked. Freshly prepared anodic or corrosion oxide on Zr is an insulator at room temperature, and a low resistance area is an indication of a conducting inclusion. Other factors which influence the data are discussed below.

Experimental

Procedure.—All measurements were made by resting the polished tip of a 10-g Pt probe on the oxidized surface of Zr specimens. The probe made electrical contact through the oxide to another Pt wire spot welded to the Zr. In all measurements the voltage across the oxide was 10 mv, and the current was read on a galvanometer with a sensitivity of 0.005μa/mm of deflection. The circuit and probe are shown in Fig. 1. The magnitude of the current was independent of polarity; usually the probe was maintained positive to the Zr. The Zr specimen rested in the center of a 1-in. diameter Pt tube fur-

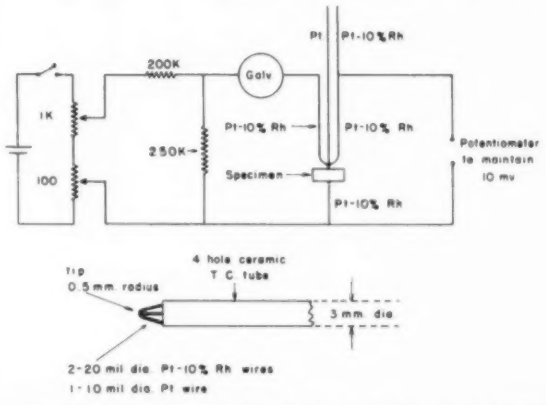

Fig. 1. Schematic drawing of circuit and construction of probe for measuring film conductivity and temperature.

nace, 8 in. long. The furnace was mounted in an 18-in. bell jar which was evacuated to 10^{-6} mm Hg pressure before heating. At 450°C the vacuum was 10^{-5} mm Hg or better.

Materials.—The study was made on reactor grade Zr, Zircaloy-1, and Zircaloy-2. Hafnium was present to approximately 0.02% in all these materials. Specimens were cut from rolled plates having the analyses given below:

Zirconium: (all ppm) 200 O, 70-350 C, 60-150 N, 30-100 Al, 2-10 Cr, 5-20 Cu, 200-700 Fe, 1-20 Mg, 2-7 Mn, 40-80 Ni; each less than 50 ppm: Si, Ti. This material is classified Grade 1 on the basis of corrosion testing in water.

Zircaloy-1: 2.5% Sn, other individual elements below 0.01%.

Zircaloy-2: 1.43% Sn, 0.108% Fe, 0.105% Cr, 0.048% Ni, 0.0032% N, with 30 ppm Al, 50 ppm Ca, 170 ppm Hf, 60 ppm Pb, 50 ppm Si, 15 ppm Ti.

All specimens were prepared by wet grinding to 400 grit paper and etching in a solution of 50 ml 70% HNO_3, 50 ml distilled water, 8 ml 47% HF. Etching time was 1 min at room temperature.

Anodic films.—Anodic films were produced by applying constant voltage to a cell with Zr as the anode and Pt as the cathode. In the present work the electrolyte was purified saturated H_3BO_3 at room temperature. This electrolyte had a high resistance but permitted anodizing up to 500 v. In anodizing of this type the film thickness is proportional to the applied voltage (1). The gain in weight of Zr anodized according to the procedure used in this study was found to be in good agreement with the data of Polling and Charlesby (6), i.e., 0.46 μg cm^{-2} v^{-1}. Charlesby assumed a density of 5.67 g cm^{-3} which gave a thickness-voltage relation of 30Å v^{-1}.

The dependence of film thickness on voltage was also shown by measuring the capacitance of the Zr anode in the electrolyte. The second electrode was Pt gauze. Effectively, the Zr and electrolyte were the plates of the condenser. A General Radio Company Type 650-A bridge was used. It was expedient to substitute acetic acid for boric acid when measuring capacitance in view of the high resistance of the latter soluton. The data are shown in Fig. 2. Zircaloy-2 could not be anodized above 300 v which limited the range in which the film thickness could be varied. This fact was attributed to oxygen evolution at inclusions.

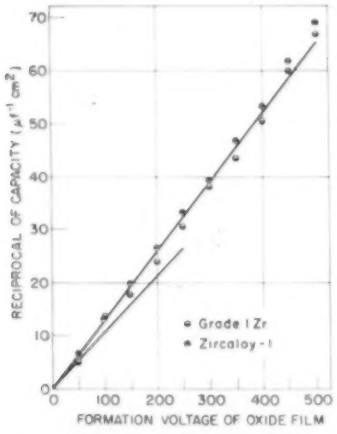

Fig. 2. Reciprocal of capacity of anodic films as a function of the voltage of anodizing of Zr and Zircaloy-1, anodized in boric acid, measured in 1N acetic acid. The short line is from data of Charlesby (14).

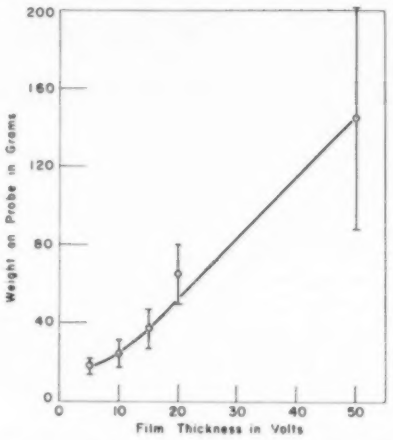

Fig. 3. Region of electrical breakdown of the anodic film on Zr as a function of probe weight and film thickness. The solid line bracketing each point indicates standard deviation.

Autoclave films.—Autoclave films were produced by exposing specimens to degassed, distilled water at 350° ±5°C for periods from 16 hr to 2 weeks. The resultant films were adherent, and weight gains were a measure of film thickness.

Weight on the probe.—The probe rested on the surface with a weight of 10 g. To be certain that the film was not damaged by this weight the maximum tolerable weight at room temperature was determined for different film thicknesses. The data are given in Fig. 3. The film broke down electrically above the line, producing a short circuit. The applied voltage was 10 mv prior to breakdown. An average of 30 points was examined for each anodic film thickness.

Contact area.—The contact area of the probe was very small. To determine this area the 10-g probe was placed on smooth Pt, the resistance was measured, and the area was calculated from the formula of Holm (7). An average of numerous measurements gave a contact area of $1.5 \pm 0.5 \times 10^{-4}$ cm^2. This is the largest error in estimating resistivity.

Results

Effect of Heating in Vacuum

No current was detected when the probe was placed on anodic or autoclave films at room temperature. However, when a specimen was heated in vacuum, current became measurable at 350°C and higher. The conductivity increased with time as well as temperature, and a reversible temperature coefficient could not be obtained. Film history, thickness, and temperature were all found to influence the conductivity changes.

Preliminary work in which specimens were heated and cooled showed that the ZrO_2 films became better conductors and remained so as long as the vacuum

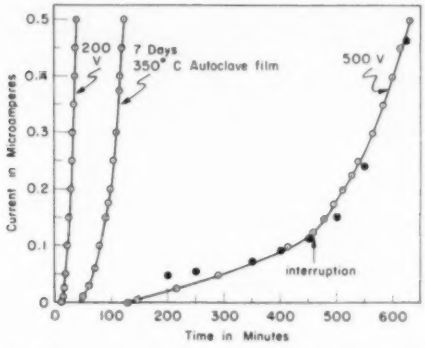

Fig. 4. Typical examples of the change in conduction of the oxide in Zr held at 450°C in vacuum.

was maintained. The conductivity often dropped when air was admitted.

At constant temperature the conductivity increased at a rate dependent on temperature. At 350°C there was no perceptible conductivity up to 16 hr. At 450°C the change in the film was apparent in a matter of minutes. Typical results for heating different specimens are shown in Fig. 4.

Weight gains of these specimens were as follows: 200 v anodized film, 9.1 mg/dm^2; autoclave film, 31.0 mg/dm^2 (somewhat higher than average); 500 v anodized film 22.8 mg/dm^2. These data were for single trials, but the reproducibility may be judged from Fig. 5-7. The "interruption" on the 500 v curve indicates an overnight interval during which the specimen was in vacuum at room temperature. When heating was resumed, the current returned within several minutes to the magnitude recorded just before cooling.

Anodic films of increasing thickness.—To measure the effect of film thickness, a series of anodic films formed at different voltages was studied. The voltages were 200, 250, 300, and 500 and the corresponding weight gains were 9.1, 11.4, 13.7, and 22.8 mg/dm^2. Assuming 5.67 g cm^{-3} as the density (6) the thicknesses of these films were 0.6, 0.75, 0.9, and 1.5μ. The conductivity was measured at 450°C in vacuum,

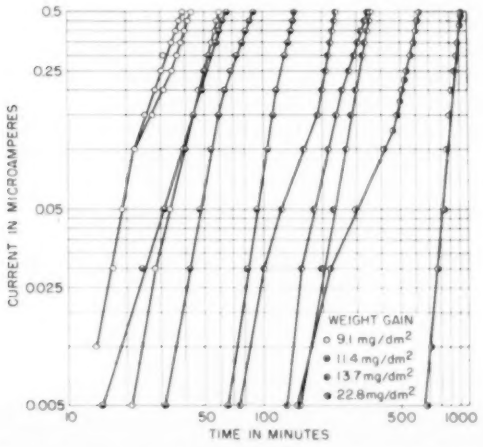

Fig. 5. Current vs. time curves for anodic oxide films on Grade I Zr held at 450°C in vacuum.

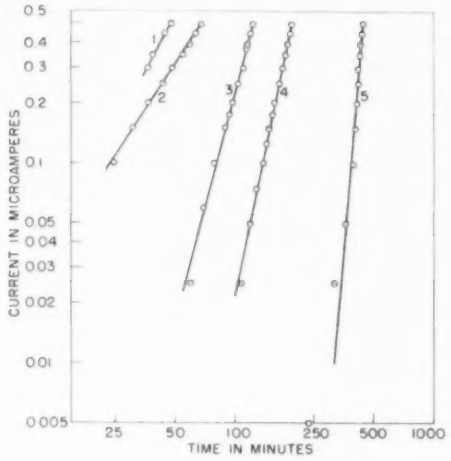

Fig. 6. Current vs. time curves for autoclave films on specimens of arc-melted Zr crystal bar having an average weight gain of 19 mg/dm^2 after 1 week in water at 350°C. Each specimen was held at 450°C in vacuum. Specimens 1, 2, and 3 exhibited patches of gray or white oxide; specimens 4 and 5 were black and uniform.

and the data are plotted as log current (with 10 mv across film) vs. log time in Fig. 5.

Autoclave films.—Here all the specimens had weight gains very close to 21 mg/dm^2. The alloys had uniform black films, while the Zr specimens showed occasional white patches. Measurements were made only on the coherent black film.

The curves for Zr are given in Fig. 6 and the curves for the two alloys in Fig. 7. In the latter case the experimental points are shown only for Zircaloy-2. The experimental data for Zircaloy-1 were in good agreement with the lines as shown, and the points were omitted to avoid overlapping. The slopes of the curves on the autoclave films were similar to those for the anodic films. The experimental spread for Zr was large as compared to the alloys.

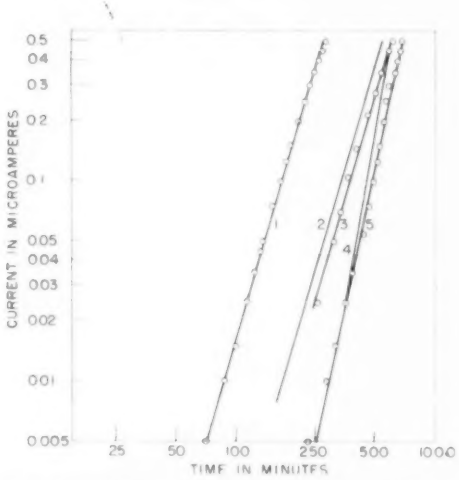

Fig. 7. Current vs. time curves for autoclave oxide films on specimens of Zircaloy-1 (curves 2 and 4) and Zircaloy-2 (curves 1, 3, and 5) having an average weight gain of 24 mg/dm^2 after 1 week in water at 350°C. Specimens were held at 450°C in vacuum.

Vacuum heating and corrosion rate.—The existence of a conductivity effect suggested that the corrosion rates might be increased by vacuum heating. With rapid heating to sufficiently high temperatures the corrosion oxide film became a good conductor at room temperature over its entire surface. The subsequent corrosion behavior should indicate whether film growth is affected. For this purpose the corrosion of Zr specimens was compared before and after a rapid heating to 600°C followed by rapid cooling. The corrosion film was conducting after this treatment. Zirconium specimens were exposed to water at 350°C, periodically removed, and vacuum heated. Comparison with controls revealed no effect of the heating. Consequently, the heating time in vacuum was extended as follows: The specimen was brought to 600°C in 30 sec, kept at 600° for 1 min, and cooled below 400° in 30 sec. The vacuum was 10^{-5} mm Hg or better. This procedure was employed on both Zr and Zircaloy-2 specimens after 16-hr intervals of exposure to degassed water at 350°C. Upon removal from the autoclave the heated films were again insulating.

One set of specimens was used as a control; the other set was vacuum heated before and during the corrosion test. An additional set of specimens was vacuum heated at the same time, but corrosion testing was not carried out until the vacuum heating was discontinued after 320 hr of corrosion exposure.

The corrosion weight gains are shown in Fig. 8 and 9. Initially, the heated specimens had lower weight gains, but they continued to gain weight when the control specimens were leveling off. It was found in a preliminary experiment that these low weight gains did not appear when the vacuum heating preceding the corrosion exposure was omitted. Consequently, the initial low weight gains may be due to a different surface after the vacuum treatment.

The effect of vacuum heating did not last, as shown by the leveling of the curve after 320 hr when this treatment was ended. The four specimens of each material which were vacuum heated and then corrosion tested (data not shown) had essentially the same weight gains as the standards which were

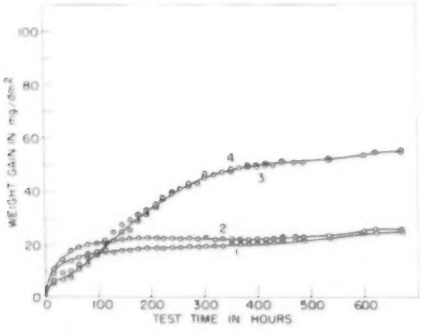

Fig. 8. Weight gains of four specimens of arc-melted Zr, corrosion tested simultaneously in water at 350°C. No. 3 and No. 4 were heated at 600°C for 1 min at the time of each weighing up to and including 320 hr (also prior to testing). Heating was discontinued after this point. Specimen No. 1 and No. 2 were not heated.

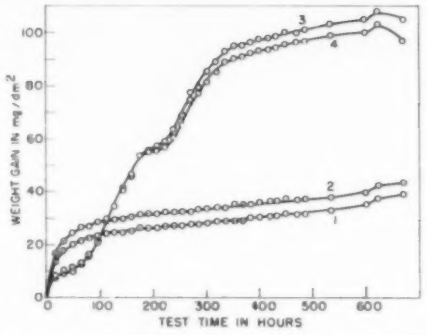

Fig. 9. Weight gains of four Zircaloy-2 specimens, corrosion tested simultaneously in water at 350°C. No. 3 and No. 4 were heated at 600°C for 1 min at the time of each weighing up to and including 320 hr (also prior to testing). Heating was discontinued after this point. Specimen No. 1 and No. 2 were not heated.

not heated. This ruled out any metallurgical effect. Specimen weights were always checked before and after the vacuum heating and did not vary by more than 0.5 mg/dm². This was negligible in comparison to the corrosion weight gains.

At the end of the test the specimens numbered 1 and 2 had a uniform dark lustrous appearance indicative of a protective oxide, for both Zr and Zircaloy-2. Specimens 3 and 4 were light gray. Under a microscope the light gray oxide was seen to vary from gray to white with white predominating. The film on the Zircaloy-2 was breaking away along the lines of inclusions. The Zr surfaces had tiny brown and black spots which were probably deposits from the autoclave.

Discussion

Vacuum heating has been shown to influence both the electrical conductivity of the oxide on Zr and its corrosion rate in water at 350°C. The reasons for electrical changes in the oxide will be considered before discussing the effect of vacuum heating on corrosion.

The nature of the Zr-ZrO_2 system suggests that diffusion is responsible for the conductivity changes. The most likely mechanism to account for the observed changes is the loss of oxygen to the metal which would be accompanied by the formation of anion vacancies in the oxide. The very low dissociation pressure of ZrO_2 (10^{-60} atm at 450°C) is evidence that oxygen will not escape to the vacuum.

The current-time curves can be explained on the basis that the resistance of the oxide drops rapidly with the penetration of anion vacancies. The mean displacement of a diffusing species is $\sqrt{2Dt}$, where D is the diffusion coefficient and t is time (12). If the major part of the observed electrical resistance is provided by the unpenetrated oxide (of unchanged resistivity), one may write

$$i = \frac{k\,V}{\delta - \sqrt{2Dt}} \qquad [1]$$

where i is the current through the film, V is the applied voltage, k is a constant proportional to the area of the contact, and δ is the film thickness. At 450°C

Table I. Diffusion coefficients, D, calculated from the data of Fig. 5 (Anodic oxide on Grade 1 Zr at 450°C)

Anodizing voltage	Film thickness μ	D x 10^{13} (cm^2 sec^{-1}) As calculated	Average for each film thickness
200	0.60	7.6 6.7 4.9	6.4
250	0.75	6.9 5.2 3.2	5.1
300	0.90	2.8 1.9 1.9	2.2
500	1.5	2.9 1.8	2.4

the change in film thickness due to dissolution can be neglected.

This equation provides a reasonable representation of the observed data as indicated in Fig. 4 where the solid points were calculated from Eq. [1] using the values $D = 2.72 \times 10^{-13}$ cm^2 sec^{-1} and $k = 3.1 \times 10^{-5}$ μa^{-1} cm^{-1}. These empirical values were calculated from two points on the experimental curve (0.05 μa, 290 min and 0.4 μa, 600 min); k was an average for these points.

Two points from a curve are sufficient to solve for D from the equation

$$\frac{i_2}{i_1} = \frac{\delta - \sqrt{2Dt_1}}{\delta - \sqrt{2Dt_2}} \qquad [2]$$

Using i_2 as 0.5 μamp and i_1 as 0.025 μamp, the diffusion coefficient was calculated for the curves of Fig. 5. The resulting values are shown in Table I. The average from all the curves was 4.0×10^{-13} cm^2 sec^{-1}.

This result may be compared with 2×10^{-15} cm^2 sec^{-1} which Pemsler (8) obtained for the diffusion of oxygen into Zr metal at 450°C. The difference between 4.0×10^{-13} and 2×10^{-15} is consistent with the observation that conductivity changes can be observed in films where dissolution is almost insignificant. However, in the absence of corroborative information it should not be concluded that the "vacancy diffusivities" presented here are valid diffusion coefficients.

The conductivity changes of the corrosion oxide films on Zr showed a wide variation although the films were of equivalent thickness. The following diffusivities for the corrosion films heated at 450°C were calculated in the same manner as for the anodic films (the designations refer to Fig. 6): Curve 1, 2.5×10^{-12} cm^2 sec^{-1}; curve 2, 2.1×10^{-12} cm^2 sec^{-1}; curve 3, 1.4×10^{-12} cm^2 sec^{-1}; curve 4, 0.86×10^{-12} cm^2 sec^{-1}; curve 5, 0.38×10^{-12} cm^2 sec^{-1}.

As would be expected, curve 5 represents a lower diffusion coefficient than curve 1.

The better reproducibility of the curves for Zircaloy-1 and 2 suggests that the oxide is more homogeneous on these alloys than on Zr. The curves for these alloys are similar to curve 5 for Zr so that a comparable diffusivity can be expected. It is possible that a low diffusivity as estimated from conductivity changes may be related to a low corrosion rate.

The effect of vacuum heating on corrosion cannot be explained readily. The increase of electrical conductivity during heating indicates that changes are taking place within the oxide. In addition, some of the oxide is dissolving as a result of oxygen diffusion into the Zr. The rate of dissolution has been used to determine the diffusivity of oxygen in Zr (8).

Considering the latter process, the effect is to make the oxide film slightly thinner. In previous work (11), using the same equipment as this study, it was shown that about 100Å of oxide was dissolved while heating 1 min at 600°C. This is somewhat smaller than the results of Pemsler (8) where approximately 250Å would be expected to dissolve in the first minute. Using the smaller number the decrease in thickness would be 0.2μ after twenty heatings. This corresponds to 3 mg/dm^2 of oxygen. The final differences in weight gains between heated and unheated specimens were much larger than this, indicating that the weight increases are not simply due to the restoration of dissolved oxide.

As already mentioned the heated film did not remain conducting after exposure in the autoclave but was apparently restored to its original insulating character. This suggests that the defect structure produced by heating is eliminated by re-exposure to water. In such a case a weight gain would be expected, corresponding to a filling of vacancies.

As shown by the data on corrosion weight gains a specimen gained weight each time it was vacuum heated and returned to the autoclave. In the case of Zr which had a weight gain of 40 mg/dm^2 without heating, the additional weight gain after each vacuum heating and re-exposure was approximately 2.5 mg/dm^2. The latter figure represents 6% of the oxygen in the film before re-exposure in the autoclave. Consequently, one may postulate that 6% of the oxygen sites were emptied by diffusion during vacuum heating and refilled upon subsequent exposure in the autoclave.

Under the same circumstances, the 40 mg/dm^2 film on Zircaloy-2 gained about 5 mg/dm^2, representing a 12.5% vacancy concentration. These percentages seem unreasonably high because the oxygen consumed in the dissolution of oxide at 600° (100Å) is only 0.15 mg/dm^2 or 0.4% of 40 mg/dm^2. This suggests that other factors are increasing the corrosion rate.

Perhaps the structure of the oxide is changed by heating, or the diffusion of oxygen into the Zr promotes the subsequent conversion of some of this diffused layer into oxide during corrosion. More evidence concerning these factors is desirable.

This phenomenon may be related to the "memory" effect noted by Thomas (13) where Zr specimens maintained a high corrosion rate after the corrosion temperature was lowered.

Acknowledgment

The authors are indebted to J. E. Draley for discussion relating to this work.

Manuscript received May 3, 1957. This paper was prepared for delivery before the Pittsburgh Meeting, Oct. 9-13, 1955. The work was performed under the auspices of the U. S. A. E. C.

Any discussion of this paper will appear in a Discussion Section to be published in the December 1959 JOURNAL.

REFERENCES

1. B. Lustman and F. Kerze, Jr., Editors, "The Metallurgy of Zirconium," Chapter 11, Corrosion of Zirconium and Its Alloys, McGraw-Hill Book Co., New York (1955).
2. J. Chirigos and D. E. Thomas, Proc. AEC Metallurgy Conf. March 1952, p. 337, Report TID-5084.
3. R. D. Misch, Unpublished research.
4. G. V. Akimov and G. B. Clark, *Trudy Inst. Fiz. Khim., Akad. Nauk SSSR*, **4**, Issledovaniya Korrozii Metallov. No. 3, 3 (1952).
5. R. H. Savage and D. G. Flom, *Ann. N. Y. Acad. Sci.*, **58**, 946 (1954).
6. J. J. Polling and A. Charlesby, *Proc. Phys. Soc. (London)*, **67B**, 201 (1954).
7. Ragnar Holm, "Electric Contacts," Hugo Gebers Forlag, Stockholm (1946).
8. J. P. Pemsler, U.S.A.E.C. Report NMI-1177 May 31, 1957; also *This Journal*, **105**, 315 (1958).
9. T. J. Gray, "The Defect Solid State" Interscience Publishers, Inc., New York (1957).
10. L. Young, *Trans. Faraday Soc.*, **51**, 1250 (1955).
11. R. D. Misch, *Acta Met.*, **5**, 179 (1957).
12. W. Jost, "Diffusion in Solids, Liquids, Gases," Academic Press, New York (1952).
13. D. E. Thomas and S. Kass, *This Journal*, **103**, 478 (1956).
14. A. Charlesby, *Acta Met.*, **1**, 340 (1953).

The Structure of Electro-Deposited Nickel

B. C. Banerjee and A. Goswami

National Chemical Laboratory, Poona, India

ABSTRACT

An electron diffraction study was made on the crystal structure, orientation, and mode of growth of nickel deposits from sulfate-chloride-boric acid and chloride-boric acid baths under various bath conditions. The effect of pH, temperature, concentration, current density, mechanical stirring, etc., and of additions such as hydrogen peroxide, nickel nitrate, and sodium chloride was investigated on polycrystalline substrates. Depending on bath conditions various preferred orientations (one-degree), mixed or otherwise, were developed and their causes have been discussed in detail. These have been correlated also with the mode of cathodic crystal growth process.

It has been shown previously that the crystal structure and orientations of electrodeposited nickel are profoundly affected by the bath conditions (1-5). In what follows an account is given of a comparative survey of the crystal orientations in deposits from nickel chloride and sulfate-chloride baths as commonly used in industrial plating.

Experimental

In order to restrict the substrate influence on crystal size and orientation of electrodeposits, mechanically polished brass disks (70:30) of about 3.0 cm^2 significant area were used as cathodes, the nonsignificant portions being covered with collodion. Compositions of the baths were: (*a*) $NiSO_4 \cdot 7H_2O$ 280 g/l + $NiCl_2 \cdot 6H_2O$ 48 g/l + H_3BO_3 31 g/l; (*b*) $NiCl_2 \cdot 6H_2O$ 150 g/l + H_3BO_3 31 g/l; (c) $NiCl_2 \cdot 6H_2O$ 280 g/l + H_3BO_3 31 g/l; and (*d*) $NiSO_4 \cdot 7H_2O$ 280 g/l + H_3BO_3 31 g/l. The chemicals used were of AR or CP quality. The above solutions were purified and adjusted to desired pH values in the manner described previously (3). Unless otherwise stated, the current density employed was 10 ma/cm^2, and the solutions were unstirred. When stirring was resorted to, the sweep of the glass propeller was close to the cathode surface.

After electrodeposition, the specimens were washed thoroughly with distilled water, with alcohol, and then immediately examined in a Finch-type electron diffraction camera (6) working with 45-65 kv electrons, the camera length being about 50 cm. The lattice parameter of the deposit was determined by dusting graphite powder over the specimens and using $11\bar{2}0$ ring of graphite ($d_{11\bar{2}0}$ = 1.230Å) as the internal standard. Since the reflection technique was used, the diffraction of electrons was due to the top surface layers only. In order to study the change of surface structure with time of deposition, specimens were examined by electron diffraction at various deposit thicknesses.

The deposition was carried out to well beyond the stage where the polycrystalline deposits had developed preferred orientations (one-degree). By preferred orientation, it is meant that the polycrystalline deposits had a common lattice row normal to the deposit surface, or in other words had a common lattice plane parallel to the deposit or substrate surface. The orientation plane is generally indicated by {hkl}.

Results

The appearance of nickel deposits varied from semibright and dull matte to dark gray or even black, depending on the deposition conditions. Pitting and pinholes were observed in deposits formed under the conditions giving rise to profuse hydrogen evolution. Electron diffraction studies of the cathode surface revealed that the deposits were initially polycrystalline but randomly disposed; with increasing thickness, the deposits developed one degree orientations determined by bath conditions. The lattice constant of the coatings (a_o = 3.543Å) was found to be similar to that of f.c.c. nickel (7). Occasionally, however, hexagonal form of nickel

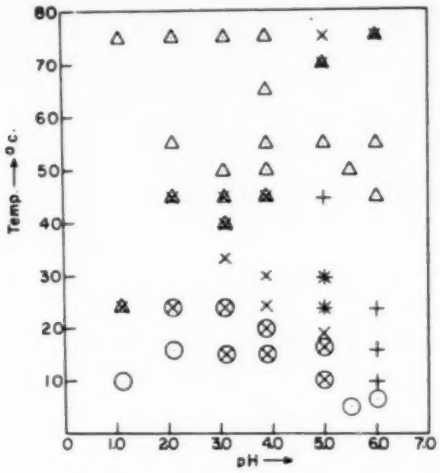

Fig. 1. Change in orientations of nickel deposits with pH and temperature; bath (a). × means {100} orn; △ means {110} orn; + means {211} + {10$\bar{1}$0} orn; O means {210} orn.

(7) also appeared along with the f.c.c. structure. The results are shown in Fig. 1-7.

Influence of Various Factors

pH and temperature.—It will be seen from Fig. 1-3 that, with increasing bath temperature, the orientations changed eventually from {210} (○) to {110} (△) irrespective of pH values. At an intermediate range, however, depending on pH and bath composition, {100} (×) and a mixed {211} + $\{10\bar{1}0\}_{hex}$ (+) orientations were generally observed.

Metal ion concentration.—The orientations of the deposit crystals were also influenced by metal ion concentrations. Baths (*a*) and (*b*) under different pH conditions were diluted in the ratio of 1:1, 1:3, and 1:9 maintaining the pH in each case the same as that of the undiluted bath. Thus with gradual dilution, the initial {211} + $\{10\bar{1}0\}_{hex}$ (+) orientations changed to {100} (×) and finally to {110} (△)

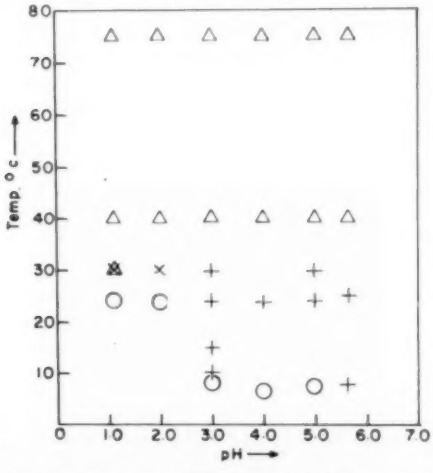

Fig. 2. Change in orientations of nickel deposits with pH and temperature; bath (b). Symbols have same meaning as in Fig. 1.

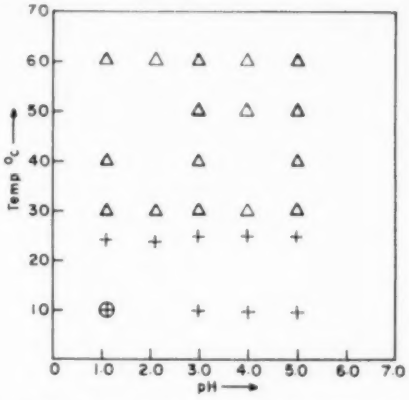

Fig. 3. Change in orientations of nickel deposits with pH and temperature; bath (c). Symbols have same meaning as in Fig. 1.

as can be seen from Fig. 4. Similar results were also obtained even when the concentration of boric acid was maintained to 31 g/l in the diluted baths. This suggests that boric acid content has no significant effect on the orientations of nickel deposits.

Oxidizing agents.—The addition of hydrogen peroxide or nickel nitrate to the baths suppressed pitting of deposits and also affected the crystal orientations (Fig. 5a and 5b). Addition of hydrogen peroxide (≅1 g/l) resulted in the {210} orientation (○) gradually changing to {100} (×) or {211} + $\{10\bar{1}0\}_{hex}$ (+) at all pH ranges and at temperatures up to 35°C. At higher temperatures, however, hydrogen peroxide decomposed without oxidizing hydrogen evolved at the cathode, and no further change in orientation was observed. With further increase in hydrogen peroxide concentration, the crystal orientations changed to {110} (△) (Fig. 5a). If the concentration of hydrogen peroxide was still further increased, the deposits became rough and were often covered with basic nickel salts.

Nickel nitrate (about 0.8 g/l), on the other hand, favored {110} (△) orientation of the deposit crystals under conditions which would otherwise have developed {210} (○), {100} (×), or {211} + $\{10\bar{1}0\}_{hex}$ (+) orientations (Fig. 5b).

Mechanical stirring.—Stirring of the solutions affected the crystal orientation by reducing the con-

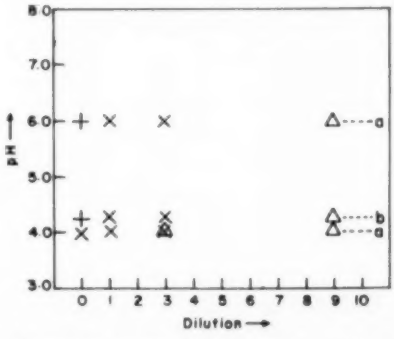

Fig. 4. Change in orientations of nickel deposits with dilution and pH; baths (a) and (b). Symbols have same meaning as in Fig. 1.

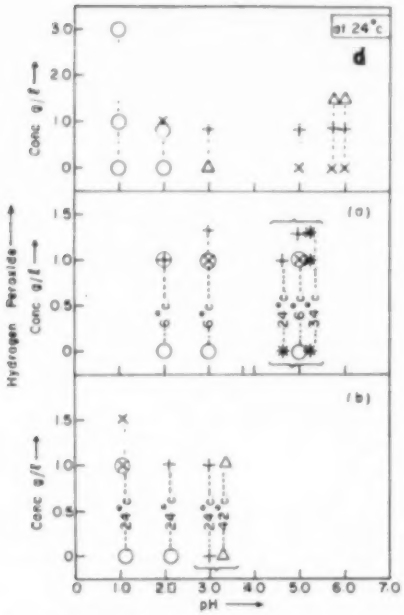

Fig. 5. (a) Change in orientations of nickel deposits with hydrogen peroxide and pH; bath (a), (b), and (d); Fig. 5 (b). With nickel nitrate. Symbols have same meaning as in Fig. 1.

centration gradient in the catholyte layer and possibly also by facilitating the removal of hydrogen from the cathode surface. Thus, instead of the {210} (○) orientation of the deposit-crystals favored at a low temperature in a still bath, a mixture of {210} (○) and {100} (×) orientations occurred at 250 rpm and, finally, {211} + $\{10\bar{1}0\}_{hex}$ (+) orientations at about 1000 rpm (Fig. 6). Similarly, instead of the {110} (△) orientation normally developed at 55°C in an unstirred bath, a {100} (×) orientation appeared at 300 rpm. Mechanical stirring, however, did not affect the continued development of {100} (×) or {211} + $\{10\bar{1}0\}_{hex}$ (+) orientations when the unstirred were favorable to the formation of these orientations.

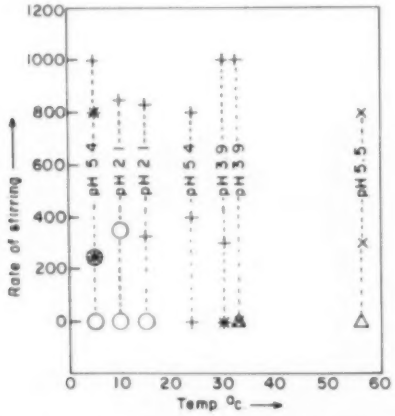

Fig. 6. Change in orientations of nickel deposits with rate of stirring and temperature; bath (a). Symbols have same meaning as in Fig. 1.

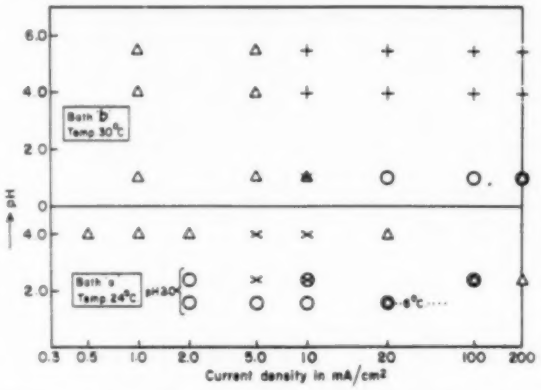

Fig. 7. Change in orientations of nickel deposits with current density and pH; baths (a) and (b).

Current density.—The effect of current density on the deposition of nickel is very interesting. It may be seen (Fig. 7) that except at low temperature, the deposits developed {110} (△) orientation in the lower current density range. At an intermediate range of current density, however, either {100} (×) or {211} + $\{10\bar{1}0\}_{hex}$ (+) orientations were favored. At a still higher current density {110} (△) orientation was developed sometimes accompanied by {210} (○) orientation, especially at low pH ranges. In bath (c), however, lateral {100} (×), {211} + $\{10\bar{1}0\}_{hex}$ (+) types of deposits were always obtained, even at a current density as high as 200 ma/cm².

Chloride ion concentration.—An increase in the chloride ion concentration in the bath generally favored {211} + $\{10\bar{1}0\}_{hex}$ (+) orientations in place of {100} (×) and the bath could tolerate a higher current density range than the usual. Figure 8 shows typical {211} + $\{10\bar{1}0\}_{hex}$ orientations of the deposit crystals.

Discussion

The mode of cathodic crystal growth and its influence on the orientation of the resulting deposits have recently been discussed by Finch and coworkers (1, 2) and ourselves (3-5, 8). The orientations developed in electrodeposits are determined primarily by the growth process of the deposits. The chief factors controlling the process are: (*a*) rate of supply of cations through the diffusion layer to

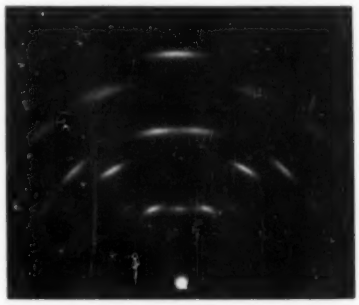

Fig. 8. 1-d {211} + $\{10\bar{1}0\}_{hex}$ orientation of nickel deposits.

the cathode; (*b*) rate of discharge of cations; (*c*) thickness of the diffusion layer; and (*d*) formation of films near the cathode surface region. Any change in the deposition conditions may materially affect one or more of the above factors determining the over-all deposition process and thus modify the orientation of the deposited crystals. When the rate of supply of metal ions to the catholyte is plentiful compared with the rate of their discharge, the deposits grow laterally with a densely packed plane lying parallel to the substrate surface. On the other hand, when the rate of supply of cations at the cathode is inadequate, resulting in an impoverishment of metal ions at the catholyte, the deposit-crystals grow outward in such a way that a densely packed atom row is normal to the cathode surface. In the case of nickel {111}, {100} (×), and also {211} + $\{10\bar{1}0\}_{hex}$ (+) orientations, as recently shown by Goswami (8), are characteristics of lateral growth-deposits whereas {110} (△) indicates an outgrowth mechanism.

Other orientations also may develop due to factors which come into play during deposition. The appearance of {210} (○) orientation, for instance, seems to be associated with the adsorption or otherwise of hydrogen, presumably atomic, by the deposits which are known to be in a highly active condition when freshly deposited (9). This is evident from the change of orientation from {210} (○) to {100} (×) or $\{10\bar{1}0\}_{hex}$ and {211} (+) effected by the addition of hydrogen peroxide to the bath (Fig. 5a). The rate of discharge of hydrogen ions at the cathode will be increased due to the oxidation of atomic hydrogen to water molecules in the presence of hydrogen peroxide. This will, no doubt, facilitate the formation, precipitation, and occlusion on the cathode surface of colloidal nickel hydroxides or basic salts, thus reducing the effective metal ion concentration in the catholyte and favoring an outgrowth mechanism.

Nickel nitrate influences the orientation of the deposits in a different manner. Hydrogen, atomic or molecular, formed at the cathode reduces the nitrate in its immediate vicinity finally to ammonia which in turn forms nickel ammonium complexes. The effective metal ion concentration thus reduced should favor outgrowth.

Mechanical stirring, as has been mentioned before, reduces the thickness of the catholyte layer and maintains metal ion concentration at the cathode surface region; hence orientations of the deposits tend to be characteristic of the lateral growth. By disturbing the adsorption of hydrogen at the cathode, mechanical agitation also reduces and ultimately eliminates pitting pinholes in the deposit surface.

When a bath is much diluted, the effective metal ion concentration is low and hence the deposits are of outgrowth type as has been experimentally observed by us.

The effect of temperature on the crystal is peculiar. A higher temperature should increase the mobility of the ions and at the same time reduce the thickness of the diffusion layer. Normally this should favor lateral growth-deposits. On the other hand, our experimental results show that higher temperatures favor outgrowth-deposits at all pH conditions excepting in bath (*a*) at 75°C at pH 5.0. This may be due to the increased rate of hydrolysis of the nickel salts with the rise of bath temperature. It is well known that nickel salts hydrolyze to hydroxides or basic salts when the pH of the solution is appropriate at room temperature and this is increased still more at higher temperatures. This leads to outgrowth-deposit.

The effect of high current density is generally to increase the rate of discharge of metal ions at the cathode without a corresponding increase in their rate of supply to cathode surface region, thereby causing an impoverishment of cations at the cathode surface and thus favoring outgrowth. The formation of lateral-growth deposits at an intermediate current density range may also be similarly understood. A very peculiar observation, as mentioned before, was the development of {110} (△) orientation at very low current densities. This cannot be explained easily. The effect of current density and temperature will be discussed in a separate paper.

An increase in chloride ion concentration generally induces crystal twinning and ultimately results in a new orientation. This has recently been studied in detail on single-crystal substrates. The development of {211} + $\{10\bar{1}0\}$ (+) orientation in the concentrated chloride bath can thus be easily understood, but it is not yet clear why chloride ions should favor twinned structures. However, it is known that these ions are adsorbed more easily by the cathode surface than the bivalent sulfate ions (12), and hence it may be possible that they influence the potential energy configuration of the substrate surface, thereby inducing a twinned structure on the deposits.

Acknowledgment

The authors' thanks are due to Professor G. I. Finch and Dr. A. B. Biswas for their keen interest in the work.

Manuscript received April 11, 1957.

Any discussion of this paper will appear in a Discussion Section to be published in the December 1959 JOURNAL.

REFERENCES

1. G. I. Finch, H. Wilman, and L. Yang, *Disc. Faraday Soc.*, **1**, 144 (1947).
2. G. I. Finch and D. N. Layton, *J. Electrodepositors Tech. Soc.*, **27**, 215 (1951).
3. B. C. Banerjee and A. Goswami, *J. Sci. Industr. Res.*, **14B**, 322 (1955).
4. B. C. Banerjee and A. Goswami, *ibid.*, **16B**, 144 (1957).
5. A. Goswami, *ibid.*, **16B**, 315 (1957).
6. G. I. Finch and H. Wilman, *Ergeb. exakt. Naturwiss.*, **16**, 353 (1937).
7. W. R. A. Wycoff, "Crystal Structure," Interscience Publications, New York (1957).
8. A. Goswami, *J. Sci. Industr. Res.*, **15B**, 322 (1956).
9. C. C. Roth and H. Leidheiser, *This Journal*, **100**, 553 (1953).
10. A. W. Hothersall and R. A. F. Hammond, *Trans. Faraday Soc.*, **30**, 1079 (1934).
11. D. J. Macnaughton, G. E. Gardam, and R. A. F. Hamond, *ibid.*, **29**, 729 (1933).
12. J. Heyrovsky, *Disc. Faraday Soc.*, **1**, 212 (1947).

The System $ZnO{\cdot}CdO{\cdot}B_2O_3$, Phase Relationships, and Fluorescence

D. E. Harrison

Luminescent Materials Laboratory, Lamp Wire and Phosphors Department, General Electric Company, Cleveland, Ohio

and

F. A. Hummel

Department of Ceramic Technology, The Pennsylvania State University, University Park, Pennsylvania

ABSTRACT

The subsolidus phase relationships were investigated using x-ray and petrographic methods. Two compounds were isolated: $2ZnO{\cdot}CdO{\cdot}B_2O_3$ which fuses at about 860°C and $ZnO{\cdot}2CdO{\cdot}2B_2O_3$ which melts congruently at 797° ± 3°C. Excitation by either 2537A or cathode rays produces a maximum orange (6200A) fluorescence in $2ZnO{\cdot}CdO{\cdot}B_2O_3$ with 0.004 wt % Mn and a maximum red (6400A) fluorescence in $ZnO{\cdot}2CdO{\cdot}2B_2O_3$ with 0.080 wt % Mn. The fluorescence of $ZnO{\cdot}2CdO{\cdot}2B_2O_3$ was examined using Ag, Sn, Tl, Pb, and Sb as single activators as well as sensitizers with Mn.

Ohno (1) claimed a region of manganese activated zinc-cadmium borate compositions which when blended with $MgWO_4$ yielded a white fluorescent substance. Interest in the zinc-cadmium borate component and the lack of any phase data in this ternary system stimulated the present investigation.

The study was limited to the determination of compatibility triangles, isolation of compounds, and examination of the fluorescence of certain compositions with various activators.

Experimental Procedure

Mallinckrodt reagent-grade boric acid and cadmium carbonate, and New Jersey Zinc Company U.S.P. zinc oxide were used as starting materials. Reagent-grade $MnSO_4$, $Mn(NO_3)_2$, $AgNO_3$, Tl_2CO_3, $Pb(NO_3)_2$, SnO_2, or Sb_2O_3 were used as activators.

The ingredients were ground in an agate mortar with acetone until dry. Calcines were prepared in platinum crucibles at temperatures ranging from 700° to 900°C for periods from 8 to 48 hr.

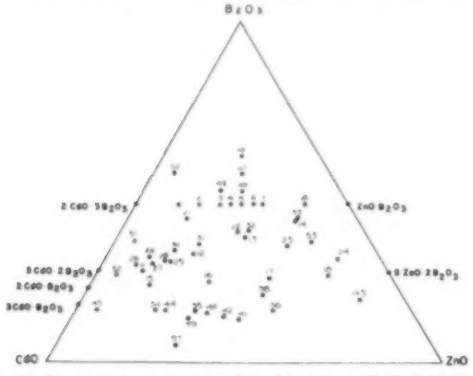

Fig. 1. Compositions examined in the system $ZnO{\cdot}CdO{\cdot}B_2O_3$.

X-ray data were obtained from Norelco and General Electric recording spectrometers using $Cu_{K\alpha}$ radiation (λ = 1.537A) filtered with nickel.

The immersion technique was used to determine the refractive indexes of crystals to an accuracy of ±0.002, using white light and index oils which were calibrated with an Abbe refractometer.

Differential thermal analysis (DTA) data were obtained with automatically recording apparatus described by Gruver (2).

Emission curves were obtained with an automatically recording General Electric spectroradiometer. Visual examinations were made under 2537A, 3650A, and cathode-ray excitation.

Compositions.—The compositions examined are listed in Table I and are shown graphically in Fig. 1.

Experimental Results and Discussion

Phase relationships.—The compatibility triangles were determined by comparing the x-ray data of ternary compositions with the data for binary compounds in the systems $CdO{-}B_2O_3$ and $ZnO{-}B_2O_3$ as reported by Subbarao and Hummel (3) and Harrison and Hummel (4), respectively.

Two new ternary compounds were discovered and individually prepared, and the compatibility triangles were determined as shown in Fig. 2. An unidentified phase is situated in the subtriangle $3CdO{\cdot}B_2O_3{-}2ZnO{\cdot}CdO{\cdot}B_2O_3{-}ZnO$, but its exact composition is not readily discernible because of the extensive solubility of $3CdO{\cdot}B_2O_3$ and ZnO in $2ZnO{\cdot}CdO{\cdot}B_2O_3$.

Table I. Composition of ZnO-CdO-B_2O_3 mixtures

No.	Molar composition ZnO	CdO	B_2O_3
1	1.00	2.61	4.91
2	1.00	1.51	3.26
3	1.00	0.97	2.46
4	1.00	1.24	2.16
5	1.00	0.65	1.97
6	1.00	0.53	1.80
7	1.00	0.43	0.89
8	1.00	0.16	1.24
9	1.00	—	1.00
10	—	1.00	0.50
11	1.00	3.71	2.86
12	1.00	1.39	0.92
13	1.00	0.62	0.71
14	1.00	0.23	1.12
15	1.00	2.68	1.74
16	1.00	0.99	0.90
17	1.00	0.45	0.62
18	1.00	0.17	0.62
19	1.00	—	0.40
20	—	1.00	1.50
21	1.00	1.88	3.22
22	1.00	0.70	1.47
23	1.00	0.31	0.87
24	1.00	0.12	0.58
25	1.00	2.00	2.00
26	1.00	4.71	3.81
27	1.00	2.91	2.61
28	1.00	2.23	2.21
29	1.00	3.17	3.31
30	1.00	2.01	2.34
31	1.00	1.29	1.86
32	1.00	0.58	1.39
33	1.00	0.22	1.14
34	1.00	2.06	0.87
35	1.00	1.16	5.83
36	1.00	0.44	0.35
37	1.00	1.37	0.20
38	1.00	0.50	0.50
39	1.00	1.25	0.50
40	1.00	0.94	0.47
41	1.00	0.67	0.33
42	1.00	0.80	0.40
43	1.00	0.10	0.30
44	1.00	1.75	0.75
45	1.00	10.21	3.52
46	1.00	0.64	2.34
47	1.00	0.63	2.86
48	1.00	0.63	3.50
49	1.00	1.00	3.00
50	1.00	5.11	12.95
51	1.00	7.66	8.25
52	1.00	8.93	5.89
53	1.00	0.19	0.82
54	—	1.00	0.67
55	—	1.00	0.33

The compound 2ZnO:CdO:B_2O_3 (2:1:1) is biaxial negative with a very small 2 v angle and R.I. of $n_\alpha = 1.709$, $n_\beta > 1.79$, $n_\gamma > 1.79$. Because of the difficulty in obtaining this composition as a glass, neither the nature of the fusion nor the exact melting temperatures could be determined by the conventional quench technique. However, DTA revealed an endothermic peak at 860°C at which temperature the sample fused. X-ray examination of 2:1:1 after firing at various temperatures supported the DTA data that no polymorphs existed between 100°C and the fusion temperature. A characteristic x-ray pattern is given in Table II.

Crystals of the compound ZnO:2CdO:2B_2O_3 (1:2:2) remained too small, even after prolonged heat treatment, to determine their optical properties accurately. However, 1:2:2 exhibited high birefringence with maximum and minimum R.I. of about 1.78 and 1.75, respectively. The 1:2:2 compound melts congruently at 797° ±3°C and it has no polymorphs between 100°C and its fusion temperature. A characteristic x-ray pattern is given in Table II.

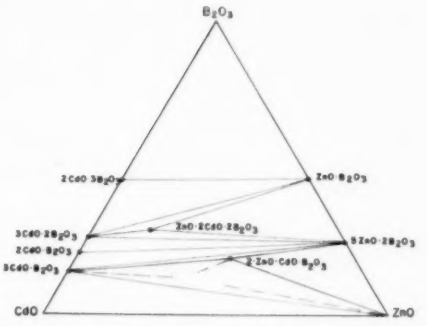

Fig. 2. Compatibility triangles in the system ZnO-CdO-B_2O_3

With the exception of the subtriangle 3CdO·B_2O_3-2ZnO·CdO·B_2O_3-ZnO, petrographic and x-ray data revealed no extensive solid solution in the ternary system. The compound 1:2:2 gave no evidence of solid solubility between it and compatible phases.

Fluorescent studies.—The compounds 2:1:1 and 1:2:2 were prepared with various Mn concentrations. Excitation by either 2537Å or cathode rays, but not 3650Å, gave an orange (6200Å) fluorescence in 2:1:1 and a red (6400Å) fluorescence in 1:2:2. Variation in Mn concentration in either 2:1:1 or 1:2:2 affected the fluorescent intensity, but it did not produce any noticeable shift in the emission

Table II. Characteristic x-ray patterns

2ZnO·CdO·B_2O_3 d	I/I_o	ZnO·2CdO·$2B_2O_3$ d	I/I_o
4.21	40	9.12	20
3.39	5	5.31	25
3.23	5	4.48	50
3.11	5	4.42	10
2.93	100	3.36	30
2.32	20	3.25	30
2.67	20	3.21	25
2.61	10	3.07	55
2.51	10	3.02	60
2.48	15	2.98	85
2.40	55	2.87	55
2.34	10	2.71	100
2.08	15	2.64	30
2.04	15	2.51	15
1.855	40	2.41	5
1.834	20	2.38	20
1.734	5	2.24	5
1.678	5	2.20	15
1.629	10	2.12	15
1.575	10	2.08	20
1.556	15	2.04	15
1.469	25	1.953	35
1.459	10	1.845	10
1.389	10	1.824	15
1.318	5	1.790	10
1.293	5	1.771	5
1.247	5	1.749	10
1.203	5	1.722	25
1.148	5	1.689	25
1.112	5	1.680	10
		1.626	10
		1.600	10
		1.556	15
		1.506	10
		1.465	10
		1.423	5
		1.388	5

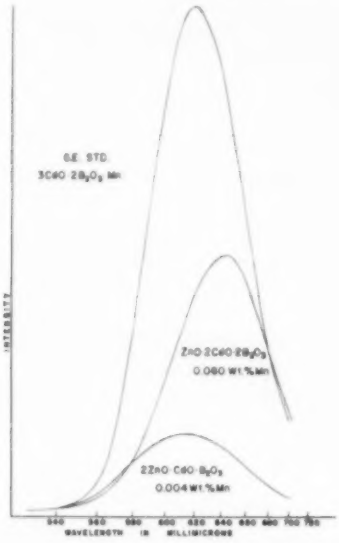

Fig. 3. Spectral distribution and relative intensities excited by 2537Å radiation.

spectrum. Optimum brightness occurred at 0.004 wt % Mn in 2:1:1 and at 0.080 wt % Mn in 1:2:2. Manganese concentrations in the range 1 to 5 ppm were sufficient to activate either 2:1:1 or 1:2:2. However, decreasing fluorescent brightness with decreasing Mn concentration indicates that the pure compounds are not luminescent. The small amounts of Mn necessary to activate the ternary compounds did not appear to introduce new phases.

Spectral distributions of 2:1:1:Mn and 1:2:2:Mn compared to Std. G.E. $3CdO \cdot 2B_2O_3$:Mn using 2537A excitation are shown in Fig. 3. The intensities are relative to Std. G.E. cadmium borate phosphor and thus give a comparison of absolute intensities obtained. Visual examination of the phosphors under cathode rays gave results comparable to those obtained by 2537A excitation.

The rarity of red (6400Å) emitting borate phosphors directed attention to 1:2:2 as a possible matrix for other activators. These included Ag, Tl, Pb, Sn, and Sb as single activators, as well as sensitizers with Mn. Only one level of activator concentration at 0.1 wt % was investigated. Since the phosphors were prepared under oxidizing conditions, Sn^{++} was probably the oxidation state involved.

After firing the singly activated 1:2:2 compositions at 700°-750°C for from 8 to 12 hr, visual examination with excitation by 2537Å, but not 3650Å, gave a weak red fluorescence. The sample prepared without the addition of an activator remained dead after this heat treatment.

When viewed through a Corning No. 2418 red filter, the Tl addition showed the greatest brightness followed in order of decreasing brightness by Sb, Ag, Pb, and Sn additions. Only the Pb-activated phosphor showed a blue band in addition to the weak red band when viewed through a Corning No. 5850 blue filter.

Increasing the firing temperature to values close to the melting temperature of 1:2:2 (797° ±3°C) produced weak red fluorescence in the activated as well as the "nonactivated" phosphors.

Evidently the addition of Tl, Sb, Ag, Pb, or Sn sensitized the residual Mn present in the nonactivated material when the phosphor was prepared at the lower temperature. Also, the additive may have had a mineralizing effect on the phosphor matrix. With the exception of Pb none of these additions introduced emission bands of their own.

When either Tl, Ag, Sn, Pb, or Sb was used as a sensitizer with Mn, all at concentrations of 0.1 wt %, and when the compositions were fired at 700°-750°C for from 8 to 12 hr, excitation by 2537Å or cathode rays, but not 3650A, produced a bright red fluorescence. Mn + Tl and Mn + Ag additions were brighter and exhibited much shorter afterglows than did Mn additions alone. Thus an Mn + Tl activated 1:2:2 composition fired at 700°-750°C was as bright as a phosphor activated with Mn alone and fired close to the melting point. When viewed through a Corning No. 2418 red filter, Mn + Tl addition showed the greatest brightness followed in order of decreasing brightness by Mn + Ag, Mn alone, Mn + Sn, Mn + Pb, and Mn + Sb additions. None of these phosphors showed a blue component when examined through a Corning No. 5850 blue filter.

The differences in fluorescent brightness between the various additions became smaller as the firing temperature approached the melting point. However, the brightness did not exceed that produced by Mn + Tl at the lower temperature. Both the Mn + Tl and Mn + Ag additions exhibited shorter afterglows at the higher firing temperature than did Mn additions alone.

Manuscript received April 18, 1958. This paper was prepared for delivery before the New York Meeting, April 27-May 1, 1958. It is a part of a thesis submitted by D. E. Harrison in partial fulfillment of the requirements for the Ph.D. degree to The Pennsylvania State University; contribution No. 57-83 from the College of Mineral Industries, The Pennsylvania State University.

Any discussion of this paper will appear in a Discussion Section to be published in the December 1959 JOURNAL.

REFERENCES

1. Y. Ohno, Japanese Pat. No. 3354, Oct. 9, 1950; *C. A.*, 46: 9998d.
2. R. M. Gruver, *J. Am. Ceram. Soc.*, **31**, 323 (1948).
3. E. C. Subbarao and F. A. Hummel, *This Journal*, **103**, 29 (1956).
4. D. E. Harrison and F. A. Hummel, *ibid.*, **103**, 493 (1956).

Activation of ZnS and (Zn,Cd)S Phosphors by Gold and Other Elements

S. T. Henderson, P. W. Ranby, and Margaret B. Halstead

Thorn Electrical Industries, Ltd., Enfield, Middlesex, England

ABSTRACT

A study has been made of the spectral emission characteristics of zinc and zinc-cadmium sulfide phosphors, activated by gold and excited by long wave ultraviolet at 25° and —120°C. The positions and heights of the Gaussian sub-bands constituting the emission were examined and compared with those derived from the series activated by copper, silver, and chloride ("self-activated"). Copper and gold produce the most similar phosphors, with 3 sub-bands each; silver and chloride give 2 sub-bands, and resemble each other particularly in the effects associated with crystallographic change. Linear relations in the peak locations and an energy diagram are discussed. Other observations concern cathode-excitation, the effects of substituting selenium for sulfur, and a recently reported emission band of higher frequency.

The zinc and zinc cadmium sulfide phosphors have been investigated very extensively, especially with activation by Cu, Au, and Mn. There has been comparatively little interest in Au as the impurity metal, and it is remarkable that these sulfides are the only phosphors, so far as is known, which can be activated by Au. In the following a survey is given of work published hitherto on the subject.

Indications of ZnS:Au as a distinct phosphor began when a blue emission band was observed in a slightly different position from that of "unactivated" ZnS under excitation by ultraviolet (1, 2) or cathode rays (3). Since then a number of observations have been made on the emission peaks of ZnS with trivalent cations and variable Au content (4), and the cathodoluminescent efficiency of this material (5); on the emission shift due to incorporation of ZnO (6); and on the glow curve of ZnS:Au,Cl (7). More recently Arpiarian has used ZnS:Au to study intensification and killing effects produced by Fe, Co, and Ni (8), and Destriau has found that field-enhanced luminescence of (Zn,Cd)S:Mn under x-rays is improved by traces of Au in the phosphor (9).

The well-known (Zn,Cd)S series has received little attention in regard to activation by Au. This activator was mentioned by Leverenz as applicable to the (Zn,Cd) (S,Se) series but no emission data were quoted (10). Byler attempted to explain the effects of changing CdS content by assuming a set of emission bands in fixed positions and independent of the activator (Cu,Ag,Au, Mn, or none) (11). The most extensive investigation on record is concerned with developing a single phosphor of white cathodoluminescence, namely, (Zn,Cd)S:Ag,Au,Al; in this case the emission data for (Zn,Cd)S:Au were presented only as chromaticity plots (12).

There is no doubt that Au is a specific activator, although in the past the blue band it produces in ZnS has sometimes been mistaken for that in ZnS without added metal activator.

The present work is concerned primarily with the effects of activation by Au, but for comparison other better known activators also have been used. The properties of ZnS phosphors with the various activators and different preparative details are first considered, particularly with regard to the effects on emission band positions and intensities of changes of temperature or of crystal form. Next, phosphors in the (Zn,Cd)S series with the same activators are discussed, with special reference to the shift of the bands as the CdS content is changed. A search for regular progressions between different series with Cu, Ag, and Au activators has been unrewarding, although interesting comparisons between Cu and Au have emerged. The individual behavior of activators is in fact much more striking than their similarities.

It has been reported previously that the frequencies of emission band peaks in the (Zn,Cd)S series, under cathode-ray excitation, give closely linear plots against weight proportions of the matrix (3). This inexplicable relation applies reasonably well to most of the data in the present work, but the apparently more rational scale of molecular proportions has been used in the graphical presentation. Other variables have been plotted against peak band wave number; of these only the c_o dimension of the hexagonal lattice gave any approach to linearity.

Measurement and Presentation of Emission Spectra

In the present work long wave-length ultraviolet excitation has been used in the main, with a few observations made under cathode-ray excitation. Samples were generally contained in a brass cell with a quartz window for exposure to 125-w mercury arc lamps in Wood's glass bulbs. This excitation by the group of lines near 3650Å produced a phosphor brightness of the order of 0.25 to 0.5 stilb. For the experiments on cooled samples the powder was used in the apparatus shown in Fig. 1. This

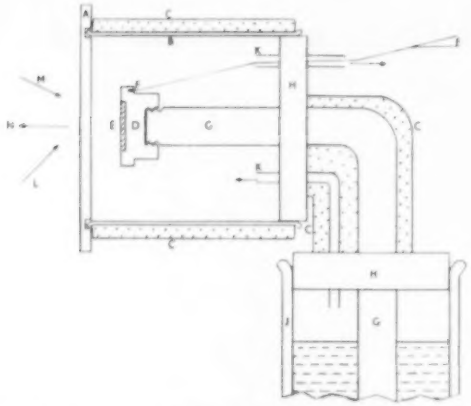

Fig. 1. Apparatus for excitation under ultraviolet at low temperature. A, Lucite plate; B, glass; C, asbestos and silica wool insulation; D, phosphor container detachable by screwing; E, phosphor compressed into cavity; F, thermocouple; G, copper rod; H, corks; J, Dewar flask of liquid oxygen; K, glass tubes for oxygen circulation; L, air stream to prevent condensation; M, ultraviolet beam; N, to spectrograph slit.

produced reasonably low phosphor temperatures without a vacuum enclosure, and condensation on the phosphor was prevented by a stream of evaporated oxygen.

Spectral emission curves were measured on a spectrophotometer previously described (13), with an exit slit width of 5Å at 4000Å and 42Å at 7000Å. Beyond the latter wave length the low sensitivity of the 1P22 photomultiplier and the background radiation from the mercury lamps made the measurements unreliable. Although wave lengths in the visible spectrum are more familiar than wave numbers and are largely used in the literature of phosphor emission bands, in the present work wave numbers have been used to permit analysis of the emission bands into Gaussian sub-bands. Therefore, emission curves are drawn with ordinates representing relative energy emitted per unit wave number interval instead of the usual energy per unit wave length interval. The Gaussian bands isolated from these curves were taken to be the ultimate components of the emission and were considered as the basic experimental data. This agreement of emission curves with a sum of Gaussians is of somewhat uncertain significance, but it provides a convenient method of analysis and presentation. Peak intensities of the bands have been examined in detail; band widths were found to be not very consistent, and therefore band areas (equivalent to energy) were not used.

ZnS with Au and Other Activators

Preparation.—Samples were prepared by mixing pure precipitated ZnS with aqueous solutions to give 5% by weight of chloride ion (added as an equimolecular mixture of sodium and magnesium chlorides) and 0.01% by weight of Au, Ag, or Cu, as chloride, nitrate, or sulfate, respectively. After drying, the finely powdered mixtures were heated in 100-g quantities for 1 hr at 1100°-1150°C in air in plugged silica tubes, then removed from the furnace to cool. The products were washed free from fluxes, dried, and sieved. Other phosphors were prepared in a precisely similar manner but omitting the heavy metal addition. Also, a few samples of cubic structure were made by firing at 800°C, and of partially cubic structure by firing at 1100°C in the presence of excess of S contained in the raw ZnS. Other workers have referred to ZnS with no other foreign ion than chloride as "self-activated," "zinc activated," or "unactivated." In the following the term "chloride activated" is used. The residual chloride in these materials is in fact of the usual order of activator proportions. The metal-activated phosphors also contain small amounts of chloride and are described as ZnS:Au,Cl, etc.

Emission characteristics.—When activated by Au instead of by Cu, Ag, or Cl, ZnS emits two closely overlapping bands with peaks about 600Å apart; these are of the same order of intensity when the excitation is by long wave-length ultraviolet. There is in addition a weaker band in the yellow region. The over-all effect is that the fluorescence is much paler than for the other phosphors examined and is of a light bluish green color, similar in hue to that of 80 mole % ZnS·20% CdS:Ag,Cl, or 85%ZnS·15%CdS:Cl, but less saturated (see Fig 2. and 3 for examples of emission curves).

Table I summarizes the average values for emission peak positions. Wave lengths are given to correspond to the wave numbers: it must be emphasized that such values are not really equivalent owing to the different shapes of the wave number and wave-length curves. Peak values read off directly from the latter curves are included for comparison.

Table II shows changes observed on cooling the samples during excitation. Details are included for preparations of similar composition but different crystal structure.

Table III summarizes changes at 25°C caused by these different structures.

For Table I accuracy is estimated at ±100 cm^{-1} except for the more uncertain bracketed values. The

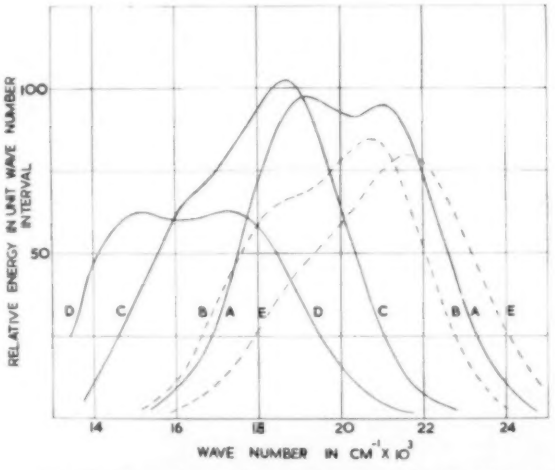

Fig. 2. Spectral emission of Au activated phosphors at 25°C. A, B, C, D: 0, 2.7, 16.5, 30 mole % CdS, respectively. E: 0% CdS, cathode-ray excitation.

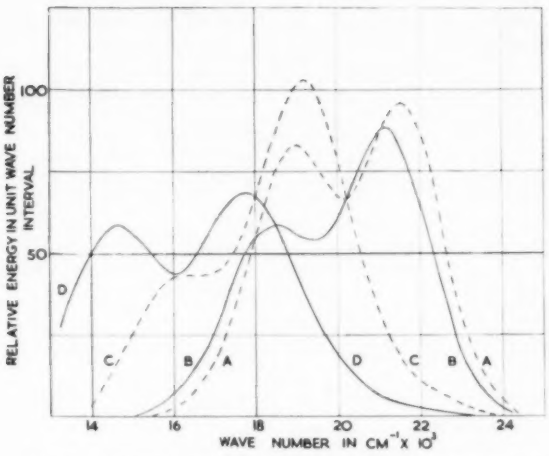

Fig. 3. Spectral emission of Au activated phosphors at −120°C. A, B, C, D: 02.7, 16.5, 30 mole % CdS, respectively.

convention adopted is to number the bands in order from the blue end of the spectrum, as Au I, II, etc. A band appearing only at low temperature is not included in this scheme (see Discussion).

Band peak positions.—The most interesting feature is the similarity between Au and Cu as activators. The well marked shifts to increased wave number on cooling and the contrary effect observed for ZnS:Cl agree with the findings of Tomlinson for his "self-blue" and "Cu-blue" bands (14) and of Shrader and Larach for their blue bands in ZnS:I, ZnS:Cu,I, and ZnS:Ag,halide (15).

For ZnS:Ag,Cl there is a small increase of wave number in Ag I on cooling. This places Ag with Cu and Au, as chemical considerations would suggest. Silver activation however is known to show anomalous behavior compared with Cu and Cl when ultraviolet excitation of cubic samples is changed to cathode-ray excitation (3). Other unusual effects have been described also for Ag in (Zn,Cd)S (16). To summarize present information on this topic:

(*A*) Cu, Ag, and Au at about 0.01% concentration and with Cl also, in cubic or hexagonal ZnS under ultraviolet, produce an increase of wave number on cooling, and Cl alone shows the reverse effect.

(*B*) A change to cathode-ray excitation increases wave number for Cl and Cu,Cl (cubic), and Au,Cl (hexagonal), but the reverse is true for Ag,Cl (cubic).

(*C*) Under cathode-ray excitation, cooling increases wave number for Cu,Cl (cubic), and decreases it for Ag,Cl and for Cl (cubic). It appears that it would be worth-while to pursue such measurements in the hope of correlating some of the variables.

Of the small bands isolated, Ag II and Cl II have not been reported before, while Cu III is probably the yellow band at 5800Å described by Froelich, but not the red band at 6700Å which moves to a lower wave number on cooling (17, 18).

Most of the samples considered in this paper were entirely hexagonal in structure. Table III shows considerable shifts of bands to lower wave numbers for cubic forms of ZnS with metal activators, and for a ZnS:Cl with about 50% cubic structure. Shifts of −400 to −600 cm^{-1} have been reported for this crystallographic change in ZnS:Cl, ZnS:Cu,Cl, and ZnS:Ag,Cl (19). The changes mentioned in this paragraph are all for excitation at room temperature; cooling introduces more complications.

Relations between band peak intensities.—The relative heights of the peaks vary with method of preparation of the phosphor, and with temperature of excitation. In almost every case the ratio of blue Au I to green Au II is increased by cooling to −120°C, that is, the green band is suppressed, as with Cu II. Another similarity to Cu is provided by an increase of the green band with more Au.

Modifications of the phosphor preparation, using several rates of cooling graded from instantaneous quenching in water to 16 hours' cooling in the furnace, made a progressive increase of Au II at the expense of Au I as the cooling became faster, and the more so for higher initial firing temperature.

Table I. Positions and ratios of peak intensities of component bands of ZnS: ultraviolet excitation at 25°C. Alternative values are for different samples. Cl is present in all samples

	Au (hex)	Au (cub)	Cu (hex)	Cu (cub)	Ag (hex)	Ag (cub)	Cl (hex)	Cl*
Band I	21150	20700	22400	21700	22900	22100	22250	21650 cm^{-1}
II	18550	18000	19250	18750	21000	20000	(19500)	(19100)
III	(16950)	(16500)	(17000)	(17200)				
Band I†	4730	4830	4460	4610	4370	4520	4490	4620Å
II	5390	5560	5190	5330	4760	5000	5130	5240Å
III	5900	6060	5880	5810Å				
Main peak‡ (wave length)	4710	4800	5150	5300	4350	4500	4460	4580Å
Ratio of peak energy								
I : II	1.2,1.4	1.7	0.13,0.11	0.16,0.15	6.1,9.9	7.4	8.8,9.9	9.4,9.0
I : III	9.3,6.7	16.8	4.5,2.9					

* 50:50 cubic:hexagonal.
† By direct conversion from the wave number data above.
‡ From wave-length emission curves.

Table II. Shifts of component bands of ZnS and peak intensity changes by cooling from 25° to −120°C (±10°). Separate results shown for 0.01% hexagonal are from different samples

Activator	% Metal activator	Crystal structure	Shift of peak in cm⁻¹ Band I	Band II	Band III	Change in peak intensity ratio I:II	I:III
		Hex	+350	+200	+400	1.20–1.22	9.3–8.7
			+340	+170	+250	1.41–1.55	6.7–10.0
	0.01						
		Cub	+125	+200	+150	1.7–1.7	16.8–17.6
Au,Cl	0.002	Hex	+160	+170	+250	2.55–2.23	11.1–15.6
	0.1	Hex	~ 0	~ 0		0.48–0.81	
		Hex	+225	+100	+800	0.13–0.20	4.5–3.0
			+230	+ 85	+600	0.11–0.19	2.9–2.9
Cu,Cl	0.01						
		Cub	+375	+ 80	+175	0.16–0.22	1.25–2.4
		Hex	− 10				
			+140				
			+100				
Ag,Cl	0.01						
		Cub	+150				
		Hex	−250				
			− 80				
Cl	(~0.01 Cl)						
		50:50 Cub-hex	−175				

Quenching also produced unusual results on the positions of Au I and II when the phosphor was excited at −120°C. The hexagonal form showed small or no shifts compared with excitation at room temperature, while the cubic suffered wave number decreases of 200-300 cm⁻¹ instead of the "normal" increases given in Table II.

Cathodoluminescence.—A few phosphors were examined when scanned by a defocused spot at 14 kv and 3 μa/cm². This produced an approximate doubling of the blue band at the expense of the others. Of the ZnS:Au,Cl samples, those with 0.01% Au showed shifts of all three bands, to wave numbers higher by 100-450 cm⁻¹, compared with ultraviolet excitation (see Fig. 2 for an example).

Selenium replacement in ZnS.—When Se replaces increasing proportions of S in ZnS:Au,Cl, phosphors result which resemble the (Zn,Cd)S:Au,Cl series under ultraviolet. The color changes are produced in part by the suppression of Au I and in part by shifts in the positions of Au I and II which are smaller than those found with equivalent substitution of CdS. For instance, a sample containing 27.6% of ZnSe has an emission curve which is nearly a pure Gaussian of Au II, peak 17875 cm⁻¹, and with a visual color close to that of (Zn,Cd)S:Au,Cl containing 20% CdS. At −120°C the Au I band is largely restored in relation to Au II for those phosphors with smaller ZnSe contents.

Table III. Shifts of component bands of ZnS at 25°C by change from hexagonal to cubic structure

	Band I	Band II	Band III
0.01% Au,Cl	−450	−550	−450 cm⁻¹
0.1% Au,Cl	−400	−350	
0.01% Ag,Cl	−800	−1000	
0.01% Cu,Cl	−700	−500	+200
Cl (50% cubic)	−600	−400	

(Zn,Cd)S Series with Au and Other Activators

Au *activator: preparation, composition, and spectral characteristics.*—Samples were prepared by the general method described above, replacing proportions of ZnS in the initial mixture by an equal weight of precipitated CdS, usually in multiples of a nominal 10% by weight of ZnS up to 80% CdS. The percentages of ZnS and CdS in the phosphors were determined by analysis involving the initial removal of Cd by precipitation with phenyl trimethyl ammonium iodide; the Zn was then precipitated by 8-hydroxyquinoline, followed by the standard volumetric estimation. The precipitated Cd was determined volumetrically by iodate. In the text and figures percentages of CdS given are molecular values unless stated otherwise. The analyzed CdS weight percentages were up to 4% less than the nominal values (increasing with CdS content), this difference arising largely from a small amount of ZnS present in the CdS raw material.

In appearance under ultraviolet the Au,Cl series varies from pale bluish green to very pale yellow to colors resembling those of higher members of the other series. The unsaturated color of phosphors low in CdS is very marked, but at 25% CdS the yellow fluorescence is similar to that of 10% CdS:Cu,Cl, 50% CdS:Ag,Cl, and 35% CdS:Cl. Examples of emission curves at 25° and −120°C appear in Fig. 2 and 3, and of resolution into sub-bands in Fig. 4. The peak wave numbers are plotted against molecular percentage of CdS in Fig. 6, which also includes a weight percentage plot for Au I.

Cathode-ray excitation gave results similar to those for ZnS, namely, a relatively doubled emis-

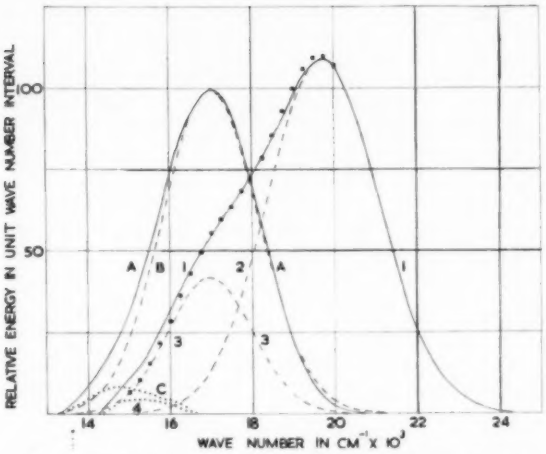

Fig. 4. Resolution of emission curves at 25°C into Gaussian sub-bands. Solid line, measured emission; broken line, Gaussian; dotted line, remainder not resolved into Gaussians; square points, sums of constituent Gaussians. 1-4: 8.5 mole % CdS: Au, Cl; A-C: 48 mole % CdS: Ag, Cl.

sion of band Au I compared with ultraviolet excitation, and band shifts between 100 and 300 cm^{-1} to higher wave numbers.

Other activators.—Samples were made with 0.01% Cu or Ag, or without metal addition, all with chloride. In the last mentioned type, analysis of well-washed samples established the residual chloride content to be 0.007% by weight in a 3.5% CdS phosphor and 0.01% in a 7% CdS phosphor, compared with 0.008% in a ZnS:Cl.

Examples of band resolution are given in Fig. 4 and 5, while peak wave number data from the complete series are presented in Fig. 7-9, where linear relations are evident as in Fig. 6. The Cu II band is also plotted on a weight percentage scale.

It will be observed that qualitatively Cu resembles Au in its band structure: to visual inspection the Cu and Au phosphors are similar in their long phosphorescence which contrasts with the short afterglow in the Ag series. There is a resemblance between the slopes of the Ag and Cl plots, but all the

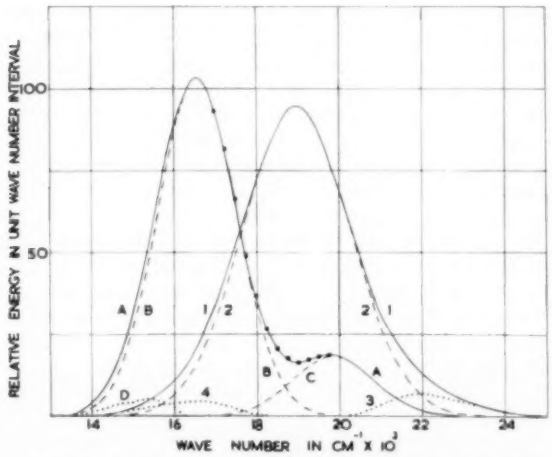

Fig. 5. As Fig. 4, at —120°C. 1-4: 20 mole % CdS:Cl; A-D: 18 mole % CdS: Cu, Cl.

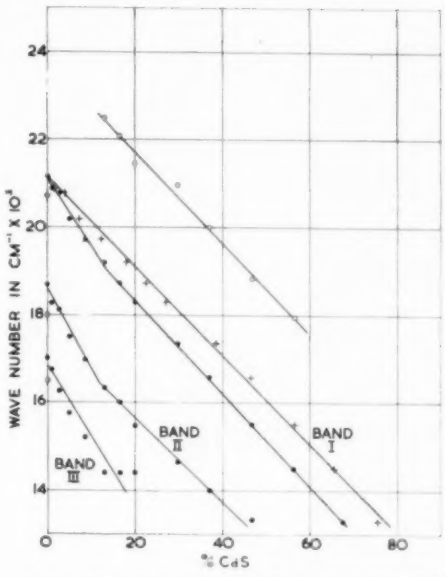

Fig. 6. Location of emission band peaks of (Zn, Cd)S: Au, Cl at 25°C. Circled points, cubic samples; open circles, low temperature peak; crosses, plot with weight percentage abscissae.

series show a break at about 15 mole % CdS. If weight proportions are used for plotting, the data for Cu and Au may be expressed by straight lines from 0 to 80% CdS, while Ag and Cl require broken lines like those in Fig. 8 and 9. These breaks occur near the point at which cubic forms can no longer be made as CdS content increases, owing to the preponderance of the hexagonal CdS structure.

Another series of samples was fired at 1100°C without metallic activator but with ZnS containing much free S, which assists the formation of the cubic structure below about 15 mole % CdS. The emission

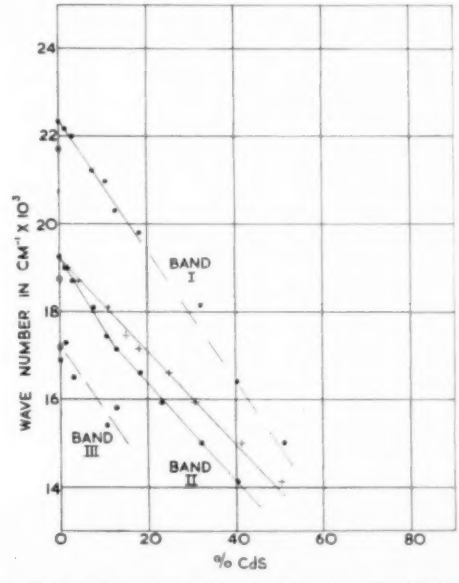

Fig. 7. Location of emission band peaks of (Zn,Cd)S:Cu, Cl at 25°C. Circled points, cubic samples; crosses, plot with weight percentage abscissae.

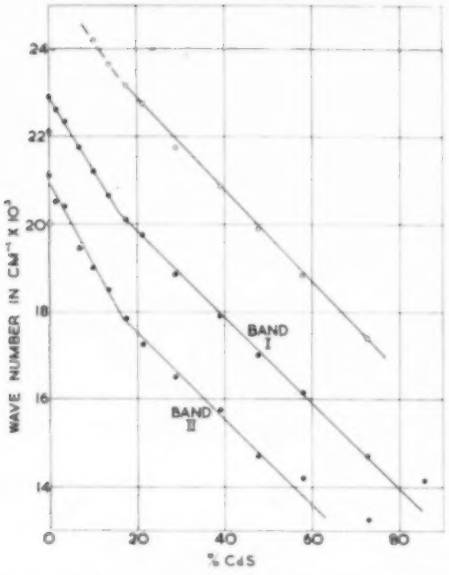

Fig. 8. Location of emission band peaks of (Zn,Cd)S:Ag, Cl at 25°C. Circled points, cubic samples; open circles, low temperature peak.

band peaks of these materials lie on the general plots above 15% CdS, but below this point the wave numbers are lower, as shown in Fig. 9 for band Cl I.

The peak intensities of the bands in the (Zn,Cd)S series with any of the four types of activator decrease as the CdS content rises to 10-15%, the fall of intensity being between 10 and 30%; a rise follows by which the values for 0% CdS may be reached or exceeded (at a CdS content of 15-30%); finally with more CdS a general fall occurs. In Fig. 2 and 3 the ordinates (except for the cathode-ray excitation example) are nearly proportional to the true intensities.

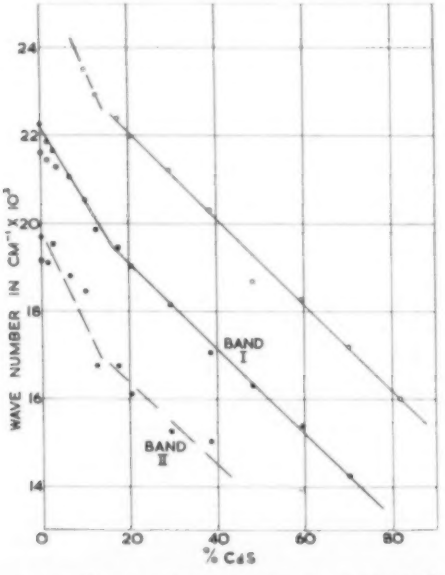

Fig. 9. Location of emission band peaks of (Zn,Cd)S:Cl at 25°C. Circled points, partially cubic samples; open circles, low temperature peak.

Table IV. Slopes of band peak plots in $-cm^{-1}$/1 mole% CdS, for main hexagonal series

Activator	Band I <15% CdS	Band I >15% CdS	Band II <15% CdS	Band II >15% CdS	Band III <15% CdS	Band III >15% CdS
Au,Cl, 25°C	152	107	180	97	174 ?	
Au,Cl, −120°	176	101	192	104	176	
Cu,Cl, 25°	150	?	158	110	150 ?	
Cu,Cl, −120°	165	125	171	113	164	
Ag,Cl, 25°	161	99	184	97		
Ag,Cl, −120°	155	97	178	101		
Cl, 25°	167	97	200 ?	95 ?		
Cl, −120°	154	95	170	98		

Low temperature effects in the (Zn,Cd)S *series.*— The emission spectra of the series with four different activators have been investigated at −120°C. When plotted in the manner of Fig. 6-9 the component band peaks lie on lines of similar slopes, and with the same breaks, as those of the corresponding bands at 25°C. These plots are not reproduced here. They show closer fit of points to lines owing to the sharper band structure at −120°C. In the case of Cu I at 25°C it is difficult to isolate this small component from the emission, and the plot in Fig. 7 is irregular. At −120°C a more normal pattern reappears; see Table IV, which summarizes all the measurements and indicates some similarity of Cu and Au on the one hand, and of Ag and Cl on the other.

The uppermost lines on Fig. 6, 8, and 9 refer to another band, not hitherto mentioned, found only at the low temperature; this is discussed in the next section.

Discussion

Reference has been made to the representation of emission band peak positions in terms of straight line plots. These varied linear relations are difficult to interpret, although their occurrence is quite striking. The data are probably not sufficiently precise to determine the exact relations which exist, but one interesting possibility is suggested below.

The emission band structure and its behavior on temperature change are important in relation to the theory of activator center structure and of energy levels. For Cu a third long wave-length band has been confirmed, and for Au three bands have been demonstrated. With both activators band II appears to be the typical one due to the metal, possibly as Cu^{+} or Au^{+} substituted for Zn^{++}. If the blue bands Cu I and Au I are assumed due to Cl producing cation vacancies, in the way that Bowers and Melamed have proposed for Cl "blue I," the anomaly arises that these bands differ from Cl I in their response to cooling (20). It is therefore suggested that, contrary to the views of Bowers and Melamed, blue Cu I and Au I are not due to the presence of cation vacancies even though all the phosphors did contain chloride. When, besides the chloride, an activating metal is also present, its effect seems to predominate.

With regard to the emission changes by cooling the main series of hexagonal phosphors, it is reasonable to attribute all the bands in ZnS and (Zn,Cd)S with Au or Cu to associated groups of acceptor levels near the valence band, whereas Cl as sole activator produces donor levels nearer the con-

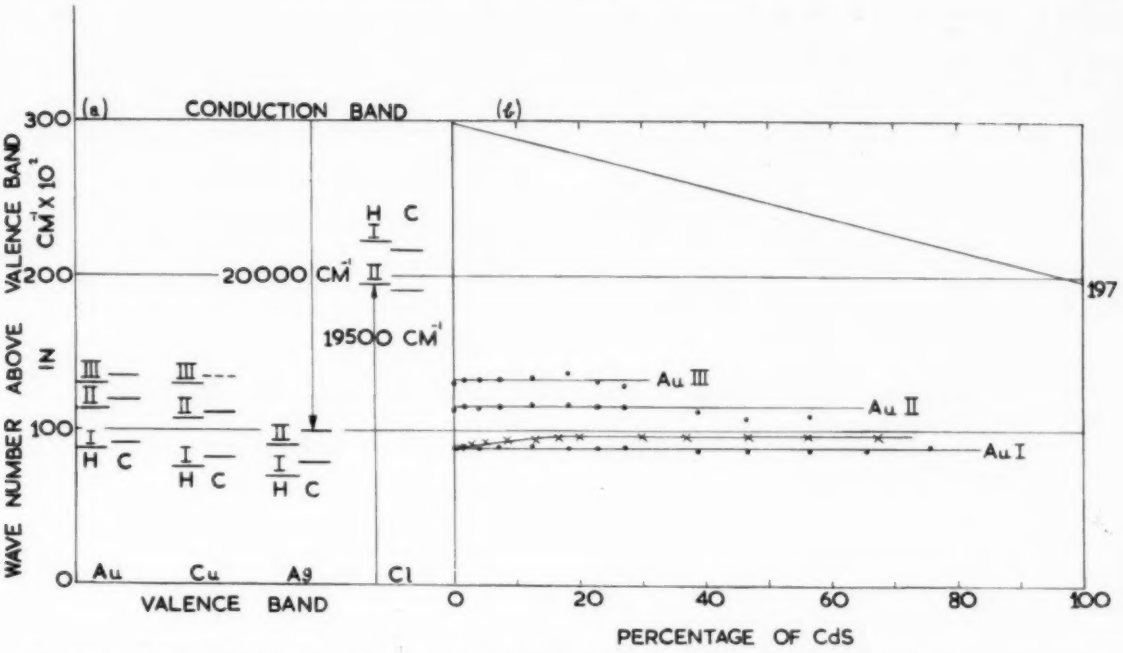

Fig. 10. (a) Energy level diagram for Cu, Ag, Au, Cl bands in ZnS at 25°C. Arrows indicate luminescent transitions; H, levels for hexagonal crystals; C, for cubic. (b) Energy level diagram for Au bands in (Zn, Cd)S. Points, plotted on weight percentage of CdS; crosses, plotted on colecular percentage.

duction band in the sense of the model of Lambe and Klick (21). These different types of radiative transition may account for the differences in temperature effects. Figure 10a gives the simplest energy diagram on these assumptions. Over the temperature range used in the work, the energy gap in the ZnS crystal increases by about 300-500 cm^{-1} according to determinations by Coogan and others (22). The observed emission band shifts on cooling suggest that the Au, Cu, and Ag levels remain nearly in the same position with respect to the valence band as the energy gap increases. In contrast, for Cl alone the levels must approach the valence band appreciably on cooling. All the shifts discussed are very small compared with the energy gap or the radiated quanta, and they are so easily altered by change of phosphor preparation method that the above details cannot be generally applicable. The approximate constancy of the separation between activator and valence band is shown better by assuming a linear variation of the energy gap between ZnS and CdS, the observed emission wave numbers being then plotted from the conduction band downward, as in Fig. 10b for the gold-activated series, where abscissae give weight percentages of CdS. A recent extensive study of (Zn,Cd)S phosphors by Hoogenstraaten develops similar ideas on activator levels (23). He refers to molecular proportions of CdS, but in Fig. 10b this scale is seen to give worse agreement with a linear relation than does the weight proportion scale; in fact the line for Au I could be drawn in two sections, as in Fig. 6, and the part above 15% CdS would be parallel to the x-axis.

A band of shorter wave length than those already discussed, and not included in the band numbering, was found only under excitation at −120°C, and for phosphors with over 10 mole % CdS. Peak locations are shown in Figs. 6, 7, and 9 on the lines which are all of the same slope (-102 ± 2 cm^{-1}/1 mole % CdS), with possibly a steeper part below 15% CdS making extrapolation difficult; however it is likely that the 0% CdS value is that attributed by Melamed (24) to the emission due to anion vacancies in cooled ZnS, namely 3950Å or approximately 25000 cm^{-1}. Similarly van Gool (24, 25) has reported a band in CdS:Ag at 6200Å or approximately 16000 cm^{-1}. The present results extrapolated would give a much higher wave length. This band did not appear with Cu activator except doubtfully in a few samples of low CdS content, and at 25°C.

There is clearly a great deal more to be discovered about the emission spectra of these phosphors and their mutual relations. Correlation with other physical parameters may be difficult or impossible but this is merely a consequence of the most striking characteristic of phosphors as a whole, namely the extreme sensitivity of their emission, both qualitative and quantitative, compared with any other measurable properties.

Manuscript received May 19, 1958.

Any discussion of this paper will appear in a Discussion Section to be published in the December 1959 JOURNAL.

REFERENCES

1. C. J. Milner, "Luminescence," Faraday Society, London, 1938, Discussion, p. 101.
2. H. W. Leverenz and F. Seitz, *J. Appl. Phys.*, **10**, 479 (1939).
3. S. T. Henderson, *Proc. Roy. Soc.* **A173**, 323 (1939).
4. F. A. Kröger and J. Dikhoff, *Physica*, **16**, 297 (1950).
5. A. Bril and H. A. Klasens, *Philips Research Repts.*, **7**, 401 (1952).

6. F. A. Kröger and J. A. M. Dikhoff, *This Journal*, **99**, 144 (1952).
7. W. Hoogenstraaten, *ibid.*, **100**, 356 (1953).
8. N. Arpiarian, *C. R. Acad. Sci. (Paris)*, **240**, 1202, 1333 (1955).
9. G. Destriau, Paper presented at Electrochem. Soc. Meeting, Washington, May 14, 1957, Abstract 24.
10. H. W. Leverenz, *et al.*, "Solid Luminescent Materials," Cornell 1946 Symposium, p. 205.
11. W. H. Byler, *J. Opt. Soc. Amer.*, **37**, 920 (1947).
12 F. A. Kröger, A. Bril, and J. A. M. Dikhoff, *Philips Research Repts.*, **7**, 241 (1952).
13. S. T. Henderson and M. B. Halstead, *Brit. J. Appl. Phys.*, **3**, 255 (1952).
14. T. B. Tomlinson, *J. Electronics*, **2**, 166 (1956).
15. R. E. Shrader and S. Larach, *Phys. Rev.*, **103**, 1899 (1956).
16. E. B. Fehr, A. I. Friedman, F. J. Studer, and G. R. Fonda, *J. Opt. Soc. Amer.*, **42**, 917 (1952).
17. H. C. Froelich, *This Journal*, **100**, 280 (1953).
18. M. H. Aven and R. M. Potter, *ibid.*, **105**, 134 (1958).
19. F. A. Kröger and J. E. Hellingman, *ibid.*, **93**, 156 (1948).
20. F. Bowers and N. T. Melamed, *Phys. Rev.*, **99**, 1781 (1956).
21. J. Lambe and C. C. Klick, *ibid.*, **98**, 909 (1955).
22. C. K. Coogan, *Proc. Phys. Soc.*, **B70**, 845 (1957).
23. W. Hoogenstraaten, Thesis, Amsterdam, Feb. 1958.
24. N. T. Melamed, *Phys. Rev.*, **107**, 1727 (1957).
25. W. van Gool, *Philips Research Repts.*, **13**, 157 (1958).

Particle Size Effects and the Distribution of Barriers in Electroluminescent Zinc Sulfide Phosphors

Paul Goldberg

Central Research Laboratories, Sylvania Electric Products Inc., Bayside, New York

ABSTRACT

The particle size of electroluminescent phosphors is found to be a significant factor in empirical equations describing brightness-voltage relationships. These observations can be understood by considering the following factors: (*a*) number and distribution of barriers in a single particle, (*b*) division among the barriers of the voltage drop per particle, and (*c*) dependence on the particle size of the voltage drop per particle. Equations are derived which permit a comparison of the brightness of different phosphors.

In the recent literature on the electroluminescence of zinc sulfide, the barrier concept finds wide support. According to this mechanism electrons are accelerated in the barrier region and cause excitation through impact ionization of luminescent centers (1-6). Radiation occurs when the ionized centers and free electrons recombine. The barrier picture is appealing for at least two reasons. First, it provides an explanation of how an electric field can raise electrons to several electron volts above their ground states without electrical breakdown of the crystals. Second, the concept of localized barriers correlates well with the observed inhomogeneous distribution of emitted light (2, 7, 8).

Information on the number and distribution of barriers is not obtained easily. This is particularly true of powder layers. Electroluminescent phosphors are reported to possess both "surface" (2) and "volume" (9) electroluminescence, reflecting possible differences in barrier distribution. The present work is one approach for obtaining information on the number and distribution of barriers in polycrystalline phosphors.

If it is assumed that the barriers are located near the surface of the particles, one may ask what happens to the electroluminescent properties as the specific surface, (i.e., particle size) is varied. To study this problem effectively, a series of electroluminescent phosphors is needed in which the members have equal chemical and physical properties but have varying particle sizes. While it is hardly feasible to synthesize separately the individual members of such a series, one promising approach is through fractionation by particle size. Most of the work presented here employed this technique.

Experimental Technique and Results

The starting materials were two phosphors representative of the blue- and green-emitting materials of Homer, *et al.* (10). These were fractionated according to particle size by settling from water or aqueous glycerine solutions. Turbulent stirring of the suspensions with a surface active agent prior to settling reduced flocculation. Also, the green-emitting phosphor was subjected to ultrasonic vibration as an added measure to break up agglomerates. Nevertheless, some aggregation undoubtedly occurred prior to settling as some of the fractions showed a plurality of log-normal distributions. Unfractionated phosphors showed only a single log-normal distribution. Individual particles were mainly globoid. A few particles showed triangular faces with rounded corners.

The measurement of the luminous emittance of the powders was made using a cell similar to that described by Lehmann with castor oil as the suspending dielectric (11). The cell dimensions were 1 x 1 x 0.005 in. A 1P22 photomultiplier was used as the detector. The phosphor concentration was held at a fixed volume fraction of 0.25 for all measurements. The experimental spread in duplicating a given emittance measurement, including factors for making the castor oil slurries, loading the cell, and aging it under an applied field, is about 10%.

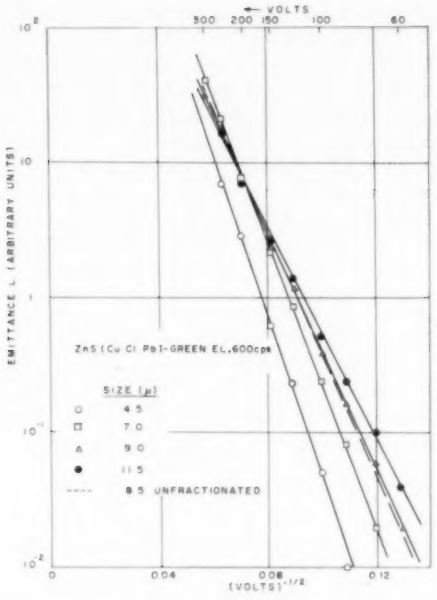

Fig. 1. Brightness-voltage characteristics of a green-emitting electroluminescent powder and some representative fractions.

It has been demonstrated by Zalm (2) and Alfrey and Taylor (3) that brightness data are well represented by straight lines when the log of the luminous emittance L is plotted vs. $V^{-1/2}$, where V is the rms applied voltage. Figure 1 shows the emittance-voltage data of four fractions and of the unfractionated green-emitting electroluminescent powder plotted in this way for a frequency of 600 cps. There is a distinct regularity in the variation of the slopes and the apparent intercepts with particle size. Variations in the emittances of up to an order of magnitude at 60-70 v are evident. Figure 2 shows the data taken at 6000 cps for the blue-emitting phosphor, with a similar result. For both phosphors the effect has been observed at other frequencies in the range 60-6000 cps.

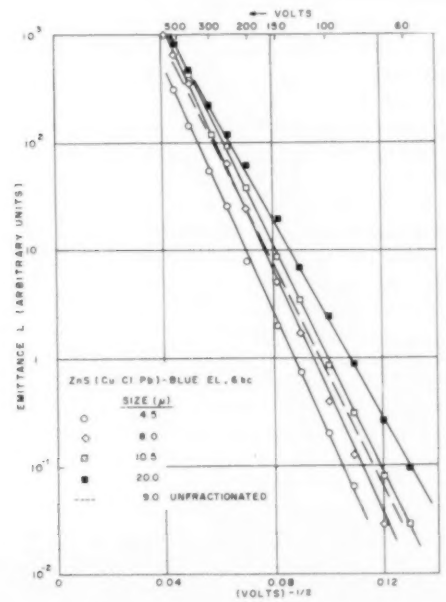

Fig. 2. Brightness-voltage characteristics of a blue-emitting electroluminescent powder and some representative fractions.

Analysis of Results

An attempt will be made to analyze the emittance data in terms of the luminous flux from each particle. This flux itself originates at point sources of emission. We shall assume that a potential barrier exists at each point source and the flux from it is determined by the voltage drop, V_B, across the barrier. V_B will be determined largely by the voltage applied to the cell. However, it may have different values depending on the particle size and the number and distribution of barriers in each particle. The procedure will be to evaluate V_B for a given applied voltage and for different types of distributions. We then may express the dependence of the flux from each point source on the applied voltage and the parameters describing the particular distribution of barriers. The emittance of the cell is obtained by summing the flux from each point source in a particle and then summing the contributions to the total emittance from each particle in the cell. Lehmann discussed this approach but did not attempt a quantitative development (12) .

For the a-c case, V_B will vary with time during a cycle and, therefore, we must visualize it as corresponding to an average value. Zalm (2) and Alfrey and Taylor (3) have discussed this point and also the factors which determine how much of the voltage applied to the crystal appears across the barrier.

The voltage dependence of the luminous flux from the individual point sources will be assumed to be of the same form as the dependence of the emittance of the whole cell.[1] Thus the flux F_B from one point source of those making up a given particle is

$$F_B = F_o \exp\left(-b'/V_B^{1/2}\right) \qquad [1]$$

where F_o and b' are parameters which are independent of voltage.

To evaluate V_B in terms of the voltage applied to the crystal we shall assume that the electroluminescent layer is represented by a mixture of two homogeneous dielectrics. The phosphor phase is considered to be a rectangular array of cubic phosphor grains of uniform size dispersed in the insulating medium between plane parallel electrodes in the manner shown in Fig. 3. Following Roberts (12), the electric field in a particle E_p is proportional to the mean applied field E_m through a factor dependent upon the ratio, r, of matrix and phosphor dielectric constants, and the volume fraction v of the phosphor, i.e., $E_p = E_m \cdot f(r, v)$. The voltage drop V_p across one of the cubes in Fig. 3 is thus

$$V_p = (Va/l) \cdot f(r, v) \qquad [2]$$

where V is the applied voltage, l the distance between electrodes, and a the cube edge.

At this point some choice must be made as to the

[1] Zalm (2) measured the flux from single grains of electroluminescent ZnS and showed that the dependence of the emission from single grains follows closely that of the composite cell.

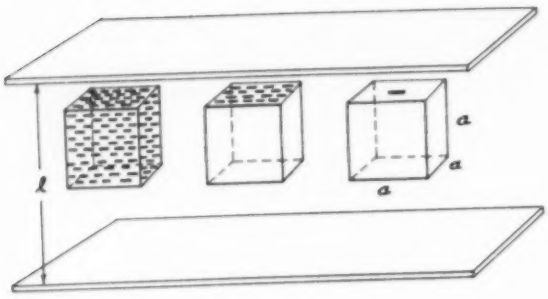

$F_B \sim \exp(-bV_B^{-1/2})$

Fig. 3. Schematic diagram of electroluminescent particles with (a) volume distribution of barriers, (b) surface distribution of barriers, and (c) a constant number of barriers per grain, unity in the case pictured.

distribution of potential barriers in the particle. The choice of the distribution will determine how much of the voltage applied to the crystal as a whole will appear across each barrier and, therefore, governs the magnitude of the luminous flux from the region near each barrier. Three cases will be considered: (*a*) uniform distribution of barriers throughout the volume of the grain; (*b*) uniform distribution of barriers over the surface of the grain; and (c) constant number of barriers per grain regardless of dimensions.

These cases are represented schematically in Fig. 3 and considered in detail below.

(*a*) *Uniform distribution of barriers throughout the crystal volume.*—Let the volume density of a system of identical barriers be n_v/cm³. Then along a line of force through a crystal with rectangular orientation relative to the electrodes there will be $n_v^{1/3}$ barriers per cm.[2] In a crystal of edge a cm there are $n_v^{1/3}a$ barriers through the crystal in the direction of the applied field. Dividing the V_p by this number of barriers gives for the voltage drop per barrier

$$V_B = V_p/n_v^{1/3}a = (V/ln_v^{1/3}) \cdot f(r, v) \qquad [3]$$

and substitution in Eq. [1] gives for the luminous flux from the region near each barrier

$$F_B = F_s \exp[-b/(V/ln_v^{1/3})^{1/2}]; b \equiv b'/f^{1/2}(r, v) \quad [4]$$

There are $n_s a^2$ barriers in the grain and the total flux F_p from the particle is $F_p = n_s a^2 F_B$. For a volume fraction of phosphor v in the suspending dielectric the number of grains N per cm³ of suspension is v/a^3. The flux per cm² of suspension is $F = F_p v/a^3 = vn_s F_B$ or from Eq. [4]:

$$F = vn_s F_s \exp[-b/(V/ln_v^{1/3})^{1/2}] \qquad [5]$$

The luminous emittance L from a layer of the suspension l cm thick is proportional to $F \cdot l$ and therefore

$$L \sim vn_s lF_s \exp[-b/(V/ln_v^{1/3})^{1/2}] \qquad [6]$$

Thus, as the particle size a does not occur in Eq. [6], neither the intercepts nor the slopes of data plotted as in Fig. 1 should depend on particle size for grains with a volume distribution of barriers.

(*b*) *Uniform distribution of barriers on the surface of the grains.*—Let us next consider the barriers to be distributed over the surface of the grains at a concentration of n_s barriers per cm². The number of barriers on one cube face is $n_s a^2$. Also, as there is only one barrier along any line of force perpendicular to the surface, the full voltage applied to the grain will appear across each barrier.[3] Thus, $V_B = V_p = (Va/l)\, f(r, v)$. Therefore from Eq. [1]:

$$F_B = F_s \exp[-b/(Va/l)^{1/2}] \qquad [7]$$

The flux from each particle is $F_p = n_s a^2 F_B$. The total flux per cm² is $F = vn_s F_B/a$ and the emittance is given by

$$L \sim (vn_s lF_s/a) \exp[-b/(Va/l)^{1/2}] \qquad [8]$$

Here both the slope and intercept of log L vs. $V^{-1/2}$ will vary with particle size. It is seen from Eq. [8] that for all particle sizes, plots of log (La) vs. $(Va/l)^{-1/2}$ should be coincident.

(*c*) *Constant number of barriers per grain.*—Next let us visualize a specific number of barriers, n, to exist on the surface of each particle and let n be constant for all particle sizes. The entire voltage drop per crystal is across the barrier as in case (*b*), and again $V_B = V_p = (Va/l)\, f(r, v)$. The total flux per particle is

$$F_p = nF_s \exp[-b/(Va/l)^{1/2}] \qquad [9]$$

and

$$L \sim (vnlF_s/a^3) \exp[-b/(Va/l)^{1/2}] \qquad [10]$$

where again

$$b \equiv b'/f^{1/2}(r, v)$$

Here too, both the intercept and the slope of log L vs. $V^{-1/2}$ vary with particle size. In contrast to the previous section, plots of log (La^3) vs. $(Va/l)^{-1/2}$ for various particle sizes should be coincident. The data in Fig. 1 and 2 eliminate the possibility of a volume concentration of barriers, as prominent particle size effects are evident. The model of a surface density of barriers is also not satisfied by the data, as Fig. 4 shows a test of Eq. [8] for the fractions in Fig. 1. While the slopes of separate fractions show some degree of uniformity in Fig. 4, there is still a wide discrepancy among the intercepts. Good agreement with case (c) is found for the data of Fig. 1. The application of Eq. [10] to these data is shown in Fig. 5. The simple model of a constant number of barriers per grain fits well for this phosphor.

While the blue-emitting phosphor of Fig. 2 shows pronounced particle size effects, the data are not satisfied by Eq. [10]. This is seen in Fig. 6; a dependence of slope on particle size still persists. For this phosphor it can be shown that the slopes in Fig. 2 vary roughly as $a^{-1/3}$.

The development presented above can also be tested with unfractionated phosphors of differing mean particle size. Figure 7 shows a plot of the slope of (log L vs. $V^{-1/2}$) vs. $a^{-1/2}$ for a group of blue-emit-

[2] The number of barriers in the direction of the lines of electrical force will actually be proportional to $n_v^{1/3}$. Setting the number of barriers/cm equal to $n_v^{1/3}$ simply introduces a different arbitrary constant at a later point.

[3] We visualize the barriers on only one side of the crystal to be operative during one half cycle of a.c. and those on the opposite side during the following half cycle.

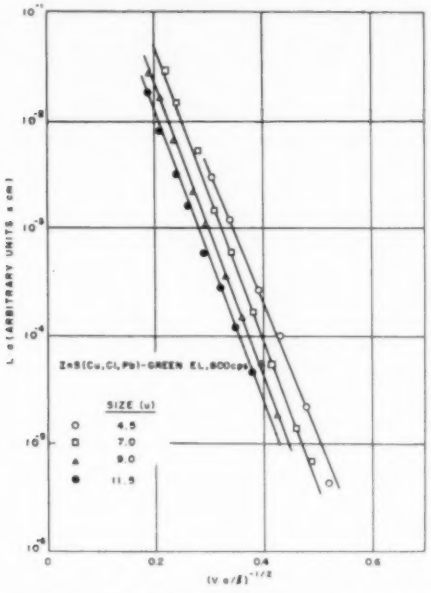

Fig. 4. Test of Eq. [8] corresponding to a surface density of barriers (case b). Data are taken from Fig. 1.

ting phosphors of the ZnS:Cu, Cl, Pb or ZnS:Cu, Cl type. The data fall close to a straight line with a slope greater than zero. This eliminates the possibility that the group is characterized by a volume distribution of barriers. It is not possible, however, to distinguish between cases (*b*) and (*c*) for these phosphors.

It should be mentioned that, for a given field strength, Eq. [10] predicts a particle size a_m which gives maximum emittance: $a_m = b^2/36(V/l)$. This condition arises from the fact that as a decreases, the number of emitting particles per cm^3 increases.

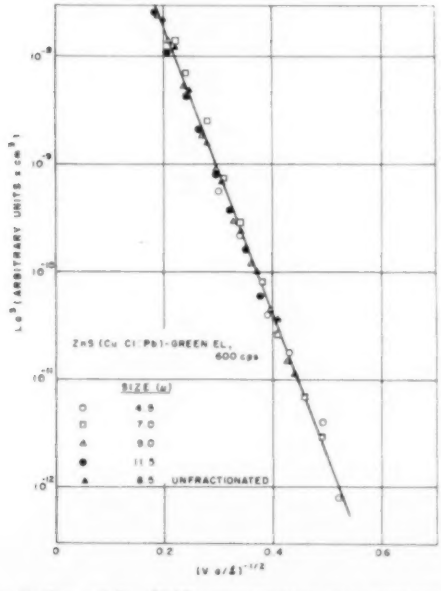

Fig. 5. Test of Eq. [10] corresponding to a constant number of barriers per grain (case c) for the data of Fig. 1.

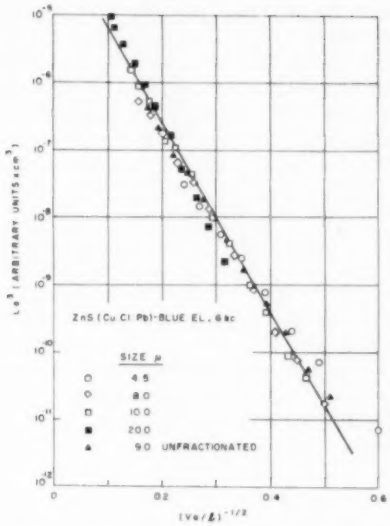

Fig. 6. Test of Eq. [10] corresponding to a constant number of barriers per grain (case c) for the data of Fig. 2.

At the same time however, the luminous flux per particle decreases with decreasing particle size.

Discussion

The data presented above show that the particle size is a significant factor in the brightness-voltage characteristics of electroluminescent phosphors. Limited agreement is obtained between the data and a simple theory based on a specific distribution of barriers in the phosphor particles. For both the fractionated green-emitting phosphor and the unfractionated group of Fig. 7 the slopes of the exp $(V^{-1/2})$ lines vary as $a^{1/2}$. In particular, the data for this fractionated phosphor support case (*c*) corresponding to a constant number of barriers per grain. It should be emphasized that this concept, being derived as it is from the emittance data, applies only to the barriers which are active in the excitation processes. Other barriers or similar physicochemical constructs may be present in the particles but are not revealed by the emittance data.

The reasons for the failure of the blue-emitting phosphor of Fig. 2 to show the same detailed behavior as the green-emitting one are not clear. The assumptions regarding the identity of chemical com-

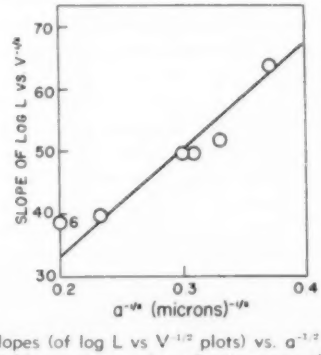

Fig. 7. Slopes (of log L vs $V^{-1/2}$ plots) vs. $a^{-1/2}$ for some unfractionated blue-emitting electroluminescent phosphors with various thermal histories and particle sizes.

position of the fractions and the existence of a simple distribution of barriers possibly need closer examination. Poor separation during fractionation may also be a factor as the blue-emitting phosphor did not have the benefit of ultrasonic dispersion prior to settling.

The development assumes that for barriers distributed as in cases (*b*) and (*c*), the voltage drop per barrier V_s will be determined largely by the grain size. This concept finds support in the work of Waymouth and Bitter (8), who studied the effects of geometric crystal orientation, relative to the field vector, on the emission from individual particles. They examined particles of elongated shape in which single spots of emission could be observed. These spots were brightest when the field was parallel to the long axis of the particle. One possible interpretation of this from the present work is that the elongated particle exhibits the greatest "effective particle size" when oriented parallel to the field, causing V_s and therefore F_s to be larger than for any other orientation.

We can only speculate at present on the number of barriers per grain for case (*c*). The choice of one barrier per grain is attractive. Waymouth and Bitter examined a large number of single grains of phosphors also synthesized by the method of Homer, *et al.* (10) and observed brightness waves with only one major emission peak per cycle. If more than one barrier were operative in a crystal, then emission during each of the two half cycles would be expected.

In practical electroluminescent cells the grains are not cubic and perfectly oriented. However, the aim of the development is to produce the correct functionality in equations relating light output to particle size. Absolute values are not of concern. The shape might have been taken to be something other than cubic with the same result; the cube of a characteristic linear dimension would enter into the pre-exponential factor in Eq. [10] and as the negative ½ power in the exponential term, regardless of particle geometry. Neither does the fact that only polydisperse materials can be obtained by fractionation limit the validity of the arguments. It is seen that the unfractionated powder behaves as if it were a fraction with the effective particle size equal to the average.

It is possible to employ the present analysis in several ways. First, it provides a possible approach to distinguishing between classes of phosphors possessing dissimilar distributions of barriers. However, the equations do not provide means for distinguishing between surface and volume barriers. For instance, Eq. [10] can be obtained by choosing a small value for the number of barriers in each grain and distributing them throughout the volume. If the density of such barriers is low, so that a single line of force through the crystal sees only one barrier, then the equation so derived is exactly of the same form as Eq. [10]. For other phosphors, distributions not considered here may be of importance.

Second, if the distribution of barriers can be established, the characteristics of phosphors with different particle sizes can be compared, with allowance for size. Thus if the data for a pair of phosphors are plotted as in Fig. 4, comparison of the ordinates for a specified value of the abscissa gives a measure of the relative light output corrected to the same particle size and applied field.

Third, it may be possible to employ the analysis for a better understanding of the factors which influence the efficiency of the excitation process. Figure 7 shows that a constant slope exists for several electroluminescent phosphors of the ZnS:Cu, Cl type. Theoretical arguments have been advanced which state that the slopes are related to the probability that an electron accelerated in the region of a potential barrier will result in impact ionization (2, 3). Changes in the composition of the phosphor which change the slopes may yield information on the chemical and physical factors which govern the properties of the barriers.

Acknowledgments

It is a pleasure to thank B. E. Bartels, D. R. Frankl, A. K. Levine, A. L. Solomon, and R. N. Summergrad for stimulating and helpful discussions. Thanks are also due D. H. Baird for reading the manuscript and suggesting improvements. The aid of J. T. Ragusin and G. Klecak in the fractionations and the particle size determinations is gratefully acknowledged.

Manuscript received May 23, 1958. This paper was prepared for delivery before the New York Meeting, April 27-May 1, 1958.

Any discussion of this paper will appear in a Discussion Section to be published in the December 1959 JOURNAL.

REFERENCES

1. G. Destriau and H. F. Ivey, *Proc. I. R. E.*, **43**, 1911 (1955).
2. P. Zalm, *Philips Research Repts.*, **11**, 353 (1956); **11**, 417 (1956).
3. G. F. Alfrey and J. B. Taylor, *Proc. Phys. Soc.*, **B78**, 775 (1955).
4. W. W. Piper and F. E. Williams, *Brit. J. Appl. Phys.*, Supplement No. 4, S39 (1955); *Phys. Rev.* **87**, 151 (1952).
5. D. R. Frankl, *Phys. Rev.*, **100**, 1105 (1955); *Sylvania Technologist*, **9**, 6 (1956).
6. G. F. Neumark, *Sylvania Technologist*, **10**, 29 (1957).
7. S. Roberts, *J. Opt. Soc. Amer.*, **43**, 590 (1953).
8. J. F. Waymouth and F. Bitter, *Phys. Rev.*, **95**, 941 (1954).
9. A. H. McKeag and E. G. Steward, *This Journal*, **104**, 41 (1957).
10. H. H. Homer, R. M. Rulon, and K. H. Butler, *ibid.*, **100**, 566 (1953).
11. W. Lehmann, *ibid.*, **103**, 24 (1956).
12. W. Lehmann, *ibid.*, **103**, 667 (1956).

A Method for the Purification of Selenium

S. Nielsen and R. J. Heritage

Royal Radar Establishment, Great Malvern, England

ABSTRACT

A method has been worked out for purifying selenium based on the formation and decomposition of hydrogen selenide. Details of an apparatus capable of producing about 10 g/hr of extremely high purity selenium are given. Several analytical methods used in examining the product are outlined.

Selenium is recovered industrially from two main sources (*a*) flue dust obtained in burning pyrites in the manufacture of H_2SO_4, and (*b*) anode slimes from electrolytic refining, particularly of Cu. Usually the crushed ore is roasted in air and the SeO_2 formed, sublimes, and is collected in water. Selenium is recovered from this solution by reaction with SO_2 according to the equation

$$H_2SeO_3 + 2SO_2 + H_2O = Se + 2H_2SO_4$$

Material prepared in this way is approximately 99.5% pure, the main impurities being S and Te (1).

Further purification has been achieved in several ways. Henkels (2) recommended a 4-stage procedure: (*a*) distillation of the Se at atmospheric pressure, (*b*) conversion to SeO_2, (*c*) purification of the SeO_2 by sublimation, (*d*) recovery of the Se by reaction of the dioxide with gaseous ammonia according to the equation

$$3SeO_2 + 3NH_3 = 3Se + 2N_2 + H_2O$$

High purity Se has also been produced commercially by the ammonia reduction of SeO_2, which has been prepared by the catalytic vapor phase oxidation of Se (3). A recent patent (4) pointed out that selenium could be obtained spectrographically pure by a direct solution method. In this process Se was dissolved in a hot aqueous solution of sodium sulfite and a small quantity of aluminum sulfate solution added. Aluminum hydroxide precipitated, carrying with it impurities present in the solution. After filtration, purified Se was precipitated on cooling. Nijland (5) recommended a sublimation procedure at a pressure of 10^{-3} mm Hg and claimed that sublimation was much better than distillation. Also methods based on the purification of SeO_2 in solution using ion exchange resins have been used (6).

Distillation and sublimation techniques are to be preferred since they are simple and the purification of other chemicals is not required. However our experiments with radiotracers suggested that to achieve a significant reduction in impurities repeated sublimation would be necessary. Our attempts to purify Se by zone melting were also without success.

Selenium doped with 10 ppm of radioactive Cu and Sb was sublimed in a simple tube-type apparatus. The results indicated that the Cu content of the sublimate was reduced to about 0.5 ppm and the Sb content to about 0.2 ppm.

An ingot of Se which had been previously doped with 100 ppm of each of the impurities shown in Table II was zone-melted in a sealed evacuated silica tube. After 30 passes, samples taken from along the ingot were examined spectrographically, but no movement of impurities could be detected. The ingot length was ~30 cm, the zone length ~2 cm, although there was a pronounced tendency for supercooling, and the rate of zone travel was 5 cm/hr.

These experiments suggested that neither sublimation nor zone melting processes were particularly effective, and we report here a new method which we believe to provide very pure Se. The method involves the formation and decomposition of H_2Se. Hydrogen selenide is formed by bubbling purified hydrogen through molten Se at 650°C. The H_2Se is decomposed by passing the gas through a silica tube maintained at 1000°C. With a suitably constructed tube about 70% of the selenide is decomposed. Undecomposed H_2Se is condensed in a liquid air trap and later allowed to recirculate through the decomposition tube. In this way practically all the H_2Se is decomposed. The Se liberated is collected by melting into a silica crucible.

The only other elements likely to form hydrides under these conditions and consequently those likely to be impurities in the final material are F, Cl, Br, I, O, S, Te, P, As, and Sb. The first 6 of these elements form hydrides more readily than Se and the others less readily. Further, the hydrides of the first 6 are less easily decomposed at 1000°C than H_2Se, while the others are more easily decomposed (cf. Table I). The difference in stability is utilized in this process. Further purification of the H_2Se could be obtained by fractional distillation (cf. Table I) or gas chromatographic procedures, but we have not found these necessary.

The advantage of the process lies in the purity which can be obtained in one operation. For instance, it has been shown using radiotracers that, if 1 ppm of the Cu or Sb is added to the starting material, there is an improvement of the order of 10^4. It is clear also that very low grade Se can be purified in this way. A serious disadvantage, however, is that H_2Se is very toxic and consequently care must be

Table I. Physical properties of hydrides

	HF	HCl	HBr	HI	H_2O	H_2S	H_2Se	H_2Te	H_3N	H_3P	H_3As	H_3Sb
MP	−92.3	−112	−88.5	−50	0	−82	−64	−51	−77	−133	−113	−88
BP	+19.4	−84	−67	−35	100	−61	−42	−4	−33	−87	−55	−17
Approx. % decomp. at 1000°C	—	10^{-2}	10^{-1}	35	0	15	75	10^2			10^2	10^2

taken to avoid leakages when assembling and handling the apparatus.

Apparatus

The general arrangement of the apparatus, as illustrated in Fig. 1, is described below, followed by details of the individual units. Hydrogen is purified (H_2 purifier) and bubbled through molten Se where a portion is converted into H_2Se (H_2Se generator). The gas stream then passes though trap I at 300°C and through trap II at −20°C. During the first ½ hour's operation the gas is led direct to waste with taps B and D being open and taps C and E closed. After this time, tap D is closed and C and E opened and the gas stream is led into condenser I. This is maintained at −196°C by surrounding it with liquid nitrogen when H_2Se is condensed. When a suitable quantity of H_2Se has been collected, the hydrogen flow is stopped, taps A and B are closed, and the H_2Se is allowed to evaporate into a silica tube maintained at 1000°C (decomposition tower). In this tower H_2Se is cracked into its elements and the Se is collected by melting into a silica tube. Most of the undecomposed H_2Se is trapped in condenser II which is surrounded by liquid nitrogen and any which passes through this is converted into copper selenide by bubbling through a solution of copper sulfate (waste). After the H_2Se in condenser I has been passed through the tower, tap E is closed and D opened and the selenide in condenser II is allowed to evaporate through the decomposition tower in the reverse direction. Any undecomposed H_2Se then passes into waste where it is converted into copper selenide.

Periodically, crude Se is added to the generator and the purified Se collected from the tower. Hydrogen selenide can be recovered from waste by reaction of the copper selenide with acid.

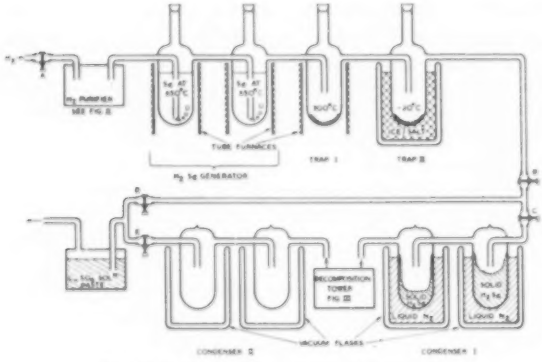

Fig. 1. General arrangement of apparatus

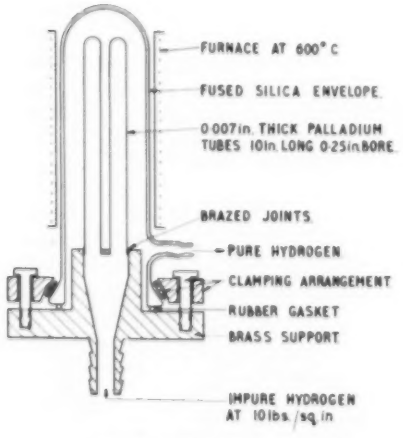

Fig. 2. Hydrogen purifier

Hydrogen Purifier

We have used oxygen-free hydrogen which has been further purified by passing through a palladium diffusion unit (Fig. 2) followed by a liquid air trap. In most of our experiments, a flow rate of 2 l/hr was maintained. When flow rates of 10 l/hr were used the hydrogen was purified by passing through a "Deoxo" catalytic purifier[1] again followed by a liquid air trap.

Generator

The purified hydrogen is passed through molten Se in a simple trap-type apparatus illustrated in Fig. 1. The apparatus is made of fused quartz and contains 150 g of crude Se. The Se is introduced in pellet form via a long arm closed with a rubber bung. For the first ½ hour's operation the Se is maintained at 550°C and after this time at 650°C.

A temperature of 550°C is used initially when volatile materials and elements which react readily with hydrogen are expelled from the Se, these being sent direct to waste. During the remainder of the operation a temperature of 650°C is maintained. At this temperature the reaction $H_2 + Se = H_2Se$ precedes more rapidly than at 575°C, the temperature at which the concentration of H_2Se in the equilibrium mixture is greatest (7). Actually we have used two generators coupled in series to insure that a near equilibrium concentration of H_2Se is attained. The fact that the second generator does not lose weight suggests that this may be so. Under these conditions, we expect those materials such as the halides, oxygen, and sulfur, which form hydrides more readily than selenium, to be removed during the preliminary ½ hr at 550°C. We have found from doping experiments that Te, As, and Sb are not carried over under the normal experimental conditions. The only

[1] Made by Baker Platinum Ltd.

impurities likely to be present in the gas stream leaving the generator are volatile materials such as hydrocarbons, etc., not removed by the preliminary stage and particles which are carried along in the gas stream.

Impurity Traps

Trap I is maintained at 300°C such that any hydrides of As, Sb, and Te which may be present would be decomposed. Trap II is cooled in an ice/salt mixture at −20°C to collect any particles carried over in the gas stream and any vapors which may be condensed at this temperature, e.g., mercury or water. Both the traps are of the same design as the generator and made of fused quartz (cf. Fig. 1).

Condensers

The gas stream is then passed into condenser I which is maintained at −183°C. The condensers are made of quartz, and a very simple design such as illustrated in Fig. 1 is satisfactory. Two condensers of 300-ml capacity, coupled in series could be used with the generator for about 4 hr. After this time, the H_2Se is allowed to evaporate over into the decomposition tower. The condensation and subsequent distillation result in further purification of the H_2Se and also enable the gas to be recirculated through the tower.

Decomposition Tower

From preliminary experiments we found that a decomposition tower of the type illustrated in Fig. 3 was very satisfactory. It appeared that the H_2Se needed to be raised to 1000°C and then the products cooled rapidly, so that they did not reform H_2Se. Selenium condenses at points shown in Fig. 3 and is melted with a bunsen burner into a silica collecting crucible.

Under equilibrium conditions, at 1000°C, about 75% of the H_2Se is decomposed. Table I indicates the extent to which the other hydrides decompose at 1000°C. From this, it is suggested that only sulfur and iodine may appear in the final product, and the concentrations of these will be appreciably reduced.

Any H_2Se which escapes the condensers, passes into waste. This consists of two bubblers. The first bubbler contains 50% H_2SO_4 to prevent water and oxygen diffusing back into the tower. The second contains copper sulfate solution in which the H_2Se decomposes according to the reaction $H_2Se+CuSO_4=CuSe+H_2SO_4$. Periodically the copper sulfate is renewed.

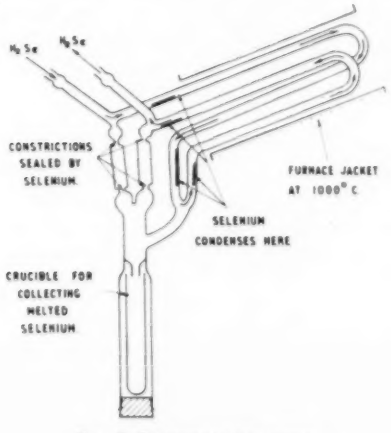

Fig. 3. Decomposition tower

Taps and Assembly

The units of the apparatus have been sealed to each other, but the final assembly is fragile. We have found it more convenient to use polythene, silicone rubber, or rubber tubing to connect the units. The tubing quickly becomes coated with a layer of Se which would tend to reduce any possible exchange reaction. The separate units are cleaned by soaking in a mixture of HNO_3 and HF, washing with metal-free water and finally with distilled acetone. The units are heated to a high temperature in air to remove adhering liquid and then heated by a flame when assembled in the apparatus with a stream of hydrogen passing through.

Results

The efficiency of the process was estimated by weighing the generator before and after an experiment and weighing the amount of purified Se obtained. In a typical experiment the following results were obtained: 28 g of Se was used in the generator and the H_2Se produced was trapped in condenser I. When this was allowed to evaporate through the tower, 20 g (70%) of Se was formed. Undecomposed H_2Se which was trapped in condenser II was recycled through the tower and yielded a further 4 g (14%) Se. The total yield of the process was, therefore, 84%. In an experiment not using condenser I, the gas mixture leaving the generator being passed directly into the decomposition tower, the following typical figures were obtained: 33 g of Se was used in the generator and 21 g (64%) of Se was obtained after passing through the tower. The undecomposed H_2Se trapped in condenser II was recirculated through the tower and a further 8 g (24%) produced, giving a total yield of 88%. The efficiency of the process is seen to be high and yields near 100% are possible if the undecomposed H_2Se is recirculated through the tower after condensing.

Analytical Tests

1. Selenium doped with 100 ppm of each of the elements Cu, Hg, Pb, Sn, Ag, Bi, Fe, Si, and 500 ppm

Table II. Results of analytical test No. 1

Impurity	Initial ppm	Final	Detection limit ppm
Cu	100	Not detected	0.2
Hg	100	Not detected	1
Pb	100	Not detected	1
Sn	100	Not detected	10
Ag	100	Not detected	0.1
Bi	100	Not detected	20
Fe	100	?*	10
Si	100	?*	20
As	500	Not detected	300
Sb	500	Not detected	50
Te	500	Not detected	200

* Traces of these were also visible with blank electrodes.

of As, Cb, and Te was used in the generator and the purified Se examined spectrographically. Ten-mg samples of Se were arced at 6 amp D.C. between graphite electrodes on Hilger Medium Quartz Spectrograph. Results are given in Table II. The limit of detection of the process was obtained by successive dilution of the doped Se.

2. Selenium doped with 1 ppm of radioactive Sb and Cu (separately) was used in the generator. After operation, traps I and II, condensers I and II, and the purified Se were examined for radioactivity. Quantitative estimation of the impurity content was obtained by dissolving the Se in HNO_3 and using a solution counting method.

3. The Li, Na, and K content of the purified Se was examined, using an Evans flame photometer. Samples of Se (10 g) were dissolved in concentrated HNO_3 (30 ml) and the solution evaporated to dryness. Selenium dioxide was then sublimed at 300°C. The residue was taken up in warm metal-free water (10 ml) and examined in the photometer. Calibration, using a series of standards, indicated that the galvanometer reading on the photometer varied linearly with concentration in the ranges 0-1 ppm for Na, 0-3 ppm for Li, and 0-5 ppm for K, with a standard deviation of ±0.05, ±0.1, and ±0.1 ppm, respectively. These tests also indicated that Na, Li, and K, were not lost during the evaporation of SeO_2. Results with purified Se are given in Table III.

4. Copper, silver, mercury, tin, zinc, lead, indium, and bismuth in the purified Se were estimated using the following procedure. Selenium (5 g) was dissolved in warm concentrated HNO_3 (20 ml) and the solution adjusted to pH 9.5 with ammonia. The solution was then extracted with 5 ml of a 0.005% solution of dithizone (diphenylthiocarbazone) in chloroform. The chloroform extract was then allowed to drip on to a sample of ammonium sulfate (5 mg) maintained at 85°C. The chloroform evaporated leaving the solute adsorbed on the ammonium sulfate; this was then arced on the spectrograph as described previously. Checks on the limit of detection were made by introducing impurities as nitrates into the solution of Se in HNO_3. Results are given in Table III. We found that it was necessary to redistill all the reagents in quartz apparatus and to carry out all operations in quartz vessels to avoid pickup of traces of impurity from glass. It was also advantageous to work in clean laboratory with still air.

5. We are also greatly indebted to the Boliden Mining Co., Skelleftehamn, Sweden, for the analytical results presented in Table IV, which, we understand, were obtained by a modified spectrographic technique.

Analytical Results

The results of the analytical experiments are shown in Tables II and III.

Our analytical techniques could detect no difference in the impurity content of the final Se whether the H_2Se was condensed before entering the decomposition tower or allowed directly through.

In the experiments with radioactive Cu no trace of radioactivity could be detected in the final Se or in any part of the apparatus except the generator.

Table III. Results of analytical tests Nos. III and IV

Method	Impurity	ppm in purified selenium	Detection limit ppm
Flame photometer	Li	Not detected	0.07
	Na	0.25	0.02
	K	0.3	0.10
Dithizone Extraction and spectrograph	Zn	Not detected	1
	Cu	0.04	0.04
	Ag	0.04	0.04
	Pb	Not detected	0.4
	Hg	Not detected	0.5
	Bi	Not detected	1
	In	Not detected	2
	Sn	Not detected	1

As 1 ppm of Cu was used, this means less than 2×10^{-5} ppm was present in the purified Se. Using radioactive Sb, however, a trace of activity was found in trap II and the final material appeared to contain about 10^{-5} ppm. Selenium obtained when H_2Se from condenser II was recycled through the decomposition tower showed no trace of activity.

Combined results of the analysis suggest that traces of Na, As, Pb, and Cu may be present in the purified material. Although the total amount of impurity appears to be small, the difficulty of analysis at these concentrations precludes an accurate estimate.

Discussion

If Cu is regarded as typical of cations which do not form hydrides, then the experiment using radioactive Cu indicates that such cations are not carried over during the purification procedure. The presence of Cu shown by direct analysis suggests that it has either been picked up from the silica apparatus or has been introduced during the transfer operation. We have also found it extremely difficult to remove traces of Cu from the reagents. It is probable that the other cations indicated by the analysis are also introduced in these ways. The experiment with radioactive Sb suggests that traces of the hydride of Sb may be formed during the experiment but an improvement of 10^5 may be expected.

It is not certain, at present, whether the As present in the final material has been transferred as the hydride or is due to pickup from the silica apparatus, in which it is known to be present. The absence of detectable S and Te in the product is encouraging

Table IV. Results of the Boliden analysis

Impurity	Impurity content in sample	Detection limit ppm	Impurity	Impurity content in sample	Detection limit ppm
Ag	Not detected	0.03	Ca	Not detected	1
Cu	0.20 ppm	0.1	Cr	Not detected	0.3
Hg	Not detected	0.5	Mg	Not detected	0.3
Fe	0.60 ppm	0.3	Mn	Not detected	0.1
K	Not detected	0.3	Ni	Not detected	0.3
Na	0.40 ppm	0.1	Pb	0.6 ppm	0.3
Te	Not detected	1	Sb	Not detected	1
Al	Not detected	0.3	Si	Not detected	1
As	1.0 ppm	1	Sn	Not detected	0.3
Bi	Not detected	0.1	S	Not detected	5
Zn	Not detected	1	Ce	Not detected	2

and suggests that these are at least substantially reduced by the process.

The amount of Se which could be purified appears to be limited only by the rate of flow of hydrogen through the Se. Flow rates of 10 l/hr result in production of about 10 g of Se/hr. It is important that the flow rate is such that H_2Se attains 1000°C in the decomposition stage. Analytical results (cf. Table II) suggest that quite impure Se may be refined in this way.

It may be mentioned that the purified H_2Se may be decomposed chemically if suitably pure reagents are available and may also be converted directly into a metal selenide should this be required.

Acknowledgment

The authors wish to acknowledge the help and interest shown by the Boliden Mining Company, Skelleftehamn, Sweden. They are also indebted to Miss I. Betteridge and Messrs. A. Fray, D. Maines, and J. Conaboy for help with the apparatus and to Miss P. Butcher for some of the analytical work. Acknowledgment is made to the Controller, Her Majesty's Stationery Office for permission to publish this paper.

Manuscript received July 16, 1957.

Any discussion of this paper will appear in a Discussion Section to be published in the December 1959 JOURNAL.

REFERENCES

1. B. S. Hopkins, "Chemistry of the Less Familiar Elements," Stipes Publishing Co., Chicago, Ill. (1939).
2. H. W. Henkels, *J. Appl. Phys.*, **21**, 725 (1950).
3. (a) C. W. Clark and E. M. Elkin (to Canadian Copper Refiners Ltd.) U.S. Pat. 2,406,666, Aug. 27, 1946; (b) C. W. Clark, E. M. Elkin, and G. R. Waitkins (to Canadian Copper Refiners Ltd.) U.S. Pat. 2,409,835 Oct. 22, 1946.
4. A. Voigt and H. Krebs (to Deutsche Gold-und-Silber-Scheideanstalt vorm. Roessler), British Pat. 698,228, Oct. 7, 1953.
5. L. M. Nijland, *Philips Research Repts.*, **9**, 259 (1954).
6. British Drug Houses, Poole, England, Private communication.
7. J. W. Mellor, "A Comprehensive Treatise on Inorganic and Theoretical Chemistry," Vol. X, p. 759, Longmans, Green and Co., London (1930).

Electrodeposition of High-Purity Chromium

F. E. Block, P. C. Good, and G. Asai

Bureau of Mines, Region I, Albany, Oregon

ABSTRACT

Thick chromium deposits were prepared by the electrolysis of aqueous chromic acid baths. Metal containing 0.005% oxygen, less than 0.002% nitrogen, and only traces of metallic impurities was obtained upon electrolysis of purified solutions at elevated temperatures. After consumable electrode arc-melting, this type of chromium could be hot-worked to rod and drawn to wire that was ductile at room temperature.

The electrolysis of chromic acid solutions was selected for study as a method of preparing high-purity chromium because metallic impurities may be excluded easily and gaseous impurities remain at very low levels. Although a low current efficiency is obtained in electrowinning chromium from hexavalent solutions and chromic anhydride is an expensive reagent, this method was adopted because it was found that metal could be prepared sufficiently pure to permit a study of its properties without additional purification steps which, in turn, are costly.

Electrodeposition from chromic acid solutions has been practiced from the time Fink (1) patented his process in 1926; however, its use has been confined mainly to decorative plating. Adcock (2) prepared massive deposits in 1927 as a means of making chromium for physical studies, but it was not until more recently that Greenaway (3) and the Bureau of Mines, United States Department of the Interior (4) employed high-temperature baths operated at high current density to yield thick deposits of low-oxygen chromium.

Brenner, Burkhead, and Jennings (5) investigated the properties of thin chromium electrodeposits plated under widely differing conditions of solution concentration, temperature, and current density. Their work indicated that the level of oxygen contamination in the electrodeposits was governed primarily by the temperature of deposition, with high temperatures favoring lower oxygen contents. Consequently, high-temperature baths were employed exclusively in this work. It has been demonstrated (6-8) that oxygen has little effect on the ductility of chromium metal; however, the object of this investigation was the preparation of the pure metal for direct study and for alloy studies, and since oxygen is generally the major contaminant in chromium, efforts were made to maintain a low oxygen level.

Experimental Work

Description of Apparatus

A number of different cells and procedures were studied during the course of the investigation, but only the more recent apparatus used in preparing metal for fabrication studies is described here.

The bath was maintained in a circular steel tank 18 in. in diameter and 16 in. in height lined on the inside with unplasticized polyvinyl chloride. This

was found to be one of the few corrosion-resistant nonmetallic materials that would withstand the operating temperatures of 90°C. A 6-in. diameter aluminum tube in the center of the cell served as cathode. In earlier runs the anode consisted of a 16-in. diameter coil of ¾-in. lead tubing which served also as a cooling coil. In later runs the cell comprised a lead vessel in a steel container, and the cell was used as an anode, the electrolyte being cooled by circulating water in the annular space between the cell and the steel container. In either type of cell the flow of water was regulated with a Powers regulator[1] activated by a temperature-sensitive, lead-sheathed bulb in the electrolyte. The tubular lead anode was more effective in removing heat and controlling temperature at high current densities, but the lead-pot type suffered less anodic corrosion.

Because the bath was operated at its boiling point and was in a constant state of violent agitation, due to the large amount of hydrogen being produced, a Micarta cover was fitted over the cell to direct the escaping mist and vapors to a glass reflux condenser which returned them to the cell. Losses of uncondensed liquid were made up from a reservoir placed above the cell and connected to a constant-level device to maintain a uniform electrolyte level in the cell.

Cell Operation

The electrolyte was made up by dissolving chromium trioxide in distilled water and adding sulfate ion as H_2SO_4.

Since the electrolyte was used repeatedly, impurities were prevented from building up by contacting the solution with a cation-exchange resin before each run. A 4-in. diameter resin bed 30 in. deep was employed. By analyzing the H_2SO_4 solution used to regenerate the resin, it was determined that Al, Cu, Fe, Ni, Si, and Sn were being removed by this treatment.

Cation-exchange resins of the sulfonated polystyrene type have been recommended (8) for treating strongly oxidizing solutions, such as chromic acid. Although this general type was employed, there was considerable variation with respect to stability among the different resins tested. Amberlite IR-120 was found to be highly resistant to oxidation at room temperature when used with solutions containing up to 250 g/l of chromic acid.

During electrolysis the chromium concentration in the electrolyte was determined twice daily by specific gravity measurements and adjusted by the addition of chromium trioxide to the feed reservoir or directly into the cell. The sulfate ion concentration was adjusted at the beginning of each run.

Direct current was supplied to the electrodes from a 4000-amp selenium rectifier.

To take advantage of the relationship between operating temperature and the oxygen content of the deposit, the electrolyte temperature was maintained near the boiling point. Since early deposition tests at lower operating temperatures had confirmed the temperature-oxygen content relationship as reported by Brenner and co-workers (5), all runs in this investigation were made in the 85°-90°C range.

During electrolysis, the deposit appeared first as a smooth surface having a matte finish, but as deposition continued it changed to a more nodular form. Because the electrolyte had poor throwing power, the nodules grew quickly into long dendrites, which eventually broke from the cathode and dropped to the bottom of the cell. Although the dendrites could be recovered as metal, it was necessary to treat them with nitric acid to remove lead chromate, which sloughed off the anode and mixed with the dendrites. Also, the dendrites consistently contained more oxygen than the adherent deposits.

For these reasons attempts were made to minimize the growth of dendrites. This could be accomplished to some degree by changing cathodes at shorter intervals before the dendrites formed; however, the thinner deposits were very difficult to remove from the cathode by mechanical methods. It was found that a deposition interval of 72 hr generally yielded a deposit between 1/16 and 3/32 in. thick, which was plated in a highly stressed condition. A deposit of this nature could be removed by striking the cathode a sharp blow with a hammer. Scoring the surface of the aluminum cathode into 1-in. squares before electrolysis caused a thinner deposit to be formed at the score marks and facilitated removal of the deposit.

Experimental Results

Table I shows the results of 72- and 96-hr deposition tests at cathode current densities ranging from 340 to 1100 amp/ft^2 and with various electrolyte compositions. Analyses were performed on specimens taken from ingots arc-melted from representative portions of the deposit. Oxygen and hydrogen were determined by vacuum fusion analysis, and nitrogen was determined either by vacuum fusion or Kjeldahl analysis.

Figure 1 is a plot of the data appearing in Table I and shows the relationship between the cathode current density and the proportion of the cathode deposit that appeared as loose dendrites. This plot indicates the advantage of operating at lower cur-

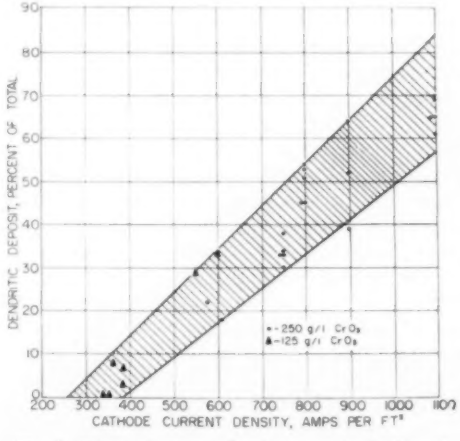

Fig. 1. Effect of current density on cathode deposit

[1] The Powers Regulator Company, Skokie, Ill.

Table I. Results of electrolytic tests

Run No.	Hr	Bath composition			Cathode current density, amp/ft²	Cathode current efficiency, %	Dendrite deposit %	*	Analysis, ppm			
		SO_4, g/l	CrO_3, g/l	Ratio, CrO_3/SO_4					O_2	H_2	N_2	C
1	72	2.5	125	50	340	12.3	0	P	410	2	10	110
2	96	1.0	125	125	350	7.7	0	P	50	1	20	80
3	96	2.2	85	39	350	10.2	20					
4	96	2.1	125	60	365	11.6	8					
5	96	2.6	125	48	385	13.1	7					
6	72	2.5	125	50	385	13.6	3					
7	72	3.9	125	32	550	10.5	29	P	55	1	<30	250
8	72	5.2	250	48	580	8.8	22	P	140	2	<50	
9	72	3.9	125	32	600	8.4	33	P	1150	7	20	55
10	72	7.8	250	32	610	8.4	18	P	50	<1	<30	
11	72	2.5	250	100	750	9.7	33	P	100	3	<20	
								D	920	3	<20	
12	72	2.5	250	100	750	8.6	38	P	120	5	<20	
								D	590	5	<20	
13	72	2.5	250	100	750	8.6	34	P	40	1	<20	
								D	600	5	<20	
14	72	2.5	250	100	750	11.2	33	P	250	4	<20	
								D	355	6	<20	
15	72	2.5	250	100	750	10.7	30	P	134	2	85	
								D	836	4	<20	
16	76	2.5	250	100	800	8.7	53	P	150	934	<20	740
								D	970	<20	<20	160
17	72	2.5	250	100	800	7.8	45	P	215	14	<20	370
								D	1170	<20	<20	<50
18	72	2.5	250	100	800	8.5	51	P	120	<20	<20	<50
								D	260	<20	<20	<50
19	72	2.5	250	100	800	7.5	45	P	130	<20	<20	<50
								D	740	5	<20	160
20	72	2.5	250	100	800	7.3	54	P	200		<20	<50
								D	920		<20	<50
21	72	2.5	250	100	900	9.4	52	P	210		<20	490
								D	1170		<20	80
22	72	2.5	250	100	900	12.8	64					
23	72	2.5	250	100	900	8.5	39					
24	72	2.5	250	100	1100	8.8	65					
25	72	2.5	250	100	1100	7.3	65					
26	72	2.5	250	100	1100	8.5	69	P	220	5	<20	
27	72	2.5	250	100	1100	8.4	70	D	1140	10	<20	
28	72	2.5	250	100	1100	8.9	61					

* P = deposit adhering to cathode; D = dendrite deposit fallen from cathode.

rent densities if a greater proportion of low-oxygen, solid deposits are desired. These data are not strictly comparable, because larger amounts of chromium usually were deposited in the tests at higher current densities, and a greater proportion of dendrites might be expected under these circumstances. However, the relationship appears to be independent of either the current efficiency or time of deposition, which might also be expected to influence the results if the relative amount of deposit was a major factor.

Table I indicates that the current efficiency was independent of the current density at constant bath composition. These data also suggest that optimum current efficiencies were obtained when baths were used having CrO_3 to SO_4 ratios of approximately 50, with somewhat lower efficiencies resulting from either higher or lower ratios. In this respect, the present investigation is in general agreement with the work of Greenaway (3).

At constant temperatures the oxygen content of the deposit appeared to be independent of both current density and bath composition. In all instances the dendritic deposits were found to contain a significantly higher amount of oxygen than the corresponding deposits which adhered to the cathode; however, the dendrites also exhibited a significantly greater amount of surface, which might account for the higher oxygen level. Usually the deposit which was removed from the cathode was found to contain between 50 and 250 ppm oxygen and less than 20 ppm nitrogen.

Metallic impurities were not determined quantitatively, but qualitative spectrographic analysis indicated that the deposits usually contained trace amounts of aluminum, iron, or silicon. There was no detectable difference between the dendritic or adherent deposits with respect to metallic impurities.

Figure 2 shows photomicrographs of arc-melted chromium representing both types of deposits. The increased amount of second-phase material in the dendritic deposit illustrates the higher oxygen level in this material.

Physical Testing

For evaluation, the deposits were consolidated by the inert atmosphere, cold mold, arc-melting technique. Homogeneous samples were prepared for analysis by melting a 50-g representative portion of

Fig. 2. Photomicrographs of arc-melted, as-cast chromium electrodeposits, chromic acid-electrolytic etch. (a) Adherent deposit 40 ppm oxygen, (b) dendritic deposit 600 ppm oxygen. Magnification 100X before reduction for publication.

each deposit, employing a nonconsumable tungsten electrode for arc melting. Larger ingots were prepared for physical studies by melting the chromium as a consumable electrode into a 2-in. diameter, water-cooled copper crucible. In this case the deposit was crushed to pass minus-8-mesh and compressed into 1-in. by 1-in. electrodes 10 in. long. The electrodes were sintered 8 hr in purified hydrogen at 1200°C to increase their mechanical strength.

Tensile tests were made on wire specimens prepared from the arc-cast ingots. Ingots were scalped, sheathed in stainless steel, and swaged at 1100°C to approximately 1-in. diameter. The 1-in. diameter swaged rods were recrystallized by heating to 1200°C sheathed in mild steel and swaged to approximately 0.25-in. diameter. After recrystallization the rods were reduced to 0.125-in. diameter test wire by drawing through tungsten carbide dies at 350°C. All of the specimens were tested in the 50% worked condition. Tensile specimens were prepared by stopping off the ends and electrolytically

Table II. Tensile strength of wire at 25°C

Specimen No.	Ingot analysis, ppm			Wire analysis, ppm N	U.T.S., 1000 psi.	Elongation, % in 1 in.
	O	H	N			
W-65	245	6.7	<50	40	69	10
				40	69	16
W-82	245	6.7	<50	50	68	15
				50	68	16
W-88	245	6.7	<50	30	57	26
SA, 17, 286	—	—	—	210	72	0
				—	70	0
SA 16, 284	40	2	<30	220	77	0
				—	74	0

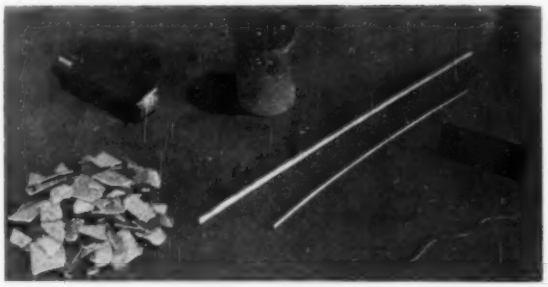

Fig. 3. Stages employed in preparing chromium wires from electrodeposit.

etching the wire surface in the center portion to yield a reduced section along the gauge length. In this work, as in previous investigations (9, 10), the full ductility of the material was not realized until a thin surface layer had been removed from the specimens by etching. Although the wires could not be bent before etching, after removal of the surface layer the wires could be reverse-bent by hand repeatedly without fracture.

Table II shows the results of tensile tests at 25°C representing specimens prepared from two ingot melts. Because of the opportunity for gaseous contamination during the sintering, arc-melting, and annealing steps, the broken tensile specimens were analyzed for nitrogen content as shown. The results indicate that material containing 50 ppm or less nitrogen is ductile, while chromium containing on the order of 200 ppm nitrogen has no ductility. This shows the importance of preparing and maintaining a low nitrogen content in the metal if ductility is desired.

Figure 3 represents the stages employed in preparing chromium wires, showing the electrodeposit, a section of partly melted consumable electrode, an ingot section, swaged rod, and drawn and etched ductile wire.

Conclusions

High-purity chromium can be prepared conveniently by high-temperature electrodeposition from purified chromic acid solutions, yielding deposits containing only trace amounts of metallic impurities, with oxygen the chief impurity. After having been melted and worked into shapes, electrolytic chromium exhibits tensile properties comparable to chromium prepared by refining commercial grade material by hydrogen treatment. The low nitrogen content of electrodeposited metal favors this method as a means of preparing chromium for physical studies.

Manuscript received Dec. 3, 1957. This paper was prepared for delivery before the Buffalo Meeting, Oct. 6-10, 1957.

Any discussion of this paper will appear in a Discussion Section to be published in the December 1959 JOURNAL.

REFERENCES

1. C. G. Fink, U. S. Pat. 1,581,188 (1926).
2. F. Adcock, *J. Iron and Steel Inst.*, **115**, 369 (1927).
3. H. T. Greenaway, *J. Inst. Metals*, **83**, 1576 (1954-55).
4. P. M. Gruzensky and F. E. Block, *U. S. Bur. Mines Rep. Invest. 5035*, January 1957.
5. G. Asai and H. Johansen, "Final Report on Massive

Chromium" to Army Ordnance Corps, Watertown Arsenal Laboratory, Watertown, Mass., Sept. 15, 1953.
6. A. Brenner, P. Burkhead, and C. Jennings, *J. Res. Nat. Bur. Standards*, **40**, 31 (1948).
7. G. Asai and E. T. Hayes, "Mechanical Properties of Bureau of Mines' Chromium," Ductile Chromium ASM, p. 138 (1957).
8. W. H. Smith and A. U. Seybolt, "Effects of Impurities on the Ductility of Chromium," Ductile Chromium, ASM, p. 169 (1957).
9. R. L. Costa, *Ind. and Eng. Chem.*, **42**, 308 (1950).
10. H. L. Wain, F. Henderson, and S. T. M. Johnstone, *J. Inst. Metals*, **83**, 133 (1954-1955).
11. H. A. Johansen and G. Asai, *This Journal*, **101**, 604 (1954).

Some Effects of Pressure on Consumable Electrode Arc Melting

J. W. Suiter[1]

Mines Branch, Department of Mines and Technical Surveys, Ottawa, Ontario, Canada

ABSTRACT

The effect of pressure in a consumable electrode arc furnace on the weight of metal melted per unit of energy dissipated was investigated while melting titanium electrodes of negative and positive polarity and steel electrodes of negative polarity. Provided that the arc length was sufficiently short, the weight of metal melted per unit of energy dissipated increased continuously as the pressure of argon was decreased from 650 to 1×10^{-2} mm Hg.

Many workers (1, 2) have reported the weight of metal melted per unit of energy dissipated in consumable electrode arc melting, but in most cases the experiments were done only at a few widely separated pressures. Beall, *et al.* (3) have reported the effects of varying the pressure in the range 10-760 mm Hg when melting titanium electrodes in an argon atmosphere. However, the present emphasis on vacuum arc melting has made it desirable to extend their investigations to lower pressures.

The paper reports the effects of varying the argon pressure in the range of 1×10^{-2} to 650 mm Hg on the weight of metal melted per unit of energy dissipated when melting titanium and steel in a consumable electrode arc furnace.

Materials and Experimental Procedure

The titanium electrodes were produced by welding, end to end, compacts of sponge titanium (20.4 x 5.1 x 5.1 cm) each weighing 1600 g. The mild steel (0.1% C) electrodes consisted of rolled bar 3.8 x 3.8 cm in cross section. These electrodes were attached to a water-cooled copper electrode stub which passed through a sliding seal in the top of the furnace. The electrodes were melted into a mold 34 cm long and 12 cm in diameter, producing ingots of 4-5 kg weight.

Power for melting was supplied by three motor-generator welding machines connected in parallel. The same generator settings were used in all experiments, and the arc current and voltage were allowed to vary with the pressure.

During melting the feed rate of the electrode was adjusted by the operator while observing the arc voltage pattern on a direct current oscilloscope and also the arc voltage and current as indicated by conventional meters. The desirable arc length was such that the pattern on the oscilloscope indicated the presence of occasional, momentary dead shorts. It was thought that these momentary dead shorts were due to droplets of molten metal shorting between the electrode and the molten pool. It was not possible to measure such an arc length but it appeared to be less than 1 cm. For some melts at pressures of 25 and 10 mm Hg, an arc length of approximately 8 cm was deliberately maintained; these were duplicates of melts made at the same pressures with a normal short arc length. The long arc length was used to determine what effect the presence of positionally unstable arcs would have on the weight of metal melted per unit of energy dissipated. It was possible to observe, through a sight glass, the presence or absence of positionally unstable arcs within the mold.

In the pressure range 10-650 mm Hg a static atmosphere of argon was used, but in the pressure range 10^{-1}-10 mm Hg it was necessary to remove gas from the system while melting to maintain a constant pressure. No argon was used for pressures less than 10^{-1} mm Hg which were obtained by continuously evacuating the furnace so that the steady pressure during melting depended on the speed of the pumps being used and the amount of gas evolved from the electrode. The gas pressure was measured in the body of the furnace, for it has been shown (4) that this pressure is very close to that in the melting region of this type of furnace if there are no volatile materials in the electrode. There were only very small quantities of volatile materials in the steel electrodes used in these experiments, but the titanium electrodes contained such volatiles as magnesium and magnesium chloride. Thus, the pressure measured in the body of the furnace did not indicate accurately the pressure in the melting region when melting titanium electrodes at very low pressures.

The energy dissipated during melting was calculated from the arc voltage, the arc current, and the time of the melting operation.

[1] Present address: Baillieu Laboratory, The University of Melbourne, Victoria, Australia.

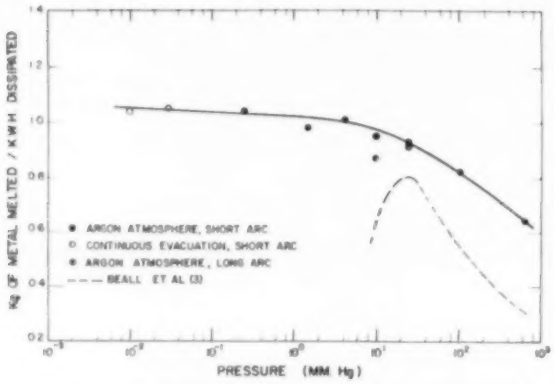
Kg OF METAL MELTED / K.W.H DISSIPATED
PRESSURE (MM. Hg)
ARGON ATMOSPHERE, SHORT ARC
CONTINUOUS EVACUATION, SHORT ARC
ARGON ATMOSPHERE, LONG ARC
BEALL ET AL (3)

Fig. 1. Effect of pressure on the weight of titanium melted per unit of energy dissipated when melting electrodes of negative polarity.

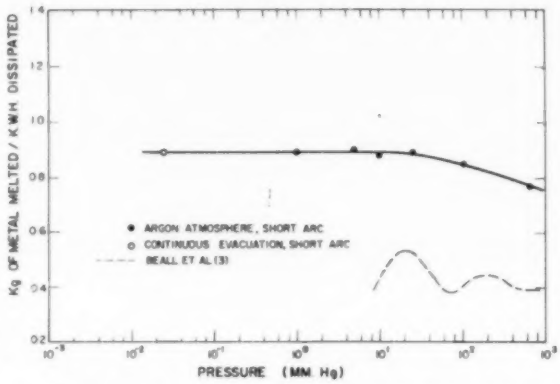
Kg OF METAL MELTED / K.W.H DISSIPATED
PRESSURE (MM. Hg)
ARGON ATMOSPHERE, SHORT ARC
CONTINUOUS EVACUATION, SHORT ARC
BEALL ET AL (3)

Fig. 2. Effect of pressure on the weight of titanium melted per unit of energy dissipated when melting electrodes of positive polarity.

Results

The effect of pressure on the weight of metal melted per unit of energy dissipated when melting titanium electrodes of negative polarity is shown in Fig. 1. As the pressure was decreased from 650 mm Hg to approximately 10 mm Hg the weight of metal melted per unit of energy dissipated increased, but at lower pressures the increase was less marked. As the pressure was decreased the arc voltage decreased from 36 v at 650 mm Hg pressure to 28 v at pressures less than 5 mm Hg, and in the same pressure range the arc current increased from 1800 to 2200 amp.

In the pressure range 2 x 10^{-1} to 20 mm Hg, positionally unstable arcs were seen occasionally within the mold, but these were eliminated by decreasing the arc length. Two electrodes were melted at 25 and 10 mm Hg pressure while maintaining an arc length of approximately 8 cm. At a pressure of 25 mm Hg, melting with a long arc had little effect on the weight of metal melted per unit of energy dissipated. At 10 mm Hg pressure, the weight of metal melted per unit of energy dissipated was less when melting with a long arc, and there was also a large increase in the amount of positionally unstable arcs within the mold.

Figure 2 shows that the weight of metal melted per unit of energy dissipated increases with decreasing pressure when melting titanium electrodes of positive polarity, but the increase is less than when melting titanium electrodes of negative polarity (compare Fig. 1 and 2). Thus, at low pressures the weight of metal melted per unit of energy dissipated was higher when melting electrodes of negative polarity, but near atmospheric pressure the position was reversed.

The effect of pressure on the weight of metal melted per unit of energy dissipated when melting steel electrodes of negative polarity is shown in Fig. 3. The results are similar to those obtained when melting titanium electrodes of negative polarity. At all pressures the weight of steel melted per unit of energy dissipated was greater than that of titanium, but this result was not unexpected in view of the different heat contents of the two materials at temperatures just above their melting points. As in the case of titanium electrodes of negative polarity, a long arc at a pressure of 8 mm Hg led to positionally unstable arcs and a decreased weight of steel melted per unit of energy dissipated.

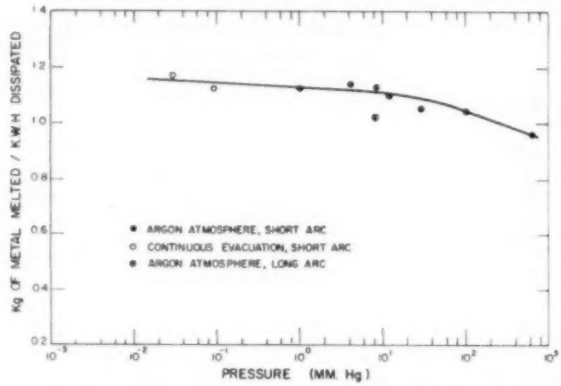
Kg OF METAL MELTED / K.W.H DISSIPATED
PRESSURE (MM. Hg)
ARGON ATMOSPHERE, SHORT ARC
CONTINUOUS EVACUATION, SHORT ARC
ARGON ATMOSPHERE, LONG ARC

Fig. 3. Effect of pressure on the weight of steel melted per unit of energy dissipated when melting electrodes of negative polarity.

Discussion

When melting titanium electrodes of negative and positive polarity and steel electrodes of negative polarity in a consumable electrode arc furnace, the weight of metal melted per unit of energy dissipated increased continuously as the pressure was decreased. Beall, *et al.*, (3) have reported the results of melting titanium electrodes in argon atmospheres in the pressure range of 10-760 mm Hg, and they found a sharp decrease in the weight of titanium melted per unit of energy dissipated as the pressure was reduced below 20 mm Hg (see Fig. 1 and 2). Beall, *et al.* suggested that this decrease was due to the formation of positionally unstable arcs. The present work confirmed that the formation of these arcs led to a decreased weight of metal melted per unit of energy dissipated but that by maintaining a sufficiently short arc length these positionally unstable arcs could be avoided. If they were avoided, then the weight of metal melted per unit of energy dissipated increased continuously as the pressure decreased. Beall, *et al.* used two horizontally opposed electrodes in a relatively large furnace in their experiments,

and the different size and arrangement of electrodes used in the two sets of experiments may account for the different values of the weight of titanium melted per unit of energy dissipated that were obtained in the two sets of experiments near atmospheric pressure.

Although most of the melting experiments were done in an argon atmosphere, no argon was used for the melts when the furnace was evacuated continuously, and the pressure during melting was less than 1×10^{-1} mm Hg. Since the results obtained under these conditions followed the same trend as those obtained when melting in an argon atmosphere, it appeared that at very low pressures the atmosphere in which melting occurred had little effect on the weight of metal melted per unit of energy dissipated. The steel electrodes contained very little volatile material, and the composition of the gas in the melting region when melting these electrodes under continuous evacuation differed greatly from the gas composition when melting titanium electrodes. These changes in the composition of the gas in the melting region appeared to affect neither the behavior of the arc nor the weight of metal melted per unit of energy dissipated.

Acknowledgments

The work was done under the general direction of H. V. Kinsey, of the Department of Mines and Technical Surveys, Ottawa, and was made possible by the award of a Fellowship by the National Research Council of Canada. Thanks are due to R. H. Landry, technician, for assistance with the experimental work.

Manuscript received May 19, 1958. This paper was prepared for delivery before the Ottawa Meeting, Sept. 28-Oct. 2, 1958.

Any discussion of this paper will appear in a Discussion Section to be published in the December 1959 JOURNAL.

REFERENCES

1. W. H. Smith, "Arcs in Inert Atmospheres and Vacuum," W. E. Kuhn, Editor, p. 41, John Wiley & Sons, Inc., New York (1956).
2. J. L. Ham and C. B. Sibley, *J. Metals*, **9**, 976 (1957).
3. R. A. Beall, F. W. Wood, J. O. Borg, and H. L. Gilbert, "Production of Titanium Castings," Rept. of Investigation 5265, Bureau of Mines, U. S. Department of the Interior, Washington (1956).
4. J. W. Suiter, *This Journal*, **105**, 44 (1958).

Tungsten Zone Melting by Electron Bombardment

R. G. Carlson

Lamp Wire and Phosphors Department, General Electric Company, Cleveland, Ohio

ABSTRACT

An apparatus for refining tungsten in vacuum by the floating zone method is described. It consists of four components: vacuum system, power supply, anode support, and traversing cathode. Included is a brief résumé on the theory of refining by this technique. Spectrographic analyses along the length of a purified tungsten rod indicate that molybdenum may not be removed by zone refining, but rather by volatilization. Further, x-ray diffraction studies show that tungsten rods purified in this manner are single crystals and these crystals as grown from the melt do not exhibit preferential growth. It is demonstrated, by bending one of the single crystals, that the purified tungsten rods have relatively high ductility.

Zone melting, developed by Pfann (1), has attracted great interest as a process for the purification of metals. In this process a small molten zone traverses the length of a solid rod. Impurities that are more soluble in the liquid phase than in the solid phase migrate with the molten zone, leaving behind a purer metal. In the case of zone melting tungsten purification also occurs because of the outgassing and volatilization of impurities.

It is exceedingly difficult, if not impossible, to retain W in a molten state by conventional techniques without impairing its purity because of the refractory nature of this metal. Tungsten can be zone melted by utilizing the floating zone technique and heating by electron bombardment. The principle of this heating, simply the blasting of a material anode with electrons through a high potential gradient, is not new nor unique since it has long been used in the outgassing of electronic vacuum tubes and occurs in the operation of x-ray tubes. However, because of the characteristics inherent in electron bombardment heating, i.e., ability to operate at low pressures, ability to direct and concentrate the heat, ease of temperature control over a wide range, and relative simplicity of the power supply, this type of heating is employed advantageously in laboratory (2-4) as well as commercial furnaces (5).

This paper covers the design and construction of an Electron Bombardment Zone Melting Apparatus (EBZMA), includes a brief discussion on the theory of purification, and presents data on the removal of Mo and on crystal orientation.

Electron Bombardment Zone Melting Apparatus

The equipment consists of four components: vacuum system, power supply, anode support, and traversing cathode.

Vacuum system.—The anode and cathode are enclosed by a Pyrex bell jar 10½ in. in diameter and 14 in. high mounted on a brass plate (Fig. 1). There

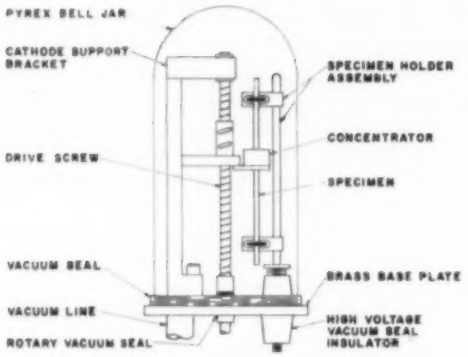

Fig. 1. Schematic drawing of the vacuum system

are five holes in this plate: three ⅝-in. diameter holes for electrical binding posts; one 2-in. diameter hole for the vacuum line; and one rotating "O" ring seal for the cathode traversing helix.

The 2-in. vacuum line is constructed with a vertical pipe extending down to a "T" section. One leg of this section forms a liquid nitrogen trap; the other leg is connected to a MCF-60 CEC oil diffusion pump, which in turn is backed up by a Kinney KC-2 mechanical pump.

Power supply.—A small power unit supplies d.c. at a maximum of 5000 v and 300 ma. It consists of a variac that limits the 110 a-c volt power to the high voltage transformer. This high voltage is then rectified by a pair of 866 A half-wave mercury rectifier tubes. The positive side of this high voltage is fed through the high-voltage-high-vacuum-throughput to the anode support. The cathode is the ground terminal. Figure 2 is a schematic of the power supply.

Anode support.—The support shown in Fig. 1 can accommodate rods up to ¼ in. in diameter. The upper and lower holding blocks are critical parts. They should possess four properties: (*a*) high melting point; (*b*) stable material in order that W is not contaminated, i.e., low vapor pressure; (*c*) high electrical conductivity; (*d*) low thermal conductivity. No one material has all these properties, but because of its superiority in the first three properties and its ability to be easily fabricated, Mo is used. A small groove in each block at the point of specimen contact reduces the heat transfer.

The specimen is held in position in each of the

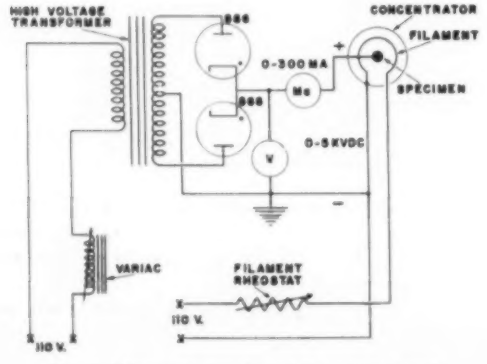

Fig. 2. Schematic drawing of the power supply

holders by flat tungsten strip that acts as a spring contact. This spring serves a dual purpose. One is to support the rod during the movement of the floating zone and the other is to allow the specimen to expand and contract in the heating and cooling operation.

Traversing cathode.—The cathode is the moving terminal; it is composed of a filament that emits the electrons, a concentrator that directs the flow of the electrons, and a mechanism that moves the cathode with respect to the stationary tungsten rod.

Traversal of the specimen occurs by the movement of a screw drive with the torque being transmitted through a rotating "O" ring seal in the brass plate. The torque is supplied through a gear train by a 3 rpm a-c reversible motor. The output of the gear train varies from 0.1 to 12 rpm producing a cathode movement of 0.3-4 cm/min.

The concentration of the electrons to the anode is an important factor. This is achieved by enclosing a W filament with a Mo concentrator of the same potential. To obtain more efficient concentration the sides of the concentrator are parabolic. The top and bottom are changeable disks with different diameter center holes, approximately ⅛ in. diameter larger than the specimen diameter.

The W filament, 15 mils in diameter, is heated by a 110 a-c power supply as shown in Fig. 2. The filament rheostat regulates the current flow to obtain sufficient emission of electrons to melt the sample, i.e., in the order of 200-250 ma.

Theory

In the zone refining process the molten zone is moved repeatedly in the same direction. Solute elements that depress the melting point of the solvent metal concentrate in the terminal end of the rod and have a distribution coefficient, k, less than one. Solute elements that increase the melting point have a k value greater than one and tend to concentrate at the starting end. The distribution coefficient is defined by the equation

$$k = \frac{N^s}{N^l} \qquad [1]$$

where N^s is mole fraction of the solute in the solid phase and N^l is the mole fraction in the liquid phase.

The distribution coefficient can be determined simply by referring to a phase diagram. From the Mo-W equilibrium phase diagram (6), the equilibrium distribution coefficient (k_o) for Mo in W is found to be 0.91.

Another approach in the determination of the distribution coefficient would be to utilize thermodynamics and, if the alloy forms ideal liquid and solid solutions, apply the well-known van't Hoff equation

$$\ln \frac{N_{Mo}{}^{l}}{N_{Mo}{}^{s}} = -\frac{\Delta H_f{}^{Mo}}{R}\left(\frac{1}{T} - \frac{1}{T_M{}^{Mo}}\right) = K_{Mo} \qquad [2]$$

or

$$\frac{N_{Mo}{}^{l}}{N_{Mo}{}^{s}} = e^{K_{Mo}} \qquad [3]$$

then

$$k_o = \frac{1}{e^{K_{Mo}}} \qquad [4]$$

where T equals the temperature considered, in this case the melting point of W, 3680°K; $T_M^{W_o}$ equals the melting point of Mo, 2900°K; $\Delta H_f^{M_o}$ equals the heat of fusion for Mo, 6700 cal/mole; R equals gas constant. From Eq. [4] we determine that k_o equals 0.78.

As originally stated, purification of W also occurs by outgassing and the volatilization of metallic impurities on fusion in vacuum. In this particular case we will consider only the volatilizaton of Mo. The vapor pressure (p^*Mo) for Mo at a temperature slightly above the melting point of W, 3800°K, equals 3.83 mm Hg, while the vapor pressure for W, at the same temperature, equals 0.046 mm Hg. If the mole fraction of Mo (N_{M_o}) is assumed to be 0.00002, by assuming ideality ($a_{M_o} = N_{M_o}$) and using Raoult's law ($p = a \cdot p^*$Mo), the vapor pressure of Mo in the melt is 7.7×10^{-5} mm Hg. This would indicate that, if the pressure of Mo in the environment was less than 7.7×10^{-5} mm Hg, Mo would volatilize from the melt. The rate of evaporation can be calculated from the formula (9)

$$\frac{m}{t \cdot A} = P\sqrt{\frac{M}{2\pi RT}} = G \qquad [7]$$

where P is pressure (microbars); M, molecular weight; A, area (cm²); t, time (sec); R, gas constant (8.31×10^7 erg/°K/mole); T, temperature (°K); m evaporation (gr), or the ratio of the evaporation rates can be determined from the equation

$$\frac{G_{M_o}}{G_W} = \frac{P_{M_o}}{P_W}\sqrt{\frac{M_{M_o}}{M_W}} \qquad [8]$$

From this equation the ratio of evaporation rate of Mo to W is found to be 1.21×10^{-3}, i.e., of the metal evaporated during melting, 0.121% by weight is Mo.

Results

Many rods have been zone melted with this apparatus; two of the zone melted rods after five passes are shown in Fig. 3. It was found on evaluation of the purified rods that they were high in purity, single crystals, and exhibited a comparatively large amount of ductility.

It is difficult to obtain quantitative data on samples containing less than 10 ppm of an impurity. The initial concentration of all elements other than Mo were less than 10 ppm and could not be detected by spectrographic analysis. The initial concentration of Mo was estimated to be of the order of 10 ppm. To determine the amount of Mo present after the bar was traversed five times at a speed of 0.33 cm/min the rod was severed at intervals along its length. Each end of the severed section was arced against its adjacent section. The initial concentration in the rod was arbitrarily assigned the value of 10. In Fig. 4, the relative amounts of Mo, as determined by quantitative optical spectrography, are plotted against the distance along the zone purified rod.

An apparent discrepancy existed at the beginning and the end of the zone melted portion. According to the theory of zone purification, if $k < 1$, a zone of higher purity should be present at the start and a concentration of the impurities at the end. Because this did not occur, it was reasoned that either a distribution coefficient greater than one existed, or possibly the Mo evaporated from the zone melted region.

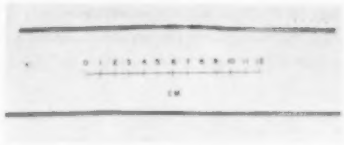

Fig. 3. Zone melted W rods, after five zone passes

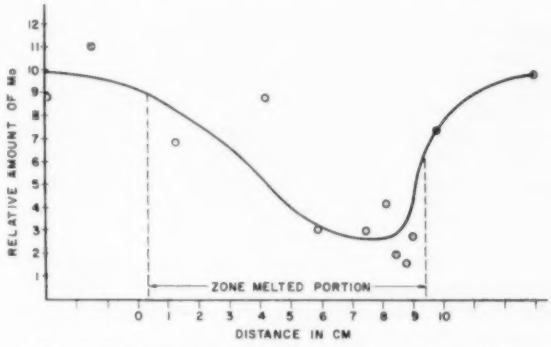

Fig. 4. Relative concentration of Mo vs. distance in zone melted portion.

To substantiate the absence of an increase in Mo concentration at the end of the rod, five separate analyses were obtained in this region. If a zone of higher Mo concentration was present, it must have existed in a length less than 4 mm long, and this is not very probable. On the basis that $k_o = 0.91$, the lowest possible concentration of Mo that could exist after 5 passes was calculated to be 6.24, assuming equilibrium existed and that the original concentration of Mo = 10. Using the same assumption and now $k_o = 0.78$, the lowest concentration was calculated to be 2.89. This latter value, as can be noted in Fig. 4, falls in the range of the lowest concentration. Of course, this lowest concentration of the solute should have occurred at the start. More work is currently being performed to support the validity of these initial results.

To determine the orientations of the rods and to ascertain if the rods after zone melting were single crystals, six were examined by x-ray diffraction utilizing the transmission Laue technique, and two were examined metallographically. Results of x-ray

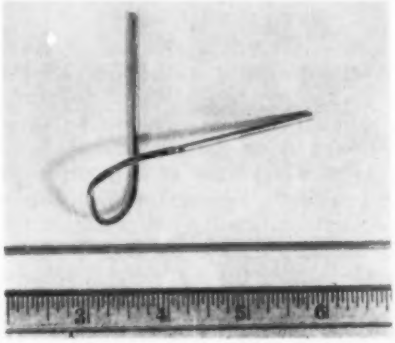

Fig. 5. Zone melted W rod bent into a loop

Table I. Crystal orientation

Plane	Angle between major plane normal and rod axis 1	1A	ZMW-1	ZMW-2	ZMW-3	ZMW-4
(100)	37	33	38	25	6	18
(110)	20	14	7	21	42	32
(111)	22	29	33	32	49	37

orientation determination are recorded in Table I. These suggest that no one preferential direction of growth existed, Rod 1A and ZMW-1 were examined at several points along the length of the crystal, and it was determined that the orientation remained the same, indicating only one crystal of the same orientation existed. Metallographic observation confirmed these results, that the rod was a single crystal along its length.

A qualitative measure of the high ductility at room temperature was obtained; this is shown in Fig. 5. Here the ⅛-in. zone melted tungsten rod was bent approximately 270° into a loop.

Conclusions

Single crystals of tungsten can be grown in the Electron Bombardment Zone Melting Apparatus. These crystals are greatly purified and exhibit a larger amount of ductility than can be obtained in an equivalent sized polycrystalline material.

Acknowledgments

The author gratefully acknowledges the assistance of J. H. Moorhead with the design and operation of this apparatus. Further, the assistance of R. Madden and J. Fagel in obtaining the spectrographic analysis, and of S. Leber for the x-ray orientation determinations is acknowledged.

Manuscript received June 9, 1958. This paper was prepared for delivery before the New York Meeting, April 27-May 1, 1958.

Any discussion of this paper will appear in a Discussion Section to be published in the December 1959 JOURNAL.

REFERENCES

1. W. G. Pfann, "Zone Melting," John Wiley & Sons, New York (1958).
2. W. A. Rocco and G. W. Sears, *Rev. Sci. Instrum.*, **27**, 1 (1956).
3. A. Calverly, M. Davis, and R. F. Lever, *J. Sci. Instr.*, **34**, 142 (1957).
4. P. G. England and H. N. Jones, *ibid.*, **35**, 66 (1958).
5. Temescal Metallurgical, *Chem. Eng. News*, Feb. 10, 1958.
6. W. P. Sykes, "A.S.M. Metals Handbook," p. 1230 (1948).
7. J. Chipman and A. Hayes, *Trans. A.I.M.E.*, **135**, 85 (1939).
8. L. S. Darken and R. W. Gurry, "Physical Chemistry of Metals," McGraw-Hill Book Co., New York (1953).
9. H. Jones, I. Langmuir, and G. MacKay, *Phys. Rev.*, (2) **30**, 201 (1927).

Vapor Pressure of Niobium

Rudolph Speiser

Department of Metallurgy, The Ohio State University, Columbus, Ohio

P. Blackburn

Research Laboratory, Westinghouse Electric Corporation, Pittsburgh, Pennsylvania

H. L. Johnston

H. L. Johnston Associates, Columbus, Ohio

ABSTRACT

The Langmuir method has been used to determine the vapor pressure of niobium. An accommodation coefficient of unity was assumed. Least square treatment of the vapor pressure data yields the equation

$$\log P_{atm} = -\frac{(40{,}169)}{T} + 8.872$$

The heat of sublimation at absolute zero, ΔH°_0, is 171.80 ± 0.49 and $\Delta H^\circ_{298.15}$ is 172.53 kcal/g atom.

Prior to this investigation, the only data (1) available for the computation of vapor pressures of Nb was the rate of sublimation from a Nb wire heated by the passage of an electric current. Since these measurements were made at only three temperatures, and since the temperature measurement depended on an accurate determination of the emissivity of the wire, it was decided to repeat these measurements using the method and apparatus described in previous publications (2). The Langmuir method was employed, and an accommodation coefficient of unity was assumed.

Experimental

The measurements consisted of determining the rate at which a Nb surface sublimed into a high vacuum. The sample was supplied by the Fansteel Corporation and was assayed at a purity of 99.9%. The sample was in a form of an annular ring 0.985 in. OD, 0.374 in. ID, and 0.357 in. thick. The effective internal area (3) of the annular ring was computed from the expression

$$\text{Eff. area} = \pi b(\sqrt{a^2 + b^2} - b) \qquad [1]$$

where a is the inside diameter and b, the thickness.

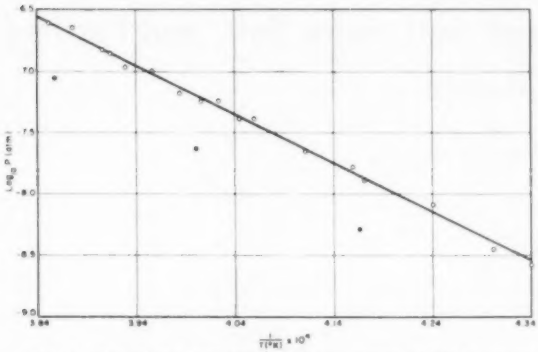

Fig. 1. Plot of the logarithm of the pressure of Nb in atmospheres vs. the reciprocal of the absolute temperature. Solid circles represent the data of Reimann and Grant (1).

Table I. Vapor pressure of Nb

Temp, °K	Weight loss, g	Eff. time, min.	Evap. rate, g/cm²/sec	Pressure, atm
2304	0.00791	326.7	2.3423×10^{-6}	2.6311×10^{-9}
2325	0.00881	274.4	3.1208×10^{-6}	3.5216×10^{-9}
2358	0.01733	236.0	7.1368×10^{-6}	8.0977×10^{-9}
2397	0.01206	105.4	1.1091×10^{-7}	1.2708×10^{-8}
2404	0.02600	174.2	1.4402×10^{-7}	1.6526×10^{-8}
2432	0.01941	97.1	1.9343×10^{-7}	2.2323×10^{-8}
2463	0.01495	41.5	3.4881×10^{-7}	4.0512×10^{-8}
2472	0.01134	30.8	3.5520×10^{-7}	4.1329×10^{-8}
2485	0.01568	30.4	4.9777×10^{-7}	5.8069×10^{-8}
2496	0.01735	33.6	4.9787×10^{-7}	5.7032×10^{-8}
2510	0.02501	42.4	5.6649×10^{-7}	6.6418×10^{-8}
2528	0.02694	30.1	8.6111×10^{-7}	1.0132×10^{-7}
2545	0.02172	23.2	9.0269×10^{-7}	1.0657×10^{-7}
2555	0.02684	21.8	1.1803×10^{-6}	1.3963×10^{-7}
2566	0.04075	31.7	1.2338×10^{-6}	1.4626×10^{-7}
2580	0.04827	25.0	1.8615×10^{-6}	2.2127×10^{-7}
2596	0.04340	20.4	2.0495×10^{-6}	2.4438×10^{-7}

Table II. Thermodynamic functions of Nb

Temp, °K	$\frac{(F^\circ - H^\circ_0)_S}{T}$	$\frac{(F^\circ - H^\circ_0)_g}{T}$	$-R \ln P$	ΔH°_0 kcal	
2304	51.41	15.66	39.28	172.87	
2325	51.46	15.71	38.70	173.10	
2358	51.55	15.82	37.05	171.62	
2397	51.65	15.92	36.15	172.30	
2404	51.67	15.94	35.63	171.55	
2432	51.74	16.02	35.03	172.06	
2463	51.82	16.11	33.85	171.33	
2472	51.85	16.13	33.81	171.88	
2485	51.88	16.17	33.13	171.07	
2496	51.91	16.20	33.17	171.92	
2510	51.94	16.23	32.86	172.11	
2528	51.98	16.27	32.02	171.22	
2545	52.02	16.31	31.92	172.11	
2555	52.05	16.34	31.38	171.41	
2566	52.07	16.36	31.29	171.92	
2580	52.12	16.40	30.47	170.77	
2596	52.16	16.46	30.27	171.26	
			Mean	171.80	±0.49

The area of the sample was also corrected for the thermal expansions from room temperature to the temperature of the measurement. The sample was placed in a metal cell (2) and after thorough outgassing was then heated by induction under a vacuum of the order of 10^{-4} mm.

The effective time at the temperature of measurement was determined as described previously (2).

Temperatures were measured under black body conditions by sighting into a hole drilled into the sample. A L&N disappearing filament optical pyrometer which had been calibrated by the National Bureau of Standards and frequently checked against a standard lamp furnished by the Bureau was used to measure the temperature. Pyrometer readings were reproduced to ±2°.

Results and Discussion

Experimental results are plotted as log P_{atm} vs. $1/T$ in Fig. 1 and summarized in Table I. Thermodynamic functions are tabulated in Table II; the thermal data for solid and gaseous Nb were taken from the compilation of Stull and Sinke (4). The computed value of ΔH°_0, the heat of sublimation at 0°K, is 171.80 ±0.49 kcal/g atom. This value is to be compared with a ΔH°_0 value of 176.82 kcal/g atom computed from the vapor pressure data of Reimann and Grant at 2600°K. Vapor pressures in this research are higher by a factor of 2.8 than those measured by Reimann and Grant. An error of 70° in the temperature scale could account for this discrepancy, and an error of this magnitude is quite possible when temperature measurements dependent on the emissivity of a surface are made.

Least square treatment of the vapor pressure data for Nb yields the equation

$$\log P_{atm} = -\frac{(40{,}169)}{T} + 8.872 \qquad [2]$$

These data also yield a value of $\Delta H^\circ_{298.15}$ of 172.53 kcal/g atom.

Manuscript received July 14, 1958. This paper was prepared for delivery before the New York Meeting, April 27-May 1, 1958.

Any discussion of this paper will appear in a Discussion Section to be published in the December 1959 JOURNAL.

REFERENCES

1. A. L. Reimann and C. K. Grant, *Phil. Mag.*, **22**, 34 (1936).
2. R. Speiser and J. W. Spretnak in "Vacuum Metallurgy," p. 155, Electrochem. Soc., Inc. (1955); R. Speiser and H. L. Johnston, *Trans. ASM*, **42**, 283 (1950).
3. R. B. Holden, R. Speiser, and H. L. Johnston, *J. Am. Chem. Soc.*, **70**, 3897 (1948).
4. D. R. Stull and G. C. Sinke, "Thermodynamic Properties of the Elements," Am. Chem. Soc. (1956).

The Occurrence of Impurities in Rock Salt, Solar Salt, and Purified Sodium Chloride

Arthur Bloomberg and Kurt Ladenburg

Research Laboratory, International Salt Company, Inc., New York, New York

ABSTRACT

Because of the known interference of certain impurities and the suspected effect of others in the electrolytic cell processes for the production of sodium and chlorine-caustic soda, the presence or absence of thirty-five elements in sodium chloride samples was investigated spectrographically, allowing detection of extremely low concentrations. Results are reported for rock salt from four different locations, for three different solar salts, and for purified salt from two separate plants.

The chlorine caustic industry has reliable information (1-4) regarding the influence of trace impurities on the electrolysis of sodium chloride by the mercury cell process. The presence of certain metals (V, Mo, Cr, and Ti) in concentrations as low as 0.25 mg/liter of brine (equivalent to 0.8 ppm in dry sodium chloride) decreases cathodic current efficiency considerably.

The sodium chloride brines used are derived from different sources and from various locations, viz., rock salt, brought to the surface dry; rock salt, dissolved underground and pumped to the surface through brine wells; natural underground brines; solar salt; vacuum pan salt.

Although rock salt and raw brines are usually purified before use, it is of considerable interest to know to what extent the harmful metals occur in the salt. Since the literature provides practically no information on this subject, a spectrographic investigation of different types of sodium chloride from different locations was undertaken. Rock salt samples were obtained from Louisiana, Michigan, New York, and the Dominican Republic; solar salt from California, The Great Salt Lake, and the Bahamas; purified vacuum pan salt from Louisiana and New York.

Considerable variation exists in quantity, and some variation in kind, of impurities found in natural salt deposits.Unrefined rock salt contains some water-insoluble matter, mostly anhydrite, plus traces of other minerals: dolomite, hematite, quartz, celestite, clay (aluminum silicate), etc. Since trace quantities were to be determined, an effort was made to determine the variance in results between duplicate analyses and between samples taken from the production line at least one week apart. The analyses on rock salt from New York, Michigan, and Louisiana were run in duplicate on two samples taken at different times. A single analysis of the purified salt was made on two samples taken several weeks apart. Kilogram samples were used in all analyses to increase precision and to compensate for the non-uniform distribution of impurities in the rock salt deposits. In no instance, where more than one analysis was made on salt from a given source, was there any wide discrepancy in results between the several samples.

Solar salt may contain traces of many of the constituents of sea water, depending on the control exercised during the evaporation and crystallization process. Most of the natural impurities are water-soluble except for mechanical contaminants such as clay or calcium sulfate from pan bottoms, or wind-blown dust.

Purified vacuum pan salt was included to indicate, by difference, the extent to which trace elements are removed by chemical purification.

Experimental

A kilogram of salt was dissolved in 3500 ml of distilled water, allowed to stand over night, and then filtered through Whatman No. 41 paper. The residue was washed with several portions of distilled water, the washes being added to the brine. The filter paper and insolubles were dried over night at 110°C. The paper was separated and ashed separately. The residue was added to the ash and the total weighed as "insolubles." This was ground in an agate mortar and analyzed spectrographically. In the case of the purified salt samples there was no insoluble portion.

The trace elements in the soluble fraction were precipitated with H_2S from slightly alkaline brine, using high-purity lead as a carrier.

The filtered brine was made alkaline with 5 ml of C.P. NH_4OH. Fifty mg of 99.99+% lead, as a lead nitrate solution, was added to act as "carrier." The precipitation of the sulfides was carried out under a slight pressure of water-washed H_2S and with stirring. A blank containing 5 ml NH_4OH and 50.0 mg Pb was run along with the brine samples. To avoid colloid formation, the solution was evaporated to 400-500 ml before the H_2S was added.

In the analysis of the sulfides, the following metals were determined quantitatively with the aid of specially prepared standards: Ni, Co, Cr, Cu, Mn, Zn, Fe, and V. All other analyses were made semiquantitatively.

Table I

Element	Limit of detection (ppm) Insol.	Sulfide	Mother liq.	Wave length Å
				3082.1
Al	0.1	0.00025	5	3092.7
				2528.5
Sb	0.1	0.00025	5	2598.0
As	0.2	0.0005	10	2780.2
Ba	0.02	0.00005	1	4554.0
Bi	0.02	0.00005	1	3067.7
Cd	0.1	0.00025	5	3261.0
Ca	0.02	0.00005	1	4226.7
Ce	0.02	0.00005	1	8521.1
Cr	0.1	0.00025	5	4254.3
Co	0.1	0.00025	5	3453.5
Cu	0.01	0.000025	0.5	3273.9
Ga	0.02	0.00005	1	2943.6
Ge	0.02	0.00005	1	3039.0
In	0.02	0.00005	1	3256.1
Fe	0.02	0.00005	1	3020.6
Pb	0.02	0.00005	1	2833.1
Li	0.02	0.00005	1	6707.8
Mg	0.1	0.00025	5	2852.1
Mn	0.02	0.00005	1	2798.2
Mo	0.1	0.00025	5	3193.9
Ni	0.1	0.00025	5	3414.7
P	1	0.0025	50	2535.6
K	0.02	0.00005	1	7664.8
Rb	0.02	0.00005	1	7800.2
Si	0.1	0.00025	5	2881.5
Ag	0.01	0.000025	0.5	3280.6
Na	0.02	0.00005	1	5889.9
Sr	0.02	0.00005	1	4607.3
Tl	0.1	0.00025	5	3519.2
Sn	0.02	0.00005	1	2839.9
Ti	0.1	0.00025	5	3078.6
W	1	0.0025	50	2944.4
V	0.02	0.00005	1	3185.4
Zn	0.1	0.00025	5	3345.0
Zr	0.1	0.00025	5	3601.2

The precipitate was allowed to settle over night and was then separated from the alkaline brine by centrifuging. It was washed several times with slightly alkaline H_2S-saturated distilled water. The washed precipitate was then transferred to a crucible, dried at 110°C, and analyzed spectrographically as was the alkaline "mother liquor." Since no information was available on the efficiency of this method of separation of trace elements, a separate spectrographic analyses was also made on the filtered mother liquor.[1]

To evaluate the contribution of the water impurities to the mother liquor analysis, the alkaline solution, after the removal of the sulfides in the blank analysis, was evaporated to dryness and the residue analyzed spectrographically.

All spectrographs were made using a Bausch and Lomb Littrow instrument. Samples were burned to completion using a d-c arc. Fifty mg of the "insolubles" or 100 mg of the salt obtained by evaporating the mother liquor was used for each analysis. The standards were prepared by adding 0.01 mg of each of the metals to 50.0 mg of high-purity lead and converting to sulfate. In each analysis of the "Sulfide Precipitate," the entire precipitate was converted to sulfates and burned to completion. The standard sulfate sample contained the equivalent of 0.01 ppm of each of the metals based on the original sample weight of 1000 g.

Discussion of Results

Table I gives the minimum concentration of each element detectable by the techniques used and the wave lengths used for detection. The data give the maximum amount of each element found.

Tables II and III give the analyses of the different salt samples. To conserve space the analyses of the sulfides and the mother liquors are combined under the heading of "Brines." The alkali metals and alkaline earth metals were not found in the sulfide precipitate. The only metallic impurities found in the filtered mother liquor were Cu, Fe, and Mn. These were close to the limit of detection and may be due largely to trace impurities in the graphite electrodes. The values listed for these metals in the brine column are based on analysis of the sulfides. Silicon

[1] Vanadium content of Pacific Coast solar salt found spectrographically, 5 ppb; independent analysis by colorimetric method, 7 ppb.

Table II

Element	Rock salt samples: Michigan Insoluble	Michigan Brine	New York Insoluble	New York Brine	Louisiana Insoluble	Louisiana Brine	Caribbean Insoluble	Caribbean Brine
	ppm Element in sample							
Al	750	0.09	900	0.9	150	0.09	>1000	0.9
Ba	25	N	10	N	N	N	100	N
Ca	—	—	—	—	—	—	—	—
Cr	N	0.01	N	0.01	N	<0.005	1.8	0.06
Co	N	<0.005	N	<0.005	N	<0.005	N	<0.005
Cu	5	0.3	1	0.09	1	0.03	18	0.2
Fe	250	0.9	1000	0.5	90	0.2	<1000	0.08
Pb	2	—	0.2	—	2	—	18	—
Mg	1000	500	1000	90	1000	90	>1000	900
Mn	10	0.04	100	0.03	100	1.2	180	0.1
Ni	N	0.08	N	0.01	N	0.012	1.0	0.03
K	200	9000	1000	5000	100	9000	180	9000
Si	1000	—	>1000	—	200	—	>1000	—
Ag	N	<0.005	N	<0.005	0.2	0.09	N	0.09
Na	100	—	200	—	1000	—	180	—
Sr	1000	9000	200	900	100	900	100	900
Sn	N	N	N	N	N	N	0.2	0.09
Ti	10	<0.005	200	<0.005	2	<0.005	180	0.09
V	N	<0.005	10	<0.005	N	<0.005	N	0.09
Zn	N	0.20	2	0.34	N	0.05	N	0.2
Zr	N	N	2	N	N	N	1.8	N

Table III

ppm Element in sample

Element	Purified salt		Solar salt					
			Caribbean		Great Salt Lake		Pacific Coast	
	New York	Louisiana	Insoluble	Brine	Insoluble	Brine	Insoluble	Brine
Al	0.09	0.05	18	0.9	15	0.009	>15	0.09
Ba	N	N	1	N	0.9	N	0.9	N
Ca	90	90	—	—	15	—	<15	—
Cr	<0.005	<0.005	N	0.02	0.05	<0.005	0.09	<0.005
Co	<0.005	<0.005	N	<0.005	N	<0.005	N	<0.005
Cu	0.57	0.04	0.2	0.2	0.9	0.008	0.5	0.1
Fe	0.25	0.20	18	0.3	<15	0.01	>15	0.08
Pb	—	—	0.1	—	0.5	—	0.05	—
Mg	9	9	—	900	>15	900	>15	900
Mn	0.002	0.009	0.2	0.003	0.9	<0.005	0.9	0.01
Ni	0.04	0.005	N	0.01	0.05	<0.005	0.09	0.009
K	90	90	1.8	9000	0.9	5000	0.9	5000
Si	—	—	—	—	>15	—	<15	—
Ag	0.009	0.009	N	0.09	N	0.009	N	0.009
Na	—	—	18	—	>15	—	<15	—
Sr	9	N	18	900	0.05	50	0.09	500
Sn	N	N	1.8	0.09	0.005	N	0.009	0.009
Ti	0.09	0.009	0.2	0.09	<15	N	<15	N
V	<0.005	0.008	N	0.06	N	<0.005	N	0.005
Zn	<0.01	<0.01	N	0.07	N	<0.005	N	0.01
Zr	N	N	N	N	0.09	N	0.09	N

was estimated only in the insoluble portion. Sufficient silicon can be extracted from laboratory glassware to show up in the spectra of the sulfides and mother liquors.

Where semi-quantitative analyses were made, the higher value of the range is listed. The symbol "N" in the tables indicates that the element was not detected, and (-) indicates that the concentration was not estimated. All values are corrected for the concentrations found in the blanks. An element listed in Table I, but not in the other tables, indicates that the element was not detected in either the insoluble or soluble portion.

Manuscript received April 2, 1958. This paper was prepared for delivery before the New York Meeting, April 27-May 1, 1958.

Any discussion of this paper will appear in a Discussion Section to be published in the December 1959 JOURNAL.

REFERENCES

1. G. Angel and T. Lunden, *This Journal*, **99**, 435 (1952).
2. G. Angel and R. Brämmland, *ibid.*, **99**, 442 (1952).
3. G. Angel, T. Lunden, and R. Brämmland, *ibid.*, **100**, 39 (1953).
4. G. Angel, T. Lunden, S. Dahlerus, and R. Brämmland, *ibid.*, **102**, 124 (1955).
5. G. Angel, T. Lunden, S. Dahlerus, and R. Brämmland, *ibid.*, **102**, 246 (1955).

The Oxygen Electrode

I. Isotopic Investigation of Electrode Mechanisms

Myron O. Davies,[1] Milton Clark,[2] Ernest Yeager, and Frank Hovorka

Department of Chemistry, Western Reserve University, Cleveland, Ohio

ABSTRACT

Isotopic techniques involving O^{18} have been used to study the cathodic and anodic properties of the oxygen-peroxide couple on partially hydrophobic, active carbon electrodes in alkaline solution. The isotopic analyses have been carried out with an analytical mass spectrometer. For the cathodic reaction, tracer and equilibration experiments prove that all of the peroxide oxygen originates from gaseous oxygen and that the O-O bond is not actually broken in the formation of the peroxide. Tracer experiments also indicate that the oxygen gas liberated during the anodic oxidation of the HO_2^- ion contains only peroxide oxygen. These results are interpreted in terms of various possible reaction mechanisms.

Various investigators (1-5) have demonstrated the reversibility of the oxygen-peroxide couple on active carbon electrodes in alkaline solution in the absence of a polarizing current. The over-all electrode reaction in alkaline solution may be represented as follows:

$$O_2 + H_2O + 2e \rightleftharpoons OH^- + HO_2^-$$

[1] Present address: N.A.S.A. Laboratory, Cleveland, Ohio.
[2] Present address: National Carbon Co., Cleveland, Ohio.

Cathodic (5,6) as well as anodic (7) polarization measurements[2] at Western Reserve University have indicated that the activation polarization associated with the oxygen-peroxide couple on active carbon in alkaline solution is generally small even at apparent current densities as high as 500 ma/cm^2. Concentration polarization involving the perhydroxide ion and molecular oxygen transport are the predominant sources of polarization under these conditions. As a result, polarization measurements have yielded only limited information concerning the electrode mechanisms associated with the oxygen-peroxide couple.

The following questions have been raised concerning the cathodic reaction:

(*A*) Does all of the peroxide oxygen originate from molecular oxygen? (*B*) Is the oxygen-oxygen bond actually broken in the formation of the peroxide? Similar questions have been proposed for the reverse anodic reaction. On a theoretical basis, the answer to the first question should be positive and to the second question negative, but no one had ever proved it conclusively.

The present experiments involving isotopic techniques represent an attempt to provide a definite proof. While tracer experiments involving O^{18} can be used to answer the first question, equilibration experiments are necessary to answer the second question. All of the isotopic experiments described in this paper have been carried out under substantially reversible electrochemical conditions.

Experimental Procedures

Isotopic concentrations in non-equilibrated oxygen gas.—In terms of the isotopes 16 and 18, oxygen gas contains the three molecular species O^{16}-O^{16}, O^{18}-O^{16}, and O^{18}-O^{18}. The O^{18}-enriched gas available for these experiments is approximately 1.4% O^{18} on an atomic basis. The concentration of O^{18}-O^{16} is twice the O^{18} concentration because there are two chances for the inclusion of an O^{18} atom in a given molecule (see Table I). The concentration of O^{18}-O^{18}, however, is approximately the square of the O^{18} concentration since the probability of two simultaneous, substantially independent events is involved. The latter is true only if the gas is completely equilibrated. Consider the results of diluting this O^{18}-enriched gas sample with oxygen gas containing no O^{18} in a 1:1 ratio. Table I indicates the concentrations for the case of nonequilibration and equilibration. For the former, the concentration of the species O^{18}-O^{18} is reduced by a factor of two, whereas in the latter case the concentration is reduced fourfold.

In the present research, various experiments have been performed in which nonequilibrated oxygen gas is converted to hydrogen peroxide. The peroxide is then oxidized to yield oxygen gas which is subsequently examined with a mass spectrometer to see if it has been equilibrated. From this information it is possible to establish whether the oxygen bond has been broken during any step.

Preparation of O^{18}-enriched gas.—The oxygen gas used in the isotope experiments was prepared by the electrolysis of O^{18}-enriched water (1.4% H_2O^{18}).[4] Sufficient H_2SO_4 was added to provide an approximately 1M solution. The electrolysis was carried out in an H-cell between smooth platinum electrodes. The oxygen gas was collected by means of an automatic system and stored as a liquid at liquid nitrogen temperatures for subsequent use.

Electrolytic cells.—Two cells of different design were required for the cathodic and anodic experiments. Figure 1 shows the cell used for the cathodic experiments. The cathode consisted of a porous graphite plug with a layer of active carbon approximately 1 mm thick on the surface exposed to the electrolyte. The apparent area of the cathode was approximately 3 cm^2. The oxygen gas was introduced through the rear side through inlet F. The side arm E, which was submerged in the water within a test tube, served as a pressure control by venting excess gas. The anode consisted of a 1-cm^2 piece of smooth platinum, which was enclosed in a separate compartment with a small hole connecting to the main cathode compartment. This arrangement reduced greatly the rate at which the peroxide generated at the cathode diffused to the anode where it would be oxidized. Oxygen liberated at the anode did not diffuse to the cathode in any appreciable amounts.

The active carbon layer on the cathode must serve the dual purpose of providing sites for the electrochemical reduction as well as a means by which molecular oxygen is readily transported to these sites. The effective transport of oxygen in the electrode structure has been shown (5, 6) to require a

[2] These polarization studies will be the subject of later papers in this series.

[4] Obtained from the Stuart Oxygen Co. of California.

Table I. Effects of dilution on isotopic concentrations

	O^{18} %	O^{18}-O^{16} %	O^{18}-O^{18} %
1. Original sample	1.4	2.8	0.02
2. Diluted sample (1:1)			
a. Equilibrated	0.7	1.4	0.005
b. Nonequilibrated	0.7	1.4	0.01

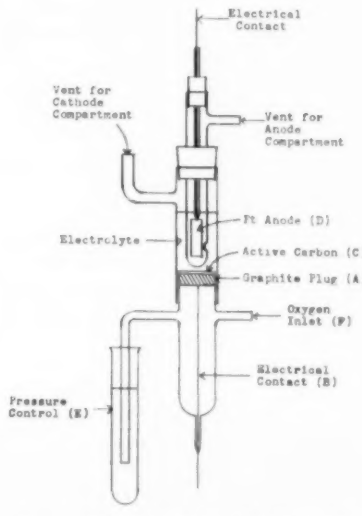

Fig. 1. Cathodic cell for O^{18} experiments

microporous structure containing no solution. For these reasons, the active carbon electrode must be partially hydrophobic to prevent the penetration of the solution into the porous structure. While active carbon itself is somewhat hydrophobic to alkaline solutions, additional waterproofing is obtained through the use of a material such as polyethylene, paraffin, or gum rubber, which also functions as a binder. In the present work, the active carbon layer was applied to the graphite plug by a technique similar to that used by Berl (1). A benzene suspension of active carbon containing gum rubber (5% by weight of carbon) was sprayed with a small atomizer onto the porous graphite plug. The graphite plug was warmed with an infrared lamp both before and after spraying and suction applied on the rear surface of the plug to expedite the rapid and complete removal of the benzene from the active carbon layer. Nuchar C 115[5] was chosen as the active carbon because cathodes prepared from this carbon have low polarization and do not decompose hydrogen peroxide very readily.

The cell used for the anodic experiments is shown in Fig. 2. The anode, A, consisted of a smooth platinum electrode with an area of approximately 3 cm^2. This platinum electrode was corrugated so that it would fit under the hood, B, and then was sprayed on both sides with active carbon by a procedure similar to that used for the preparation of the cathodes in Fig. 1. A small piece of platinum foil, C, located outside of the hood served as the cathode. The oxygen gas resulting from the anodic oxidation of the hydrogen peroxide in the solution was collected in the tube, E.

Cathode measurements.—Two types of cathodic experiments were carried out with the cell in Fig. 1. In one, ordinary oxygen (Linde) was used in conjunction with an enriched 1M KOH solution, prepared by dissolving analytical grade KOH in O^{18}-enriched water. In the second, the electrolytic solution was unenriched, but a 1:1 mixture of enriched oxygen and ordinary oxygen gas was fed to the cathode. No hydrogen peroxide was added to the electrolyte in the cathodic experiments.

[5] Product of West Virginia Pulp and Paper Co.

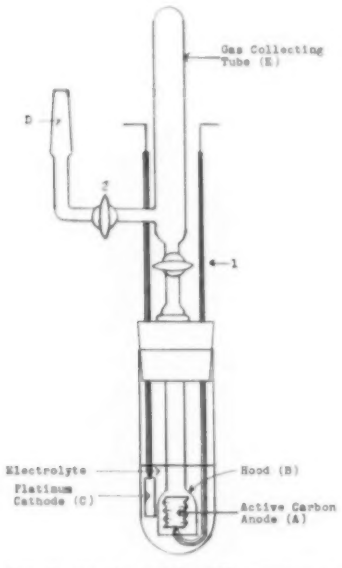

Fig. 2. Anodic cell for O^{18} experiments

In the experiment using the enriched oxygen mixture, the 1:1 mixture of enriched and unenriched oxygen was prepared by condensing an equal volume of Linde tank oxygen (U.S.P.) into the same tube in which the electrolytically produced, O^{18}-enriched oxygen had been collected. The two gases were mixed by distilling them over into another tube which was kept in a Dewar of liquid nitrogen until used in the electrochemical experiment. The outlet of this tube was connected to inlet F of the cathodic cell, the stopcock opened, and the Dewar lowered just enough to allow the oxygen to boil at such a rate that a steady stream of bubbles came from the outlet tube immersed in test tube E. For the majority of the experiments using only unenriched oxygen, the oxygen tank was connected directly to inlet F and the appropriate rate of flow obtained by means of the needle valve of the tank regulator.

After the oxygen flow had been adjusted, approximately 10 ml of electrolyte was added to the cell and the current turned on. Reduction was continued for 15 min after which the sample was quickly transferred to the peroxide decomposing system to be described shortly. Although it is possible for O^{18} to exchange between HO_2^- and H_2O, it has been shown (as will be described later) that no significant exchange occurs within 30 min. In all experiments this was the maximum time allowed to elapse from the beginning of the experiment until the solution was frozen in the peroxide decomposing system.

Anodic measurements.—The electrolyte consisted of 5M KOH prepared with O^{18}-enriched water to which sufficient 90% unstabilized H_2O_2 was added to yield a solution of approximately 0.9M with respect to peroxide. A volume of 25 ml of solution was required to fill the cell in Fig. 2. The solution was sucked up within the cell as far as stopcock 1. This stopcock was then closed and tube E was evacuated through outlet D, after which stopcock 2 was closed. The current was then turned on.

All of the oxygen liberated from the anode, as well as some oxygen resulting from the decomposition of hydrogen peroxide, was collected in the upper part of the tube above the hood below stopcock 1. Hydrogen from the cathode escaped into the atmosphere. From time to time oxygen which had collected in the upper part of the hood tube was admitted to the evacuated collecting tube E by opening stopcock 1. Care was taken to allow as little electrolyte as possible to be sucked into the upper tube. When sufficient oxygen gas had been obtained for the pressure in tube E to be 1 atm, the current was turned off. The total length of time from the introduction of the peroxide to the electrolyte until the end of the electrolysis was not more than 30 min.

After the completion of the electrolysis, the oxygen gas in tube E was passed through a dry ice-methanol trap to remove moisture and transferred to a storage bulb for subsequent mass spectrometer analysis.

Table II. Results of isotopic experiments

Conditions	O^{18}-O^{16} %	O^{18}-O^{18} %
A. Adsorption of enriched, nonequilibrated oxygen on active carbon at liquid nitrogen temperature, followed by desorption.		
1. Experimental	1.54	0.012
Expected if equilibration occurred	1.58	0.0062
Expected if no equilibration occurred	1.58	0.012
2. Experimental	1.50	0.0096
Expected if equilibration occurred	1.48	0.0055
Expected if no equilibration occurred	1.48	0.0086
B. Unenriched hydrogen peroxide in alkaline solution with enriched water for 30 min.		
Experimental	0.41	0.0008
Expected if no exchange	0.40	0.0004
Expected if complete exchange	2.8	0.020
C. Peroxide formed cathodically at an active carbon electrode in basic solution, using enriched, nonequilibrated oxygen and unenriched water.		
1. Experimental	1.27	0.0078
Expected if the oxygen in the peroxide came from the water only	0.40	0.0004
Expected if the oxygen in the peroxide came from the oxygen gas only		
With equilibration	1.24	0.0038
With no equilibration	1.24	0.0067
2. Experimental	1.37	0.0086
Expected if the oxygen in the peroxide came from the water only	0.40	0.0004
Expected if the oxgen in the peroxide came from the oxygen gas only		
With equilibration	1.41	0.0050
With no equilibration	1.41	0.0083
D. Peroxide formed cathodically at an active carbon electrode in basic solution, using tank oxygen and enriched water.		
1. Experimental	0.45	0.0023
Expected if the oxygen in the peroxide came from the water only	2.80	0.020
Expected if the oxygen in the peroxide came from the oxygen gas only	0.43	0.0026
2. Experimental	0.45	0.0021
Expected if the oxygen in the peroxide came from the water only	2.80	0.020
Expected if the oxygen in the peroxide came from the oxygen gas only	0.41	0.0022
3. Experimental	0.42	0.0029
Expected if the oxygen in the peroxide came from the water only	2.80	0.020
Expected if the oxygen in the peroxide came from the oxygen gas only	0.41	0.0021
E. Peroxide formed cathodically at an active carbon electrode in basic solution using enriched water and unenriched oxygen gas prepared by partial evaporation of liquefied tank gas.		
1. Experimental	0.42	0.00088
Expected if the oxygen in the peroxide came from the water only	2.80	0.020
Expected if the oxygen in the peroxide came from the oxygen gas only	0.40	0.00089
2. Experimental	0.43	0.00094
Expected if the oxygen in the peroxide came from the water only	2.80	0.020
Expected if the oxygen in the peroxide came from the oxygen gas only	0.40	0.00089
F. Oxygen gas formed anodically at an active carbon electrode in basic solution containing unenriched hydrogen peroxide.		
1. Experimental (with unenriched water)	0.39	0.00076
2. Experimental (with enriched water)	0.38	0.0014
Expected if the oxygen came from the water	2.80	0.020
Expected if the oxygen came from the peroxide	0.39	0.00076

Analytical procedures.—The hydrogen peroxide samples were decomposed with ceric sulfate as an oxidant in order to recover the peroxide oxygen for mass spectrometer analysis. Cahill and Taube (8) have shown that oxidation with this reagent liberates oxygen exclusively from the peroxide without exchange with oxygen of the water. These workers also believed that the rupture of the oxygen-oxygen bond does not occur in the oxidation of hydrogen peroxide with this reagent. The present experimental work verifies this conclusion.

Prior to the oxidation with ceric sulfate, the hydrogen peroxide solutions as well as the ceric sulfate-sulfuric acid solutions were degassed[6] to remove any dissolved molecular oxygen. The oxygen gas from the oxidation of the hydrogen peroxide was dried by means of a dry ice-methanol trap and then stored in a glass bulb for subsequent isotopic analysis.

A Consolidated Engineering analytical mass spectrometer (modified type 21-101) was used for all the isotopic analyses. This instrument was equipped with a nonmagnetic stainless steel analyzer tube in which the ionization zone was thermostated to 250° ±0.3°C. The surface of the tungsten filament within the analyzer tube was kept well carbided to minimize the attack of the filament by the oxygen gas. The mass spectrum for each sample was scanned from mass number 26 to 42 in order to include the peaks for nitrogen and argon, if present, as well as the various isotopic O_2 peaks. It was necessary to scan this range twice for each sample, once at high amplifier sensitivity and once at low amplifier sensitivity, because the high sensitivities required to give measurable 36 peaks (O^{18}-O^{18}) gave 32 peaks (O^{16}-O^{16}) which were too large to record. Mass 34 peaks (O^{18}-O^{16}) were measurable at both sensitivities.

The calculations of the relative isotopic concentrations are based on the assumption that the isotopic concentrations are directly proportional to the peak heights minus the background peak heights on the records from the mass spectrometer with the same proportionality constant for all three mass numbers: 32, 34, and 36. This assumption is justified only if the accelerating voltages used in the mass spectrometer are approximately the same for the various mass numbers. Such was the case in the present work. Corrections were made for nonlinearity in the recording system. An additional correction was necessary for the 36 peaks corresponding to O^{18}-O^{18}. Argon occurs as an impurity in oxygen gas prepared by liquefaction of air to the extent of about 0.5%. Evidence of this situation is readily apparent from the relatively prominent mass number 40 peaks in the mass spectra. Since argon has an isotope of mass 36, it has been necessary to apply a correction for this isotope. The ratio of the 36 to 40 peaks for argon is 0.31 to 99.68 in argon in the air (10). This ratio was assumed to apply to the argon in the oxygen gas as an approximation, although the actual ratio is probably higher because of the fractional distillation involved in the preparation of oxygen gas from air. The height of the 40 peak multiplied by 0.003 was subtracted from the 36 peak.

[6] For details concerning the procedure used for the recovery of the peroxide oxygen, see Ref. (9).

Experimental Results

Preliminary Experiments

Several preliminary experiments were carried out to become familiar with the techniques as well as to check certain aspects of the electrochemical experiments which might prove troublesome. The first experiment involved the adsorption of nonequilibrated oxygen gas on an active carbon sample (Nuchar C115) from which physically adsorbed gas had been removed previously. After 45 min at liquid nitrogen temperatures, the gas was desorbed by warming the sample of carbon to room temperature. The amount of gas adsorbed at the liquid nitrogen temperatures was just slightly less than that corresponding to a monolayer coverage as determined by earlier surface area measurements. The data in part A of Table II indicate that no equilibration occurred within the limits of reproducibility of the experiment. Since this experiment was for the most part at liquid nitrogen temperatures, the results do not imply that equilibration does not take place at room temperatures to some extent. Reproducibility generally was limited by contaminants in the oxygen gas, and to a lesser extent, background associated with the mass spectrometer.

The second preliminary experiment involved a check to see if appreciable exchange between oxygen in the water and oxygen in the peroxide occurs in alkaline solution during the time periods required for the electrochemical experiments. If such an exchange had occurred to any significant extent, the electrochemical experiments would have been invalidated. Sufficient 90% unenriched, nonstabilized hydrogen peroxide was added to a 1.4M KOH solution containing enriched water (approximately 1.4% O^{18}) to yield approximately 0.4M H_2O_2 solution. After 30 min the H_2O_2 was decomposed by the procedure described previously. The results are given in part B of Table II and indicate no exchange of peroxide oxygen and water oxygen within the limits of reproducibility during a period of 30 min. This was the maximum length of time during which H_2O_2 and H_2O were in contact in alkaline solution in the subsequent electrochemical experiments.

Electrochemical Experiments

In parts C to E of Table II are summarized the results of the cathodic experiments with O^{18}-enriched gas and water. In part F the results for the anodic experiments with O^{18}-enriched water are given.

All of the expected values for the O^{16}-O^{18} percentages in Table II are based on the original concentration of this species in the oxygen gas or the water involved in the experiment, as the case may be. In parts A and C the expected non-equilibration values for O^{16}-O^{16} are the same as for the original nonequilibrated enriched gas, while the expected equilibration values for O^{16}-O^{16} are calculated from the concentration of O^{16}-O^{18} in the original oxygen gas. The expected values for the concentration of O^{18}-O^{18} in parts D, E, and F of the table are based on the original oxygen gas used in the experiment or calculated on the basis of the atomic per cent O^{18} in the water, depending on which prediction is involved. In the predictions based on the O^{18} content of the original water used in preparing the solution, no correction was made for the small dilution effect of the base on the O^{18} content of the resulting solution.

Examination of the data revealed one fact which required further investigation. Unenriched oxgyen should contain only 0.0004% of O^{16}-O^{18}. Experimental values were consistently higher than this, as is evident in part D of Table II. If the unenriched oxygen gas was first liquefied and a fraction distilled off, the results were found to be closer to the expected values. An unenriched oxygen sample thus treated gave results of 0.40% for O^{16}-O^{16} and 0.0009% for O^{16}-O^{18}.

The remaining discrepancy of approximately twofold between the calculated value of 0.0004% for O^{16}-O^{18} and the measured value of 0.0009% for O^{16}-O^{18} is not surprising because these values are near the limit of sensitivity of the mass spectrometer and because relatively large background corrections are involved. The analyses of oxygen obtained from H_2O_2 produced cathodically from unenriched oxygen gas which had been fractionally distilled in the above manner also gave lower results for O^{16}-O^{18}. The data for two such experiments in 1M KOH with enriched water are given in part E of Table II. The agreement is considerably better than in part D. The nature of the impurity in the unenriched Linde U.S.P. oxygen which caused the discrepancies is not known, but apparently it is carried through the entire experimental procedure when the oxygen is not first distilled.

Conclusions

The data in parts C to F of Table II support the following conclusions concerning the oxygen-peroxide couple on active carbon in alkaline solution:

1. In the reduction of oxygen gas to hydrogen peroxide, all of the peroxide oxygen originates from the molecular oxygen. The reverse is also true for the anodic oxidation of peroxide to oxygen gas.

2. In the cathodic formation of hydrogen peroxide, the O-O bond is modified in type but not actually broken. In addition it is evident that the O-O bond is not broken in the oxidation of hydrogen peroxide with ceric sulfate in acid solution.

The following are three possible mechanisms for the oxygen cathode on carbon in alkaline solution:

Mechanism 1

$$H_2O + e \rightarrow H\ (ads) + OH^- \quad [1a]$$
$$O_2\ (gas) \rightarrow O_2\ (ads) \quad [1b]$$
$$O_2\ (ads) + H\ (ads) \rightarrow HO_2\ (ads) \quad [1c]$$
$$HO_2\ (ads) + e \rightarrow HO_2^- \quad [1d]$$

Mechanism 2

$$H_2O + e \rightarrow H\ (ads) + OH^- \quad [2a]$$
$$O_2\ (gas) \rightarrow O_2\ (ads) \quad [2b]$$
$$O_2\ (ads) + H\ (ads) \rightarrow HO_2\ (ads) \quad [2c]$$
$$HO_2\ (ads) + H\ (ads) \rightarrow H_2O_2 \quad [2d]$$
$$OH^- + H_2O_2 \rightarrow H_2O + O_2H^- \quad [2e]$$

Mechanism 3

$$O_2\ (gas) \rightarrow O_2\ (ads) \quad [3a]$$
$$O_2\ (ads) + H_2O + 2e \rightarrow HO_2^- + OH^- \quad [3b]$$

where step [3b] is intended to represent the direct electrochemical reduction of O_2 (ads) to HO_2^- without intermediate reactions involving adsorbed hydrogen. Step [3b] may proceed by several steps: for example,

$$O_2 \text{ (ads)} + H_2O + e^- \rightarrow HO_2 \text{ (ads)} + OH^-$$
$$HO_2 \text{ (ads)} + e^- \rightarrow HO_2^-$$

The authors favor mechanism 3, but the first two mechanisms involving chemi-adsorbed hydrogen cannot be discarded on the basis of information available at present.

It is not possible to distinguish between these mechanisms on the basis of the present isotope experiments. Mechanisms 1 and 2 may be considered as corresponding to hydrogen electrodes with the surface concentration of adsorbed hydrogen depressed by the reactions with adsorbed oxygen.

In later papers in this series, an attempt will be made to elucidate further the electrode mechanism in terms of cathodic and anodic polarization measurements for the oxygen-peroxide couple. In addition, fractionation experiments involving the oxygen-peroxide couple are planned.[7]

Acknowledgments

The authors are pleased to acknowledge the support of this research by the Office of Naval Research under Contract Nonr 58100 and by E. I. du Pont de Nemours and Company through a graduate fellowship to one of the authors (M.O.D.)

Manuscript received April 3, 1958. This paper was prepared for delivery before the Cincinnati Meeting, May 1-5, 1955.

Any discussion of this paper will appear in a Discussion Section to be published in the December 1959 JOURNAL.

[7] It is interesting to note that fractionation experiments involving the anodic formation of oxygen on various surfaces have been reported by Anbar and Taube (11).

REFERENCES

1. W. G. Berl, *Trans. Electrochem. Soc.*, **83**, 253 (1943).
2. R. Weisz and S. Jaffe, *ibid.*, **93**, 128 (1948).
3. K. Kordesch and A. Marko, *Oster. Chem. Ztg.*, **53**, 125 (1951).
4. K. Kordesch and F. Martinola, *Monatsch.*, **84**, 39 (1953).
5. R. Witherspoon, H. Urbach, E. Yeager, and F. Hovorka, Technical Report 4, Office of Naval Research Contract Nonr 58100, Western Reserve University, 1954.
6. M. Davies, M. Clark, E. Yeager, and F. Hovorka, Paper 163, Cincinnati Meeting, Electrochemical Society, May 1-5, 1955. (Theoretical Division Enlarged Abstract Booklet, pp. 52-4.)
7. M. Clark, M. Davies, E. Yeager, and F. Hovorka, Paper 28, Cleveland Meeting, Electrochemical Society, October 3, 1956.
8. A. Cahill and H. Taube, *J. Am. Chem. Soc.*, **74**, 2312 (1952).
9. M. Davies, M. Clark, E. Yeager, and F. Hovorka, Technical Report 6, Office of Naval Research, Contract Nonr 58100, Western Reserve University, 1956.
10. F. Aston, "Mass Spectra and Isotopes," p. 262, Edward Arnold and Co., London (1948).
11. M. Anbar and H. Taube, *J. Am. Chem. Soc.*, **78**, 3252 (1956).

Technical Notes

Magnesium-Bismuth Oxide Dry Cells

C. K. Morehouse and R. Glicksman

RCA Laboratories, Radio Corporation of America, Princeton, New Jersey

The oxides of mercury, thallium, and lead have been studied extensively as cathode materials for electrochemical cells. Mercuric oxide and lead dioxide are of practical significance, finding use as cathode materials in the zinc-mercuric oxide dry cell (1, 2) and the lead-acid storage cell (3, 4). Thallium(III) oxide (5), despite its desirable electrochemical properties, has not proved of practical value probably because of its high cost and two step voltage-time discharge curve during current flow (6). Bismuth oxide, the next oxide in this series, also has some attractive physical and chemical properties for use as a cathode material in electrochemical cells. For example, it has a low solubility in neutral solutions, is stable over a wide temperature range, and has a flat voltage-time discharge curve during current flow (6). Although bismuth oxide has a considerably lower reversible electrode potential than manganese dioxide and mercuric oxide cathode materials used at present in commercial dry cells, it does have greater theoretical ampere-minute capacity per unit of weight (20.7 amp-min/g) and volume (176 amp-min/cc) than these materials. Using the half-cell technique for evaluating cathode materials (7), it has been found that a bismuth oxide electrode operates at a potential (vs. hydrogen) of −0.30 to −0.40 v over a wide range of current densities and at an electrode efficiency in exeess of 90% when discharged at a constant current drain of 0.005 amp/g in an aqueous solution of magnesium bromide (250 g/l $MgBr_2 \cdot 6H_2O$).

Heil (13) describes a cell containing a mixture of bismuth oxide and manganese dioxide coupled with a zinc anode, while Edison (14-17) refers to the use of bismuth oxide in a nickel-iron storage cell, claiming that the addition of bismuth oxide to the electrodes results in improved performance. However, no practical dry cells containing this material have

been reported, probably because of the low resultant voltage obtained when coupling this cathode with a zinc anode.

In this paper the construction and performance characteristics of magnesium-bismuth oxide dry cells are described.

Experimental

Magnesium-bismuth oxide dry cells were assembled, using an impact extruded magnesium AA-size (height 1.82 in., OD 0.521 in., ID 0.441 in.) can, composed of AZ10A Dow Chemical Company alloy. The magnesium cans were lined with a piece of Nibroc salt-free paper (2¼ x 2¼ x 0.002 in. thick), and an extruded slug of cathode mix inserted in the lined can and consolidated. A carbon rod (height 1.787 in., diameter 0.159 in.) containing a brass cap was then inserted in the center of the cathode mix and the cells sealed with a rosin base wax seal in the conventional manner. Each cell contained approximately 10 g of cathode mix of the following formulation:

	% by weight
Bismuth oxide	54.7
Shawinigan acetylene black	6.8
Barium chromate	1.9
Electrolyte (an aqueous solution of 500 g/l $MgBr_2 \cdot 6H_2O$ and 1.0 g/l $Li_2CrO_4 \cdot 2H_2O$)	36.6

The open-circuit voltage of the bismuth oxide dry cells ranges between 1.60 and 1.65 v, the high voltage being due either to adsorbed air in the cathode mix or to the small amount of chromate which is added to inhibit the corrosion of the magnesium anode. When current is withdrawn from the cells, the voltage drops to a low value followed by a gradual increase to its operating voltage level. After the initial voltage drop, the cells have a flat voltage discharge curve operating slightly above 1.00 v for most of their useful discharge life as illustrated in Fig. 1. The initial voltage drop, which is believed to be due to changes which occur at the bismuth oxide electrode, is more noticeable at the high current drains and is different from that experienced with other magnesium dry cells.

Performance data in terms of hours of continuous service to a 0.90 v end voltage vs. load resistance are presented in Fig. 2. Also included are watt-minute capacity per unit of weight and volume data plotted against average continuous power output in milliwatts.

A favorable shelf life for the magnesium-bismuth dry cell is indicated by the fact that AA-size dry cells have given 75-80% of initial capacity as measured on 50- and 150-ohm continuous discharge tests to a 0.90 v end voltage after storage for 18 and 24 months at 70°F, 50% R. H.

The magnesium-bismuth oxide dry cells described in this paper have a flatter voltage-discharge curve and give more hours of service on continuous tests to end voltages of 1.00 v and lower than both the zinc-manganese dioxide Leclanché and magnesium-manganese dioxide (18) dry cells. At the present state of the development the technical difficulties

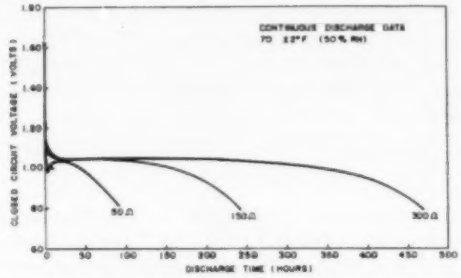

Fig. 1. AA-size magnesium-bismuth oxide dry cells discharged continuously through 50-, 150-, and 300-ohm resistances at 70° ± 2°F (50% R. H.).

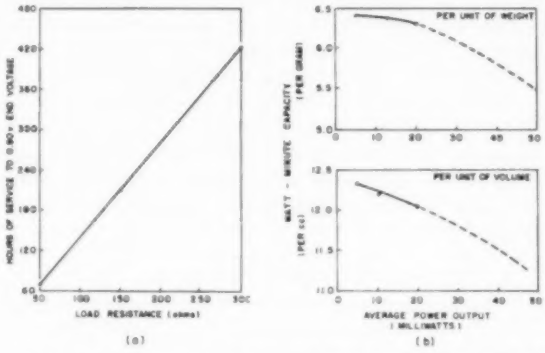
HOURS OF SERVICE TO 0.90 v END VOLTAGE
LOAD RESISTANCE (ohms)
(a)
WATT - MINUTE CAPACITY (PER GRAM)
PER UNIT OF WEIGHT
WATT - MINUTE CAPACITY (PER cc)
PER UNIT OF VOLUME
AVERAGE POWER OUTPUT (MILLIWATTS)
(b)

Fig. 2. Capacity data for AA-size magnesium-bismuth oxide cells in (a) hours of service to a 0.90 v end voltage vs. load resistance (b) watt-minutes per unit of volume and weight vs. average power output (capacity and average power computed to 0.90 v end voltages from continuous discharge data).

associated with these new cells are: (*a*) "delayed action," (*b*) high internal impedance, and (*c*) loss in capacity on light intermittent tests. These difficulties are believed to be associated with the magnesium electrode and can be solved with further research and development. It should be recognized, however, that bismuth oxide is inherently more expensive than manganese dioxide and, even if the technical problems can be overcome, these magnesium-bismuth oxide dry cells probably would find only limited application.

Acknowledgment

The authors wish to express their appreciation to Mr. G. R. Ganges for assisting in gathering some of the cell data.

Manuscript received March 7, 1958. This paper was prepared for delivery before the Ottawa Meeting, Sept. 28-Oct. 2, 1958.

Any discussion of this paper will appear in a Discussion Section to be published in the December 1959 JOURNAL.

REFERENCES

1. S. Ruben, *Trans. Electrochem. Soc.*, **92**, 219 (1947).
2. M. Friedman and C. E. McCauley, *ibid.*, **92**, 81 (1947).
3. G. W. Vinal, "Storage Batteries," 4th ed., John Wiley & Sons, Inc., New York (1954).
4. C. Drucker and A. Finkelstein, "Galvanische Elemente und Akkumulatoren," Akad. Verlag, Leipsig (1932).
5. S. Glasstone and A. Hickling, "Electrolytic Oxidation and Reduction," p. 105, D. Van Nostrand Co., Inc., New York (1936).

6. R. Glicksman and C. K. Morehouse, *This Journal*, **104**, 589 (1957).
7. C. K. Morehouse and R. Glicksman, *ibid.*, **103**, 94 (1956).
8. G. W. Vinal, *Elec. Eng.*, **67**, 456 (1948).
9. W. S. Herbert, *This Journal*, **99**, 190C (1952).
10. G. Leclanchés, *Mondes*, **16**, 532 (1868).
11. W. M. Latimer, "Oxidation Potentials," Prentice-Hall, Inc., New York (1952).
12. A. Walkley, *This Journal*, **99**, 209C (1952).
13. A. Heil, U.S. Pat. 1,195,677, Aug. 22, 1916.
14. T. A. Edison, U.S. Pat. 946,540, Jan. 18, 1910.
15. T. A. Edison, U.S. Pat. 999,762, Aug. 8, 1911.
16. T. A. Edison, U.S. Pat. 1,034,002, July 30, 1912.
17. T. A. Edison, U.S. Pat. 1,036,471, Aug. 20, 1912.
18. R. C. Kirk, P. F. George, and A. B. Fry, *This Journal*, **99**, 323 (1952).

Corrosion Product and Inhibitor Films on Aluminum

H. W. McCune

Miami Valley Laboratories, The Procter & Gamble Company, Cincinnati, Ohio

Effect of Inhibitors on Triphosphate Sorption

When aluminum corrodes in an alkaline sodium triphosphate solution, phosphate is incorporated into the surface oxide film on the metal (1). Corrosion in such sequestering solutions is more rapid than in most other alkaline solutions at the same pH, perhaps because a complex of Al(III) and sequestrant forms in the oxide surface at the solution-solid interface and plays an important role. Sodium silicate, potassium permanganate, and sodium chromate have been suggested as inhibitors for Al exposed to alkaline solutions (2). Sodium silicate has been suggested specifically for sodium pyrophosphate and sodium triphosphate solutions and has found wide application as an inhibitor in household detergent mixtures containing polyphosphates (3, 4). A comparison of the character of the corrosion product film with the inhibitor films was thought to bear on the mechanism of corrosion by sequestering agents and on the inhibition of such corrosion. The effect inhibitors have on the amount of triphosphate appearing on the surface of Al exposed to inhibited solutions of sodium triphosphate was first determined.

In Table I, the entries under "$Na_5P_3O_{10}$ deposited" were calculated from the phosphorus-32 activity sorbed on the Al specimens which were exposed to uninhibited and inhibited radioactive sodium triphosphate solutions. Triphosphate ion is probably the chief phosphate species sorbed. Hydrolysis in the bulk test solution is negligible, so only if a surface-catalyzed hydrolysis takes place would much lower phosphate be sorbed. The sorbed phosphate will be spoken of as "triphosphate," recognizing that its identity has not been proven. The specimens were weighed before and after exposure under stagnant conditions and after a standard dip in concentrated HNO_3 (5). Determination of the weight loss in HNO_3 is usually a rough measure of corrosion products. The "Total weight loss" of Table I is the sum of weight lost during exposure and during the HNO_3 dip. The metal was prepared as was described previously (1). The reported weight loss data were determined using 7.62 x 1.90 cm specimens. In the tracer determination of phosphate deposition, 1.90 x 1.90 cm specimens were used for convenience in counting. The sensitivity of the radiochemical determination was 0.001 mg/cm^2 and the precision was ±0.001 mg/cm^2 (95% confidence level).

Table I. Effect of inhibitors on triphosphate sorption

(0.02% inhibitor, 0.18% $Na_5P_3{}^{32}O_{10}$, 3.0 hr, 60°C, pH 9.5, 6.9 ml solution/cm^2 3003 Al)

Inhibitor	$Na_5P_3O_{10}$ deposited, mg/cm^2	Weight loss in HNO_3, mg/cm^2	Total weight loss, mg/cm^2
None	0.017	0.05	0.59
SiO_2 (sod. silicate)	0.000	0.00	0.01
$KMnO_4$	0.003	0.03	0.06*
K_2CrO_4	0.024	0.07	0.39

* Weight gain.

When sodium silicate was present at inhibitory concentrations, triphosphate was prevented from depositing in the film. Potassium permanganate almost eliminated phosphate deposition and formed a highly effective inhibitory coating. The film was highly colored, indicating that permanganate had been included in it. Potassium chromate increased the amount of phosphate deposited and had a slight inhibitory effect. The concentrated HNO_3 removed all of the radioactive phosphorus in these experiments except in the permanganate experiment, where it removed none. In the permanganate experiment determination of weight loss in HNO_3 obviously does not represent all of the corrosion products. The adsorbed triphosphate was roughly one-third of the total corrosion product in the uninhibited test and in the potassium chromate test. Not enough silica or corrosion product to be weighed was deposited with the silicate inhibitor in these experiments.

The attack of uninhibited alkaline triphosphate solutions on Al might be by way of the complexing of aluminum ions in solution, or by the formation of surface complexes with the oxide film, which is suggested by the incorporation of triphosphate into the film. The fact that the effective corrosion inhibitors, silicate and permanganate, largely prevent the incorporation of phosphate in the film and a poor inhibitor, chromate, does not prevent incorporation of triphosphate adds some support to the suggested role of the surface complex in increasing corrosion.

Sorption of Silicate

It has been reported that the hydrous metal oxide corrosion product plays an essential part by inter-

acting with silicate ions or silica to attach the protective film to the metal; chemical analysis, microscopic examination, and x-ray diffraction indicate that the film is mostly amorphous silica (6). The report that the siliceous film cannot continue to grow on itself (7) is a further indication of the importance of the metal oxide. Examination of the sorption of silicate on Al might indicate whether an inhibitory concentration is sufficient to cover the metal surface.

A sorption isotherm was determined using granular Al, reported to contain 1% or less impurity, which was given a wash with very dilute alkali followed by three washes with distilled water, a rinse in ethanol, and air drying. The 200-270 mesh fraction was taken, and the average particle size with respect to surface was determined microscopically. The specific surface was calculated to be 7.9×10^4 cm²/g. Sodium silicate solutions were made from filtered stock solution and analyzed for silica colorimetrically before and after shaking with the metal for 0.5 and 1.5 hr; there was no difference in the results obtained at these two times. The weight of the sorbate was calculated as SiO_2 from the decrease in solution concentration. The error introduced by loss of solvent to sorbent is estimated to be negligible compared to the variability of the data. If the weight of water sorbed is equal to the weight of the siliceous aluminum oxide film (see below), the volume of the solution would be changed less than 1%. Sodium triphosphate was absent in these experiments, but this appears to be justified by the absence of triphosphate from the inhibitory film formed when both silicate and triphosphate were in the solution.

The results in Fig. 1 show that at 60°C sorption on Al from a sodium silicate solution is essentially complete at about 0.45 mg SiO_2 per g of Al. From the specific surface of the Al granules used, this is 5.7×10^{-5} mg/cm². If it is assumed that the true area was determined microscopically and that SiO_2 molecules with an area of 12.3 sq A are sorbed (8), calculation indicates a coverage of 0.7. However, these are not very good assumptions, and whether less than a monolayer, a monolayer, or a few monolayers saturate the surface is unimportant for understanding corrosion inhibition in this case. The equilibrium concentration of SiO_2 corresponding to saturation of the surface is 150-250 mg/100 ml, which is an order of magnitude greater than the concentration of about 10-20 mg/100 ml which inhibits corrosion at the same temperature (4) (Table I). Apparently silicate by itself does not cover the metal but cooperates with the hydrous aluminum oxide to form the protective film.

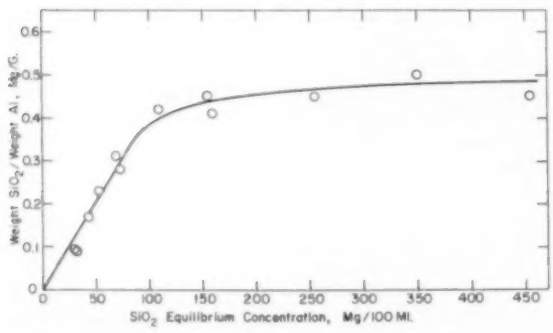

Fig. 1. Sorption isotherm of silica on Al at 60°C

Hypotheses advanced to explain how Si is built into the surface film on protected metals involve interaction of some combination of ions of the metal or the hydrous metal oxide with silicate ions or "silica micelles" (6). It is not possible to progress much further by examining the existence of possible reactants under pertinent conditions. The possibility of reaction of free aluminum ions can be dismissed in favor of aluminum ions bonded with water, hydroxide ions, and oxide ions and forming a continuous hydrous oxide film covering the metal surface. A reasonable picture of the reaction might be hydrous aluminum oxide reacting with monomeric or low molecular weight silicic acid, perhaps slightly ionized, depending on the pH (9), to produce an aluminum silicate. The aluminum ion is small enough to replace Si to some extent, adopting a coordination number of four toward oxygen, as half of the aluminum ions do in sillimanite, Al_2SiO_5, and as is common in other aluminosilicates (10). Aluminum is corroded much more rapidly by uninhibited triphosphate solutions and is protected much more effectively from sodium triphosphate solutions at low concentrations of silicates than is Zn, Ni, Ag, brass (4), Cu, or Pb. The decreased effectiveness of the inhibitor may be because the ions of these metals and alloys are larger than the aluminum ions and are not incorporated easily into metallosilicate structures.

Characterization of Isolated Films

Surface films were collected by exposing 50 to 150 dm² of Al foil (1100 purity, 0.0002 in. thick), then dissolving the metal in 5% bromine in methanol. The remaining solid film was filtered off on sintered glass, washed with methanol, and dried at 80°C before weighing. An exposure of 3 hr in 0.18% sodium triphosphate solution at 60°C gave 0.04 mg of corrosion products film per cm². This weight agreed fairly well with the weight loss in HNO_3 (Table I). It was found by chemical analysis that a similar film contained phosphorus equivalent to 0.016 mg $Na_5P_3O_{10}$ per cm² (1) which agrees well with the value in Table I determined by the use of P-32. Evidently the Al_2O_3 film contains a substantial fraction of phosphate. The triphosphate solution with sodium silicate equivalent to 0.02% silica added and also adjusted to pH 9.5, gave a film weighing 0.0013 mg/cm² under the same conditions. A correction of 0.0008 mg/cm² for the insoluble material in the clean, untreated foil must be subtracted from the weights collected. Clearly the inhibitory film is very thin, a few tens of angstroms thick. X-ray diffraction indicated that the insoluble material from the foil itself contained crystalline Si and a little Cu; after ignition, a pattern for a crystalline aluminum silicate was obtained, indicating the presence of Al from the air-formed film initially present on the foil.

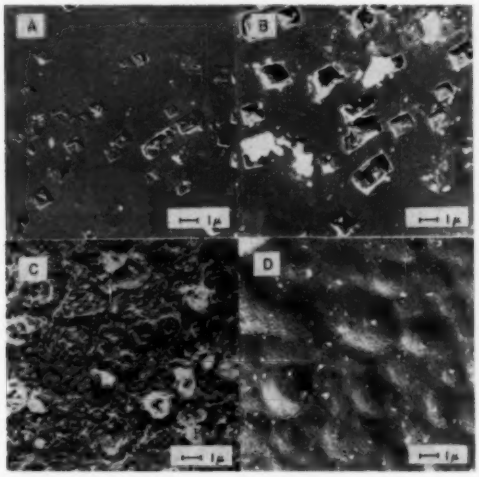

Fig. 2. Electron micrographs of Al surfaces: A, polished and etched; B, after exposure to 0.18% $Na_5P_5O_{10}$, 0.02% SiO_2, 3 hr, 60°C, pH 9.5; C, same as B without the SiO_2; D, same as C after corrosion products were removed in concentrated HNO_3.

Neither sample of film from treated foils gave crystalline x-ray diffraction lines other than those of Si and Cu, with CuK_α radiation.

Electron Microscopy of the Surface

Portions of the 3003 sheet Al were electropolished in an aqueous solution of methanol and perchloric acid. The samples were then lightly etched in a methanol solution of bromine for 15-30 sec, washed, and exposed to the corrosive conditions of interest. After removal of the metal from the test solutions, liquid was blown off with an air jet. Chromium replicas about 150Å thick were prepared by oblique evaporation and freed by dissolving the aluminum in bromine-methanol. To demonstrate that the results were not affected by the method of sample preparation, additional samples were prepared by polishing with an abrasive and etching with a dilute HNO_3-HF-HCl solution. Similar electron micrographs were obtained, but electropolishing followed by bromine-methanol etch gave more nearly reproducible surfaces and more sharply defined etch pits.

Sheet Al is polycrystalline, but the electron micrographs shown include portions of only one or a few crystallites. Electropolishing gave a smooth, abrasive-free surface like the background of Fig. 2A. The samples were all etched in bromine-methanol to remove, by dissolving the metal, any film left by polishing and to give a texture to the surface which might permit observation of surface films. Rectangular etch pits developed and, from their orientation, show that Fig. 2A includes parts of two crystallites. In electron micrographs of samples exposed to triphosphate solutions inhibited with sodium silicate there was no evidence of a continuous film covering the surface and obscuring the edges of the pits (Fig. 2B). Evidently the siliceous film is textureless, and probably it is very thin. The white, irregular unshadowed particles prominent in Fig. 2B and 2D are absent in many other micrographs of similar subjects; hence it is concluded that they are accidental contamination. The set of micrographs shown in Fig. 2 was chosen from the sets available as the most informative over-all despite the contamination. In a majority of micrographs, the rectangular pits appear larger in samples exposed to inhibited triphosphate solution than in the etched blanks, but this does not necessarily represent a real difference. When the inhibitor was omitted, corrosion product was built up, and the metal was attacked within the crystallites (Fig. 2C). A dip in concentrated HNO_3 removed the corrosion products and revealed that corrosion gave rise to shallow circular pits (Fig. 2D).

Acknowledgment

The author wishes to express his thanks to A. P. Murphy, who is responsible for the light and electron microscopy, and to W. E. Cooley for aid in preparing the manuscript.

Manuscript received April 10, 1958.

Any discussion of this paper will appear in a Discussion Section to be published in the December 1959 JOURNAL.

REFERENCES

1. H. W. McCune, *Ind. Eng. Chem.*, **50**, 67 (1958).
2. J. M. Bryan, "Aluminium and Aluminium Alloys in the Food Industry," H. M. Stationery Office, London (1948).
3. J. C. Harris, "Metal Cleaning Bibliographical Abstracts," Am. Soc. Testing Materials, Spec. Tech. Publ., 90B (1953) and 90C (1954).
4. R. Getty, N. W. McCready, and W. Stericker, ASTM Bull. No. 205, April (1955).
5. "ASTM Standard, 1952, Part 2, Non-ferrous Metals," p. 1045. ASTM Designation: B185-43T.
6. L. Lehrman and H. L. Shuldener, *J. Am. Water Works Assoc.*, **43**, 175 (1951).
7. J. G. Vail, "Soluble Silicates," Monograph No. 116, Am. Chem. Soc., Vol. II, p. 248ff, Reinhold Publishing Corp., New York (1952).
8. P. F. Holt and D. T. King, *J. Chem. Soc.*, **1955**, 773.
9. R. K. Iler, "The Colloid Chemistry of Silica and Silicates," Cornell University Press, Ithaca, N. Y (1955).
10. A. F. Wells, "Structural Inorganic Chemistry," 2nd ed., p. 569, Oxford University Press, London (1950).

Additives and Grain Refinement

D. A. Vermilyea

Research Laboratory, General Electric Company, Schenectady, New York

Most commercial plating baths contain some addition agent which is added to produce a desirable structure in the deposits. These addition agents are usually high molecular weight organic compounds or colloids, small ions or molecules being generally not very effective (1). The purpose of this note is to suggest a mechanism by which such addition agents may modify the crystal structure of electrodeposits. Silver will be used as an example.

It has often been observed (2-4) that the deposition of Ag from a $AgNO_3$ solution containing high molecular weight organic compounds may result in the formation of filaments or "whiskers" of Ag. Whiskers of Cu have also been reported (5, 6). A theory to account for such growth has been given by Price, Vermilyea, and Webb (7). According to the theory, organic molecules adsorb on the crystal and interfere with the motion of lattice steps over the surface. When the concentration of molecules adsorbed on the surface is above a critical value depending on the overvoltage, step motion is completely blocked and no further growth of the crystal occurs. On the other hand, molecules adsorbed on a rapidly growing surface are thought to be incorporated into the crystal as lattice steps move around and past them. According to this picture, therefore, molecules adsorbed on the surface interfere with growth; they may be removed from the surface by incorporation into the crystal. If the crystal grows rapidly enough, the surface will be kept clean because adsorbed molecules are buried as fast as they reach the surface by diffusion. At slower growth rates adsorbate reaches the surface faster than it can be buried; the surface becomes severely contaminated, and growth stops.

A major prediction of the theory of Price, Vermilyea, and Webb (7) is that there is a critical current density for the continued growth of a metal crystal in a solution containing large, strongly adsorbed molecules. At the critical current density there is a balance between the rate of diffusion of molecules to the surface and the rate of incorporation into the crystal. The equation for the critical current density for a spherical crystal of a given metal for a given metal ion concentration and temperature is

$$I_c = \text{const}\left(\frac{C_i}{r}\right)^{1/2} \qquad [1]$$

where C_i is the concentration of adsorbate in the solution, and r is the radius of the crystal. Equation [1] is valid for crystals with radii less than about 10 μ. Typical critical current densities observed from whisker growth experiments range from 0.1-10 amp/cm^2; somewhat larger values may be expected with the larger additive concentrations used commercially.

Now consider the electrodeposition of a metal from a solution containing some substance, either organic compound or colloidal material, which is strongly adsorbed on the electrode surface. Before the application of current, the electrode will be completely contaminated. When a current is passed through the cell the electrode potential will rise until deposition begins to occur on the most active sites of the electrode. Crystals would probably start growing at many points on the surface. The overvoltage required to start the deposition would be large because of the initial contamination of the electrode, and the crystals once nucleated would grow very rapidly. Consequently, there would be a rapid and considerable concentration polarization in the vicinity of each growing crystal.

Now consider just one of the many small growing crystals. Around the crystal there will be a hemispherical diffusion field, and if the crystal is small ($< 10\mu$ diam) the gradient at the crystal surface will be proportional to the concentration difference between the bulk of the solution and the surface of the crystal and to the reciprocal of the crystal radius. As the crystal grows a larger concentration difference is required to maintain the same concentration gradient at the surface. When the concentration of metal ions at the surface has become essentially zero it will no longer be possible to maintain the same gradient at the crystal surface, and further growth of the crystal will result in a rapid decrease in the current density.

It is clear, therefore, that eventually it will not be possible to maintain the critical current density of Eq. [1], and that the crystal surfaces will become contaminated and stop growing.

On the electrode as a whole, crystals will continually nucleate, grow, reach a limiting size, become contaminated, and stop growing. It is unlikely that a new crystal will nucleate near or on one which has just stopped growing because the solution in that area is depleted of metal ions. The tendency of new crystals to start as far as possible from ones which just stopped will insure a uniform coverage of the electrode.

It is possible to estimate the size of the crystals which result from such a process. The current density at a growing crystal is given by

$$I = zFD\frac{dC}{dr} \qquad [2]$$

where I is the current density, z the ionic charge, F the Faraday constant, D the diffusion coefficient, and dC/dr the concentration gradient at the crystal surface. For a small hemispherical crystal $dC/dr \sim \Delta C/r$, and hence with $D \sim 10^{-5}$ cm^2/sec, $\Delta C_{max} = 10^{-3}$ mole/cc, $I_{max} = 10^{-8}/r$. Hence, if the critical current density is

10 amp/cm² the maximum particle size is about 1μ, a reasonable size for a fine-grained deposit.

This simple picture accounts for the very fine grain size produced by additives and for the uniformity of the deposit. It also accounts for the fact that the addition agents which are effective in altering the structure of the deposit are invariably incorporated into the deposit in rather large quantities (of the order of a percent) (8). It also accounts for the absence of specificity reported by Fischer (9); since almost the only requirements for effectiveness are that the units of the additive be large and strongly adsorbed, it is apparent that many substances can accomplish about the same result.

Manuscript received June 18, 1958.

Any discussion of this paper will appear in a Discussion Section to be published in the December 1959 JOURNAL.

REFERENCES

1. H. Fischer, "Elektrolytische Abscheidung und Elektrokristallisation Von Metallen," p. 270, Springer, Berlin (1956).
2. K. M. Gorbunova and A. I. Zhukova, *J. Phys. Chem. U.S.S.R.*, **23**, 605 (1949).
3. K. M. Gorbunova and P. D. Dankov, *ibid.*, **23**, 616 (1949).
4. L. Graf and W. Morgenstern, *Z. Naturforsch.*, **10a**, 345 (1955).
5. P. A. Van der Meulen and H. V. Lindstrom, *This Journal*, **103**, 390 (1956).
6. T. C. J. Ovenston, C. A. Parker, and A. E. Robinson, *ibid.*, **104**, 607 (1957).
7. P. B. Price, D. A. Vermilyea, and M. B. Webb, to be *Acta Met.*, **6**, 524 (1958).
8. Ref. (1), p. 519.
9. Ref. (1), p. 236.

Measurement of Carbon-Metal Contact Resistances

H. L. Foltz and M. R. Hertz

Technical Division, Goodyear Atomic Corporation, Portsmouth, Ohio

The use of large quantities of elemental fluorine in AEC gaseous diffusion plants has led to numerous research projects concerning materials suitable for use in fluorine generators. The cell being used at present to generate fluorine consists basically of a Monel shell and head assembly from which wire mesh diaphrams, steel cathode, and carbon anode subassemblies are suspended.

One of the major causes of low power efficiency and early cell failure has been the electrical deterioration of the carbon anode-metal connection in the anode subassemblies. Since an initially high contact resistance would be conducive to heating of the carbon anode-bus-bar joint with further corrosion of the contact areas, still higher resistance, and so on, work has been completed to determine the relation between contact pressure and contact resistance for various carbon-metal joints. From this work it has been determined that of five metals tested, copper and beryllium copper give the lowest contact resistance, followed by phosphor bronze, magnesium, and steel.

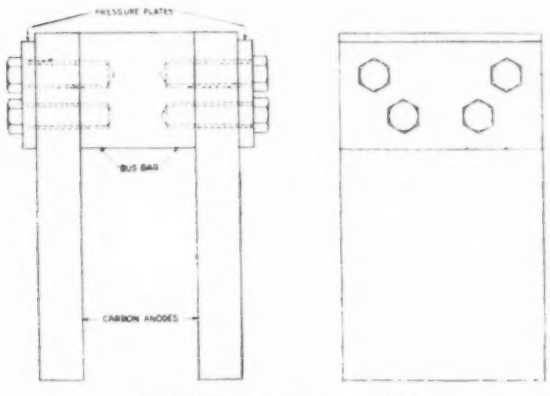

Fig. 1. Anode clamping assembly

Measurements of anode-bar contact resistance as a function of torque did not give consistent results, possibly because of pressure plate warping or a nonlinear increase in thread friction as torque was increased.

As shown in Fig. 1, the carbon anodes are clamped between the bus bar and pressure plates by four ¾-in. steel cap screws per anode. The contact areas of the anodes are specified to be ground smooth and parallel. Original cell assembly specifications called for the cap screws to be torqued to 85 ft lb, which is approximately equivalent to 1400 psi pressure on the anode contact area, the exact pressure being a function of the condition of the threads and their lubrication.

In Fig. 2 the test set-up used is shown. A carbon sample block was compressed between the two metal contact plates by means of a hand operated hydraulic press; the force was applied through a Baldwin SR-4, Type U-1 load cell, which was coupled to a type M strain indicator. Precautions were taken to make sure that the load was applied to the specimen on the vertical axis. The load cell-indicator combination was checked against an Olson testing machine and was found to have an accuracy of ± ¼% of full range (5000 lb). One metal contact plate was insulated from the press so that resistance measurements could be made between the two plates.

For resistance measurement current and potential leads, attached to the contact plates, were connected to a Biddle Model 713 "Ductor" Low Resistance Ohmmeter. This instrument operates on a somewhat similar principle to that of a Kelvin bridge, except that it incorporates a special highly sensitive D'Arsonval-type meter with both a current and a voltage coil to replace the bridge circuit. Thus, increased current tends to decrease the reading, while increased voltage increases the reading. The meter has a basic 0 to 100 micro-ohm range with five

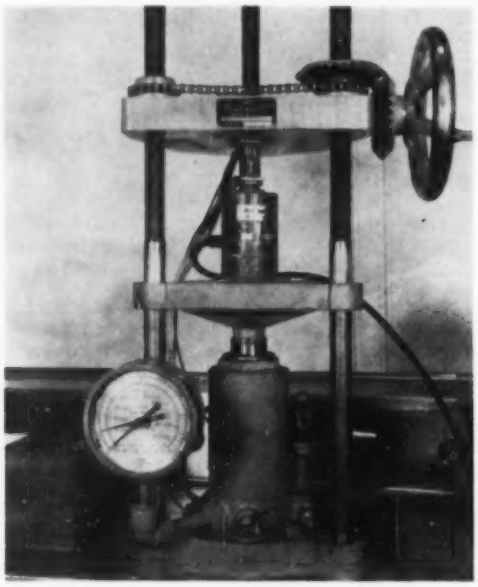

Fig. 2. Compressing carbon block samples between metal contact plates.

decade multiplying ranges giving an over-all range of 0-1 ohm with an accuracy of 1% of full scale for any range. This permits an error approaching 10% at certain readings.

Carbon sample blocks, 1 in.^{2} in cross section and approximately 2 in. high, were cut from the contact area of anodes so that the original surface was retained for the contact pressure vs. resistance measurements. For steel contacts, sections were cut from actual steel pressure plates, while for other metal contacts various metal stock was used, finished with a series of grades of emery paper of increasing fineness.

The actual resistance reading was that for two 1-in.^{2} carbon-metal contact areas and of a 2-in. length of carbon 1 in.^{2} in cross section, all in series. Contact resistance per square inch of area is then:

$$R = (R_t - R_c)/2$$

where R_t is the resistance measured on the meter and R_c is the specific resistance of the carbon in ohms per cubic inch. Since the potential leads were attached directly to the contact plates, the resistance of the metal plates themselves could be disregarded. This was checked by pressing the two plates together while resistance was measured. The resistance was found to be negligible even though an added metal-metal contact was involved.

The specific resistance of National Carbon Company Type YBD carbon, which is not graphite, as given by the manufacturer, is 1550 μ ohms/in.^{3}. This value was obtained by measuring the resistance of a large number of full size anodes lengthwise, using a Kelvin bridge. When this figure was used for the specific resistance of carbon in preliminary tests, the results were somewhat variable from sample to sample. However, when resistance vs. pressure curves were run several times on the same carbon sample block, there was little variation.

Variation could be attributed either to differences in the condition of the carbon contact surfaces from sample to sample, or to differences between the specific resistance of the carbon in the various samples. Since the anodes are formed by extrusion in a lengthwise direction, there should be some difference in carbon density in various locations in the anode, and some pore orientation should occur in the lengthwise direction. This in turn could be expected to result in a lower specific resistance of carbon lengthwise than across the anodes, the latter applying to this experiment. In addition, the National Carbon Company has measured air permeabilities twice as great in the lengthwise as in the transverse direction. Twenty-eight blocks, nominally 1 x 1 x 2 in., were cut from each of two anode blades, half lengthwise, as National Carbon measured resistance, and half transversely, the ends being the normal contact area. They were each placed in the press between pressure plates in the normal manner and resistance measured between two scribe marks, 1 in. apart. Exact dimensions were measured with a micrometer calipers. Values for transverse specific resistance varied from 1600 to 2100 μ ohms/in.^{3} with an average of 1810 μ ohms/in.^{3}. Standard deviation was approximately 100 μ ohms/in.^{3}. With samples cut in the lengthwise direction, variation was similar but the average value of specific resistance was 1190 μ ohms/in.^{3}. This was somewhat lower than that obtained by National Carbon Company. In view of the large variation between samples, the specific resistance was measured for each block and this value used in calculating contact resistance.

Several samples were loaded over a range of pressures from 600 to 5000 psi. Pressure was increased by 400-lb increments up to 5000 lb and then decreased by the same increments back to 600 lb, 5000 psi approaches the compressive strength of carbon and should be avoided for design purposes. The plots of contact resistance vs. pressure were found to approximate straight lines on a log-log graph, although the slopes were slightly smaller for the unloading curves. These plots are shown in Fig. 3.

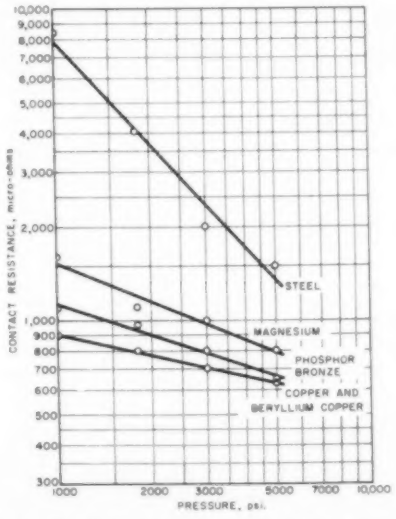

Fig. 3. Contact resistance as a function of pressure

It can be seen that, while the steel-carbon contact resistance decreases rapidly when pressure increases, it never approaches the copper-carbon contact resistance and is greater than the contact resistance of any of the other metals tested.

It has been proposed that the measured contact resistance in newly assembled cells might give some indication of the expected performance of the cell. Since humidity of the anode storage and assembly environment is one factor that is not controlled, a test was made to determine the contact resistance-pressure function of anode material which had been oven dried as compared to that which had been stored for some time in an atmosphere at 100% humidity. Some samples were dried for 165 hr at 210°C, while others were stored for 96 hr in a desiccator containing a wet sponge. When tested with both copper and steel no significant difference in contact resistance was found between dried samples, those which were in equilibrium with the laboratory atmosphere, and those stored at 100% humidity.

In the cell, the carbon metal contact is exposed to a mixture of fluorine and hydrogen fluoride gases, as well as to the liquid electrolyte which may enter the joint through capillary action in the somewhat porous carbon anode.

With the experimental set-up used it was impossible to expose the contact to a fluorine atmosphere while under pressure. The metal plates, however, were fluorinated for 48 hr with 100% fluorine at 100°C. The metal plates were then removed and contact resistance against carbon determined as before. Care was exercised that the fluorinated layer was undisturbed. Results are shown in Table I.

The increase in contact resistance was negligible for beryllium-copper, a factor of approximately three for copper and magnesium, and a factor of five for phosphor-bronze. Contact resistance for steel could not be measured with the normal equipment and was found to be greater than 20 megohms when measured with a conventional ohmmeter. It must be noted that the fluorination was done with dry fluorine which contained no hydrogen fluoride. Fluorination in a cell might not affect the micro-areas of the metal actually in contact with carbon. However, the extreme insulating value of the fluoride layer on steel indicates that this metal is of doubtful value as a contact material in a fluorine cell.

Table I. Contact resistance-pressure values for carbon-fluorinated metal

Pressure psi	Steel megohms	Contact resistance in micro-ohms/in.^{2} Mg	Phosphor-Bronze	Cu	Be-Cu
1000	>20	3560	4830	2330	900
1800	>20	2440	3170	1610	683
3000	>20	1760	2260	1140	575
5000	>20	1230	1600	858	517

The resistance-pressure relationship for any metal has the general equation:

$$R = a\,P^m$$

where R is contact resistance, a, a constant, P, pressure, and m, slope of log-log plot. Both a and m are different for each metal.

From the results it is apparent that the largest unit pressure possible, applied uniformly over the contact surfaces, results in the lowest contact resistance. The use of copper alloys and magnesium result in lower contact resistance than does the use of steel. Copper contact plates have been used for at least fifteen years and the tests confirm the suitability. Steel appears to be of doubtful value in this application.

Manuscript received May 16, 1958. The work on this paper was performed under Contract AT-(33-2)-1 with the U. S. Atomic Energy Commission.

Any discussion of this paper will appear in a Discussion Section to be published in the December 1959 JOURNAL.

REFERENCE

1. R. L. Murray, S. G. Osborne, and M. S. Kircher, *Ind. Eng. Chem.*, **39**, 249 (1947).

Technical Review

Electrodeposition of Powders for Powder Metallurgy

C. L. Mantell

Department of Chemical Engineering, Newark College of Engineering, Newark, New Jersey

ABSTRACT

A very large number of articles are made by powder metallurgical methods from electrolytically reduced powders. In powder production, cathode current densities are much higher than those of refining; loosely adherent deposits are produced. These are dried, surface oxides removed, and classified by screening. Important electrolytic powders are those of copper, iron, nickel, zinc, some alloys, as well as duplexes. Operating details are reviewed.

Metal deposited at the cathode varies widely in its characteristics, depending on the electrolyte itself, the ions present, and operating conditions. Silver deposited from a solution of $AgNO_3$ forms large, readily visible crystals. Tin from a solution of $SnCl_4$ will form long needles which may rapidly "bridge" from the anode to the cathode. Lead from a chloride or acetate solution gives crystals different from those from a chlorate or perchlorate electrolyte. Nickel deposits from a sulfate bath are hard and may be polished but not with ease, while nickel from a naphthalene sulfonate gives bright deposits needing little if any polishing.

In plating, efficiency of utilization of electrical energy is secondary to quality. High current and energy efficiencies may be sacrificed without upsetting the economics of the operation. Particularly where thermal or chemical processes compete, power cost in refining is a major item; maximum current and energy efficiencies are vital. In electroforming, of which metal powder production is a form, conditions approach refining to a far greater degree than plating, as the procedures compete with thermal and mechanical disintegration procedures.

The nature of the electrolyte, its pH, metallic ion concentration, anodic and cathodic current density, temperature, the simplicity or complexity of the metallic ion including its primary and secondary ionization, as well as the presence of modifying or "addition" agents, have effects on the character of the deposit.

The crystalline structures of cathode deposits may be classified as follows:

Group I. The initial nuclei or crystals continue to grow throughout the deposit forming (*A*) isolated crystals: which are (*a*) symmetrical or (*b*) acicular; or giving rise to (*B*) contiguous crystals: which may be (*a*) columnar or (*b*) fibrous.

Group II. Part of the initial nuclei or crystals continue to grow. These are (*A*) conical ("normal") or (*B*) twinned.

Group III. The nuclei or crystals do not grow for any extended period. Their shapes are (*A*) broken (compact), or (*B*) arboreal, sometimes called "fernlike" ("treed"), or (*C*) powdery (spongy), and (*D*) slimelike.

If any addition which would increase the cathode polarization be made to the solution, the number of crystal nuclei increases. The current densities may be increased, and the effective metal ion might be decreased in the film or thin layer of solution adjacent to the cathode by (*a*) diluting the solution; (*b*) decreasing the temperature, which in turn reduces diffusion and convection; (*c*) adding a salt having an ion common with those already present; (*d*) introducing a colloid; (*e*) increasing the viscosity of the solution; and (*f*) causing the formation of complex ions. These factors increase the difference in cathode potential, the number of crystal nuclei, and the production of fine-grained deposits.

Dissociation, ionic migration, diffusion, and convection, particularly at the surface of the cathode, replenish the metal ion concentration. Growth of existing crystals may be favored by acceleration of these factors. The tendency of metals such as silver and lead, when deposited from nitrate solutions, to form isolated crystals is partly the result of the relatively large change in density of the solution produced by the removal of the metal. The effects of various factors upon the structure of deposits are summarized in Table I.

Decreasing the metal ion concentration decreases the size of the crystals. Fine-grained, bright, or hard deposits are produced at low temperatures, while increase of temperature causes coarse or soft deposits. The effects of increases of current density and

Table I. Direction of effects on structure of deposits

Change in operating condition	Change in structure group*
Increase metal salt concentration	III → II → I
Increase metal ion concentration	III → II → I
Agitate solution	III → II → I
Elevate temperature	III → II → I
Increase conductivity of solution	III → II → I
Add colloids to solution	I → II → III
Increase viscosity of solution	I → II → III
Increase current density	I → II → III

* Groups as described above in the text.

temperature are in opposite directions. Therefore, it is possible to obtain fine-grained deposits in warm solutions at a high current density. Addition of colloids in more than small amounts, increase of viscosity, and increase in current density tend in the direction of broken crystals, arboreal, or powdery electrolytic precipitates.

Deposited metal powders are represented by the Group III type of crystals. They are "poor" electroplates. Powder production is favored by low metal concentration, low metal ion concentration, unagitated solutions, low temperatures, solutions of low conductivity, addition of colloids, increases in viscosity, and marked increases in current density. The effect of each variable is not of the same order of magnitude; the effects are cumulative and interdependent; changes in concentration may be of greater importance than variation of temperature; vigorous agitation may offset the effect of increase of current density.

Electrolytic powders of commercial importance are of two varieties. Loose crystals may be formed in the cells as nonadherent powders, or the powder may result from grinding relatively hard, brittle, partially coherent deposits. Examples of the first class are Cu, Zn, Ni, Ag, and Pb; of the second Fe and Mn. These will be briefly described from the viewpoint of their production. While electrolytic Zn, Ni, and Pb powders are interesting, they are commercially unimportant in that powders of these metals are the result of other methods; industrially only electrolytic Cu, Fe, and Mn command markets. Silver crystals are the conventional result of electrolytic refining. Disintegration converts them to a powder.

The powders all command "shape" premiums in price over ingot metal or cathode chip of the same purity.

In practice, cathode current densities are higher than those of refining, so that loosely adherent spongy deposits which are periodically removed by scraping or tapping devices or by electrolyte circulation may be produced. In the case of Cu powder, acid electrolytes of lower metal and higher acid concentration than those used for refining or plating are preferred. When operated at high cathode density and with hydrogen evolution, the finely divided metal crystals often have a fernlike appearance under the microscope. It is necessary to remove the cathode frequently; otherwise the effective area of the deposit is increased to such an extent that the current density is lowered and coarse deposits formed.

The fineness of the powder may be varied over a considerable range by changes in the composition, temperature of the electrolyte, and variation of the cathode current density, as well as by the introduction of addition agents, reducing compounds, or substances which are cathodically reduced and anodically oxidized but are not plated out. Cathode current densities are different from those at the anode, usually higher. The deposited powders are washed, dried in inert or reducing atmospheres, and cooled to room temperature.

Copper

French electrolytic copper powders were produced through the addition of colloidal materials, such as H_2SO_4-treated glucose, for example, to the electrolyte (1). The colloid was thought to make possible the production of extremely fine powders with the elimination of hydrogen evolution at the cathode and higher current efficiencies. American production of copper powder made the material in modified refining tanks from selected regular anodes and smooth copper cathodes.

Large quantities of industrial Cu powders are electrolytic. They are made by electrodeposition using a soluble anode and a nonattackable cathode. The electrolytic step transforms solid Cu into discrete, finely divided particles of controlled and reproducible characteristics. Since high purity is essential, the anodes are electrolytically refined Cu. Large-scale attempts to use anodes of lower purity so that refining and powder formation could be combined have been commercial failures because of the wide variations in the characteristics of the end product. Insoluble anodes have been investigated, but have not proved commercially feasible for the production of high-grade Cu powders.

The cathodes are lead alloy sheet. Silicon-iron, briquetted iron oxide, various stainless steels, magnetite, and graphite, have not been satisfactory.

The electrodes are arranged in parallel in lead-lined or rubber-lined tanks, and are frequently inspected as in refinery practice for irregularities to insure uniform current density and elimination of short circuits in the cells.

In contrast to the copper refining practice, electrolysis is carried out at current densities from 5 to 10 times higher, at lower temperatures and low concentrations, and low circulation. By control at various levels, marketable copper powder is produced varying from 1.5 to 3.5 g/cm^3 in apparent density and from 30 to 98% minus 325-mesh in particle size. The widely differing demands of powder metallurgy make this necessary.

Copper deposits as discrete particles at the cathode and is collected at the bottom of the cell, or as a loosely adherent deposit which may be lifted from the cell and washed off the cathodes. Periodically the sludge is removed, filtered, and washed free of electrolyte. The large surface area and activity of wet Cu powder make thorough washing and immediate drying essential to avoid oxidation of the Cu particles.

The powder is dried in controlled-atmosphere, continuous furnaces. Reducing conditions are main-

Technical Review

Electrodeposition of Powders for Powder Metallurgy

C. L. Mantell

Department of Chemical Engineering, Newark College of Engineering, Newark, New Jersey

ABSTRACT

A very large number of articles are made by powder metallurgical methods from electrolytically reduced powders. In powder production, cathode current densities are much higher than those of refining; loosely adherent deposits are produced. These are dried, surface oxides removed, and classified by screening. Important electrolytic powders are those of copper, iron, nickel, zinc, some alloys, as well as duplexes. Operating details are reviewed.

Metal deposited at the cathode varies widely in its characteristics, depending on the electrolyte itself, the ions present, and operating conditions. Silver deposited from a solution of $AgNO_3$ forms large, readily visible crystals. Tin from a solution of $SnCl_2$ will form long needles which may rapidly "bridge" from the anode to the cathode. Lead from a chloride or acetate solution gives crystals different from those from a chlorate or perchlorate electrolyte. Nickel deposits from a sulfate bath are hard and may be polished but not with ease, while nickel from a naphthalene sulfonate gives bright deposits needing little if any polishing.

In plating, efficiency of utilization of electrical energy is secondary to quality. High current and energy efficiencies may be sacrificed without upsetting the economics of the operation. Particularly where thermal or chemical processes compete, power cost in refining is a major item; maximum current and energy efficiencies are vital. In electroforming, of which metal powder production is a form, conditions approach refining to a far greater degree than plating, as the procedures compete with thermal and mechanical disintegration procedures.

The nature of the electrolyte, its pH, metallic ion concentration, anodic and cathodic current density, temperature, the simplicity or complexity of the metallic ion including its primary and secondary ionization, as well as the presence of modifying or "addition" agents, have effects on the character of the deposit.

The crystalline structures of cathode deposits may be classified as follows:

Group I. The initial nuclei or crystals continue to grow throughout the deposit forming (*A*) isolated crystals: which are (*a*) symmetrical or (*b*) acicular; or giving rise to (*B*) contiguous crystals: which may be (*a*) columnar or (*b*) fibrous.

Group II. Part of the initial nuclei or crystals continue to grow. These are (*A*) conical ("normal") or (*B*) twinned.

Group III. The nuclei or crystals do not grow for any extended period. Their shapes are (*A*) broken (compact), or (*B*) arboreal, sometimes called "fernlike" ("treed"), or (*C*) powdery (spongy), and (*D*) slimelike.

If any addition which would increase the cathode polarization be made to the solution, the number of crystal nuclei increases. The current densities may be increased, and the effective metal ion might be decreased in the film or thin layer of solution adjacent to the cathode by (*a*) diluting the solution; (*b*) decreasing the temperature, which in turn reduces diffusion and convection; (*c*) adding a salt having an ion common with those already present; (*d*) introducing a colloid; (*e*) increasing the viscosity of the solution; and (*f*) causing the formation of complex ions. These factors increase the difference in cathode potential, the number of crystal nuclei, and the production of fine-grained deposits.

Dissociation, ionic migration, diffusion, and convection, particularly at the surface of the cathode, replenish the metal ion concentration. Growth of existing crystals may be favored by acceleration of these factors. The tendency of metals such as silver and lead, when deposited from nitrate solutions, to form isolated crystals is partly the result of the relatively large change in density of the solution produced by the removal of the metal. The effects of various factors upon the structure of deposits are summarized in Table I.

Decreasing the metal ion concentration decreases the size of the crystals. Fine-grained, bright, or hard deposits are produced at low temperatures, while increase of temperature causes coarse or soft deposits. The effects of increases of current density and

Table I. Direction of effects on structure of deposits

Change in operating condition	Change in structure group*
Increase metal salt concentration	III → II → I
Increase metal ion concentration	III → II → I
Agitate solution	III → II → I
Elevate temperature	III → II → I
Increase conductivity of solution	III → II → I
Add colloids to solution	I → II → III
Increase viscosity of solution	I → II → III
Increase current density	I → II → III

* Groups as described above in the text.

temperature are in opposite directions. Therefore, it is possible to obtain fine-grained deposits in warm solutions at a high current density. Addition of colloids in more than small amounts, increase of viscosity, and increase in current density tend in the direction of broken crystals, arboreal, or powdery electrolytic precipitates.

Deposited metal powders are represented by the Group III type of crystals. They are "poor" electroplates. Powder production is favored by low metal concentration, low metal ion concentration, unagitated solutions, low temperatures, solutions of low conductivity, addition of colloids, increases in viscosity, and marked increases in current density. The effect of each variable is not of the same order of magnitude; the effects are cumulative and interdependent; changes in concentration may be of greater importance than variation of temperature; vigorous agitation may offset the effect of increase of current density.

Electrolytic powders of commercial importance are of two varieties. Loose crystals may be formed in the cells as nonadherent powders, or the powder may result from grinding relatively hard, brittle, partially coherent deposits. Examples of the first class are Cu, Zn, Ni, Ag, and Pb; of the second Fe and Mn. These will be briefly described from the viewpoint of their production. While electrolytic Zn, Ni, and Pb powders are interesting, they are commercially unimportant in that powders of these metals are the result of other methods; industrially only electrolytic Cu, Fe, and Mn command markets. Silver crystals are the conventional result of electrolytic refining. Disintegration converts them to a powder.

The powders all command "shape" premiums in price over ingot metal or cathode chip of the same purity.

In practice, cathode current densities are higher than those of refining, so that loosely adherent spongy deposits which are periodically removed by scraping or tapping devices or by electrolyte circulation may be produced. In the case of Cu powder, acid electrolytes of lower metal and higher acid concentration than those used for refining or plating are preferred. When operated at high cathode density and with hydrogen evolution, the finely divided metal crystals often have a fernlike appearance under the microscope. It is necessary to remove the cathode frequently; otherwise the effective area of the deposit is increased to such an extent that the current density is lowered and coarse deposits formed.

The fineness of the powder may be varied over a considerable range by changes in the composition, temperature of the electrolyte, and variation of the cathode current density, as well as by the introduction of addition agents, reducing compounds, or substances which are cathodically reduced and anodically oxidized but are not plated out. Cathode current densities are different from those at the anode, usually higher. The deposited powders are washed, dried in inert or reducing atmospheres, and cooled to room temperature.

Copper

French electrolytic copper powders were produced through the addition of colloidal materials, such as H_2SO_4-treated glucose, for example, to the electrolyte (1). The colloid was thought to make possible the production of extremely fine powders with the elimination of hydrogen evolution at the cathode and higher current efficiencies. American production of copper powder made the material in modified refining tanks from selected regular anodes and smooth copper cathodes.

Large quantities of industrial Cu powders are electrolytic. They are made by electrodeposition using a soluble anode and a nonattackable cathode. The electrolytic step transforms solid Cu into discrete, finely divided particles of controlled and reproducible characteristics. Since high purity is essential, the anodes are electrolytically refined Cu. Large-scale attempts to use anodes of lower purity so that refining and powder formation could be combined have been commercial failures because of the wide variations in the characteristics of the end product. Insoluble anodes have been investigated, but have not proved commercially feasible for the production of high-grade Cu powders.

The cathodes are lead alloy sheet. Silicon-iron, briquetted iron oxide, various stainless steels, magnetite, and graphite, have not been satisfactory.

The electrodes are arranged in parallel in lead-lined or rubber-lined tanks, and are frequently inspected as in refinery practice for irregularities to insure uniform current density and elimination of short circuits in the cells.

In contrast to the copper refining practice, electrolysis is carried out at current densities from 5 to 10 times higher, at lower temperatures and low concentrations, and low circulation. By control at various levels, marketable copper powder is produced varying from 1.5 to 3.5 g/cm^3 in apparent density and from 30 to 98% minus 325-mesh in particle size. The widely differing demands of powder metallurgy make this necessary.

Copper deposits as discrete particles at the cathode and is collected at the bottom of the cell, or as a loosely adherent deposit which may be lifted from the cell and washed off the cathodes. Periodically the sludge is removed, filtered, and washed free of electrolyte. The large surface area and activity of wet Cu powder make thorough washing and immediate drying essential to avoid oxidation of the Cu particles.

The powder is dried in controlled-atmosphere, continuous furnaces. Reducing conditions are main-

tained to remove surface oxides. The furnaces are operated at 315°-760°C (600°-1400°F) in atmospheres of 10-30% hydrogen and 5-20% carbon monoxide. Furnace conditions are closely controlled. Excessive fritting or sintering of the powder into a ductile mass must be avoided.

The discharge from the furnaces is fed to high-velocity impact mills to break up clusters without excessive cold working and hardening. Powder which is milled too lightly will contain a high percentage of agglomerated fines. Powder milled too heavily will contain flakes, roughly spherical, or cold-worked particles which will destroy its compacting qualities.

Size fractionation is by screening and air separation. The various fractions are stored in airtight, dessicated containers. Blending of the various fractions produces desired types of powder.

Lead

Mantell described the preparation of Cu-coated Pb powder using an acetate electrolyte with Cu and Pb anodes and Ni cathodes at cathode current densities of 18 amp/ft² at a power consumption of 1.5 kwhr/lb of 200-mesh powder containing 60% Cu and 40% Pb (2). These have been used for bearings whose operating temperatures may exceed the melting point of Pb. No lead "bleeding" results.

Zinc

Electrolytic zinc powder is made from flue dust with a caustic leach liquor and an electrolyte of sodium hydroxide and sodium zincate. The product shows a typical fern-leaf appearance of sizes 45-60 μ long. Zinc dust is employed as a reducing agent in the manufacture of hydrosulfites and in the preparation of organic compounds. Commercial operating data of a plant employing hollow magnesium alloy cathodes are given in Table II.

Nickel

Electrolytic Ni has been made by Mantell (3) employing an NH_4Cl electrolyte whose *p*H was adjusted by means of NaOH, using Ni anodes and cathodes. Operating details are given in Table II.

Lead

The inter-relation of operating conditions in producing lead powder was shown by Crownover (4) who found: "Spongy deposits were formed at lead concentrations between 7.23 and 16.2 oz per gal and free HBF, concentrations between 51.5 and 27.6 oz per gal at current densities ranging from 1,325 to 177 amp per sq ft for 2 minute deposition periods. Particle size increased with increasing time of deposit and decreasing current density. Dendritic growths formed on the edge of the cathodes at current densities between 257 and 835 amp per sq ft and electrolyte concentrations of 16.6 to 28.1 oz per gal lead and 27.6 to 12.4 oz per gal free HBF, for deposition periods of 4 to 30 minutes. Easily removable powdered lead could not be produced at current densities between 299 and 835 amp per sq ft when the electrolyte contained 28.1 oz per gal lead and 12.4 oz per gal free HBF$_4$. A firm adhering deposit formed on the cathode at a current density of 1,100 amp per sq ft. No difference was noted in the use of copper, carbon steel or stainless steel for cathodes."

Table II. Operating details—electrolytic Zn and Ni powders

	Electrolytic zinc powder	Electrolytic nickel
Raw material	High-grade Zn flue dust	Ni
Cell:		
Material of construction	Steel, rubber-lined	Steel, rubber-lined
Capacity, lb/day	110	
Electrolyte:		
Feed	200 g/l NaOH, 10 g/l Zn	300 g/l NH_4Cl, 2 g/l NaOH
Effluent	200 g/l NaOH, 9 g/l Zn	
Temperature, °C	30	23-26
Method of feed	Gravity	
Circulation method	Rubber-lined pump	
Current:		
Current per cell, amp	2,500	
C.d. anode, amp/ft²		10-20
C.d. cathode, amp/ft²	120-150	20-30
Current efficiency, %	80-90	55
Volts per cell	3.4	1.4-1.5
Power consumption:		
Kwhr per lb metal	1.37	1.13
Lb metal per kwhr	0.73	0.88
Anode	Ni sheet	Ni
Cathode	Hollow iron or Mg alloy (Elektron)	Sheet Ni
Electrode spacing	1.18 in. (30 mm)	1.5 in.
Final product, % metal	Paste 35-45 Zn, dry dust 85-95	98-99

Iron

Electrodeposition of iron dates back to 1846 when Bottger used a bath of $FeSO_4 \cdot 7H_2O$ and NH_4Cl. Bietz in 1869 produced electrolytic Fe and employed it for making magnetic tests. Siemens (5) in 1889 proposed a general process in which sulfide-iron minerals were leached with ferric chloride or sulfate, the Fe deposited from the leach liquors on a cathode in a diaphragm cell, and the leach regenerated. The first serious attempt to produce electrolytic Fe in quantities was in 1904 (6), when the metal was deposited from a mixture of ferrous and ammonium sulfates at a current density of 6-10 amp/ft² (0.65-1 amp/dm²) at 30°C and an average emf of 1 v. In the plant of the Western Electric Company (7) the anodes were cast steel and the bath carried slightly on the alkaline side so that a considerable amount of oxides would be deposited in the cathode to make the latter brittle and easily ground up in connection with the manufacture of electrical "loading coils." It was not necessary to make a pure grade of Fe. A further modification of the Burgess process was used by the Westinghouse Electric & Manufacturing Company (8) in which a pure grade of Fe was produced for use in the manufacture of alloys for electromagnetic machinery and instruments. Commercially pure Fe anodes were used, but the refining range of the process was very small. Cathodic products would often be produced which were too high in either C or S or both.

In 1914 an electrolytic iron plant was installed at

Table III. Data on production of electrolytic Fe powder and electrolytic Mn

	Iron	Manganese
Electrolyte:		
Sp gr	1.1	
Percentage Fe	4.6 (50 g/l)	
pH	4.5	
Temperature, °C	50	35-40
Circulation, gal/min	3.0	
Circulation apparatus	Centrifugal pumps	Centrifugal pumps
Anolyte:		
Mn, g/l, as $MnSO_4$		10-18
H_2SO_4, g/l		25-35
$(NH_4)_2SO_4$, g/l		120-140
pH		1-1.4
Catholyte feed:		
Mn, g/l, as $MnSO_4$		25-35
$(NH_4)_2SO_4$, g/l		125-135
pH		7.2-7.6
Current:		
Amp/ft²	25	40
Voltage per tank	2.5	5+
Current, voltage, and kw of d-c apparatus	2940 amp 85 v 250 kw	6000 amp 600 v
Current efficiency, %	90	65-70
Kwhr/lb metal, d.c.	1.20	4-4.5
Kwhr/lb metal, a.c.		5-5.25
Lb metal per kw-day	20.0	4.07
Anodes:		
Composition	Steel plate, 99%	Lead alloy
Length, width, thickness	24 x 18 x 1 in.	
Weight, lb	120	
Mode of suspension	Welded to hanger bars	Welded to hanger bars
Anode spacing, in.	5	
Life	12 days	3 years
Scrap, %	20	None
Number per cell	21	21
Cathodes:		
Length, width, thickness	18 x 22½ x 20 in. gauge	36 x 18 x 1/16 in.
Weight, lb	5½	
Mode of suspension	Welded to hanger bars	Welded to hanger bars
Replaced after ? days	2-3	1.5-2
Weight, lb	15-22	
Material		Stainless steel
Number per cell	20	20
Deposition tanks		
Material of construction	Haveg	Concrete, lead or plastic lined
Length, width, depth	10 ft x 30 in. x 30 in.	
Number of anodes, cathodes	21, 20	21, 20
Electric connection	Series	Series
Amp/in.² cross section of busbar	1000	1000
Anode mud:		
Percentage of anode	17	
Composition	Metallic iron and other metal oxides and sulfates	MnO_2
Removed after ? days	8	

Grenoble, France (9), in which a hot neutral solution of ferrous chloride was employed as an electrolyte to which iron oxide was added as a depolarizer, with cast-iron anodes and rapidly rotating mandrels for cathodes. Both tubing and plates were produced of electrolytic Fe of good purity, showing Fe 99.967%, C 0.008%, Mn 0.009%, P 0.002%, Si 0.014%, S trace (10). In commercial operation the electrolyte was circulated over Fe turnings, and iron oxide was added; or else air was blown in to keep the H^+ ion concentration of the solution low. Current density was 93-105 amp/ft² (10-11 amp/dm²) at a temperature of 80°C. The small hydrogen content of the metal was removed by annealing at 900°C. Power requirements were of the order of 1.8 kwhr/lb.

A bath used in Germany, originated by Fischer (11), contained 450 g $FeCl_2$, 500 g anhydrous $CaCl_2$, 750 g water, operated at 90°-110°C at 93-185 amp/ft² (10-20 amp/dm²). Owing to the high working temperature, the Fe deposited is relatively free from hydrogen and is therefore not brittle. It has a purity of at least 99.95% and can be deposited in thick, dense layers.

With the development of powder metallurgy, a demand for Fe powder arose. Part of this is met by electrolytic iron made by Plastic Metals of Johnstown, Pa. The operating conditions are tabulated in Table III (12).

Manganese

Manganese powder is the product of grinding electrolytic "cathode chip" metal in ball mills in nitrogen, helium, or argon atmospheres with particular care to keep temperatures low because of the pyrophoric nature of the powder. More recently Mn powder has been made successfully on crushing rolls. Manganese powder finds tonnage applications in welding rods and coatings therefore, as well as magnetic materials.

Manganese is electrowon from reduced ores or equivalent Mn containing materials which are

leached with return electrolyte, which when purified becomes cell feed (13). Operating conditions are given in Table III.

In the preparation of electrolyte from which the metal is deposited, the solution is purified completely of Fe, As, Sb, Sn, Pb, Ni, Co, Mo, SiO_2, Al; Ca and Mg are also removed. Diaphragms are around the cathodes, and the anolyte fills the cell around the diaphragms.

The electrowinning of Mn depends on very pure solutions. In addition, there is dependence on the combination of factors such as concentration, pH, temperature, current density, cathode and anode material, rate of flow to the cells, as well as other variables. Problems of dealing with an alkaline catholyte and an acid anolyte in a two-compartment cell, as well as the impossibility of considering any of the variables separately because of their influence on each other, cause Mn electrowinning to be almost in a class by itself. It demands much more delicate control than does the electrowinning of Zn and Cu, for it carries all their problems and many more.

Manuscript received July 15, 1957. This paper was prepared for delivery before the Buffalo Meeting, Oct. 6-10, 1957.

Any discussion of this paper will appear in a Discussion Section to be published in the December 1959 JOURNAL.

REFERENCES

1. E. Drouilly, U. S. Pat. 1,799,157 (1931); S. A. Tréfileries et Laminoirs du Havre, British Pat. 303,984 (1929); B. Leach and Henry and Leigh Slater Ltd., French Pat. 511,428 (1920); S. A. Tréfileries et Laminoirs du Havre, French Pat. 656,777 (1929).
2. C. L. Mantell, U. S. Pat. 2,182,567 (1939).
3. C. L. Mantell, U.S. Pat. 2,233,103 (1941).
4. J. B. Crownover, M.S. in ChE Thesis, Newark College of Engineering, Newark, N. J. (1952).
5. H. Siemens, U. S. Pat. 415,576 (1889).
6. C. F. Burgess and C. Hambuechen, *Trans. Am. Electrochem. Soc.*, **5**, 201 (1904).
7. B. Speed and G. W. Elman, *J. Am. Inst. Elec. Eng.*, **40**, 596 (1921).
8. P. H. Brace, *ibid.*, **44**, 922 (1925).
9. L. Guillet, *Electrician*, **74**, 79 (1914); *Engineering*, **98**, 413 (1914).
10. J. Escard, *Génie civil*, **75**, 165, 199, 225 (1919); *Elec. Rev.*, **76**, 610 (1920).
11. F. Fischer, *Z. Elektrochem.*, **15**, 595 (1909); O. W. Storey, *Trans. Am. Electrochem. Soc.*, **29**, 357 (1916).
12. B. T. du Pont, Private communication.
13. C. L. Mantell, *J. (and Trans.) Electrochem. Soc.*, **94**, 323 (1948).

Brief Communication

On the Hydrogen Evolution Reaction

Ralph J. Brodd

National Bureau of Standards, Washington, D. C.

Theoretical calculations of the rates of electrochemical reactions have been the subject of many publications. Most treatments in recent years involve the assumption of an activated complex and suffer in that the energy terms for the activated complex cannot be evaluated accurately. In the case of electrode reactions it would appear that a promising line of approach to take would involve the assumption that the charge transfer at the electrode occurs by a tunneling process and that this tunneling process is the controlling factor in the rate of the reaction (1).

Kinetic theories of the hydrogen evolution reaction usually assume that the initial reaction step at an elecrode is

$$H^+ \text{ (sol'n)} + e \underset{M}{\rightarrow} H \qquad [1]$$

It can be shown that the rate of this reaction may be approximated from (1) by

$$\text{rate} = \Gamma \exp(-\Delta U/kT) \qquad [2]$$

where

$$\Gamma = \exp\left[-\frac{(2m)^{1/2}}{h}(\phi)^{1/2}R\right] \qquad [3]$$

and

$$\Delta U = \phi - E_a - \frac{e^2}{4R} + (E_{zpc} + \chi) \qquad [4]$$

In these equations e, h, k, m, and T have their usual significance. ϕ is the work function of the metal electrode, E_a is the electron affinity of H^+ in Eq. [1], E_{zpc} is the potential of the hydrogen electrode vs. the zero point of charge, χ is the surface potential for hydrogen adsorption on the metal, and R is the distance of approach of hydrogen ions to the surface of the metal when the charge transfer occurs. R is assumed to be 0.49Å, the average of the Goldschmidt and Bohr radius of the hydrogen atom.

In Table I are found the results of calculations

Table I. Calculated and experimental rates of hydrogen evolution reaction

Metal	Cal'd. rate, amp/cm²	Expt'l. rate (2), amp/cm²
Hg	5.8×10^{-13}	2×10^{-12}
Ni	2.5×10^{-4}	1×10^{-6}
Cu	2.5×10^{-7}	2×10^{-7}
Ta	7.2×10^{-6}	1×10^{-5}

of the rates of the hydrogen evolution reaction at the reversible potential, and H^+ (sol'n) concentration of unity. Experimental rates of the hydrogen evolution reaction at approximately the same conditions are given for comparative purposes.

The table shows that the calculated and experimental values are in fairly good agreement. Since the calculated values are very sensitive functions of R, $E_{i,pc}$, and χ, as seen in Eqs. [3] and [4], the agreement is fortuitous in some cases.

The following model may be associated with the process given in Eq. [1]. The metal electrode is assumed to be a perfect conductor. The electron from the metal electrode moves through an energy barrier at the surface of the electrode described by the Γ function in which the barrier height is ϕ and the barrier width is R. Then, at distance R from the electrode the electron combines with a proton from the hydrogen ion solvation complex in the electrical double layer to form a hydrogen atom. A somewhat similar model in principle has been proposed by Gurney (3).

Manuscript received Aug. 22, 1958.

Any discussion of this paper will appear in a Discussion Section to be published in the December 1959 JOURNAL.

REFERENCES

1. J. Weiss, *Proc. Roy. Soc. (London)*, **A222**, 128 (1954).
2. J. O'M. Bockris, National Bureau of Standards "Electrochemical Constants," Circular 524 (1953), P243.
3. R. W. Gurney, *Proc. Roy. Soc. (London)*, **A134**, 137 (1931).

Manuscripts and Abstracts for Fall 1959 Meeting

Papers are now being solicited for the Fall Meeting of the Society, to be held at the Deshler-Hilton Hotel in Columbus, Ohio, October 18, 19, 20, 21, and 22, 1959. Technical sessions probably will be scheduled on Batteries, Corrosion (including a joint Corrosion—Electronics-Semiconductors session), Electrodeposition (including symposia on "Electrodeposition from Organic Solvents" and "Electro- and Chemical-Polishing"), Electronics (Semiconductors), Electro-Organics, and Electrothermics and Metallurgy.

To be considered for this meeting, triplicate copies of abstracts *(not exceeding 75 words in length)* must be received at Society Headquarters, 1860 Broadway, New York 23, N. Y., *not later than June 1, 1959. Please indicate on abstract for which Division's symposium the paper is to be scheduled, and underline the name of the author who will present the paper.* Complete manuscripts should be sent in triplicate to the Managing Editor of the JOURNAL at the same address.

* * *

The Spring 1960 Meeting will be held in Chicago, Ill., May 1, 2, 3, 4, and 5, 1960, at the Lasalle Hotel. Sessions will be announced in a later issue.

FUTURE MEETINGS OF
The Electrochemical Society

Philadelphia, Pa., May 3, 4, 5, 6, and 7, 1959

Headquarters at the Sheraton Hotel

Sessions probably will be scheduled on

Corrosion, Electric Insulation, Electronics (Including Luminescence and Semiconductors), Electrothermics and Metallurgy (including a Projected Symposium on "Mechanical Properties of Intermetallic Compounds"), Industrial Electrolytics, and Theoretical Electrochemistry (including a symposium on "Electrode Processes")

* * *

Columbus, Ohio, October 18, 19, 20, 21, and 22, 1959

Headquarters at the Deshler-Hilton Hotel

Sessions probably will be scheduled on

Batteries, Corrosion (including a joint Corrosion—Electronics-Semiconductors session), Electrodeposition (including symposia on "Electrodeposition from Organic Solvents" and "Electro- and Chemical-Polishing"), Electronics (Semiconductors), Electro-Organics, and Electrothermics and Metallurgy

* * *

Chicago, Ill., May 1, 2, 3, 4, and 5, 1960

Headquarters at the Lasalle Hotel

* * *

Houston, Texas, October 9, 10, 11, 12, and 13, 1960

Headquarters at the Shamrock Hotel

* * *

Papers are now being solicited for the meeting to be held in Columbus, Ohio, October 18-22, 1959. Triplicate copies of each abstract (*not exceeding 75 words in length*) are due at Society Headquarters, 1860 Broadway, New York 23, N. Y., *not later than June 1, 1959* in order to be included in the program. *Please indicate on abstract for which Division's symposium the paper is to be scheduled, and underline the name of the author who will present the paper.* Complete manuscripts should be sent in triplicate to the Managing Editor of the JOURNAL at 1860 Broadway, New York 23, N. Y.

Feature Section

William J. Kroll—Medalist[1]

J. W. Marden

The history of William J. Kroll's life reads like a novel. He was born in 1889 in story-book Luxembourg, son of the director of an iron blast furnace plant. He attended the Technische Hochschule at Charlottenburg where he studied iron and steel metallurgy. With his doctor's thesis on boron began a distinguished career with the less common elements and, although he worked in several European metallurgical plants and on many alloys, he seems always to have been most interested in the rarer metals.

Dr. Kroll has been, for many years, an international figure in his line of work. He has published about 80 scientific papers and has at least 40 patents to his credit. Thirteen of his more recent and very important papers on ductile titanium, zirconium, chromium, and electric furnaces are published in the JOURNAL of The Electrochemical Society.

Not only have Kroll's researches been of great scientific value but many have found practical application. Among these are: calcium lead bearing alloys; production of calcium lead by reduction of calcium chloride with sodium lead; production of calcium lead by reaction of calcium carbide with lead; debismuthizing of lead with calcium; deantimonizing lead solder with aluminum; aluminum silicon piston alloy with more than 20% silicon; production of beryllium by reduction of the fluoride with magnesium; dezincing of lead by vacuum treatment; age hardened copper titanium alloys; age hardened nickel aluminum and nickel titanium steels; cerium magnesium alloys for high-temperature applications; production of titanium and zirconium by halide metallurgy.

Between the years 1923 and 1940, Kroll worked in his laboratory in Luxembourg on titanium and, in 1938, he came to America and offered to develop his process for any one of several firms interested in nonferrous metals and electrical fields. The reception was discouraging and, even though some of us were sympathetic, he returned home with no takers. Since many of our executives have now retired, I can report to Dr. Kroll that often (as some of you well know from experience) vice-presidents and general managers who control plant expenditures do not agree with the recommendations of the members of their research staff. Also, the factory in question was located in a congested area and we were hardly in a position to start a production involving the use of much chlorine.

However, I remember our conference well. Dr. Kroll drew on the blackboard pictures of the equipment he proposed to use for producing commercial quantities of titanium and zirconium. Although his schematic drawings did not look exactly like the apparatus I saw years later at Albany, Ore., or the melting furnaces at Salt Lake City, basically the ideas for production of these metals were the same as those which finally proved to be so successful.

Two stories were told by Dr. Kroll at these conferences regarding the living conditions near the German border where he had his laboratory and home. One of Hitler's ministers was named Von Ribbentrop. On one side of a river stood a man from Luxembourg, and on the other a German. The Luxembourgian called to the German, "We have butter on our bread," and the German replied, "We have Von Ribbentrop on ours." Rübe means beets.

Also, Dr. Kroll told me that his home and laboratory in Luxembourg would be directly in the path of the Germans if they attacked France. He said he had a bicycle hidden in the woods and when the first gun went off he would ride away as fast as he could. Perhaps he will tell us tonight whether or not he ever used his bicycle.

Fortunately, Kroll got out of Luxembourg ahead of the German invasion and came back to America in 1940 as No. 13 of a quota of 200 immigrants. It now seems quite fitting that the development of the commercial processes for titanium and zirconium were sponsored by the U. S. Bureau of Mines and that patent rights to some of these inventions should be the property of the people of the United States who made a refuge for him in time of war. A very small portion of these significant inventions still belongs to Kroll as a naturalized citizen of the U. S. A.

I wrote to Dr. Kroll and asked him to tell me more about "Kroll, the man." A paragraph from his reply follows:

"As to 'Kroll, the Man' . . . he has had his share of troubles in his life, had to run away from the Nazis, was forced to adjust himself sometimes to a changed ambiance with fair success and did his best to use his opportunities. Unfortunately he was hollering during many years in the desert, and nobody wanted to listen to him. He did not marry but was (and is) not adverse to feminine charm. He liked water sports and skiing which he practiced as long as youth permitted. He has interests in art, especially in its history. Otherwise he spends his time reading, writing and travelling to advise people how to get along with titanium and zirconium."

Dr. Kroll is a true scientist who does not require elaborate equipment or a large group of assistants. Forty hours of work is only a part of his week's efforts. He has had his full share of failures and laboratory explosions. Those of us who have also worked on chromium, titanium, and zirconium know that very great ingenuity and many years of effort were needed to overcome the difficulties encountered in their successful production. One cannot overemphasize the value of Kroll's work in making such important metals commercially available.

[1] Introductory remarks by J. W. Marden on the occasion of the Acheson Medal Award to W. J. Kroll on September 30, 1958.

Dr. Kroll has been awarded many honors in the last few years, including the following: Francis J. Clamer award of the Franklin Institute; James Douglas medal of the A.I.M.E.; The Heyn Award of the Deutsche Gesellschaft für Mettallkunde; Albert Sauveur Achievement Award of the A.S.M.; Honorary Degrees from the University of Grenoble, Oregon State College, and the University of Missouri School of Mines; Perkin Medal of the Society of Chemical Industry, American Section.

Since the methods developed by Dr. Kroll for the production of titanium, zirconium, and other less common metals are truly electrochemical, it is particularly fitting that he be given the high honor of the Edward Goodrich Acheson Award by this Society.

Ladies and Gentlemen, it is now my great honor and privilege to introduce . . . Dr. William Justin Kroll.

Acheson Medal Award Address[2]

W. J. Kroll

It is a great favor to have Dr. Marden, the pioneer of the rare metals, introduce me to my audience. When we met for the first time, around 1932, he had already been engaged for some years in this type of research, to which his occupation with lamp filaments had conducted him. His report on the methods of zirconium production was for a long time a classic on the metallurgy of this metal, and his work on malleable chromium, which I checked and found confirmed, led finally to cold ductile metal. Thank you, Dr. Marden, for the many invaluable things I learned in your school.

When I was a student at the Technische Hochschule in Charlottenburg around the year 1910, a fascinating book fell into my hands. It was a translation of a monograph by Fitzgerald on Acheson's methods for producing artificial graphite and silicon carbide. My youthful and receptive mind was deeply impressed by Acheson's electrothermal methods, which in my later years I was able to use repeatedly. I never thought, at that time, that some day I would be destined to be selected by the American Electrochemical Society as recipient of a medal created by Acheson, which I modestly accept today as a posthumous reward by a great master and pioneer to one of his many devoted and anonymous students. To The Electrochemical Society and to the members of the award committee, I address my deep feelings of gratitude for having been found worthy of this high honor.

When I studied at college, metallurgy was still to a large extent an Art. This was the time when, in Europe, the teachings of Roozeboom, Le Chatelier, Martens, Ostwald, Tammann, and Bragg started elucidating metal structures and throwing light on metallurgical processes; while, in this country, Richards, Hofman, and Peters gave American nonferrous metallurgy world repute with their textbooks. In these days, too, Duralumin was accidentally discovered in Germany by Wilm, who opened the era of age hardening.

However, fate did not bring me in contact with these great men of the past. My teacher in iron metallurgy, which I selected as my future breadwinner, had some ideas on how to make artificial diamonds, and he took me, after having me swear absolute secrecy, as his best man for this job. We brought one of the finest autoclaves for this study, for 1500 atm of pressure, with a fretted steel barrel, and filled its belly with black gunpowder which we blew off with a hot wire, just to see what would happen. The autoclave held, but the residue from the powder was just plain carbon. Then we followed Moissan's prescriptions, melted iron in a graphite crucible, and, after overheating the melt under high pressure, poured it into mercury within the autoclave. But the sample of iron obtained showed only ordinary ledeburite eutectic, and the chemical treatment left behind plain graphite. Then my professor had an inspiration. He suggested that we react acetylene with insufficient oxygen. We produced the former in the autoclave by dripping water on calcium carbide, and blew oxygen in from a cylinder through a long copper tube. A spark plug provided for ignition if the mixture did not go off by itself. Careful week-long leaching of the residue with various acids left microscopic crystals which the professor claimed to be diamonds, but, as a skeptic, I never believed him. He thought that the only thing left for us to do was to make these crystals grow bigger with the help of a suitable catalyst, for which he selected carbon disulfide. This choice sounded quite logical to us, the operators, and we went ahead with the experiments. My helper had to empty the autoclave afterwards, and this was worse than receiving the full blast of a skunk, since our catalyst produced mercaptans. My unhappy assistant had trouble with streetcar conductors, who admitted him for home transportation only if he stood in the well-ventilated front section of the car, after the door had been carefully locked behind him. For weeks, people passing in front of the Technische Hochschule sniffed the air, asking what animal could have died unnoticed and left unburied on the grounds of our Alma Mater. I had endless squabbles with my landlady because of odor, and the semester, which was about to start, had to be delayed two weeks to let the ozonized Berlin air decontaminate the building. The diamond production along such promising lines had to be discontinued for understandable reasons. I hope that the General Electric people, who now make real diamonds, get by without the addition of carbon disulfide if by any chance they use acetylene in their process.

Progress in one branch of science is frequently brought about by advances in other lines. When around 1908 Tammann patented the use of cobalt-chromium alloys for gas turbine blades, he was hopelessly ahead of his time. When von Bolton at about the same time produced the first ductile tantalum, he succeeded largely due to better mechanical and mercury diffusion vacuum pumps, built by Gaede. When sodium lighting was introduced, it was a special duplex glass, inert to this element, that made this progress possible. Sodium was not used in the reduction of titanium chloride until recently, after the Atomic Energy Labs. recognized the solubility of the oxide in the metal and worked out methods for its removal, since it caused corrosion. When titanium and zirconium, as well as other rare or active metals, became commercial the inert gas industries had an essential part in their successful production. The greatest advance of the century in steel making, the "Linz" bessemerizing with oxygen, was brought about largely by Fraenkl's improvements in heat exchangers for oxygen liquefaction, which lowered the price of this gas. Our specialized college training makes

[2] Acheson Medal Address delivered September 30, 1958 at the Ottawa Meeting of The Electrochemical Society.

this kind of invention increasingly more difficult. Encyclopedic knowledge is evidently out of the question for most of us today, but, nevertheless, the research man with a shallow but more universal education may be more capable of bridging two or more fields of techniques and may, therefore, be more successful as an inventor than the specialist.

Research projects are still being started in many laboratories without any serious library work. One research manager of my acquaintance claimed that a study of the literature would discourage the searcher because he would become aware of his ignorance. Another wrote that library work is so expensive that a direct attack of the problem by experiments is, in the end, cheaper. Also, the Patent Office could always be used as a rather cheap source of information. Both objections are, of course, rationalizations of conduct, but with a core of truth. They miss the main point, however, namely, that library work is not just collecting data, which any librarian can do, but it is the main, perhaps even the sole, opportunity for the research scientist to take time out for thinking and for evaluating.

Literature searches are expensive because we make them so. Most technical magazines force the reader constantly to keep his mind "dejunking" the advertisements, sandwiched in the text, and, if after this effort and waste of time he condenses the article, the useful substance matter as a rule does not comprise more than a few words. This frustrating rejection of bulk makes rapid reading techniques necessary, and, conversely, concentration, when needed, difficult. The starting point of any library search should be good modern textbooks, which, in the field of electrochemistry, and still more in nonferrous metallurgy, are wanting. We lack modern monographs on the electrolytic production of copper, zinc, lead, aluminum, magnesium, sodium, lithium, calcium; on the production of graphite, calcium and silicon carbide, silicon metal, and ferroalloys. For reliable, up-to-date, and thorough information on modern copper refining, we have to consult the West German Handbook of Inorganic Chemistry, "Gmelin"; for ferroalloys, another West German book by Durrer-Volkert; for magnesium and aluminum electrolysis, an East German and, respectively, a Russian monograph. Are we going to be overtaken by Russia also in this field? I do not want to criticize the laudable efforts of the many book committees of our various technical associations, but, in the light of our increased needs, such projects must be speeded up. Plenty of money has been available, however, for monographs on fancy metals such as beryllium and zirconium. The lack of textbooks greatly handicaps the education of our future metallurgists. This gap cannot be filled any more by the efforts of one individual author; the support of our technical associations, combined with the active help of plant owners, who earn all the benefits, is needed for this vast project. The almost complete absence of good textbooks on descriptive, extractive metallurgy in general is perhaps symptomatic of a miscarried principle. Could it be that the emphasis put in our universities on physical chemistry and physical metallurgy has killed the urge to describe the processes to which these branches of science apply? This, if true, would explain our recession in process metallurgy, which took us within one generation from leaders and exporters of ideas such as those of Cottrell's and Dwight Lloyd's, to importers and copyists of 100,000-amp aluminum cells, rotating hearth electric furnaces, and electrothermic metal refining processes using fused slags, to mention only electrochemistry.

Another justified criticism of today's metallurgical research is the frequent overemphasis on thermochemistry, used as window dressing in publications, despite the fact that this branch of science is still in its infancy and lacks accuracy. Indiscriminate use of thermodynamics leads frequently to grievous mistakes which discredit it. For instance, some years ago one outstanding thermochemist calculated the vapor pressure of magnesium over a magnesia-silicon mixture. He found it to be so low that he disclaimed the possibilities of this process. It was discovered later that his values were about 10,000 times too low, due to the unreliable old data he used, and, if at that time American industrialists had taken his calculations seriously, there would not have been any magnesium made by the Pidgeon process. Confirming the results of experiments would have been better than trying to predict their outcome. Thermodynamics must consider chemical facts first. All efforts should be directed toward establishing new and more precise free energy data instead of using old ones for vain calculations, made by thermochemists who frequently neglect their chemistry. Few institutes contributed more to thermochemistry than Dr. K. K. Kelley's Bureau of Mines laboratory in Berkeley, which earned him and the sponsoring government recognition all over the world. It deserves much more financial help than it has at present.

Frequently, the opinion is expressed that humanity has reached approximately the end of outstanding discoveries. This, I do not believe. It is astonishing how unexpectedly a great advance is made, often by laymen with the most primitive means, while huge laboratories, provided with the most powerful research tools and plenty of money, miss the discovery entirely. For example, powdered aluminum has been available for half a century, but, only a few years ago, an up to then unknown chemist named Irrmann, of the Swiss "Aluminium Industrie Neuhausen," had the idea of sintering such powder and of checking the mechanical properties of the compacts at medium temperatures. He thus discovered with the simplest means a broad line of new materials, the so-called "SAP" aluminum-alumina alloys, suitable for lightweight construction at temperatures at which normal aluminum alloys fail.

Progress usually proceeds in leaps. Since the time of Richard Lorenz, 40 years ago, fusion electrolysis with a solid cathode deposit remained dormant despite the fact that it is applicable to many more metals than is electrolysis with a fused cathode. Fused salt electrolysis for refining impure metals with a soluble solid anode has recently been rediscovered and put to use for the purification of titanium and other metals. It was, however, broadly described and known to be successful in the refining of aluminum-silicon alloys, plain iron, and ferroalloys, on the pilot-plant scale. This method has opened large horizons for the electrolytic refining of raw metals, and we know now that the Van Arkel iodide process is replaceable by the much cheaper method of soluble anode electrolysis, which also allows removal of oxygen, nitrogen, carbon, and many metallic impurities. Another rediscovery is the reaction of fused or gaseous halides with solid metals or alloys in powder form, in order to extract certain constituents. This idea has been described for the extraction of manganese from ferromanganese, of iron from ferronickel, and of copper from monel metal. It is now one of the leading suggestions in titanium electrolyte production. If someday the great difficulties in cell construction and operation can be overcome for the direct production of titanium and zirconium crystals, with graphite anodes, the processes which use metal reduction of the chloride will have had their day. In the case of titanium, the

raw material will probably not be a master alloy to be refined, but tetrachloride solubilized in alkali chloride after partial reduction to lower chlorides. This is by far the cheapest and purest titanium compound, since it can be made by chlorination in a fluidized bed, and it does not create the problem in sludge treatment which exists in the anodic dissolution of impure master alloys.

The collateral of the fusion electrolysis of chlorides is, of course, a halide chemistry. We already have learned a great deal in the now commercial chlorination of magnesium, beryllium, silicon, titanium, and zirconium materials and ores, and we also have learned how to purify the raw chlorides obtained. In the more general development of chloride chemistry, one big hurdle has to be overcome, which is the reclaiming of the chlorine contained in byproduct chlorides, especially in iron trichloride. This problem has world importance. Today, we know how to make titanium oxide pigment and chlorine from $TiCl_4$ by burning this compound in oxygen, but the same method, when applied to iron trichloride, has not yet found commercial uses because of special difficulties. Yet, on this method depends the possibility of economical beneficiation of iron-bearing ores with chlorine, such as bauxite, chromite, ilmenite, and low-grade nickel ores. The difficulties with plurivalency in the electrolysis of iron chloride in a carrier salt with graphite anodes are almost identical with those encountered in titanium winning from a lower valency, fused halide bath. The problem of iron fusion electrolysis is also one that concerns the world, since it might allow nations which have cheap hydropower, but no coal, to produce iron by electricity. While the Hall-Heroult process of aluminum winning has not yet been menaced by any competitive or cheaper method, it may well have to count on a rival, which may be the electrolysis of aluminum chloride in a carrier salt. This depends mainly on cheap aluminum chloride of high purity. The power consumption would be much lower, especially if the metal were deposited in solid form, as it can be, around 200°C, in closed cells. There would be barely any anode carbon consumption, while the chlorine would be recovered. New anode materials might, however, have to be discovered since, at low temperatures, aluminum chloride, as well as iron trichloride, reacts with graphite, forming some curious addition compounds which disintegrate the carbon.

The many unorthodox methods that we have seen introduced in titanium metallurgy have had their happy repercussions in many other branches of metal extraction and purification. The special steel producer, faced with the necessity of competing with titanium in airplane construction on a weight to strength ratio basis, has been forced to look for new and much stronger alloys of the age-hardenable stainless steel type, of greater cleanliness, and, especially, free of gases. Vacuum arc melting is now applied to such alloys. The little arc melting button furnace used in the control of the hardness of titanium has developed into the most precious tool for metallographic laboratories because of clean melting conditions. Vacuum retorts as used in titanium metallurgy now spread to the bright-annealing of metals.

We lack, to a considerable degree, basic knowledge of fused salt electrolysis and, as an example, the problem of the anode effect may be cited. It has been encountered again in the fusion electrolysis of titanium with graphite anodes, and those who made the observation erroneously called it "polarization." It has nothing to do with this, since the anode effect is a gas skin which is electrically charged and which adheres tightly to the graphite surface. It can be broken up by adding oxide to the bath. This phenomenon is much more pronounced in fluoride electrolysis, which is made possible only because of oxide addition to the electrolyte. While the chloride electrolysis does not require much oxide, this might nevertheless impart some extra hardness to gas-sensitive metals deposited at the cathode. Anode gases coming off a titanium cell with graphite anodes reveal the presence of CO and CO_2. A very soft metal could not be expected under these conditions.

Many of those involved in titanium electrolysis also ignore some elementary facts of chloride chemistry. Few are conscious of the behavior of alkali and alkaline earth metal chlorides when these are exposed to air in the hot state, and few know that chlorine can be displaced by oxygen, or that moisture, in an equilibrium reaction, oxidizes chlorides and produces HCl from such salts. In this way, the bath is provided naturally and unexpectedly with the oxide it needs to avoid anode effect. One recent study proved how difficult it is to produce an oxide-free fused sodium chloride for conductivity measurements.

This short survey shows the bright future of the fused salt electrolysis of halides, with solid cathode deposit, which is bouncing back after 40 years of stagnation. The whole field of raw metal purification by anodic dissolution in a fused salt bath is now open to us. It extends to a great many metals. We are learning now about cell construction, salt handling and purification equipment, about the chemistry of electrolytes. This might well have repercussions on other established electrolytic processes.

It is exactly 18 years since a congress of The Electrochemical Society took place in Ottawa. I attended that meeting as a refugee from the Old Country and came here to deposit the calling card of titanium. I gratefully remember that The Electrochemical Society in those days started me on my way to success by extending to me the favor of presenting, in this very same Chateau Laurier, my first report on my new titanium process which is going to be important also for ilmenite-rich Canada. This favor was repeated later with an article in our JOURNAL which started the zirconium industry, and with another one laying the foundations of fusion electrolysis with soluble anodes for the industrial refining of metals.

Looking back at my life, I may say that it went the way Isaac Newton said: "I do not know what I may appear to the World, but to myself I seem to have been playing only like a boy on the sea shore and diverting myself in now and then finding a smooth pebble, or a prettier shell than ordinary, whilst the great ocean of truth lay all undiscovered before me." To all those who opened this great ocean of truth with me, to all those who lent me their hands and who made something big out of titanium and zirconium, I am deeply indebted. It is a great satisfaction for me to have lived through these thrilling years of adventure and to have received for my contribution so many honors, among which I will cherish particularly the one of our association, the Acheson Medal Award.

Current Affairs

William Blum Receives Electrochemical Award

Dr. Blum receives first William Blum Award of the Washington-Baltimore Section from the Section's Chairman, Dr. Gwendolyn Wood.

Dr. William Blum, Past President of The Electrochemical Society (1926), was presented the newly established Electrochemical Award of its Washington-Baltimore Section at an award dinner on the evening of November 20, 1958. At the same time, the Section announced that this semiannual award in recognition of outstanding contributions to electrochemistry would be named the "William Blum Award" in honor of its first recipient.

Dr. Gwendolyn Wood, Chairman of the Washington-Baltimore Section, made the presentation which consisted of a check for $100 and a certificate which cited the recipient for "fundamental contributions to the science of electrochemistry, with special reference to the techniques and theories of electroplating."

Dr. Blum received his Ph.D. degree from the University of Pennsylvania in 1908, and joined the staff of the National Bureau of Standards the same year. Here he remained, until his retirement in December 1951, at which time he was chief of its Electrodeposition Section and assistant chief of its Chemistry Division.

His entire career has been one of dedicated service to his Government, to science, and particularly to the field of electrodeposition. His attention was directed to the latter during World War I and it became his life's work.

His scientific endeavors have produced over 100 publications, dealing with various phases of the theory and practice of electrodeposition. With George B. Hogaboom, he published "Principles of Electroplating" in 1924. The principles were so well presented that, even after three editions, the book remains fundamentally unchanged and one of the main texts in this field.

Dr. Blum's outstanding work has been recognized through the following: the medal of the American Institute of Chemistry (1926); an honorary membership in the American Electroplaters' Society and its special award (1928); honorary membership in The Electrochemical Society and its Acheson Award (1944); Exceptional Service Award of the Dept. of Commerce (1950); Award of Merit of the American Society for Testing Materials (1951); Special Award from Frankford Arsenal (1951).

Since retiring, he has received an honorary membership in the Institute of Metal Finishing and its Hothersall Medal in 1954. The University of Pennsylvania conferred on him the honorary degree of Doctor of Science in 1953. In the same year, he received the Elliott Cresson Medal of the Franklin Institute of Philadelphia. In May 1958, he received the American Electroplaters' Society Achievement Award established to honor truly distinguished service to the field of electroplating, metal finishing, and allied arts.

Despite a busy technical life, Dr. Blum has found time to engage in a number of activities. He once served as mayor of his community, Chevy Chase, Md., doing an outstanding job in this capacity. He also has been an active member of the Chevy Chase Presbyterian Church where he has taken particular interest in its youth work.

June 1959 Discussion Section

A Discussion Section, covering papers published in the July–December 1958 JOURNALS, is scheduled for publication in the June 1959 issue. Any discussion which did not reach the Editor in time for inclusion in the December 1958 Discussion Section will be included in the June 1959 issue.

Those who plan to contribute remarks for this Discussion Section should submit their comments or questions in triplicate to the Managing Editor of the JOURNAL, 1860 Broadway, New York 23, N. Y., *not later than March 2, 1959*. All discussion will be forwarded to the author, or authors, for reply before being printed in the JOURNAL.

Division News

Corrosion Division

The Division sponsored, with the Electrothermics and Metallurgy Division, a half-day session on stress-corrosion cracking of stainless steels, at the Spring New York Meeting. This well-attended session included six papers representing new advances in the field.

The major activity of the Division was concentrated at the Fall Meeting held in Ottawa. The Division participated in eight sessions (four full-day meetings). Five sessions were sponsored jointly with the Battery Division and the Theoretical Electrochemistry Division. The topic of mutual interest was "Films Formed in Contact with Liquids."

The annual luncheon and business meeting was held on October 1, 1958 at the Chateau Laurier. Approximately 50 attended, with Mr. J. F. Stanners of the British Iron and Steel Research Association as a guest.

The Treasurer's report indicated that there was a balance of $21.68 in the Division treasury. There were no expenses during the year.

The following officers were nominated and elected for the 1958-1959 term:

Chairman—M. A. Streicher, E. I. du Pont de Nemours & Co., Wilmington, Del.

Vice-Chairman—R. T. Foley, General Electric Co., Schenectady, N. Y.

Secretary-Treasurer — Milton Stern, Electro Metallurgical Co., P.O. Box 580, Niagara Falls, N. Y.

R. T. Foley,
Sec.-Treas., 1957-1958

Electrodeposition Division

At the Electrodeposition Division luncheon meeting held in Ottawa on October 1, 1958, with 66 members present, the following officers were elected:

Chairman—Abner Brenner, National Bureau of Standards, Washington 25, D. C.

Vice-Chairman—D. G. Foulke, Hanson-Van Winkle-Munning Co., Matawan, N. J.

Secretary-Treasurer—D. R. Turner, Bell Telephone Labs., Inc., Murray Hill, N. J.

Members-at-Large—C. A. Snavely and E. B. Saubestre.

Abner Brenner announced that two symposia, "Electrodeposition from Organic Solvents" and "Electro- and Chemical-Polishing," were planned for the 1959 meeting, and urged those interested in presenting papers to contact him at the National Bureau of Standards with regard to the first and Dr. Foulke at Hanson-Van Winkle-Munning Co. regarding the second. Other symposia discussed for future meetings included: (*a*) Electrorefining and Electrowinning; (*b*) Kinetics of Electrodeposition Processes, and Hydrogen Embrittlement of Metals.

Dr. Petrocelli was appointed Chairman of a committee to determine whether a change in term of officers was in order at this time.

F. A. Lowenheim reported that the Editor and Advisory Board for the third edition of "Modern Electroplating" had been selected and that the revision was already under way, with the target date for publication being mid-1961.

D. G. Foulke, *Sec.-Treas.*

Section News

Boston Section

The 11th meeting of the Boston Section was held on October 14, 1958 at the Arthur D. Little Research Labs. at Acorn Park. Dr. R. B. Mears, Director of Applied Research of United States Steel, spoke on the "Electrochemistry of Localized Corrosion."

Dr. Mears stated that: "Localized corrosion is the type of corrosion that normally occurs where there is little anodic polarization and where the anodic corrosion products are soluble. Use is made of localized corrosion in determining the sites of dislocations in very pure metals and in structures of practically all types of metals and alloys. Under laboratory conditions, it is possible to demonstrate that at least 20 different factors can individually cause localized corrosion. However, under the more complex conditions encountered in service, it is frequently impossible to determine which one of the various possible factors was effective in producing localized corrosion."

R. A. Peak, *Sec.-Treas.*

India Section

New Patrons-India Section.—The following have joined the India Section as Patrons: (*a*) Grauer and Weil (India) Private Ltd., Kalbadevi Rd., Bombay 2; (*b*) S. Mitra & Co., Dadhabhai Navroji Rd., Bombay 1.

Associates-India Section. — The Section has recently established the grade of "Associate" with a view to enabling those who are not members of The Electrochemical Society to associate themselves with the Section activities. So far, the Section has enrolled 27 Associates.

T. L. Rama Char,
Regional Editor, India

Ontario-Quebec Section

J. M. Noy has resigned as Secretary-Treasurer (1958-1959) of the Ontario-Quebec Section. The Executive Committee has appointed R. P. Bailey, Quebec Metallurgical Industries, Box 340, Billings Bridge P.O., Ottawa, Ont., to take over for the remainder of the term.

Philadelphia Section

The November 5, 1958 meeting of the Philadelphia Section featured a talk by Dr. Simon Larach on "Chemical Aspects of Electroluminescence." Dr. Larach is head of the Photoelectronic and Magnetic Research Group, Sarnoff Research Center, RCA.

Luminescence is the emission of light from materials without thermal means. In electroluminescence, the excitation is produced by an a-c field. A phosphor contains in the host crystal (e.g., ZnS) an activator (e.g., Cu^+) and a coactivator (e.g., halogen). These additions introduce additional energy levels in the forbidden gap of the host crystals. By varying the activator, the wave length of the emitted light can be changed. A more effective way to change the color of the phosphor is the variation of the forbidden band width by using solid solutions of, e.g., ZnS + ZnSe. Also, the frequency of the a-c field influences the color somewhat. A large variety of colors can be produced with these techniques. Applications of electroluminescence are found in lightning, x-ray amplifiers, and computers.

The next meeting of the Section will be held on January 7, 1959. Dr. Ralph Roberts of the Office of Naval Research will be the speaker.

Paul Rüetschi

Battery Division Extended Abstracts

Battery Division Extended Abstracts from the Ottawa Meeting, September 28-October 2, 1958, may be ordered from the Secretary-Treasurer, Chas. H. Clark, 34 Pleasant Place, Deal, N. J.

Their price is $2.00 per copy, postpaid, and payment must accompany all orders (by action of the Battery Division Executive Committee).

New Members

In November 1958, the following were approved for membership in The Electrochemical Society by the Admissions Committee:

Active Members Sponsored by a Sustaining Member

J. W. Glenn, Jr., Metals & Controls Corp., P.O. Box 898, Attleboro, Mass. (Corrosion)

Harold B. Goldberg, General Transistor Corp., 91-27 138th Place, Jamaica 35, N. Y. (Electronics)

Robert H. Herrmann, Grace Electronic Chemicals, Inc., Baltimore 1, Md. (Electronics, Semiconductors)

John R. Hofto, Westvaco Chlor-Alkali Div., Food Machinery & Chemical Corp., Box 8127, So. Charleston 3, W. Va. (Industrial Electrolytic)

John A. McDonald, Northern Electric Co., Ltd., Dept. 8220, P.O. Box 6123, Montreal, Que., Canada (Electronics)

Nathan Yagol, Hoffman Semiconductor Div., 930 Pitner Ave., Evanston, Ill. (Electrodeposition, Electronics, Theoretical Electrochemistry)

Active Members

William Arbiter, Nuclear Development Corp. of America; Mail add: 59 Windermere Dr., Yonkers, N. Y. (Electronics, Electrothermics & Metallurgy)

Robert J. Barry, CBS-Hytron; Mail add: 32 Barstow St., Salem, Mass. (Electronics)

Richard W. Blue, Bendix Aviation Corp.; Mail add: P.O. Box 5115, Detroit 35, Mich. (Electronics)

Joseph M. Blum, Bendix Aviation Corp.; Mail add: 4 Heddin Place, Red Bank, N. J. (Electronics)

William E. Boggs, U. S. Steel Co., Applied Research Lab., P. O. Box 38, Monroeville, Pa. (Corrosion, Electrothermics & Metallurgy)

John H. Bruns, Jr., Corning Glass Works; Mail add: 20 Townsend Ave., Corning, N. Y. (Corrosion, Electrothermics & Metallurgy)

Thomas M. Buck, Bell Telephone Labs., Inc.; Mail add: 1427 Marlborough Ave., Plainfield, N. J. (Electronics)

Donald J. Doan, Eagle-Picher Co.; Mail add: 216 No. Byers, Joplin, Mo. (Battery)

David L. Douglas, General Electric Co.; Mail add: 948 Westholm Rd., Schenectady, 9, N. Y. (Battery)

George Elliott, Industrial Research & Development Labs., 220-222 Elgar Rd., Reading, Berkshire, England (Electronics, Electrothermics & Metallurgy)

Alexander L. Feild, Jr., Universal-Cyclops Steel Corp.; Mail add: 1510 Missouri Ave., Bridgeville, Pa. (Electrothermics & Metallurgy)

Leonard P. Fox, Radio Corp. of America, Somerville, N. J. (Electric Insulation, Electrodeposition, Electronics)

Paul E. Friebertshauser, Pacific Semiconductors, Inc.; Mail add: 14927 Greenleaf St., Sherman Oaks, Calif. (Electronics)

Henry A. Fuggiti, Exide Industrial Div.; Mail add: 547 E. Centre Ave., Newton, Bucks County, Pa. (Battery)

John Fuller, Jr., Kendall Mills; Mail add: 91 Pleasant St., E. Walpole, Mass. (Battery)

John P. Hammes, Minneapolis-Honeywell; Mail add: Box 431D, Rt. 1, Mound, Minn. (Electronics)

Howard F. Gemperline, Union Carbide Corp.; Mail add: 39 Morrison Ave., Tonawanda, N. Y. (Electrodeposition)

Louis Habraken, Centre National de Recherches Métallurgiques—Liège, Rue du Val Benoit 69, Liège, Belgium (Corrosion, Electrodeposition, Electrothermics & Metallurgy, Theoretical Electrochemistry)

Robert N. Hall, General Electric Co., Research Lab., Schenectady, N. Y. (Electronics)

Harold K. Hughes, Markite Co.; Mail add: 98-20 62nd Dr., Rego Park 74, N. Y. (Battery)

Leopold Jungfer, Akkumulatorenfabrik Dr. Leopold Jungfer, Feistritz i.R., Kärnten, Austria (Battery)

Tadashi J. Kagetsu, Electro Metallurgical Co.; Mail add: 1070 Roberts St., Apt. 7, Niagara Falls, Ont., Canada, (Electrodeposition, Electrothermics & Metallurgy)

Charles B. Kenahan, U. S. Bureau of Mines; Mail add: 2813 Nicholson St., Hyattsville, Md. (Electrodeposition)

Ralph F. Koontz, Magnavox Co.; Mail add: RR #2, Fort Wayne, Ind. (Battery)

Edward R. Landry, Electro Metallurgical Co., 1425 Mountain St., Montreal, Que., Canada (Electrothermics & Metallurgy)

By action of the Board of Directors of the Society, all prospective members must include first year's dues with their applications for membership.

Also, please note that, if sponsors sign the application form itself, processing can be expedited considerably.

Bruce C. Olmsted, Jr., Electro Metallurgical Co.; Mail add: 34 Brookville Dr., Tonawanda, N. Y. (Electrothermics & Metallurgy)

Alan W. Postlethwaite, Raytheon Mfg. Co.; Mail add: 6 Blanchard Rd., Cambridge, Mass. (Electronics)

Hubert F. Quinn, Burroughs Corp.; Mail add: 536 West Wayne Ave., Wayne, Pa. (Electronics)

John R. Rairden, III, General Electric Co.; Mail add: 2 Dover Dr., Latham, N. Y., (Electric Insulation)

Arthur M. Ross, Gould-National Batteries, Inc., Easthampton, Mass. (Battery)

Milton R. Sherman, Texas Instruments, Inc.; Mail add: 1128A Sangamon Dr., Dallas 18, Texas (Electronics)

Philip J. Smith, Jr., Metal & Thermit Corp.; Mail add: 1401 No. Washington, Royal Oak, Mich. (Electrodeposition)

Naomi S. Suloway, General Telephone Labs., Northlake, Ill. (Electronics)

John D. S. Turnbull, Electro Metallurgical Co., Div. of Union Carbide Canada, Ltd., Welland, Ont., Canada (Electrothermics & Metallurgy)

Henry R. Weiler, Carborundum Metals Co.; Mail add: 14 Sylvan Pkway., Akron, Ohio (Electrothermics & Metallurgy)

Jay Y. Welsh, Manganese Chemicals Corp.; Mail add: 1818 Graydon Ave., Brainard, Minn. (Battery)

Edward J. Williams, Dow Chemical Co.; Mail add: 135 Holly St., Lake Jackson, Texas (Industrial Electrolytic)

Associate Members

Robert C. Dierderich, Electro Metallurgical Co.; Mail add: 1850 Broadway, Grand Island, N. Y. (Electrodeposition, Electrothermics & Metallurgy, Industrial Electrolytic)

Edward H. Sage, Frank R. Cook Co.; Mail add: Mt. Vernon Country Club, Rt. #3, Golden, Colo. (Battery)

Student Member

David S. Newman, New York University; Mail add: 3209 163rd St., Flushing 58, N. Y. (Corrosion, Theoretical Electrochemistry)

Reinstatements to Active Membership

Ernest R. Ramirez, General Electric Co.; Mail add: 17161 Denver St., Detroit 24, Mich. (Corrosion, Electrodeposition, Electrothermics & Metallurgy, Theoretical Electrochemistry)

William J. Schlotter, Electric Storage Battery Co.; Mail add: 608

Noble St., Norristown, Pa. (Battery)

Ernest C. Evers, University of Pennsylvania; Mail add: 225 Washington Ave., Haddonfield, N. J. (Theoretical Electrochemistry)

Reinstatement and Transfer from Active to Active Sustaining Membership

Leslie G. Jenness, Kennecott Copper Corp., 161 E. 42 St., New York 17, N. Y. (Industrial Electrolytic)

Transfers from Associate to Active Membership

George B. Cobel, Dow Chemical Co.; Mail add: 116 Jones St., Midland, Mich. (Electrothermics & Metallurgy)

Marjorie B. Smith, Sprague Electric Co., North Adams, Mass. (Electronics)

Deceased Members

David Hart, Dover, N. J.

E. L. Hauman, Tonawanda, N. Y.

A. T. Lincoln, Northfield, Minn.

William Y. Westervelt, Jackson, Miss.

Personals

Ralph M. Hunter, coordinator of electrochemical activities for Dow Chemical Co., Midland, Mich., has been appointed project manager in a major research project for the Government on solid fuel missile propellants. **Harold A. Robinson,** assistant head of the Metallurgical Lab., will be laboratory director for the project. Dow is one of four U. S. chemical companies selected for research contracts by the Advance Research Projects Agency.

Hyman Chessin has been appointed director of research and development for the Van der Horst Corp. of America, Olean, N. Y. Dr. Chessin had been assistant director of research since 1954.

Eugene N. Schroeder, IBM Corp., Military Products Div., Owego, N. Y., has been promoted to manager, advanced component development.

J. F. Wenckus recently joined the staff of Ewen Knight Corp., Needham Heights, Mass. He formerly was with Airtron, Inc., in Cambridge, Mass.

C. H. Aall, formerly director of research of AMCO Research, Inc., has transferred to the parent company, American Metal Climax, Inc., New York City, as manager of copper smelting and refining operations.

H. H. Rogers, previously research chemist, is now research group leader, inorganic chemistry, for Allis-Chalmers Co., Milwaukee, Wis.

E. R. Breining resigned on October 15, 1958 as manager of the Gas Plating Labs., Commonwealth Engineering Co. of Ohio, Dayton, to enter into business as a chemical consultant with office at 262 Liberty St., Muir, Mich.

Clark E. Thorp has resigned as manager of the Dept. of Chemistry and Chemical Engineering, Armour Research Foundation, Chicago, to take the position of president and director of Fiber Products Center, Inc., Beaver Falls, N. Y.

T. N. Rhodin has joined the staff of Cornell University, Ithaca, N. Y., as associate professor of engineering, physics, and metallurgical engineering. His duties involve teaching courses on the physics of engineering materials, and directing graduate research in surface physics on an Office of Naval Research contract. He had been with E. I. du Pont de Nemours & Co. in Wilmington, Del.

R. H. Coleman, U. S. Industrial Chemicals Co., Ashtabula, Ohio, has transferred to the company's metals division, Mallory Sharon Metals Corp.

S. K. Panikkar has been appointed production assistant-cum-chemist in Grauer and Weil (India) Private Ltd., Bombay.

M. S. Thacker, of New Delhi, India, attended the meeting of the Standing Committee of the British Commonwealth Scientific Conference held in Canada during August 1958. He also visited several universities and research organizations. On his way to Canada, he visited the United Kingdom and East and West Germany.

S. Ghosh has been appointed senior scientific officer, Central Electrochemical Research Institute, Karaikudi.

S. Soundararajan has been appointed senior research assistant in the Dept. of Inorganic and Physical Chemistry, Indian Institute of Science, Bangalore.

T. L. Rama Char has been appointed assistant professor in physical chemistry in the Dept. of Inorganic and Physical Chemistry, Indian Institute of Science, Bangalore. In October 1958, he went to Germany to attend the Third International Symposium on Electrodeposition held at Ilmenau. He also visited some laboratories and electroplating factories.

J. Vaid has returned to Bangalore and resumed his duties at the Indian Telephone Industries on completion of his deputation work in the National Physical Lab., New Delhi.

News Items

Nominations for ECS Honorary Membership

Harold M. Scholberg, Chairman of the Honors and Awards Committee of The Electrochemical Society, would like to receive suggestions for candidates for two Honorary Memberships in the Society, to be awarded in May 1959.

Nominations should carry a resumé of the candidate's career and of his contributions to the Society and the Science.

Nominations should be submitted as soon as possible to H. M. Scholberg, Inorganic Division, Research Dept., Monsanto Chemical Co., Lindbergh & Olive St. Rd., St. Louis 24, Mo.

New Sustaining Members

The following recently became new Sustaining Members of The Electrochemical Society:

Fairchild Semiconductor Corp., Palo Alto, Calif.

General Transistor Corp., Jamaica, N. Y.

Hoffman Electronics Corp., Evanston, Ill.

Kennecott Copper Corp., New York, N. Y.

Metals and Controls Corp., Attleboro, Mass.

Northern Electric Co., Montreal, Que., Canada.

Phelps Dodge Refining Corp., Maspeth, N. Y.

Universal-Cyclops Steel Corp., Bridgeville, Pa.

1958 Annual Index

The Annual Index for Vol. 105 (1958) of the JOURNAL will appear in the February 1959 issue. Reprints of the Index can be obtained about the middle of March by writing to The Electrochemical Society, 1860 Broadway, New York 23, N. Y.

New Process to be Used in Production of Ultrapure Chromium

Chromalloy Corp. and Chilean Nitrate Sales Corp. jointly announced the completion of an exclusive license agreement providing for a program of expanded production, and increased research and development by the Chromalloy Corp., of a new ultrapure form of chromium metal through the use of an iodide chromium process devel-

oped by Battelle Memorial Institute, Columbus, Ohio. The new technique will be used extensively in the development of alloys for nuclear reactors and gas turbines as well as for many other purposes. The program will be carried forward in cooperation with Battelle.

Film on Corrosion

A new film on corrosion, in 16 mm color with sound, tells what causes anodes and cathodes to form on steel surfaces, how they produce electrolytic corrosion, and what can be done about it. Discussed are inhibitors, alloys, hot-dip galvanizing, cathodic protection, metallizing, organic coatings, and Dimetcote inorganic zinc coating. Case histories show how corrosion problems are solved in various industries. The film, running time 19 minutes, contains many useful ideas for those interested in corrosion control. For showing, write Amercoat Corp., 4809 Firestone Blvd., South Gate, Calif.

Delahay 1958 Sigma Xi Lecturer

Dr. Paul Delahay, Boyd Professor of Chemistry at Louisiana State University, discussed "Electrochemistry and Kinetics" in an address at Porter Hall Auditorium, Carnegie Institute of Technology, Pittsburgh, on October 24, 1958. The lecture was under the joint sponsorship of the Carnegie Tech and University of Pittsburgh chapters of the Society of Sigma Xi, the national research honorary fraternity.

Dr. Delahay, who was the 1958 Sigma Xi national lecturer at a number of colleges and universities, was educated in Belgium and taught at the University of Brussels. He has done extensive work in electrode kinetics, diffusion, adsorption, electroanalytical chemistry, and instrumentation.

In 1951 Dr. Delahay received the Turner Book Prize of The Electrochemical Society, and in 1955 the Award in Pure Chemistry of the American Chemical Society. He was a Guggenheim Fellow at Cambridge University in 1955.

Book Reviews

The Physical Chemistry of Electrolytic Solutions, Third Edition, by Herbert S. Harned and Benton B. Owen. ACS Monograph No. 137. Published by Reinhold Publishing Corp., New York City, 1958. xxxiii + 803 pages; $20.00.

The first edition of this book was published in 1943 and was recognized immediately as outstanding, authoritative, and indispensable in its field. The third edition is equally authoritative and indispensable, and will be extremely useful to a host of people who deal with thermodynamic and other properties of weak and strong electrolytes.

The same outline of presentation and the same chapter headings have been used in all three editions. Chapters 1-5 deal with fundamental theory: general thermodynamics; interionic attraction theory; thermodynamics of solutions; irreversible processes (conductance, diffusion, viscosity); numerical computations and compilation of useful functions, slopes, constants. Numerical parameters have been adjusted to conform to modern values of the fundamental constants.

Later chapters deal mainly with experimental results, their analysis, and interpretation, although specific theory is included at appropriate points. Some of the subjects covered are conductance, transference numbers, diffusion, ion association, high field and frequency effects, partial molal quantities, osmotic and activity coefficients from colligative properties and from galvanic cell measurements. Chapters 11-15 especially are concerned with the evaluation and treatment of activity coefficients of strong and weak electrolytes in dilute and in more concentrated solutions, valence type effects, mixed electrolytes and mixed solvents, etc. Chemical kinetics is not treated at all in the book.

The chapters on theory have been expanded by about 60 pages and include a new section on thermodynamics of irreversible processes, discussion of newer contributions to theories of conductance and high field effects, and the general verification of Debye-Hückel theory by methods of statistical mechanics. The later chapters (6-15) have been lengthened by 100 pages, mostly required by new experimental work but including discussion of newer theory as well. The number of Tables of data in the Appendix (67 pages) has also been increased. There are now three Indexes: Author, Subject, and a useful Chemical Index. An index of Tables would be helpful, since there are more than 225 numerical Tables and it is not easy to find a specific one or even to learn if it exists.

This is not a textbook for beginners in the field, and it is a difficult book for study even by experienced workers. It is a valuable reference book; most of the best data of the world on osmotic and activity coefficients, salting-out coefficients, dissociation constants, and other properties have been collected and tabulated, and many hundreds of references to the literature are given. The text is well written and each section can be useful to one with sufficient background in the particular field. The chapters dealing with experiment are the outstanding contribution; the authors are past-masters in fitting data to theoretical, empirical or semiempirical equations, making extrapolations or interpolations to obtain critical values, in putting results in convenient and useful form.

Not everyone will be pleased with every part of the book. The discussion of "electrode potentials" and the theory of galvanic cells is one of 30 years ago, although there is no fault to find with the thermodynamic treatment. Little attention is given to the calculation or use of standard free energies and entropies of ions, and one is referred to tables published in 1938, although there are newer and better tables available. The Brönsted principle of specific interaction of ions does not seem well presented, and there is no mention of the possible enhancement of specific effects by complexing or ion-pair formation (unusual effect of sulfates on certain solubilities, for example). Some would question the relative space allotted to theories of more concentrated solutions, for instance the matter of ion distribution (page 545); the discussion of this problem by Robinson and Stokes in their book "Electrolyte Solutions" is ignored.

Most of the typographical errors are ones which should have been caught by the publisher's own proofreader. The caption of Fig. (11-6-1) is somewhat puzzling.

The authors are to be congratulated on their accomplishment in presenting this valuable contribution to their fellow workers and successors. It summarizes part of the results of their many years of experience and many thousands of hours of devoted toil.

C. V. King

The Powder Method in X-Ray Crystallography, by Leonid V. Azaroff and Martin J. Buerger. Published by McGraw-Hill Book Co., New York City, 1958. XV + 342 pages; $8.75.

The powder method is probably the simplest and most universal technique in x-ray crystallography. Consequently, this book has something to offer workers in diverse fields, such as biochemists and battery makers. The book is based

Third Printing of "Vacuum Metallurgy" Now Available

The third printing of "Vacuum Metallurgy," edited by J. M. Blocher, Jr., of Battelle Memorial Institute, is now available from Society Headquarters, 1860 Broadway, New York 23, N. Y., at the price of $5.00, less a 20% discount to ECS members.

The 216-page book, in hard paper binding, contains papers presented at the Vacuum Metallurgy Symposium held in Boston, Mass., October 6 and 7, 1954.

Sponsored by the Electrothermics and Metallurgy Division of The Electrochemical Society, this symposium brought together, for the first time, those interested in the relation of vacuum to metallurgy.

In the keynote address, J. D. Nisbet, director of research of the Universal-Cyclops Steel Corp., outlines the rapid progress in this field, together with a consideration of what the future may hold. Eighteen papers follow on vacuum melting, vacuum heat treating, vacuum distillation of metals, and on new apparatus. A valuable review of the present status of theory and techniques for the determination of the vapor pressures of metals and alloys is included.

---

on notes and lectures to students at M.I.T., and is an excellent introduction to the use of this technique

Beginning with a very brief introduction to the theory of x-ray diffraction, the authors take up principles of powder photography, and then practice, in detail. There is discussion of the cameras used, the procedures for taking photographs, the interpretation and indexing of photographs, and finally the most important subject, the discussion at great length of the sources of error, the anomalies, and corrections for the errors and anomalies.

The book is well written and accompanied by an excellent series of photographs and diagrams. It is invaluable for both the practitioner and the beginner.

M. M. Fishman

Process Instruments and Controls Handbook. Edited by Douglas M. Considine. Published by McGraw-Hill Book Co., Inc., New York City, 1957. $19.50.

This book presents a well-organized and fairly complete treatment of instruments and controls, specifically for the process fields. The fundamental principles of the instruments are carefully outlined, including excellent sketches, pertinent formulas, and in many instances a critical evaluation.

The subjects covered include measurement standards, primary elements, measurement systems, indicators and recorders, automatic controllers, timers and program controllers, electric and pneumatic telemetering, final control elements, fundamental principles of process control, and mathematical techniques for solving automatic control problems. Specific fields of measurement and control covered are temperature, pressure, flow, liquid-level, chemical composition, and miscellaneous other process measurements. This is a valuable handbook not only for the chemical engineer in the process industry but for the experimentalist concerned with measurement, control, and recording of physical and chemical properties.

Sylvan M. Edmonds

Technology of Columbium (Niobium). Edited by E. M. Sherwood and B. W. Gonser. Latest volume in ECS Series, sponsored by the Society, and published by John Wiley & Sons, Inc., New York City, 1958. 120 pages; $7.00.

The papers in this compilation were presented at the May 1957 symposium on Columbium (Niobium) of the Electrothermics and Metallurgy Division of The Electrochemical Society. Certainly, this volume should achieve the aim of the editors, and both stimulate and aid further work on columbium.

The reviews include the properties and sources of the metal, economic aspects, and supply and extraction metallurgy. Experimental papers are on separation, purification, analysis, alloys, and effects of addition and related subjects. The experimental reports present much quantitative data, and the articles have bibliographies extending into 1957.

The treatment, of course, could not be expected to be comprehensive, and not only do the editors recognize this but, actually, commendably, they recommend that the papers presented in the British symposium on "Metallurgy of Niobium," published in the *Journal of the Institute of Metals*, Vol. 24, pp. 367-392, be used to supplement those presented here.

It is too bad, however, that the oral discussion following the presentations could not be included.

H. W. Salzberg

Literature from Industry

Carbon and Graphite for Chemical Applications. An up-to-date description of its complete line of carbon, graphite, and impervious carbon and graphite equipment for chemical processing applications is available from National Carbon Co., Div. of Union Carbide Corp. The 4-page illustrated bulletin discusses each of a wide range of products, and refers to specific catalog sections that contain complete technical data.

The equipment described includes shell and tube heat exchangers; cascade, concentric, and immersion type heat exchangers; centrifugal pumps; entrainment separators; pipe and fittings; towers and accessories; and brick, structural shapes, and cements. Other products discussed are anodes and backfill for cathodic protection; electrolytic anodes; and activated carbon. Phosphoric acid systems; sulfuric acid diluting equipment, pump injectors and ejectors; and porous carbon and graphite are described, and falling-film type hydrochloric acid systems are discussed in considerable detail.

For a copy of catalog section S-5008, write National Carbon Co., 535 Fifth Ave., New York 17, N. Y.

Gas Chromatography. Best techniques for increasing quantitative accuracy in gas chromatography are covered in detail in a new data sheet published by Beckman Applications Labs. Advantages of the peak or integrated area measurement and peak height measurement methods are given, and several typical analyses are worked out in step-by-step fashion to show how each method is used. The peak area technique is demonstrated with chromatograms run on a Beckman GC-2 Chromatograph and using a new type integrator. This integrator computes peak area within 0.1% accuracy and has been especially designed to operate with recorders used with Beckman Gas Chromatographs.

Free copies of data sheet GC-86-MI and technical information on the integrator are available from Beckman/Scientific and Process Instruments Div., Fullerton, Calif.

Carbon and Graphite Properties and Uses. A new 56-page manual just issued by the Stackpole Carbon Co., gives detailed property, application, and performance data on a wide range of carbon and graphite products. Complete even to showing how carbon and graphite are made, the manual also describes how the basic qualities of the carbon atom form the basis for different carbon and graphite grades. Detailed information for a number of mechanical, chemical, electrical, and refractory uses is described and illustrated throughout.

A copy of the manual, catalog 40B, is available on letterhead request to the Stackpole Carbon Co., St. Marys, Pa.

Pumpless Mercury Arc Rectifiers. Bulletin GEA-6848, 12 pages, describes the operation, construction features, and applications of General Electric's Pumpless Mercury Arc Rectifiers ranging from 750-kw, 250-v units for industrial service to units rated over 5000 kw, 850 v for electrochemical service. It includes cross-section line drawing of pumpless tank, photographs, charts, system diagram, and rating tables. Available from General Electric Company, Schenectady 5, N. Y.

Battery Engineering Manual. Burgess Battery Co., of Freeport, Ill., which produces more than 3000 different types of dry cells, has published as an aid to product design engineers the most comprehensive manual on the use and selection of dry batteries ever prepared by the battery industry. The 100-page compendium was created to provide industrial designers and research specialists with an invaluable engineering reference guide.

Rapid advances in modern electrochemical research and engineering have greatly expanded the potential uses of batteries by industry, the Armed Services, and for scientific purposes. The new manual is intended to help design engineers bring practical application of today's battery technology to bear on all product design problems calling for portable electric power.

Batteries shown in the handbook range from 1½ to 510 v and weigh from 0.013 to 16 lb. They are used for thousands of purposes requiring portable electrical power, from flashlights and portable radios to transistorized electronic equipment and giant space-age missiles.

Practical data provided on each type of battery in 14 different volt-

The Lepel line of induction heating equipment represents the most advanced thought in the field of electronics as well as the most practical and efficient source of heat yet developed for industrial heating.

If you are interested in induction heating you are invited to send samples of the work with specifications. Our engineers will process and return the completed job with full data and recommendations without any cost or obligations.

TYPICAL INDUCTION HEATING APPLICATIONS IN THE MANUFACTURE OF TRANSISTORS

SOLDERING TRANSISTOR ASSEMBLIES BY INDUCTION HEATING

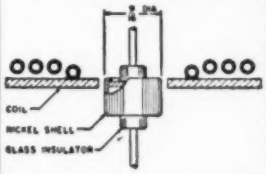

Concentrator-type coil creates high intensity, restricted heating at joint of nickel shell and tinned glass, thus causing solder to flow for permanent seal.

SINGLE CRYSTAL PULLER

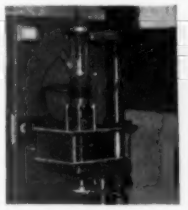

General arrangement for pulling single crystals. Induction heating coil is shown surrounding quartz tube containing crucible with molten germanium in suitable atmosphere.

MULTIPLE ZONE REFINING

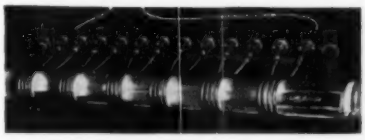

Induction heating apparatus used in zone refining. The six coils shown provide simultaneous molten zones in the ingot as it passes through the tube containing the protective atmosphere.

Electronic Tube Generators from 1 kw to 100 kw.
Spark Gap Converters from 2 kw to 30 kw.

WRITE FOR THE NEW LEPEL CATALOG . . . 36 illustrated pages packed with valuable information.

All Lepel equipment is certified to comply with the requirements of the Federal Communications Commission.

LEPEL HIGH FREQUENCY LABORATORIES, INC.
55th STREET and 37th AVENUE, WOODSIDE 77, NEW YORK CITY, N. Y.

age classifications include: ASA reference letters and numbers; the number and size of cells used; weight; maximum physical dimensions; detailed service life graphs; voltage taps, and types of terminals used. Sketches of 69 different kinds of terminals are included in a separate section of the book.

Engineers engaged in the design of battery-powered equipment are invited to write to Burgess Battery Co., Dept. PR-I, Freeport, Ill., to secure their copy of the new battery engineering manual. Others may purchase the manual at a cost of $1.00.

Announcement from Publisher

"Rocket Refractories," H. B. Porter, Naval Ordnance Test Station, Aug. 1955. Report PB 131503, 55 pages; $1.50.

This review (to 1955) of development of high-temperature refractories for use in rockets has been released for industry use by the Naval Ordnance Test Station. The volume is available from the Office of Technical Services, U. S. Dept. of Commerce, Washington 25, D. C.

The report brings together scattered literature on refractories appearing to 1955, and sets forth required characteristics of acceptable rocket refractories. Basic refractory substances, including metal oxides, metal-metalloid compounds, and intermetallic compounds, are also discussed, both individually and as ingredients of bonded-ceramic and cermet compositions.

Practices then current for the use of refractories as protective coatings, combustion chamber liners, and nozzles are reviewed, with special emphasis on commercial materials. Design and fabrication are discussed, and physical and chemical properties, manufacturers, and products listed. Areas for future research are pointed out.

New Products

Junction Transistor. A new germanium p-n-p alloy-junction transistor (RCA-2N331) for audio-frequency amplifier service was announced recently by the RCA Semiconductor and Materials Div., Somerville, N. J.

The new transistor is especially designed for use in critical industrial and military equipment where rugged construction, extreme stability, and excellent uniformity of characteristics are important design considerations. It has a current-transfer-ratio characteristic which is essentially constant over the useful operating current range for the device This feature, in addition to low collector- and emitter-cutoff currents, low base resistance, a typical power gain of 44 db, and a typical noise factor of 9 db, makes the new transistor particularly useful in low-power audio-frequency amplifier service.

Water-Cooled Silicon Rectifier. A new water-cooled silicon rectifier designed to provide either regulated or unregulated d-c power for steel, electrochemical, plating, and other continuous processing lines has been developed by General Electric's Low Voltage Switchgear Dept., Schenectady 5, N. Y.

The rectifier employs saturable reactor-amplistat control to maintain the desired current level within plus or minus 1% with unit efficiencies ranging from 90 to 95% depending on voltage rating of the equipment. Available in ratings of 1000-10,000 amp at voltages up to 300 v, the rectifier may be either manually or automatically controlled by means of the saturable reactor which provides smooth, stepless control from 10 to 125% current output.

One outstanding feature of the new rectifier is the short circuit limiting capabilities of the saturable reactor which successfully restricts short circuit current to a value about 20% greater than the current prior to the short circuit. The rectifier is designed to withstand such an output without damage to components.

Spectrofluorometers. Farrand Optical Co., Inc., announces that, in addition to its standard spectrofluorometer, two new types of spectrofluorometer are now available. One is a dual-purpose instrument for spectrofluorometic transmission measurements in the spectral region from 220 to 650 mu. The second is a triple-purpose instrument which can be utilized as a spectrofluorometer, spectrophotometer, or for reflectance measurements of solid samples such as textiles, plastics, paints, paper, powders, etc.

Farrand spectrofluorometers can be supplied for manual operation, for automatic operation with recorders, or for oscilloscope presentation.

Descriptive bulletin No. 820, Supplement 1, is available upon request from Farrand Optical Co., Inc., Dept. C-17, Bronx Blvd. and E. 238 St., New York 70, N. Y.

Nonfoaming Spray-Wash Cleaners. Cleaners SW-57 and SW-58, powered alkaline materials for use in pressure spray-washing machines, have been introduced by Enthone, Inc., New Haven, Conn., subsidiary of American Smelting and Refining Co.

The two new products contain surfactants which are designed to give maximum detergency with a minimum of foam. They remove oil, solid dirt, and other shop soils quickly and completely. Cleaner SW-57 is mild in alkalinity and safe for use on reactive metals such as zinc and aluminum. Cleaner SW-58 is designed for cleaning steel, copper, brass, and magnesium.

Both cleaners are effective at concentrations of 1-4 oz/gal and at temperatures of 150°-200°F. They can be used in all types of spray-washing machines or for tank applications using various types of agitation. For most applications, either Cleaner SW-57 or Cleaner SW-58 alone will do the complete cleaning job; for buffing compound removal, either cleaner, used in the second stage of the washing machine, rapidly removes the emulsions or solvents remaining on the work from the first or buffing compound removal stage.

Literature on Cleaners SW-57 and SW-58 is available from the manufacturer.

Employment Situations

Please address replies to box shown, c/o The Electrochemical Society, Inc., 1860 Broadway, New York 23, N. Y.

Positions Wanted

Physical Chemist, Ph.D. 1958, desires research position in electrochemistry and/or solid state. Strong instrumentation background; research experience; publications; honor societies. Will consider position in New York City or Metropolitan New Jersey area only. *Reply to Box 365.*

Battery Chemist, 11 years' experience with manufacturers of automotive, stationary, and industrial lead-acid batteries. Thoroughly experienced in grid design and casting,

oxide production, paste formulation, assembly, fast formation, and dry charging; development, quality control, and cost reduction. B.Sc. degree. Age 32. *Reply to Box 366.*

Positions Available

Electrochemist for Basic Studies in Corrosion, position open in small laboratory in Virginia. Opportunity for solid-state physics approach or conventional electrochemical approach to aqueous corrosion. Position is such that either a strong individualist or a team man could be happy. *Reply to Box A-277.*

Electrochemist. Nationally known company located in Northern N. J. has challenging product research opportunity. Steady employment for B.S. or M.S. with imagination and initiative for development work on oxygen electrodes and air-depolarized cells. Good salary and working conditions, also all usual benefits. Please send complete résumé . *Reply to Box A-278.*

Research Chemists. Research and Development group seeks experienced Chemists or Chemical Physicists for solid-state work on luminescent materials and inorganic chemicals for rapidly developing electronic applications. Candidate should have Ph.D. or equivalent and be capable of independent work. Challenging position in new research and development laboratories located in Northeast Pennsylvania. Publication of work encouraged.

Send résumé to: Dr. J. S. Smith, Manager of Chemical Research and Development, Chemical and Metallurgical Division, Sylvania Electric Products, Inc., Towanda, Pa.

Engineers (Aeronautical, Electrical, Electronic, Industrial, General, Mechanical, and Power Plant), **Electronic Scientists, Metallurgists, Physicists, Technologists**—Vacancies exist for professional personnel in the above positions. Starting salaries range from $4490 to $10,130 per annum. The Naval Air Material Center is currently engaged in an extensive program of aeronautical research, development, experimentation, and test operations for the advancement of Naval aviation. Experimental work is also being conducted in the guided missile field. Personnel are needed for work on projects involving modification, overhauling, and testing of aeronautical equipment, materials, accessories, power plants, launching and arresting devices, and for modification and structural testing of aircraft. Also, for work involving the basic design of catapults, launchers, arresting gear and their component parts; test and development work at shore stations and on board U. S. Navy ships; evaluation of new equipment and establishment of performance parameters, and applied research on the many problems relevant to this field.

Interested persons should file an Application for Federal Employment, Standard Form 57, with the Industrial Relations Dept., Naval Air Material Center, Naval Base, Philadelphia 12, Pa. Applications may be obtained from the above address or information as to where they are available may be obtained from any first or second class post office.

Physical Chemist, Physicist, or Metallurgist. The British Columbia Research Council has a vacancy for a physical chemist, physicist, or metallurgist for research on anodic oxide films. Salary range to $7000 depending upon qualifications and experience. Applications with names of two referees should be sent to Dr. G. M. Shrum, Director, British Columbia Research Council, University of British Columbia, Vancouver 8, B. C., Canada.

SEMICONDUCTOR ENGINEERS AND SCIENTISTS

An expanding program, the result of increasing production and sales of the 4-layer bistable diode, is creating openings in basic research, advanced device development and application engineering.

Opportunities exist also in the techniques of device packaging, as well as crystal growing and diffusion in silicon.

Openings are currently available and others will develop. Your resume, which will be held in strict confidence, may be sent to the Director, Professional Employment.

(Ref: EI-6)

SHOCKLEY TRANSISTOR CORPORATION

A Subsidiary of Beckman Instruments, Inc.

Stanford Industrial Park

Palo Alto, California

JOURNAL ELECTROCHEMICAL SOCIETY

Wanted to Buy.

Back sets, volumes, and issues of this JOURNAL and TRANSACTIONS.

Especially volumes 1, 3 and from volume 60 to date.

We pay good prices.

Buy also Technical and Scientific Periodicals.

E. O. ASHLEY, 27 E. 21 St., New York 10, N. Y.

Advertiser's Index

Bell Telephone Laboratories, Inc. 5C
Enthone, Incorporated ..... Cover 4
Grace Electronic Chemicals, Inc. 6C
Great Lakes Carbon Corporation ..... Cover 2
Lepel High Frequency Laboratories, Inc. 17C
E. H. Sargent & Company 2C
Shockley Transistor Corporation 19C
Sylvania Electric Products Inc. 3C

The Electrochemical Society

Patron Members

Aluminum Co. of Canada, Ltd.,
Montreal, Que., Canada

International Nickel Co., Inc.,
New York, N. Y.

Olin Mathieson Chemical Corp.,
Niagara Falls, N. Y.
Industrial Chemicals Div., Research
and Development Dept.

Union Carbide Corp.
Divisions:
Electro Metallurgical Co.,
New York, N. Y.
National Carbon Co., New York, N. Y.

Westinghouse Electric Corp., Pittsburgh, Pa.

Sustaining Members

Air Reduction Co., Inc.
New York, N. Y.

Ajax Electro Metallurgical Corp.,
Philadelphia, Pa.

Allied Chemical & Dye Corp.
General Chemical Div., Morristown, N. J.
Solvay Process Div., Syracuse, N. Y.
(3 memberships)

Alloy Steel Products Co., Inc., Linden, N. J.

Aluminum Co. of America,
New Kensington, Pa.

American Machine & Foundry Co.,
Raleigh, N. C.

American Metal Co., Ltd.,
New York, N. Y.

American Potash & Chemical Corp.,
Los Angeles, Calif. (2 memberships)

American Zinc Co. of Illinois,
East St. Louis, Ill.

American Zinc, Lead & Smelting Co.,
St. Louis, Mo.

American Zinc Oxide Co., Columbus, Ohio

M. Ames Chemical Works, Inc.,
Glens Falls, N. Y.

Auto City Plating Company Foundation,
Detroit, Mich.

Bart Manufacturing Co., Bellville, N. J.

Bell Telephone Laboratories, Inc.
New York, N. Y. (2 memberships)

Bethlehem Steel Co., Bethlehem, Pa.
(2 memberships)

Boeing Airplane Co., Seattle, Wash.

Burgess Battery Co., Freeport, Ill.
(4 memberships)

C & D Batteries, Inc., Conshohocken, Pa.

Canadian Industries Ltd., Montreal, Que.,
Canada

Carborundum Co., Niagara Falls, N. Y.

Catalyst Research Corp., Baltimore, Md.

Chrysler Corp., Detroit, Mich.

Ciba Pharmaceutical Products, Inc., Summit,
N. J.

Columbian Carbon Co., New York, N. Y.

Columbia-Southern Chemical Corp.,
Pittsburgh, Pa.

Consolidated Mining & Smelting Co. of
Canada, Ltd., Trail, B. C., Canada
(2 memberships)

Continental Can Co., Inc., Chicago, Ill.

Cooper Metallurgical Associates, Cleveland,
Ohio

Corning Glass Works, Corning, N. Y.

Crane Co., Chicago, Ill.

Diamond Alkali Co., Painesville, Ohio
(2 memberships)

Dow Chemical Co., Midland, Mich.

Wilbur B. Driver Co., Newark, N. J.
(2 memberships)

E. I. du Pont de Nemours & Co., Inc.,
Wilmington, Del.

Eagle-Picher Co., Chemical Div., Joplin, Mo.

Eastman Kodak Co., Rochester, N. Y.

Electric Auto-Lite Co., Toledo, Ohio

Electric Storage Battery Co.,
Philadelphia, Pa.

Englehard Industries, Inc., Newark, N. J.
(2 memberships)

The Eppley Laboratory, Inc., Newport, R. I.
(2 memberships)

Erie Resistor Corp., Erie, Pa.

Fairchild Semiconductor Corp., Palo Alto,
Calif.

Federal Telecommunication Laboratories,
Nutley, N. J.

Food Machinery & Chemical Corp.
Becco Chemical Div., Buffalo, N. Y.
Westvaco Chlor-Alkali Div., South
Charleston, W. Va.

Ford Motor Co., Dearborn, Mich.

General Electric Co., Schenectady, N. Y.
Chemistry & Chemical Engineering
Component, General Engineering
Laboratory
Chemistry Research Dept.

(Sustaining Members cont'd)

General Electric Co. (cont'd)
Metallurgy & Ceramics Research Dept.
General Motors Corp.
Brown-Lipe-Chapin Div., Syracuse, N. Y. (2 memberships)
Guide Lamp Div., Anderson, Ind.
Research Laboratories Div., Detroit, Mich.
General Transistor Corp., Jamaica, N. Y.
Gillette Safety Razor Co., Boston, Mass.
Gould-National Batteries, Inc., Depew, N. Y.
Grace Electronic Chemicals, Inc., Baltimore, Md.
Great Lakes Carbon Corp., New York, N. Y.
Hanson-Van Winkle-Munning Co., Matawan, N. J. (3 memberships)
Harshaw Chemical Co., Cleveland, Ohio (2 memberships)
Hercules Powder Co., Wilmington, Del.
Hoffman Electronics Corp., Evanston, Ill.
Hooker Electrochemical Co., Niagara Falls, N. Y. (3 memberships)
Houdaille-Hershey Corp., Detroit, Mich.
Hughes Aircraft Co., Culver City, Calif.
International Business Machines Corp., Poughkeepsie, N. Y.
International Minerals & Chemical Corp., Chicago, Ill.
Jones & Laughlin Steel Corp., Pittsburgh, Pa.
K. W. Battery Co., Skokie, Ill.
Kaiser Aluminum & Chemical Corp.
Chemical Research Dept., Permanente, Calif.
Div. of Metallurgical Research, Spokane, Wash.
Kennecott Copper Corp., New York, N. Y.
Keokuk Electro-Metals Co., Keokuk, Iowa
Libbey-Owens-Ford Glass Co., Toledo, Ohio
P. R. Mallory & Co., Indianapolis, Ind.
McGean Chemical Co., Cleveland, Ohio
Merck & Co., Inc., Rahway, N. J.
Metal & Thermit Corp., Detroit, Mich.
Metals and Controls Corp., Attleboro, Mass.
Minnesota Mining & Manufacturing Co., St. Paul, Minn.
Monsanto Chemical Co., St. Louis, Mo.
Motorola, Inc., Chicago, Ill.
National Cash Register Co., Dayton, Ohio
National Lead Co., New York, N. Y.
National Research Corp., Cambridge, Mass.
National Steel Corp., Weirton, W. Va.
Northern Electric Co., Montreal, Que., Canada
Norton Co., Worcester, Mass.
Olin Mathieson Chemical Corp., Niagara Falls, N. Y.
High Energy Fuels Organization (2 memberships)
Pennsalt Chemicals Corp., Philadelphia, Pa.
Phelps Dodge Refining Corp., Maspeth, N. Y.
Philips Laboratories, Inc., Irvington-on-Hudson, N. Y.
Pittsburgh Metallurgical Co., Inc., Niagara Falls, N. Y.
Poor & Co., Promat Div., Waukegan, Ill.
Potash Co. of America, Carlsbad, N. Mex.
Radio Corp. of America, Harrison, N. J.
Ray-O-Vac Co., Madison, Wis.
Raytheon Manufacturing Co., Waltham, Mass.
Reynolds Metals Co., Richmond, Va. (2 memberships)
Schering Foundation, Inc., Bloomfield, N. J.
Shawinigan Chemicals Ltd., Montreal, Que., Canada
Speer Carbon Co.
International Graphite & Electrode Div., St. Marys, Pa. (2 memberships)
Sprague Electric Co., North Adams, Mass.
Stackpole Carbon Co., St. Marys, Pa. (2 memberships)
Stauffer Chemical Co., Henderson, Nev., and New York, N. Y. (2 memberships)
Sumner Chemical Co., Div. of Miles Laboratories, Inc., Elkhart, Ind.
Superior Tube Co., Norristown, Pa.
Sylvania Electric Products Inc., Bayside, N. Y. (2 memberships)
Sarkes Tarzian, Inc., Bloomington, Ind.
Tennessee Products & Chemical Corp., Nashville, Tenn.
Texas Instruments, Inc., Dallas, Texas
Titanium Metals Corp., of America, Henderson, Nev.
Udylite Corp., Detroit, Mich. (4 memberships)
Universal-Cyclops Steel Corp., Bridgeville, Pa.
Upjohn Co., Kalamazoo, Mich.
Victor Chemical Works, Chicago, Ill.
Wagner Brothers, Inc., Detroit, Mich.
Western Electric Co., Inc., Chicago, Ill.
Wyandotte Chemicals Corp., Wyandotte, Mich.
Yardney Electric Corp., New York, N. Y.

How to make metal cleaning an exact science: Enthone's broad range of cleaning and degreasing compounds are the end result of more than 20 years of applied research in the laboratory and in the field on metal finishing problems. These compounds include emulsifiable and solvent cleaners, alkaline cleaners for soak or electrolytic cleaning of iron, steel, copper, brass, zinc and zinc base die castings. And if there's no Enthone stock cleaner that meets your requirements, Enthone will develop a special one that does. Write us about it. Enthone, Inc., 442 Elm St., New Haven 11, Conn.

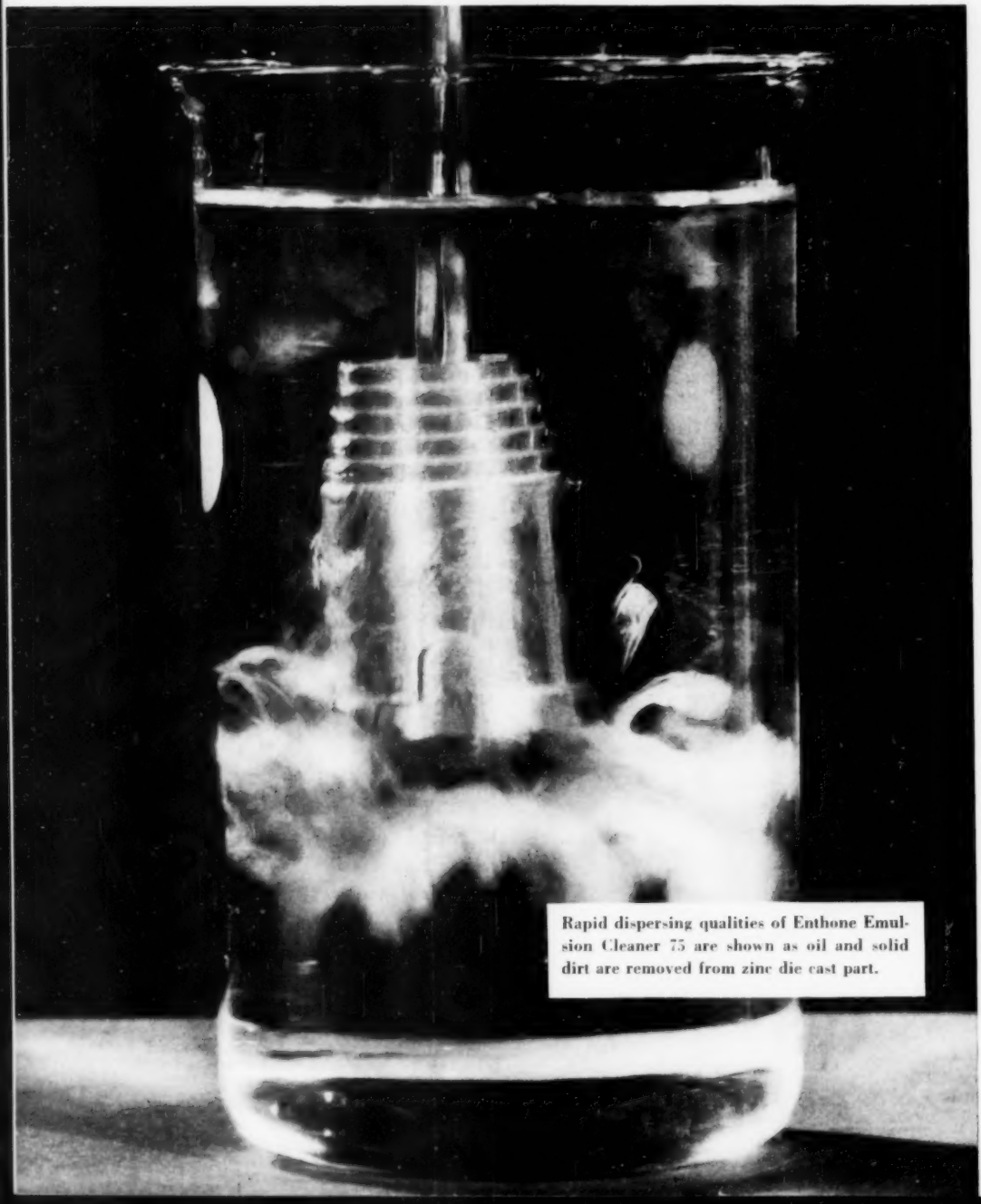

Rapid dispersing qualities of Enthone Emulsion Cleaner 75 are shown as oil and solid dirt are removed from zinc die cast part.

ENTHONE

ENTHONE, INC. IS A SUBSIDIARY OF AMERICAN SMELTING AND REFINING COMPANY